Exploiting the chick embryonic environment to reprogram neuroblastoma cells to a benign phenotype

Thesis submitted in accordance with the requirements of the University of Liverpool for the degree of Doctor of Philosophy

By

Rachel Jane Carter

June 2013

Declaration

This thesis entitled:

“Exploiting the chick embryonic environment to reprogram neuroblastoma cells to a benign phenotype”

is entirely my own work, except where indicated in the text.

This material has not been presented for any other qualification

Abstract

Neuroblastoma is a paediatric cancer that arises from the sympathetic ganglia and adrenal medulla. Tumours with MYCN amplification have the worst prognosis, and make up around 30% of neuroblastoma diagnoses. Neuroblastoma exhibits an unusually high propensity for spontaneous regression, which occurs most frequently in the youngest patients (under 18 months of age), perhaps because developmental cues still present prompt belated differentiation of the tumour cells. This led to the hypothesis that factors from an appropriate embryonic environment may be capable of activating the correct molecular switches to encourage the differentiation and/or apoptosis of neuroblastoma cells, reprogramming the tumour to a benign phenotype.

To test this hypothesis, EGFP-labelled MYCN-amplified Kelly cells were injected into the extra-embryonic vitelline veins of embryonic day 3 (E3) and E6 chick embryos, and the responses of injected cells were analysed at E10 and E14. Kelly cells injected at E3 respond to neural crest migratory cues and integrate into neural crest-derived tissues: some neural, notably the sympathetic ganglia and enteric nervous system, although never the adrenal gland; and others non-neural, such as the meninges and tail. Cells injected at E6 do not show such targeting, integrating into various tissues such as the liver, kidney and meninges. The cells respond to their respective microenvironments, and in sympathetic ganglia some cells differentiate, show reduced cell division, and crucially such cells have undetectable MYCN expression by E10. In non-neural locations, cells form more rapidly dividing clumps and continue to express MYCN. The downregulation of MYCN is dependent on continuous and direct interaction with the sympathetic ganglion environment.

Kelly cells' morphology, behaviour and gene expression are altered by the sympathetic ganglia microenvironment. Taking these key observations, we speculate that the Kelly cells' MYCN amplicon may likely contain the required DNA regulatory sequences to enable MYCN expression to be altered in response to the embryonic environment. If the factors responsible for MYCN repression can be elucidated, they may represent effective new therapeutic targets.

Acknowledgements

The biggest thanks of all goes to Diana Moss for her unwavering support and much-needed advice, I couldn't have asked for a better supervisor. And of course I can't express enough gratitude for The Neuroblastoma Society, who funded this project. They are an amazing charity run by volunteers, whose trustees and members are all so friendly and enthusiastic about the work. Thanks also to my second supervisor, Jes, for his input of ideas and for coming up with the concept behind this project in the first place. Dhanya Mullassery has been a massive help, particularly in my first year, "passing the reins" on to me, after she had completed the neural tube injections that were the preliminary work for this thesis.

Huge thanks have to go to all the lab members, past and present: Christine McNamee, who is always willing to help, and gives amazing motivational talks; as well as Michael Lyons, Mohammed Akeel, Rabiu Inuwa, Kejhal Khursheed and Heba Karosh – all of you have kept me smiling throughout the past four years. As has Sokratis Theocharatos, who deserves extra appreciation for performing the GFP lentiviral transduction of the Kelly cells, which was a real turning point in this work. Thank you to Anne Herrmann, who transduced the BE(2)C and SH-EP cells, and is one of the most polite, helpful people I know, and over the last year or so has become a friend. Thanks also to Lou Chesler for donating the Kelly and SH-EP cells, Prof. Dot Bennett for the B16 F1s, and Omar Pathmanaban for allowing the injection of his glioblastoma primaries. Thank you to Haleh Shahidipour, who completed the medulloblastoma chick injections, Violaine See, who has been supportive right the way through this project, and also to Dave Spiller, who was a big help when using the confocal microscope.

Much appreciation goes to the doctors at Alder Hey for their neuroblastoma expertise: Paul Losty, Barry Pizer and Heather McDowell; and I am so, so grateful to the patients and their families for allowing us access to their tumour material at such a terrible time.

The final thank you must go to all of my family and friends. To my mum and dad – I couldn't have done it without you. And to the rest of my family and my amazing friends – thanks for always being there and for keeping me sane, particularly through the write up!

Abbreviations

ABC	ATP binding cassette
Akt	Protein kinase B
ALK	Anaplastic lymphoma receptor tyrosine kinase
AG	Adrenal gland
ANS	Autonomic nervous system
ATP	Adenosine triphosphate
AURKA	Aurora kinase A
BDNF	Brain-derived neurotrophic factor
bHLH	Basic helix-loop-helix
BMP	Bone morphogenetic protein
BrdU	5-bromo-2'-deoxyuridine
BSA	Bovine serum albumin
CAM	Cell adhesion molecule OR Cancer-associated myofibroblast
CDK	Cyclin dependent kinase
CFDA-SE	Carboxyfluorescein diacetate N-succinimidyl ester
ChAT	Choline acetyltransferase
CMV	Human cytomegalovirus
c-Myc	v-myc avian myelocytomatosis viral oncogene homologue
CNS	Central nervous system
CO_2	Carbon dioxide
DAPI	4',6-diamidino-2-phenylindole
DBH	Dopamine-β-hydroxylase
DiI	Indocarbocyanine dye
DM	Double minute
DMSO	Dimethylsulfoxide

DNA	Deoxyribonucleic acid
DRG	Dorsal root ganglia
E	Embryonic day
EDTA	Ethylenediaminetetraacetic acid
EdU	5-ethynyl-2'-deoxyuridine
EGF	Epidermal growth factor
EGFP	Enhanced green fluorescent protein
EMT	Epithelial to mesenchymal transition
ENS	Enteric nervous system
FACS	Fluorescent activated cell sorting
FCS	Foetal calf serum
FGF	Fibroblast growth factor
G418	Geneticin
GAP43	Growth associated protein 43
GFP	Green fluorescent protein
GSK3β	Glycogen synthase kinase 3 β
H&E	Haematoxylin and eosin
HBSS	Hanks balanced salt solution
HDAC	Histone deacetylase
hESC	Human embryonic stem cell
HH	Hamburger Hamillton (chick embryo staging)
HMB-45	Human melanoma black antigen 45
HSR	Homogeneously staining region
hTERT	Human telomerase reverse transcriptase
INRG	International neuroblastoma risk group
INSS	International neuroblastoma staging system
ki67	Antigen identified by monoclonal antibody ki67
LOH	Loss of heterozygosity

miR	Micro RNA
miRNA	Micro RNA
MM	Malignant melanoma
mRNA	Messenger RNA
MRP	Multidrug resistance protein
mTOR	Mammalian target of rapamycin
MYCN	Neuroblastoma-derived v-myc avian myelocytomatosis viral related oncogene
NB	Neuroblastoma
NB84	Uncharacterised antigen from neuroblastoma tissue
NC	Neural crest
N-CAM	Neural cell adhesion molecule
NCC	Neural crest cell
N-cym	MYCN antisense gene
NEAA	Non-essential amino acids
NF	Neurofilament
NGF	Nerve growth factor
nNOS	Nitric oxide synthase (neuronal)
NO	Nitric oxide
NT	Neurotrophin
PBS	Phosphate buffered saline
PBST	Phosphate buffered saline containing 0.25% Triton X100
PI3K	Phosphatidylinositol 3-kinase
PNS	Peripheral nervous system
PP2A	Phosphatase 2A
qPCR	Quantitative polymerase chain reaction
RA	Retinoic acid
RNA	Ribonucleic acid
rpm	Rotations per minute

S62	Residue serine 62
SA	Sympathoadrenal
SDS	Sodium dodecyl sulphate
SFFV	Spleen focus-forming virus
SG	Sympathetic ganglia
Shh	Sonic hedgehog
shRNA	Short hairpin RNA
siRNA	Small interfering RNA
SMA	Smooth muscle actin
T58	Residue threonine 58
TH	Tyrosine hydroxylase
TUJ-1	Antibody to neuron-specific β-III-tubulin
VAChT	Vesicular acetylcholine transporter
VIP	Vasoactive intestinal peptide
VSV-G	Vesicular stomatitis virus glycoprotein

Contents

Chapter One:

Introduction

1.1. Neuroblastoma: an introduction

Neuroblastoma is a paediatric cancer of the sympathetic nervous system, with tumours primarily arising in the paravertebral sympathetic ganglia and, more commonly, in the adrenal glands (Brodeur 2003; Matthay 1997; Park, Eggert & Caron 2008) (Figure 1.1). Metastasis is usually to the lymph nodes, bone, bone marrow, liver and/or skin (Brodeur et al. 1988). Affecting 7.5 in every 100,000 children (Schwab et al. 2003), neuroblastoma is the most common solid tumour outside of the cranium in children and accounts for around 15% of all paediatric oncology deaths (Maris et al. 2007). Patients are usually diagnosed before the age of 5 years (90% of all cases) (Schwab et al. 2003), but can, in rarer circumstances, present with the disease up to 14, or even occasionally up to 19 years of age. Neuroblastoma is almost unheard of in adults. In the vast majority of cases, neuroblastoma occurs sporadically, although in 1-2% of diagnoses, the disease is inherited (Shojaei-Brosseau et al. 2004). Familial neuroblastoma is usually diagnosed at an earlier age, often within the child's first year of life (Maris et al. 1997), and multiple primary tumours at diagnosis is a feature much more common in those with a genetic predisposition than in patients with sporadic disease. Hereditary neuroblastoma is often associated with mutations in the ALK and Phox2b genes, which, it is postulated, may prolong the process of sympathetic neurogenesis during embryonic development, thus increasing the window in which mutational events may likely occur (Bourdeaut et al. 2005; Mosse et al. 2008; Perri et al. 2005).

Neuroblastoma is a peculiar disease with a diverse range of clinical behaviours, ranging from rapid malignant progression, complete with metastasis and extremely poor prognosis, to tumours that (occasionally) differentiate into benign ganglioneuroblastoma or ganglioneuroma (Maris et al. 2007). In addition, neuroblastoma has the highest rates of spontaneous regression of any human cancer (Castleberry 1997). However, even with an increasing wealth of research into the disease, medicine is still failing those deemed "high risk" patients, with survival often less than 40% (De Bernardi et al. 2003) (Figure 1.1).

Figure 1.1. Kaplan-Meier curve to show event-free survival of patients classed as low-, intermediate- or high-risk. Taken from Maris et al. 2007.

1.2. The sympathetic nervous system

The human body is controlled by its extensive networks of neurons which, via the brain, innervate skeletal muscles to facilitate movement, sense touch, pain and temperature, stimulate glands to emit their secretions, allow us to taste, smell and see, and keep viscera like the heart functioning efficiently – to name but a few of the nervous system's numerous and wide-ranging functions. The network itself can be separated into various hierarchical subdivisions (Figure 1.2): principally the central nervous system (CNS), composed of the brain and spinal cord and arising from the embryonic neural tube; and the peripheral nervous system (PNS), which connects the brain and spinal cord to the limbs and organs, and is derived from the embryonic neural crest. The PNS itself can be split into the somatic nervous system, responsible for voluntary bodily movements, and the autonomic nervous system (ANS), which operates largely at a subconscious level to control visceral functions. The ANS can then be split into three subdivisions: the enteric (ENS), the parasympathetic, and the sympathetic nervous systems. The ENS controls digestion, by regulating movement, blood flow and secretions in the digestive system, and exists as two plexuses: the submucosal (more externally) and myenteric plexuses, located in the wall of the gastrointestinal tract (Sasselli, Pachnis & Burns 2012). The parasympathetic nervous system, in general, is associated with "rest and digest" functions, for example salivary gland secretion, constriction of the pupil, urination and defecation. Its preganglionic neurons come from cranial nerve nuclei III, VII, IX and X and the sacral segments of the spinal cord, and both pre- and post-ganglionic neurons release the neurotransmitter acetylcholine (Le Douarin 1982). The sympathetic division of the ANS is composed of the sympathetic ganglia and the adrenal medullas (often referred to as modified sympathetic ganglia), and is associated with "fight or flight" responses, like increasing heart rate and contractional force, bronchiole dilation, induction of sweat secretion, and inhibition of peristalsis in the gut. Its effects are complimentary (often antagonistic) to those of the parasympathetic nervous system, for example it functions in pupil dilation, whereas the parasympathetic acts to constrict the

pupils. Sympathetic neurons arise from the thoracic and lumbar regions of the spinal cord. The preganglionic neurons synapse within the sympathetic chains, or in plexuses nearer to body organs, utilising the neurotransmitter acetylcholine. Postganglionic fibres' mediator is noradrenaline (Langley & Grant 1999).

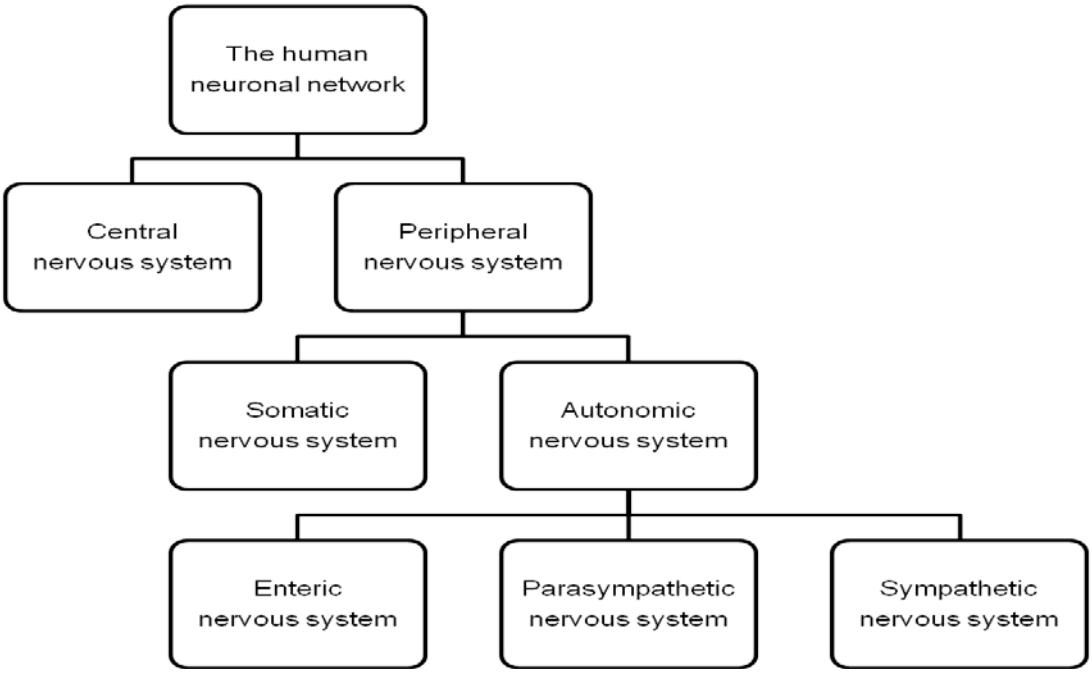

Figure 1.2. Overview of the human nervous system, split into subdivisions.

The segmentally-arranged sympathetic ganglia, as mentioned above, are the sites where preganglionic sympathetic neurons synapse and from which postganglionic neurons arise. They lie either side of the vertebral column, and are connected by bundles of longitudinal nerve fibres to form the bilateral sympathetic trunks/chains.

The two bilateral adrenal glands that lie superior to the kidneys are composed of an outer collagenous capsule, which surrounds the cortex, derived from the embryonic intermediate mesoderm, and the inner neural-crest-derived medulla. It is the medullary cells that can develop into malignant neuroblastic cells (Castleberry 1997). It has been said that the adrenal medulla could be considered as "a modified sympathetic ganglion whose postganglionic neurons lost their processes during development and became secretory cells" (Junqueira et al. 1986). The adrenal medulla is the only organ to be stimulated by preganglionic sympathetic neurons, and in response secrete either adrenaline or, like postganglionic sympathetic neurons, noradrenaline, with the effect of increasing the

metabolic rate, raising blood pressure, and other functions associated with the fight or flight response of the sympathetic nervous system (Le Douarin 1982).

Neuroblastoma tumours can appear at any point along the length of the sympathetic ganglia, although a more favourable disease outcome can be expected for those patients with tumours in the cervical or thoracic regions than those with tumours in the abdomen: it is not known why this is the case (Evans, Dangio & Randolph 1971). Overall, 65% of neuroblastomas occur in the abdomen, and of these, over half arise from the adrenal medulla (Maris et al. 2007). The adrenal glands are in fact the most common site for neuroblastoma masses, and prognosis for these tumours depends on a number of different factors (see “staging”).

1.3. The neural crest

Neuroblastoma develops from cells that would/do form the sympathetic ganglia and adrenal medulla, as well as the extra-adrenal paraganglia such as the organ of Zuckerkandl, therefore, like the aforementioned structures, can be said to originate from the embryonic neural crest.

Figure 1.3. Illustration of neural crest formation and migration. Taken from Jessen & Mirsky 2005.

Early in development, embryos undergo the process of neurulation, in which the neuroepithelial cells that constitute the neural plate invaginate to initially form the neural groove, and subsequently the neural tube, following fusion of the bilateral neural folds (Figure 1.3). The neural tube is the primordium of the central nervous system, and as such, will go on to form the brain and spinal cord. The neural crest is a group of neuroectodermal cells that detach from the crests of the neural folds during neural tube formation. They transiently exist as a multipotent subpopulation of cells that, according to the signals they

encounter from the neural tube, migrate in two waves through the embryo: the first "wave" of NCCs travel along a ventromedial route, and the second follow the dorsolateral pathway (Erickson & Goins 1995). The formerly multipotent neural crest cells' gene expression changes as they advance through the mesoderm and their fate is progressively restricted, until they eventually undergo terminal differentiation and become the cellular components of structures including the melanocytes of the skin, the dorsal root ganglia, sensory nerves, the sympathetic, parasympathetic and enteric nervous systems, the meninges (pia and arachnoid maters), the great vessels of the heart, and many of the muscular and skeletal structures of the head (Moore & Persaud 2003). Temporo-spatial factors are extremely influential in the determining the fate of these multipotent cells. Their destiny depends on their location along the rostro-caudal axis of the embryo – for example, the craniofacial cartilage comes only from cranial neural crest cells, and only the trunk neural crest cells give rise to the autonomic nervous system (Le Douarin 1982). In addition, their timepoints of migration also determine their fate – in the trunk, the earliest migrating neural crest cells travel more ventrally to form structures such as the sympathetic ganglia, adrenal medulla and DRGs, whereas those that migrate in the "second wave", 24 hours later than the first, form the melanocytes (Erickson, Duong & Tosney 1992; Weston & Butler 1966). Migration and hence cell fate seems to be a result of factors in the cells' local environments rather something that is intrinsically pre-programmed into the cells. This can be demonstrated by experiments in which vagal crest cells that would not normally go on to form sympathetic neurons, do so when transplanted into the embryonic trunk region (Le Douarin 1982), and another in which neural crest cells from slightly older embryos (destined to migrate more dorsally) were transplanted into younger embryos, where they migrated both ventrally and dorsally (Weston & Butler 1966). An additional experiment of interest found that the first wave of migrating neural crest cells tended to "fill" the ventral neural crest target locations, so that the later-migrating cells were unable to do so – if early neural crest migration was halted shortly after delamination, the later-migrating cells would then target both ventral and dorsal locations (Baker et al. 1997). The overriding theme of the above investigations is that neural crest cells show a great deal of plasticity, in that they behave according to the environment they find themselves in.

Since neuroblastoma is a malignancy of childhood, and not often an inherited condition, one can conclude that it arises from a defect within normal embryonic development and/or neonatal growth. If we look at the multitude of genes involved in the development of the sympathetic nervous system, and assess which of these may be implicated in the pathogenesis of neuroblastoma, we can further our understanding of the disease and identify potential therapeutic targets.

1.3.1. Genes involved in neural crest specification and delamination

Prior to neurulation, cells of the ectoderm are susceptible to becoming either epidermal or neural. High levels of bone morphogenetic proteins (BMPs) specify an epidermal fate, whereas inhibition of BMP signalling (by molecules such as noggin, chordin and follistatin) induces a neural phenotype, via initiation of expression of Sox2, Zicr-1 and Zic3 transcription factors, which in turn induce expression of N-CAM and N-tubulin (Mizuseki et al. 1998; Wilson & Hemmatibrivanlou 1995). Intermediate levels of BMPs likely result in an "initial, weak specification of neural crest cell fate" with "additional signals from the adjacent non-neural ectoderm, the underlying mesoderm, or both required to enhance and maintain this induction" (LaBonne & Bronner-Fraser 1998b). The expression of neural plate border specifier genes Zic1/3, Msx1/2 and Pax3/7, precede the activation of the downstream neural crest specifier genes: Snail (also termed Snail1), Slug (aka Snail2), AP-2, FoxD3, Sox9, Sox10 and c-Myc, that are transcribed in response to Wnt, FGF and Notch signalling (Aoki et al. 2003; Bellmeyer et al. 2003; LaBonne & Bronner-Fraser 1998b) (Figure 1.4). All neural crest specifier genes are expressed in both pre-migratory and migrating neural crest cells, and display extensive crossregulation/interdependence (Meulemans & Bronner-Fraser 2004).

Figure 1.4. Representation of factors and processes involved in preparing neural crest cells for delamination, and subsequent migration. Arrow represents increasing time. Taken from Morales, Barbas & Nieto 2005.

1.3.2. Neural crest delamination and migration

Overexpression experiments have shown that LSox5, Slug, AP-2 and FoxD3 are heavily involved in the delamination of neural crest cells (Meulemans & Bronner-Fraser 2004). In order to delaminate from the neural folds/neural tube, the neural crest cells must undergo changes both in their morphology and migratory potential (for example, via downregulation of N-cadherin) and accomplish an epithelial to mesenchymal transition (EMT) (Duband

2000). Sox9's key function is thought to be in neural crest specification and cell survival, as well as interacting with Slug in inducing EMT, whereas FoxD3 has been shown to regulate changes in cell adhesion molecules in order to allow delamination to occur (Cheung et al. 2005). N-cadherin and cadherin-6B are lost from NCCs, to be replaced by cadherin-7 which is permissive of cell migration (Akitaya & Bronnerfraser 1992; Nakagawa & Takeichi 1995). The transcription factor Id3 is thought to help segregate the neural crest cells, at the same time stabilising this population, ready to undergo EMT (Kee & Bronner-Fraser 2005). This transition "involves a profound reorganisation of the cytoskeleton that may be incompatible with a high rate of cell division" (Meulemans & Bronner-Fraser 2004), and hence Snail expression prevents the cells from progressing from G1 to S phase. During this cell cycle arrest, alterations in expression of proteins such as cadherins and Rho GTPases (which are targets of the neural crest specifiers) alter neural crest cell shape and adhesion, facilitating the process of delamination (Fukata & Kaibuchi 2001). Cell-cell adhesions must be broken, and interactions between NCCs and the extracellular matrix increased (Delannet & Duband 1992). BMP signalling (BMP2 in the cranial neural crest and BMP4 in the trunk) is thought to be the key trigger for delamination, and its onset is controlled by a gradient of Noggin along the antero-posterior axis of the trunk (Sela-Donenfeld & Kalcheim 1999). BMP4 permits the G1/S transition to occur in a synchronous manner, which is essential for delamination, and this occurs through Wnt1 signalling, which upregulates cyclin D1 (Burstyn-Cohen et al. 2004). Delamination occurs at the same stage as somite development, i.e. occurs next to the epithelial somites. The earliest migrating NCCs travel between the somite and neural tube, following the path of the intersomitic blood vessels, but after somitic dissociation into dermomyotome and sclerotome, NCCs are repelled from the intersomitic spaces by semaphorins, and attracted into the somites by CXCR4/CXCL12 signalling (Kulesa & Gammill 2010). They migrate along two major pathways: what will become the melanocytes migrate dorsolaterally on top of the dermomyotome, 24 hours later than the prospective sympathetic and enteric nervous systems, DRGs and glia, which migrate ventrally through the rostral sclerotome (Thiery, Duband & Delouvee 1982). Ephrins prevent the first wave of NCCs expressing Eph receptors from entering the dermomyotome and following the dorsolateral pathway, but later promote migration of the primitive melanocytes along this route by enhancing their adhesion to fibronectin (Meulemans & Bronner-Fraser 2004; Santiago & Erickson 2002). In addition, ephrins help guide migration of NCCs on the ventromedial pathway through the somites in a segmental manner, by producing both migration-promoting and -inhibitory effects, depending on the class of ephrins encountered (Krull et al. 1997; McLennan & Krull 2002). In addition to ephrins, semaphorins prevent the Neuropilin-expressing NCCs from entering the posterior half of the somites (Gammill et al. 2006), and also restrict migration of the prospective DRG cells to a more dorsal position than

those NCCs destined for the sympathoadrenal lineage (Roffers-Agarwal & Gammill 2009). Prospective SA cells are drawn out of the somites by CXCR4/CXCL12 and ErbB2/Neuregulin signalling, and Neuropilin/Semaphorin repulsion from the surrounding tissues results in aggregation at the dorsal aorta (Kulesa & Gammill 2010). This aggregation is not segmental as may be expected; rather the NCCs disperse along the entire length of the dorsal aorta. The repulsive effects of ephrinB in the mesoderm, in addition to CXCL12 attraction and N-cadherin-mediated adhesion, results in cell condensation, thus the formation of segmental ganglia (Kasemeier-Kulesa et al. 2006).

In post-migratory neural crest cells, i.e. once cells have reached their respective targets and begun to differentiate, expression of the neural crest specifier genes Id, AP-2, Slug, Snail and FoxD3 is switched off. As a consequence, the cells' migratory ability and multipotency is lost. However, Sox9, Sox10 and LSox5, initially involved as neural crest specifiers, continue to be expressed and play a part in cell differentiation – Sox9 in the formation of cartilage, Sox10 in the differentiation of enteric neurons, melanocytes and glia, and LSox5 also in glial differentiation (Meulemans & Bronner-Fraser 2004).

There are a multitude of genes implicated in all of the processes involved in neural crest development, and rather than a linear hierarchy of events, they all interact in a complex network to illicit sometimes multiple, often different, but nevertheless coordinated functions.

1.3.3. Migration and early differentiation of trunk neural crest cells, destined to become structures of the sympathetic nervous system

The sympathetic ganglia and adrenal chromaffin cells arise from the neural crest cells caudal to somite 5. Although their catecholaminergic phenotype, as indicated by tyrosine hydroxylase (TH) expression, is not apparent until they reach the vicinity of the dorsal aorta (around embryonic day 2.5 in the chick), the signals they encounter during their ventral migration, from the somites, ventral neural tube and notochord, are important for this adrenergic induction (Reissmann et al. 1996). The significance of the ventral neural tube and notochord, raises the possibility that sonic hedgehog (Shh) may be involved. However, it is only next to the dorsal aorta that cells begin to differentiate, and Reissmann et al. (1996) concluded that BMP-4 and BMP-7 from this structure were the most critical proteins for adrenergic differentiation. Therefore it can be said that the neural crest cells aggregate at the dorsal aorta to form the primary sympathetic ganglia, and in response to the BMPs expressed by the dorsal aorta, the cells begin to undergo neuronal and catecholaminergic

differentiation (Huber 2006). However, BMP signalling is also essential for differentiation of other neural crest derivatives, such as parasympathetic neurons, therefore other factors may be additionally required for specification of the sympathoadrenal lineage. One such factor, the EGF-like growth factor neuregulin-1, in conjunction with its tyrosine kinase receptor ErbB3 (which is expressed on the surface of migrating neural crest cells), is extremely important in migration of the neural crest cells to the mesenchyme lateral to the dorsal aorta (Britsch et al. 1998). Mutations in the genes of either of these proteins result in a lack of neural crest cells finding their way to the primary sympathetic ganglia, hence hypoplasia of the resultant sympathetic chain and absence of the adrenal medulla (Britsch et al. 1998).

Figure 1.5. A) depicts the migration of trunk neural crest cells from their origin dorsal to the neural tube (nt), past the notochord (no), to aggregate next to the dorsal aorta (da), where they form the primary sympathetic ganglia (sgp). Following BMP signalling, the cells the separate into the nascent sympathetic ganglia (sg) and adrenal gland (ag). B) Shows the genes involved in the progression from a neural crest cell into a sympathoadrenal (SA) cell. Taken from Huber 2006.

1.3.4. Differentiation of neural crest sympathetic precursors

Neuroblastoma may arise from impaired sympathoadrenal differentiation that results in a pool of rapidly proliferating cells susceptible to mutations and malignant transformation. Therefore an understanding of the key factors involved in normal sympathetic development may help determine causes of neuroblastoma pathogenesis.

1.3.4.1. MASH-1

Achaete-Scute homolog-1 (MASH-1 in rodents, hASH-1 in humans, and CASH-1 in chicks, but termed ‘MASH-1’ here for simplicity) is the first marker specifying a neural fate expressed upon the neural crest cells’ arrival at the dorsal aorta (HH stage 15 in the chick). It is a basic helix-loop-helix transcription factor that is essential for the proper development of

the autonomic nervous system and is transiently expressed in response to BMP2 signalling (LaBonne & Bronner-Fraser 1998a). However, high hASH-1 levels are seen in neuroblastoma tumours and cell lines (Soderholm et al. 1999). Phox2b, whose expression is also induced by BMPs, is critical for the maintenance of MASH-1 (Pattyn et al. 1999). MASH-1 activates Phox2a, and is necessary for gene expression of tyrosine hydroxylase (TH) and dopamine-β-hydroxylase (DBH), enzymes involved in the biosynthesis of noradrenaline (Hirsch et al. 1998). MASH-1 may also be required for the expression of neuronal proteins such as SCG10 and peripherin, but not for early SA proteins, as MASH-1 inactivation had no effect on the expression of Phox2b, Hand2, c-Ret and neurofilament (Sommer et al. 1995). It has been concluded that MASH-1 promotes further development of early precursors that are already committed to a neuronal fate, allowing the transition into a mature sympathetic neuron or chromaffin cell (Huber 2006).

1.3.4.2. Phox2b

Phox2b is a homeodomain protein expressed in all noradrenergic neurons, both in the central and peripheral nervous systems. Phox2b expression occurs as soon as the migrating neural crest cells aggregate on either side of the dorsal aorta, driving the NCCs along the pathway of sympathoadrenal differentiation. All autonomic ganglia fail to form properly and then degenerate in mice lacking Phox2b (Pattyn et al. 1999). It is therefore absolutely fundamental to the development of the autonomic nervous system, even more so than MASH-1, as in the absence of Phox2b the only autonomic marker expressed by the neural crest cells aggregated at the dorsal aorta is MASH-1 – Hand2, c-Ret and the neuronal protein neurofilament, which were not affected by a loss of MASH-1, are absent in this scenario. Even MASH-1 is downregulated prematurely, indicating its dependence on Phox2b for maintenance (Huber 2006). As well as being necessary for the maintenance of MASH-1, it is required for the expression of Ret, the receptor subunit for the glial-derived neurotrophic factor (GDNF), which is normally expressed in early aggregating sympathoblasts (Pattyn et al. 1999). Phox2b also induces expression of both TH and DBH, the two enzymes needed for the synthesis of noradrenaline, to the extent that they are absent in the sympathetic and enteric progenitors and in the adrenal medulla of mice lacking Phox2b (Pattyn et al. 1999). The Phox2b gene has been reported to be mutated in a small proportion of familial neuroblastomas, and mutated Phox2b is now known to predispose an individual to developing neuroblastoma (Raabe et al. 2008; Trochet et al. 2004). Mutated Phox2b can lead to increased proliferation and dedifferentiation of sympathoadrenal cells (Reiff et al. 2010), both of which would contribute to malignant transformation. Phox2b mutations have

also been detected rarely in sporadic cases of neuroblastoma (van Limpt et al. 2004), but overexpression of both Phox2b and Phox2a is regularly observed in both primary tumours and cell lines (Longo et al. 2008). The Phox2 genes are involved in the Delta-Notch signalling pathway to regulate sympathetic neuroblast differentiation, therefore deregulation of said genes may lead to disruption of the differentiation pathway and eventually tumourigenesis (van Limpt et al. 2005). It has also been reported that MYCN, a potent oncogene for neuroblastoma, promotes proliferation of the Phox2b-expressing population of neuronal precursors during development, preventing their further development and leading to hyperplasia (Alam et al. 2009).

In SA cells, the expression of MASH-1 and Phox2b is followed by Hand2 (dHAND), Phox2a and GATA2/3.

1.3.4.3. Hand2

This basic helix-loop-helix transcription factor's expression proceeds (and is dependent on) Phox2b, yet precedes Phox2a, and in addition, is expressed independently of MASH-1. It is essential for both the proliferation of sympathetic neuron precursors and their noradrenergic differentiation – in Hand2 knockout embryos there is a much reduced number of sympathetic neurons, as well as a strong decrease in TH and DBH expression in those neurons that developed. Schmidt and colleagues reported that in post-mitotic differentiated sympathetic neurons, Hand2 is required for maintenance of the noradrenergic phenotype – this was the conclusion of experiments where knockdown of the gene had no effect on pan-neuronal genes such as SCG10, TUJ-1 and HuC, but dramatically reduced the expression of TH and DBH (Schmidt et al. 2009). Hand2 is routinely detected in neuroblastomas, regardless of stage, suggesting that in these tumours, sympathetic differentiation is blocked at a relatively early stage in development (Gestblom et al. 1999).

1.3.4.4. Phox2a

The Phox2a homeodomain transcription factor is closely related to Phox2b. Like Phox2b, it is expressed throughout the entire developing autonomic nervous system, although Phox2a's expression occurs a little later, and it also is directly involved in the transcription of DBH and TH (Longo et al. 2008). However, Phox2a is much more dispensable for SA

differentiation: inactivation of this gene has no effect on the majority of autonomic structures, only on the parasympathetic ganglia of the head (Morin et al. 1997). MASH-1 and Phox2b, which are activated independently of each other in sympathoblasts, are both required for Phox2a expression (Hirsch et al. 1998; Pattyn et al. 1999). Like Phox2b, Phox2a is highly expressed in neuroblastomas (Longo et al. 2008).

1.3.4.5. GATA2/3

These zinc finger transcription factors are expressed after MASH-1, Phox2b, Hand2 and Phox2a, but before the expression of the noradrenergic enzymes TH and DBH (Tsarovina et al. 2004). They are required for the manifestation of noradrenergic traits: in the absence of embryonic GATA3, sympathetic ganglia lack TH and DBH (Lim et al. 2000); therefore a function in sympathetic differentiation is implied. Chromaffin cells from GATA3-null embryos also showed reduced levels of MASH-1, Hand2 and Phox2b, implying that feedback from GATA3 is required to maintain expression of supposed upstream transcription factors (Moriguchi et al. 2006). In neuroblastomas, GATA3 has been shown to induce expression of cyclin D1, a promoter of cell cycle progression (Molenaar et al. 2010).

Although the five transcription factors detailed above are expressed in a somewhat sequential manner (MASH-1 before Phox2a and Hand2; Phox2b before Phox2a, Hand2 and Gata3), rather than functioning in a linear cascade, they form a cross-linking regulatory network, with the end result being sympathoadrenal cell formation. From their location in the primary sympathetic ganglia, the presumptive chromaffin cells then migrate to the adrenal gland anlagen, and the cells destined to become sympathetic neurons travel dorsally to the position of the secondary sympathetic ganglia “proper” (Le Douarin 1982) (Figure 1.5 A). Once in their final position, their gene expression will change accordingly as the cells differentiate further (Figure 1.6).

Figure 1.6. Diagram to illustrate the fundamental differences in protein markers between chromaffin cells and sympathetic neurons, both of which originate from sympathoadrenal precursor cells. Adapted from Huber (2006).

1.3.4.6. Differentiated sympathoadrenal cell characteristics

Sympathetic neurons and chromaffin cells are similar in their ability to synthesize, store, release, and take up catecholamines such as tyrosine hydroxylase and dopamine β-hydroxylase, both of which are involved in the production of noradrenaline (Figure 1.7). However, the two cell types are distinct in their morphologies, with sympathetic neurons extending axons and dendrites, and expressing neuronal markers, whereas chromaffin cells' early neuronal commitment is repressed, potentially by glucocorticoids (Schober, Krieglstein & Unsicker 2000). Chromaffin cells are named as such because of the large chromaffin granules they contain (Figure 1.6). In addition, a large proportion of chromaffin cells produce adrenaline (Huber, Kalcheim & Unsicker 2009).

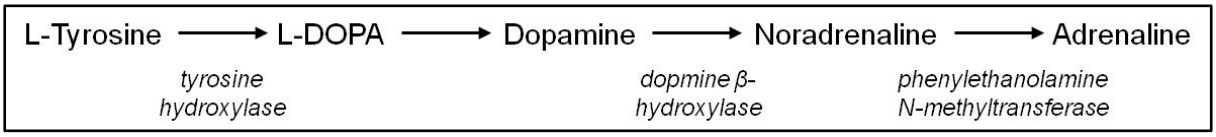

Figure 1.7. The adrenaline/noradrenaline synthesis pathway. Enzymes that catalyse each step are in italics.

1.3.4.7. The Trk neurotrophin receptors

The neurotrophin family of growth factors are heavily involved in the formation of a neuronal phenotype, and their effects are brought about via binding to their respective receptor tyrosine kinases. TrkA is the high affinity receptor for NGF, TrkB for BDNF and neurotrophin-4/5 (NT-4/5), and TrkC for neurotrophin-3 (NT-3). P75 is a low affinity receptor, capable of binding all neurotrophin ligands (Barbacid 1994). In normal sympathetic neuron

development, TrkA/NGF supports the survival and differentiation of sympathetic neurons (Nakagawara 2005). TrkC/NT-3 is also thought to promote the survival of sympathetic neuroblasts, although it is not quite as critical as TrkA (Fagan et al. 1996). TrkB/BDNF is not known to be required for sympathetic neuron differentiation (Pahlman & Hoehner 1996).

In normal development, TrkC is the first neurotrophin receptor to be expressed, in migratory neural crest cells following detection of insulin-like growth factors (IGFs) and bFGF (Pahlman & Hoehner 1996). Stimulation with NT-3 induces expression of TrkA and p75 after cell aggregation at the dorsal aorta (Pahlman & Hoehner 1996). Therefore although required for sympathetic neuron development, NGF does not initiate differentiation of sympathetic neurons, but enhances an already-initiated process (Hall & Ekanayake 1991). Within the primary sympathetic ganglia, two subpopulations of cells can be seen: early differentiating neurons that express TrkA along with TrkC, and sympathoblasts that will differentiate later that express TrkC and TrkB (Straub, Sholler & Nishi 2007). A further increase in TrkA expression is then seen to coincide with a reduction in TrkC (Fagan et al. 1996), and in addition, during normal development, all TrkB-expressing cells eventually differentiate into neurons. It appears that all SA precursors have the ability to differentiate into sympathetic neurons, but maybe those that settle near to the dorsal aorta experience a microenvironment rich in NGF, facilitative of neuronal differentiation, but those that migrate to the site of the prospective adrenal gland encounter an environment rich in glucocorticoids but lacking in NGF, therefore go on to adopt a chromaffin cell endocrine phenotype (Hall & Ekanayake 1991).

In culture, addition of BDNF to TrkB-positive sympathoblasts strongly promotes cell proliferation, although this is not the case in vivo where only 10-20% of $TrkB^+$ cells incorporate BrdU, perhaps because endogenous BDNF does not reach the threshold required for massive proliferation (Straub, Sholler & Nishi 2007). Nevertheless, their results suggest a role in development for TrkB in expanding/maintaining the sympathoblast population, and that if TrkB downregulation is impaired during development, this may be a trigger for the development of neuroblastoma.

High levels of TrkA are found in many neuroblastoma tumours with a good prognosis (Kogner et al. 1993), often those destined to undergo spontaneous regression – in cells with a single MYCN copy, the presence of NGF induces cells to mature into neurons, and in its absence, undergo apoptosis (Nakagawara 1998). This may suggest that regressive neuroblastomas originate from early sympathetic neurons that expressed TrkA (Straub, Sholler & Nishi 2007). Conversely, TrkA is downregulated in aggressive tumours, often

associated with MYCN amplification. TrkB, a marker of poor prognosis, is usually expressed along with its preferred ligands in MYCN amplified tumours, giving cells an added growth advantage (Nakagawara 2005).

1.4. The MYCN oncogene

In 1983, Schwab and colleagues published a paper detailing the discovery of multiple copies of the MYCN oncogene in various neuroblastoma cell lines and one primary tumour (Schwab et al. 1983). Since then, clinical analyses have identified amplification of the MYCN gene in around 25-30% of newly diagnosed patients' tumours, which invariably results in high levels of the protein being expressed, and this has been shown to be associated with an aggressive phenotype and poor prognosis (Cohn & Tweddle 2004). The MYCN gene is found on chromosome 2p24, and this is where it remains as a single copy, even in MYCN-amplified cells. The amplified copies of DNA are situated at an alternate locus – either as a homogeneously stained region (HSR) on a different chromosome (this varies from tumour to tumour), or as extra-chromosomal double minutes (DMs) (Corvi et al. 1994).

The MYCN basic helix-loop-helix/leucine zipper (bHLH/Zip) protein is 60-63kD transcription factor, located in the nucleus, with a short half life of roughly 30 minutes (Ikegaki, Bukovsky & Kennett 1986). It was first identified owing to its similarity to c-Myc and amplification in neuroblastomas (Schwab et al. 1983). Incidentally, MYCN expression is associated with low levels of c-Myc. The normal expression of MYCN and c-Myc differs somewhat in terms of location – c-Myc is expressed in a variety of tissues at all stages of the cell cycle in dividing cells, whereas MYCN is restricted to the CNS, PNS, kidney, spleen and lungs during embryonic development (Thomas et al. 2004b; Zimmerman et al. 1986).

1.4.1. MYCN in normal development

In the embryo, MYCN is critical for neural crest-derived neuronal development. MYCN-deficient mice show a massive reduction in the number of mature neurons present in the sympathetic and dorsal root ganglia (Sawai et al. 1993). During normal development, MYCN is initially expressed rather uniformly in nuclei of the entire neural crest cell population, but following ganglion colonisation, its expression is turned off in those cells destined to fulfil a glial fate, but retained in the cells undergoing neuronal differentiation (Wakamatsu et al. 1997). MYCN expression is then turned off in PNS neurons by E14 in the chick. It is thought

that MYCN is required for the proliferation and expansion of the population of neuronal progenitors, but in neural progenitor cell sphere culture, removal of growth factors EGF and bFGF resulted in MYCN degradation, allowing cell cycle exit and differentiation (Knoepfler, Cheng & Eisenman 2002). High levels of endogenous MYCN can induce early ventral neural crest cell migration in vivo, as well as actively promoting neuronal differentiation (Wakamatsu et al. 1997). Since some early-migrating neural crest cells located to the spinal nerve cord and formed Schwann cells rather than neurons, they concluded that although it is likely that high MYCN expression drives neuronal differentiation, the final cell phenotype is "determined within the allowance of the microenvironment". Within the sympathetic ganglia, BMPs from the dorsal aorta induce expression of MASH-1, and since MASH-1 null mutant mice fail to express any SA markers, it is entirely possible that sympathetic neuron differentiation is initiated by the cooperative action of MYCN and MASH-1.

MYCN is a part of the Myc/Max/Mad/Mnt network of proteins that together regulate cell proliferation, differentiation and apoptosis (Grandori et al. 2000; Henriksson & Luscher 1996). MYCN can act as a transcriptional enhancer by forming a heterodimer with Max, which binds to E-box sequences (CACGTG) in the promoter regions of target genes. There, the MYCN:Max complex executes its function via recruitment of histone acetyltransferase enzymes (Bouchard et al. 2001; McMahon, Wood & Cole 2000). This acetylation modifies chromatin in gene promoter regions and enhances transcription. Mad also dimerises with Max, reducing the amount of Max available for MYCN binding, as well as competing with the MYCN:Max complexes for the same promoter E-boxes (Nikiforov et al. 2003). Mad is an antagonist of MYCN and a negative regulator of cell growth, usually present in differentiated cells (Chin et al. 1995; Larsson et al. 1994). The Mad:Max heterodimers recruit histone deacetylases (HDACs) through the adaptor protein Sin3, resulting in transcriptional repression of many MYCN target genes such as TERT and Id2 (McMahon, Wood & Cole 2000). Mnt is another MYCN transcriptional antagonist, expressed in differentiated, but also proliferating cells, where it heterodimerises with Max and represses MYCN target gene transcription (Hurlin, Queva & Eisenman 1997). In addition, MYCN:Miz1 heterodimers can also inhibit transcription (Eilers & Eisenman 2008). Mad and Mnt's transcriptional repression of MYCN target genes is primarily due to chromatin remodelling (Alland et al. 1997; Wolffe 1997). The relative levels of Myc versus Mad may well determine whether a cell undergoes cell cycle progression to remain in a proliferative state or begins to differentiate (Ayer & Eisenman 1993). However in differentiating SK-N-BE(2) neuroblastoma cells, although MYCN is significantly downregulated (and therefore MYCN:Max DNA binging is reduced), expression of Mad and Mnt, and indeed their DNA binding is hardly affected (Smith et al. 2004). When Mad or Mnt was overexpressed, cells were still able to differentiate following

administration of retinoic acid. This work supports the theory that downregulation of MYCN, rather than alterations in Mad or Mnt expression, is critical to allow differentiation of neuroblastoma cells.

1.4.2. MYCN in oncogenesis

Myc family members (c-Myc, MYCN, L-Myc) play fundamental roles in the control of normal (and oncogenic) cell proliferation, growth, metabolism, differentiation and apoptosis. Myc is also one of the four genes, along with Sox2, Oct4 and Klf4, required to induce “stemness” in fibroblastic cells (induced pluripotency stem cells) (Takahashi & Yamanaka 2006). Deregulation/overexpression of MYCN (e.g. by amplification) could therefore enhance tumourigenesis by creating a population of rapidly dividing, self-renewing cells that would be increasingly vulnerable to further oncogenic mutations. Indeed amplification of the MYCN gene has been demonstrated in a number of cancers, including glioblastoma, medulloblastoma, retinoblastoma, rhabdomyosarcoma, and small cell lung carcinoma (Vita & Henriksson 2006), but for the purpose of this project, we will focus on its occurrence in neuroblastomas.

Consistent with its occurrence in pools of undifferentiated, proliferating cells, high MYCN levels are found in aggressive neuroblastomas. The highest MYCN expression is found in MYCN-amplified tumours. The highest expression of MYCN target genes occurs in both MYCN-amplified and stage 4 MYCN-non-amplified tumours, although not in those classified as stage 4S (a special stage which undergoes spontaneous regression) – even though 4S have the highest levels of MYCN in all non-amplified tumours (Westermann et al. 2008). It was therefore proposed “only partial activation of MYCN target genes occurs in 4S disease”.

MYCN is known to have a causal role in neuroblastoma tumourigenesis, as demonstrated by the transgenic TH-MYCN mouse model (Weiss et al. 1997). Overexpression of MYCN was targeted to sympathoadrenal cell precursors by placing the gene downstream of the TH promoter, and consequently several months after birth, these mice developed neuroblastoma tumours, which were similar in location, histology and chromosomal gains and losses to their human counterparts. MYCN overexpression is associated with an aggressive phenotype, with decreased growth factor dependence and contact inhibition, as well as a raised metastatic potential (Lutz et al. 1996; Schweigerer et al. 1990).

Paradoxically, MYCN also triggers barriers to tumourigenesis, such as sensitising cells to apoptosis, and initiating DNA damage responses and cell senescence (Larsson & Henriksson 2010). Therefore, for MYCN-driven tumourigenesis to occur, mutations that disrupt said tumour repressor functions will be strongly selected for.

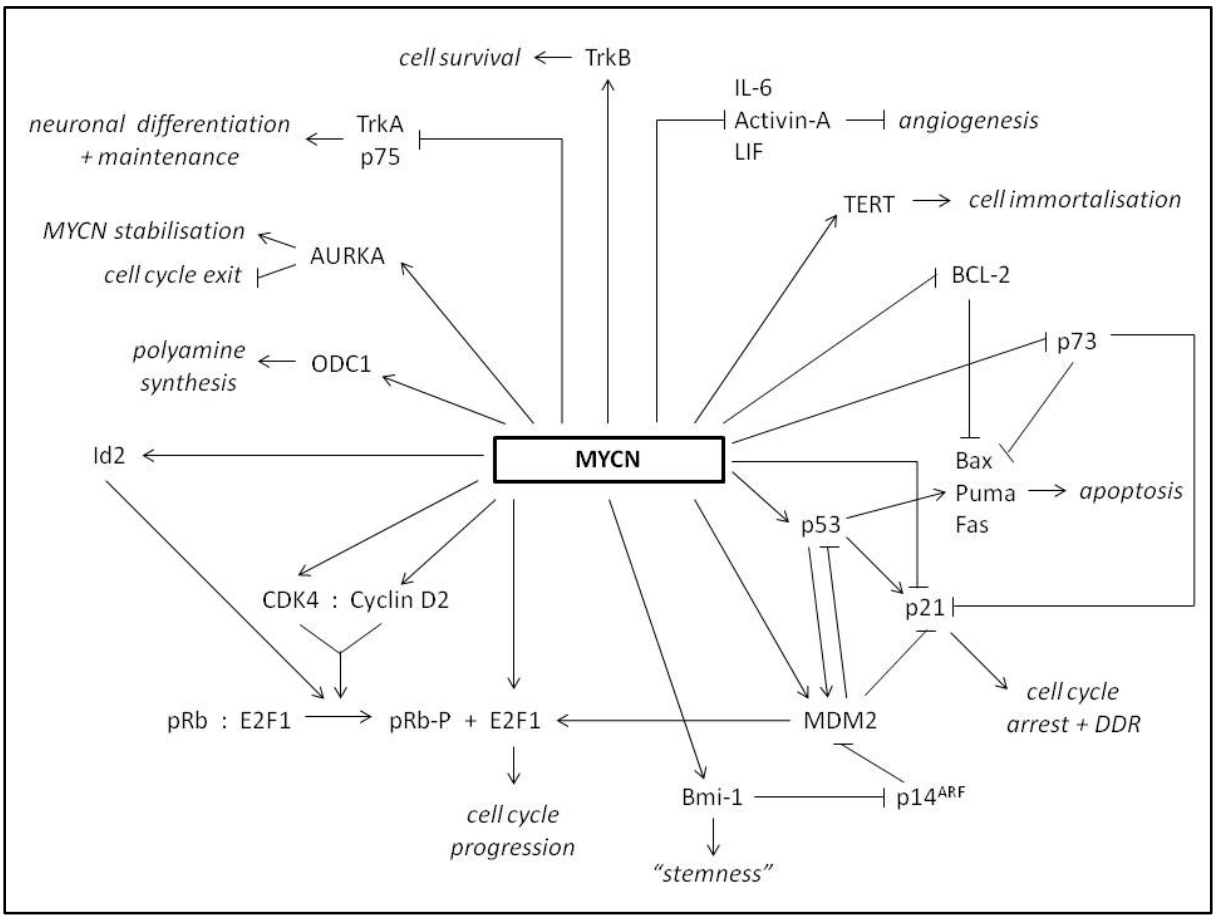

Figure 1.8. Overview of the major genes targeted by MYCN, by means of transcriptional promotion or repression, and their normal functions.

1.4.3. MYCN targets involved in cell cycle control

1.4.3.1. CDK4/Cyclin D2/E2F1

Cyclin-dependent kinase 4 (CDK4) is a direct transcriptional target of MYCN (Westermann et al. 2008). It facilitates the transition from G1 to S phase of the cell cycle, within its complex with cyclin D2 (also a MYCN target), by phosphorylating pRb, thereby dismantling the pRb:E2F1 complex and allowing E2F1 to activate transcription of genes involved in cell cycle

progression (Figure 1.8) (Alberts et al. 2010). One such gene is SKP2, which primarily targets negative regulators of the cell cycle for degradation, for example p27 and p21 (Muth et al. 2010). High SKP2 and E2F1 (which also activates MYCN expression (Strieder & Lutz 2003)), and low p27 have all been associated with MYCN amplification in neuroblastomas (Bell et al. 2010), as well as tumour dedifferentiation and aggressiveness in various other cancers (Muth et al. 2010).

1.4.3.2. Id2

Id2 expression may be induced by MYCN in neuroblastomas. Id2 is an inhibitor of the tumour suppressor pRb, therefore promotes cell proliferation by interacting with this protein and allowing E2F1 to be released and initiate transcription of S-phase proteins (Bell et al. 2010). Id2 also prevents differentiation by forming heterodimers with other bHLH proteins such as MASH-1 and HES1, and inhibiting their transcriptional function (Massari & Murre 2000). In primary neuroblastomas, Id2 has been shown to be strongly correlated with a poor outcome, and maintains the malignant proliferative behaviour of tumour cells (Lasorella et al. 2002).

1.4.3.3. MDM2

MDM2 is known as a proto-oncogene, due to its role in inactivation of the constitutively-expressed tumour suppressor p53 by sequestration/degradation – hence inhibiting its apoptotic activity. However, it also functions independently of p53 to regulate genes involved in the cell cycle (reduces levels of p21 and pRb, and prevents ubiquitination and degradation of E2F) and differentiation (prevents expression of MyoD) (Fiddler et al. 1996; Ganguli & Wasylyk 2003). MYCN has been shown to bind to an E-box within the MDM2 promoter and directly induce its expression, and conversely, MYCN inhibition reduces MDM2 levels, stabilises p53 and leads to apoptosis (Slack et al. 2005). MDM2 has also been implicated in MYCN mRNA stabilisation and hence increased protein translation (Gu et al. 2012). Hence there are multiple ways in which MDM2 contributes to neuroblastoma progression.

1.4.3.4. ODC

Ornithine decarboxylase (ODC) is the rate-limiting enzyme in the pathway for polyamine synthesis. It is a direct transcriptional target of MYCN (Lutz et al. 1996), and in addition, with its gene being located on chromosome 2p24-25, is amplified with MYCN in around a fifth of MYCN-amplified neuroblastomas (Hogarty et al. 2008). This leads to an increased availability of polyamines, critical for cell survival, stabilisation of the DNA structure and promotion of cell division.

1.4.4. MYCN targets involved in apoptosis

MYCN activates both proliferative and apoptotic pathways, therefore for MYCN-expressing neuroblastoma precursors to progress to a full-blown malignancy, the balance must be tipped in favour of cell proliferation.

1.4.4.1. p53

The tumour suppressor gene p53 is very rarely mutated in neuroblastomas (in less than 2% of tumours at diagnosis), and the p53 pathways are typically functionally active (Hosoi et al. 1994), thus for malignant progression, inhibition of p53-mediated apoptosis is essential. p53 is a direct transcriptional target of MYCN in neuroblastoma and is associated with high expression/amplification of the MYCN gene (Chen et al. 2010). It promotes a G1 phase cell cycle arrest upon DNA damage, by upregulating the CDK inhibitor p21, and allows the relevant DNA repair mechanisms to occur. However, MYCN amplification has been shown to correlate with failure to arrest in the G1 phase of the cell cycle following DNA damage (Bell et al. 2006). If growth arrest is not possible, p53 sensitises the cell to apoptosis by inducing genes such as Bax, Puma and Fas (Tweddle et al. 2003) (Figure 1.9). However, MYCN directly represses expression of p21, via its complex with Miz-1, and also promotes transcription of MDM2, hence overriding p53-induced cell cycle arrest. Therefore, in a highly MYCN-expressing neuroblastoma precursor, increased levels of MDM2 may provide that counterbalance to apoptosis needed for mass proliferation of a developing tumour.

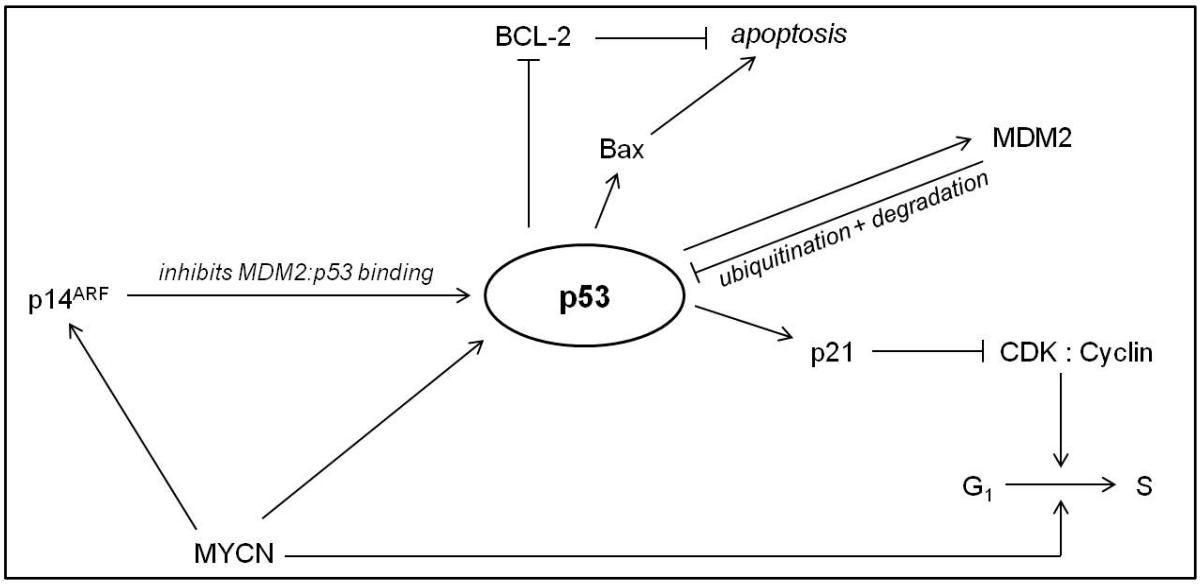

Figure 1.9. Basic illustration identifying major p53 interactions.

1.4.4.2. p73

p73 is a member of the p53 family of tumour suppressor proteins, which are involved in growth arrest and/or apoptosis in neuronal cells (Pozniak et al. 2000). p73 is not a MYCN target gene, rather it is a regulator of MYCN – p73 directly activates transcription of the MYCN gene, but can also post-transcriptionally inhibit the stability of MYCN mRNA (Horvilleur et al. 2008). p73 has been mapped to chromosome 1p36, a region often associated with loss of heterozygosity in neuroblastomas, but when present, it is thought that the protein, along with p53, is involved in apoptosis of TrkA-expressing neurons upon NGF withdrawal (Nakagawara 2005).

1.4.4.3. BCL-2

MYCN also represses anti-apoptotic proteins such as BCL-2, which allows Bax to act and eventually trigger a caspase cascade that will kill the cell (Bell et al. 2010).

1.4.4.4. ALK

Anaplastic lymphoma receptor tyrosine kinase (ALK), of the insulin receptor superfamily, is a protein which plays a role in the developing CNS and PNS (including synaptogenesis of the

sympathetic ganglia), but in adults its presence is restricted to within only a few cells in the CNS (Iwahara et al. 1997). In the presence of its ligands (e.g. pleiotrophin), ALK has an anti-apoptotic role, and is involved in processes such as differentiation and axon guidance. However, with no ligand binding the ALK receptor is cleaved by caspases, exposing its pro-apoptotic domain (Mourali et al. 2006). It has been implicated in the development of human cancers such as anaplastic large-cell lymphoma, non-small-cell lung cancer and neuroblastoma. Germline mutations in ALK have been discovered in the majority of familial neuroblastoma cases, and point mutations have been found in 7-10% of somatic tumours. Constitutive ALK signalling is thought to contribute to oncogenic transformation via control of cell cycle progression, survival, cell shaping and cell migration (Carpenter & Mosse 2012). The ALK gene is located on chromosome 2p23, and although this is only amplified in around 2% of neuroblastomas, unsurprisingly, this almost always occurs alongside MYCN amplification (whose gene is located at 2p24) (Azarova, Gautam & George 2011). No associations between these activating ALK mutations alone and disease stage or survival have yet been established. However one of the most potent ALK mutations, F1174 (which appears mostly in tumours with amplification of MYCN), when coupled with MYCN amplification, is associated with a poor prognosis in humans, a fact that is supported by recent animal models. When mice overexpressing the F1174 mutation were crossed with the MYCN transgenic mice, their progeny developed aggressive neuroblastomas with increased penetrance, an early onset, and decreased overall survival (Berry et al. 2012). Likewise, coexpression of these two aberrations in zebrafish increased the frequency of tumours and accelerated tumour onset, compared to MYCN alone (Zhu et al. 2012). It should be noted that animals carrying the ALK mutation alone, without increased MYCN expression did not form tumours, suggesting that ALK accelerates MYCN-driven tumourigenesis. It is thought that ALK regulates the stability of the MYCN protein, as ALK:MYCN tumours display an increased intensity of MYCN staining, and in the Kelly cell line, which overexpresses both ALK and MYCN, ALK knockdown results in decreased MYCN protein levels and the half-life of the MYCN protein being reduced (Berry et al. 2012). These authors also discovered that although proliferation levels in ALK:MYCN versus MYCN tumours were similar, apoptosis was massively reduced in the mouse tumours with elevated ALK^{F1174} and MYCN coexpression – a feature that was confirmed in human neuroblastomas. They propose that this reduction in apoptosis is mediated by increased expression of BCL-2, and lowered expression of pro-apoptotic genes such as Bax, and since this is in contrast with MYCN's repression of anti-apoptotic proteins (see section 1.4.4.3), concluded that an evasion of MYCN-induced apoptosis may be ALK's key role in MYCN-driven tumourigenesis.

1.4.4.5. Bmi-1

Bmi-1 is an oncogene belonging to the polycomb group of proteins, which tend to suppress genes by means of chromatin remodelling, i.e. in an epigenetic manner. Bmi-1 knockout mice have suggested a role for the protein in haematopoiesis and development of the central and peripheral nervous systems, as defects in all of these areas are observed in the absence of Bmi-1 (Vanderlugt et al. 1994). A role in self-renewal of neural crest stem cells has also been documented, although it is not required for their survival or differentiation (Molofsky et al. 2003). High levels are routinely found in both primary neuroblastomas and cell lines, and in Weiss' TH-MYCN transgenic mouse model, the tumours formed have high Bmi-1 expression. Bmi-1 inhibits the apoptotic activity of MYCN, as cells of the SHEP cell line forced to overexpress both MYCN and Bmi-1 were highly resistant to a variety of apoptosis-inducing agents, compared to cells with high MYCN expression alone, which were extremely sensitive to apoptotic induction (Cui et al. 2007). These apoptosis-resistant Bmi-1-expressing SHEP cells showed a reduction in p53 protein, which would probably have been repressed indirectly, via MDM2 binding and subsequent degradation – Bmi-1 represses the expression of $p14^{ARF}$, an MDM2 inhibitor, so high levels of Bmi-1 would result in an increase in MDM2 protein. Other groups have shown that Bmi-1 downregulates p53 and helps drive tumour progression by reducing levels of apoptosis of damaged cells (Alajez et al. 2009; Chatoo et al. 2009). Bmi-1 directly binds to p53 in a complex and results in increased p53 ubiquitination and degradation (Calao et al. 2012). Since Bmi-1 is also highly expressed in neuroblastomas without MYCN amplification, a more general, yet essential role in tumourigenesis seems likely, possibly in the maintenance/self-renewal of tumour cells, in addition to it helping override MYCN-expressing cells' tendency to undergo apoptosis. And indeed, Bmi-1 knockdown impaired the ability of neuroblastoma cells to form tumours in immunodeficient mice (Cui et al. 2007).

1.4.4.6. Survivin

Survivin (SVV) is an inhibitor of apoptosis, which binds to caspase and inhibits its function (Tamm et al. 1998). It probably has a vital role during development, where there is an ongoing readdressing of the critical balance between proliferation and apoptosis, to allow proper structural formation of the various organs. SVV is highly expressed in most embryonic tissues, as well as in most human cancers, but it is absent in terminally differentiated cells (Adida et al. 1998b; Pina-Oviedo et al. 2007). This in theory could make SVV an exciting therapeutic target, in the hope that cancer cells would be targeted, but

normal cells unaffected. Its gene has been mapped to chromosome 17q, in a region frequently gained in neuroblastoma, and consistent with this, high levels of SVV are associated with MYCN amplification and a poor prognosis (Adida et al. 1998a). Pro-apoptotic p53 represses SVV transcription, however *in vitro* studies have shown that SVV overexpression (potentially akin to that in MYCN-amplified neuoblastomas) inhibits p53-mediated apoptosis induced by DNA damage (Hoffman et al. 2002).

MYCN generally favours induction of apoptotic pathways in response to DNA damage, over the initiation of cell senescence (Larsson & Henriksson 2010). Although apoptosis seems to defeat the object of tumourigenesis, if overexpression of MYCN can override this default (by the ways described above) and allow cell cycle progression in just a few DNA-damaged cells, this could lead to neuroblastoma tumourigenesis.

1.4.5. Other MYCN targets that may contribute to tumour progression

1.4.5.1. TERT

MYCN is able to bypass cell senescence by inducing expression of the TERT subunit of telomerase. This prevents the erosion of chromosomal telomeres, resulting in cell immortalisation. Telomerase is found in almost all neuroblastomas and is associated with MYCN amplification and a poor prognosis (Hiyama et al. 1995; Krams et al. 2003).

1.4.5.2. Angiogenesis-associated proteins

Angiogenesis in neuroblastoma, as a partial consequence of vascular endothelial growth factor (VEGF), is beneficial for tumour progression and therefore associated with a poor prognosis (Fukuzawa et al. 2002). PI3K activation results in raised MYCN levels (due to protein stabilisation), with a consequent increase in VEGF secretion (Kang et al. 2008). MYCN also contributes to tumour vascularity through direct transcriptional repression of angiogenesis inhibitors Activin-A, LIF and IL-6 (Breit et al. 2000; Hatzi et al. 2000; Hatzi et al. 2002). These factors normally modulate endothelial cell proliferation, so their inhibition results in less restricted blood vessel formation.

1.4.5.3. Trks

For TrkB (whose expression is associated with MYCN amplification), TrkA and p75 (both repressed by MYCN), see section 1.3.4.7: “the Trk neurotrophin receptors”.

1.4.5.4. Ndrg1

Ndrg1 is a growth inhibitory gene induced by p53 and DNA damage that functions as an inhibitor of cell growth. It is transcriptionally repressed by MYCN, and low levels of the protein (found in MYCN-amplified neuroblastomas) are associated with a poor prognosis (Li & Kretzner 2003).

1.4.5.5. Aurora kinase A

Aurora kinase A (AURKA) is indirectly upregulated by MYCN, particularly in MYCN-amplified cells. It has been found to bind to and stabilise the MYCN protein, inhibiting its degradation (Otto et al. 2009). This group therefore propose that the elevated levels of Aurora A kinase which are commonly found in MYCN-amplified neuroblastomas, in stabilising MYCN, inhibit the cell-cycle exit of neuroblasts during development, resulting in a population of cycling cells that may contribute to the generation of neuroblastoma tumours.

Mutations in, or atypical expression of, any of these genes involved in sympathetic nervous system development and/or maintenance could be implicated in oncogenic transformation (as secondary/passenger mutations) and development of neuroblastoma. As detailed above, altered levels/activity of many of these proteins have indeed been associated with the disease.

1.4.6. Control of MYCN as a potential therapeutic target

MYCN amplification and/or high expression correlates with poor patient prognosis in neuroblastoma, therefore control of this oncogenic product is an attractive therapeutic target.

As illustrated in Figure 1.10, stabilisation of the MYCN protein depends on phosphorylation at residue serine 62 (S62), which occurs in proliferating cells and is mediated by CDK1 (Sjostrom et al. 2005). This phosphorylation then allows active GSK3β to phosphorylate MYCN at threonine 58 (T58). The S62- and T58-phosphorylated MYCN is stable and transciptionally active when bound to Max (Gustafson & Weiss 2010). Activity of GSK3β depends on upstream signalling. Receptor tyrosine kinases (potentially including ALK and the Trk neurotrophin receptors) activate phosphatidylinositol 3-kinase (PI3K), which in turn activates protein kinase B (Akt). Akt causes phosphorylation and hence inactivation of GSK3β, which has the consequence of stabilising MYCN by preventing phosphorylation at T58. The singly S62-phosphorylated protein is able to enter the nucleus and induce transcription. Although doubly-phosphorylated MYCN is also transcriptionally active, this protein can potentially be dephosphorylated at S62 by the phosphatase PP2A, which would result in ubiquitination and degradation. However, as an added complexity, Aurora kinase A (AURKA) can bind to and stabilise the T58-monophosphorylated and ubiquitinated MYCN, hence AURKA's association with a poor prognosis (Otto et al. 2009). Akt also activates mammalian target of rapamycin (mTOR), which prevents dephosphorylation at S62 (and consequent degradation), allowing the stable, doubly-phosphorylated MYCN to enter the nucleus and induce gene transcription (Gustafson & Weiss 2010).

Figure 1.10. Depiction of signalling pathways involved in MYCN protein stability. Taken from Gustafson & Weiss 2010.

In correlation with the above data, Chesler et al. (2006) used PI3K inhibitors to reduce both levels of phosphorylated Akt (pAkt) and MYCN proteins, with no significant decrease in MYCN mRNA levels. This observation was reproduced in the MYCN-amplified cell lines Kelly and LAN-1, and extended to demonstrate that MYCN protein degradation resulted in reduced levels of the MYCN targets MDM2 and MCM7 (Chesler et al. 2006). The reduction in proliferation and increase in apoptosis following PI3K inhibition was less pronounced in the non-MYCN-amplified SK-N-SH cell line compared to the Kelly and LAN-1. The effects of PI3K signalling inhibition were determined to be at least in part due to GSK3β, as MYCN

proteins lacking the GSK3β phosphorylation sites were stabilised and resistant to the effects of PI3K inhibition (Chesler et al. 2006). Since disruption of the MYCN phosphorylation pathway (by means of PI3K inhibition) halted growth of tyrosine hydroxylase-driven neuroblastoma tumours *in vivo* in mice, the potential of MYCN as a therapeutic target in neuroblastoma is substantiated, and therefore is an area that should be further delved into.

1.5. Neuroblastoma diagnosis

In a suspected case of neuroblastoma, levels of urinary catecholamine metabolites HVA (homovanillic acid) and VMA (vanillylmandelic acid) are generally analysed to confirm the adrenergic character of the tumour, as like the non-malignant sympathetic cells it arises from, neuroblastomas produce and secrete catecholamines (Berthold & Simon 2005). Histologically, the tumour tissue would typically appear somewhat heterogeneous, perhaps with regions of neuronal differentiation, as well as areas of densely packed, rapidly proliferating small round blue cells – the higher the proportion of the latter, the more aggressive the tumour. Immunohistochemisty is used to detect proteins which may help distinguish the disease from other tumours such as Wilm's and pheochromocytoma. Protein markers suggestive of neuroblastoma include N-CAM (neural cell adhesion molecule), NB84, NSE (neuron specific enolase), synaptophysin, CGA (chromogranin A) and the GD2 ganglioside. In addition, cytogenetic and genetic analyses to asses MYCN status, incidences of 1p deletion etc are performed to further support the diagnosis and determine treatment stratification (Brodeur et al. 1993).

1.5.1. Staging Systems

In order to distinguish between patients with low- or high-risk neuroblastoma, and determine the appropriate disease management, all tumours are placed in a particular "stage" bracket, the most commonly used being the International Neuroblastoma Staging System (INSS), as defined by Brodeur and colleagues in 1988, according to tumour location and spread (Table 1.1).

Table 1.1. International Neuroblastoma Staging System (INSS). Adapted from Brodeur et al. 1988.

Although a universal staging system is extremely useful in a broad sense – for determining each patient's likely prognosis and comparing the efficacy of various drugs in comparable groups of patients – for a disease which is extremely diverse in its nature, this alone is not enough to stratify tumour risk. With an increasing wealth of knowledge on the genetic aberrations, epigenetic modifications and chromosomal rearrangements that can be found in the tumour genome, and their prognostic impacts, the International Neuroblastoma Risk Group (INRG) Classification System was established in 2008, by carefully analysing the cases of 8,800 neuroblastoma sufferers in North America and Australia. The study concluded that "stage, age, histologic category, grade of tumour differentiation, the status of the MYCN oncogene, chromosome 11q status, and DNA ploidy were the most highly statistically significant and clinically relevant factors" (Table 1.2) (Cohn et al. 2009). They detailed that disease outcome worsens as patient age increases, and that those diagnosed before 18 months, and particularly in the first year of life, have a significantly better prognosis. The cohort with undifferentiated or poorly differentiated tumours had lower rates of event free survival (EFS) than those with differentiating neoplasms, and patients with primary tumours situated in the adrenal glands had the poorest prognosis. Although some of the listed factors were mutually dependent, in general, MYCN amplification, the presence of aberrations in chromosome 11q, and diploid tumour DNA, were all indicators of a poor prognosis. This classification system is now being used to allow all patients worldwide to be treated in a manner more suited to their specific tumour, and rather than a generic 'one-size-fits-all' approach, therapy of an appropriate intensity can be employed. As well as the obvious benefits for the patient, this has the added advantage of improving the efficiency of data obtained from clinical trials, and is another step in the journey towards the eventual target of personalised medicine for cancer sufferers.

This text box is where the unabridged thesis included the following third party copyrighted material:

Cohn, S.L., Pearson, A.D.J., London, W.B., Monclair, T., Ambros, P.F., Brodeur, G.M., Faldum, A., Hero, B., Iehara, T., Machin, D., Mosseri, V., Simon, T., Garaventa, A., Castel, V. & Matthay, K.K. (2009) 'The International Neuroblastoma Risk Group (INRG) Classification System: An INRG Task Force Report', *Journal of Clinical Oncology*, vol. 27, no. 2, pp. 289-297. *[Figure 2]*

Table 1.2. International Neuroblastoma Risk Group (INRG) Classification System. GN, ganglioneuroma; GNB, ganglioneuroblastoma; Amp, amplified; NA, non-amplified. Taken from Cohn et al. 2009.

It is evident that tumour stage is a huge prognostic factor, and from the Kaplan-Meier curves in Figure 1.11, one can deduce how heterogeneous the bracket of "neuroblastoma tumours" is, with recovery excellent in those patients with low stage tumours, but extremely poor in those with aggressive forms of the disease.

This text box is where the unabridged thesis included the following third party copyrighted material:

Berthold, F. & Simon, T. (2005). 'Clinical Presentation'. In: Cheung, N.V. & Cohn, S.L. (2005). *Neuroblastoma*. Berlin: Springer. *[Figure 7.3]*

Figure 1.11. Kaplan-Meier curves to show A) event free survival, and B) overall survival in 2779 neuroblastoma patients, staged according to the INSS. Taken from Berthold & Simon 2005.

1.5.2. Chromosomal aberrations

1.5.2.1. DNA ploidy

Ploidy is defined as the number of sets of chromosomes in each cell. Diploid is the normal occurrence of two copies of each chromosome: one maternal and one paternal. DNA ploidy of the tumour cells is an important prognostic factor in neuroblastoma. Tumours with hyperdiploidy/near-triploidy have the best prognosis, often with whole chromosome gains

rather than structural rearrangements (Brodeur & Nakagawara 1992). The near-diploid neuroblastomas have an poor prognosis, often encompassing several cytogenetic rearrangements, including deletions and translocation (Brodeur 1995).

1.5.2.2. 1p deletion

Around a third of neuroblastoma tumours have loss of heterozygosity (LOH) of chromosome 1p (Maris et al. 2000). Outcome is worse in patients with the largest 1p deletions, and this is often associated with MYCN amplification and diploidy/tetraploidy (Schwab 2005). It is thought that at least one, possibly multiple neuroblastoma tumour suppressors are located within chromosome 1p, although the large size of the deletions in addition to the genomic complexity of the region make identification of such genes difficult.

1.5.2.3. 11q deletion

Deletions in chromosome 11q have been found in around 15% of neuroblastomas, usually of a high stage, but rarely coincides with MYCN amplification (Spitz et al. 2003; Van Roy et al. 2009). 11q deletion is therefore sometimes considered to be an indicator of poor prognosis in non-MYCN-amplified tumours (Mertens et al. 1997). Loss of the whole chromosome 11 seems to be associated with a better prognosis.

1.5.2.4. 17q gain

Comparative genomic hybridisation (CGH) experiments have shown that around half of neuroblastomas have an additional segment of chromosome 17q, making 17q gain the most common genetic aberration in the cancer. After 1p, 11q is the second most common partner for chromosome 17q translocations. 17q gain is most common in tumours of a high stage, in children older than one year, and in tumours with MYCN amplification and diploidy or tetraploidy (Maris 2004).

Figure 1.12. Kaplan-Meier curve displaying cumulative patient survival for 133 neuroblastoma tumours with various genetic aberrations. Red line, chromosome segmental aberrations (not involving MYCN amplification, 11q deletion or 17q gain); Blue line, numerical changes only (whole chromosome loss and/or gain); Purple line, chromosome 17q gain (without MYCN amplification or 11q deletion); Yellow line, MYCN amplification (without 11q deletion); Green line, 11q deletion (without MYCN amplification). Taken from Caren et al. 2010.

1.6. Spontaneous regression

Neuroblastoma has a “special” stage, termed “4S”, in which, following a period of aggressive disseminated growth (involving liver, skin or bone marrow in addition to the primary tumour), tumours spontaneously regress (diminish, disappear and/or differentiate) with little, or often no treatment. Such tumours have favourable histology, a single MYCN copy, and are generally classed as low-risk (Maris et al. 2007; Nickerson et al. 2000). Regression very rarely occurs in patients older than one year of age and usually occurs within the first six months after birth. However, it is extremely difficult to establish precisely what proportion of tumours undergo this phenomenon, particularly when one takes into account the results of neuroblastoma screening programmes performed in Japan, North America and Europe at the end of the last century.

1.6.1. Screening

Urinary catecholamine metabolites were analysed in infants up to one year of age, and those with elevated levels were investigated further for a potential neuroblastoma diagnosis. The three main trials took place in Japan (the most preliminary and least robust), Quebec and Germany, and although different in their designs, they all noted an increase in the incidences of neuroblastoma to almost double in the screened population compared to the control cohorts, regardless of age (≤6months, or 1 year), and this was coupled with no decrease in

mortality rates or the incidences of advanced stage disease at any age. These data led to two key outcomes: the determination that incidences of spontaneous regression may be much higher than previously thought, with many patients (in an unscreened population) never even presenting at the clinic; and the conclusion that the preclinical screening methods utilised were not beneficial and should be abandoned, as earlier detection made no difference to the mortality rates of patients with high risk disease (Woods et al. 1996).

1.6.2. Possible reasons/mechanisms for spontaneous regression

It has been established that a massive pre-programmed, regulated death of sympathetic neurons occurs around the time of birth, probably due to a lack of neurotrophins (particularly NGF). Exposure of TrkA-expressing neurons to NGF results in survival and differentiation, whereas NGF withdrawal leads to apoptosis, therefore the limited availability in the foetus permits only the survival of the required number of neurons (Oppenheim 1991). Nakagawara reported that this same apoptotic mechanism seemed to occur in neuroblastoma tumours in infants, potentially as the onset of spontaneous regression. He detailed that MYCN amplification inhibits spontaneous regression, but in tumours that do regress, caspases are induced and survivin, an apoptotic inhibitor which is overexpressed in advanced stage tumours, is downregulated (Nakagawara 1998).

1.7. Neuroblastoma treatment

Current treatment regimens for neuroblastoma range from surgical resection alone in some low risk cases, to intense multi-agent modalities in high risk patients. In advanced stage disease intensive chemotherapy is often the first treatment given, which is followed by stem cell collection and then surgery to remove as much of the tumour tissue as possible. Next is myeloablative therapy, which must be followed by autologous stem cell transplantation. This may then be followed by radiotherapy. In addition, some children are then given retinoid therapy to induce tumour cell differentiation (Bhatnagar & Sarin 2012). However, it is extremely difficult to eradicate all tumour cells in high risk patients, so in recent years immunotherapy has been used in combination with the retinoic acid treatment to target residual disease. GD2 is a ganglioside expressed on all neuroblastoma cells, but rarely on normal tissues, therefore is seen as an efficient way to target the cancer cells specifically. Monoclonal antibodies are administered to the patient and target GD2, leading to immune-

mediated cell death. However, patient responses have varied, and unfavourable toxicities have been observed (Castel, Segura & Canete 2010).

Chemotherapeutic drugs, still often the most effective treatment, usually cause severe toxicity and target all dividing cells in a non-specific manner, causing devastation to many body tissues. It would be favourable to kill neuroblastoma cells *in vivo* in a less destructive manner, whilst administering minimal toxicity. Since deregulation of MYCN contributes to tumourigenesis, not just in neuroblastoma but in a variety of tumours, selectively inhibiting MYCN is an attractive prospect. One way of doing this may be to find a way of reprogramming the cells, and encouraging them to either differentiate or undergo apoptosis of their own accord.

1.8. Embryonic microenvironment reprograms tumour cells

Numerous methods of experimentation have been underway for decades, attempting to transform various types of malignant cells to a more benign phenotype, by exposing them to assorted embryonic environments. In early experiments in 1975, Mintz & Illmensee injected malignant mouse teratocarcinoma cells into mouse blastocysts, which were then implanted into pseudo-pregnant mouse uteri. They discovered that the blastocyst microenvironment reversed the malignancy of the teratocarcinoma cells, and not only that, but in some of the mice that developed from said blastocysts, the formerly malignant cells had contributed to the make-up of many developmentally unrelated tissues, in what the authors termed “cellular genetic mosaics” (Mintz & Illmensee 1975).

It had been documented that aggressive cancer cells (particularly relevant to the following experiments, malignant metastatic melanoma (MM)) share several characteristics with human embryonic stem cells (hESCs), most notably their multipotency. It was therefore proposed in 1982 that “an embryonic microenvironment capable of differentiating a stem cell lineage should be able to reprogram cancers derived from that lineage" (Pierce et al. 1982). Decades later, in 2006, Postovit and colleagues developed a system to determine the influence of a stem cell microenviroment on MM cells. They cultured hESCs on 3D matrices, before removing aforementioned stem cells and adding human MM cells to the culture system (i.e. the matrices had been conditioned by the hESCs’ secreted factors, but the complication of cell-cell interactions between them and the MM cells had been eliminated – the melanoma cells were effectively only exposed to the stem cells’ extracellular microenvironment). Morphologically, the MM cells grew as spheroids, reminiscent of the

colonies formed by hESCs. More remarkably, the conditioned matrices induced the expression of MLANA, a melanocytic marker that was absent from the malignant melanoma cells, and in addition reduced the invasive capacity of the MM cells *in vitro* and impaired their ability to form tumours *in vivo*, in nude mice (Postovit et al. 2006). All in all, proving an embryonic stem cell environment could have a dramatic effect on these multipotent melanoma cells.

At around the same time, a paper was published using the zebrafish embryo as a model system, again attempting to reprogram MM cells (Lee et al. 2005). Five days subsequent to implantation into the blastula-stage zebrafish, the MM cells were found to be scattered throughout the embryo, and the expression of a pan-melanoma marker was found to have been downregulated. This de-differentiated phenotype was still apparent after three months of observation, by which time no tumours had been formed. This so-called “reprogramming” of the MM cells, was found to be critically time-dependent, when a different group injected MM cells into a zebrafish embryo 2 days post-fertilisation, and found that tumour-like masses developed, and within some of these, angiogenesis was beginning to occur (Haldi et al. 2006).

The first paper published transplanting melanoma cells into a chick embryo model was in 2005. Melanocytes, of which melanoma is their malignant counterpart, originate from the neural crest. Since the dedifferentiated plastic/multipotent phenotype of melanoma cells, and the ability of an early embryonic environment to reverse their tumourigenicity had already been established, they reasoned that transplanting MM cells back into the neural crest environment from which they originally developed, may illicit a more pronounced response than had been seen in other model systems. SK-Mel28 cells, suspended in matrigel, were transplanted into the Hamburger and Hamilton stage (HH) 11-13 neural tube, and 48 hours later, HNK-1 negative, HMB-45 positive melanoma cells were discovered in the medial neural crest migratory stream, as well as in the sympathetic ganglia (Schriek et al. 2005). Kulesa et al., in 2006, then extended these observations further. They first injected DiI into the chick embryo neural tube to label the host neural crest cells, then transplanted blocks of around 1,500 aggressive MM cells into the neural tubes of chick embryos aged around HH9, the time when host NCCs are just about or beginning to emerge from the neural tube. These cells were analysed within the chick embryo 48h or 96h after transplantation. They were never found to form tumours, and instead, rather than lying dormant, a proportion of them migrated out into the surrounding chick tissues along with the chick’s endogenous NCCs, and were morphologically reminiscent of normal migrating neural crest cells. In addition, some MM cells were found to have invaded host NC target tissues, such as the branchial

arches, dorsal root ganglia and sympathetic ganglia. Not only this, but 34% of the migrating melanoma cells were found to express the melanocyte-specific marker MART-1, and another 13% of the migrating MM cells had been induced to express TUJ1, a neuronal marker (Kulesa et al. 2006). In contrast, when fibroblastic cells were transplanted into the neural crest cell migratory pathway, they remained intact at the graft sites, and did not migrate or invade the surrounding tissues (Erickson, Tosney & Weston 1980).

This neural tube transplantation technique was utilised by another group, this time using only moderately aggressive murine B16-F1 melanoma cells, at HH12-12. Like the human MM cells, they migrated with the host NCCs, along both the ventral and lateral pathways, and colonised structures such as the sympathetic ganglia (Oppitz et al. 2007). However after 48h, many cells were found to have undergone apoptosis rather than differentiation – the latter perhaps being a feature restricted to the most aggressive (and potentially most "stem"-like) cells. To both check cell viability within the embryo, and prove that this tumour-reversing phenomenon was unique to cells transplanted back in to their environment of origin, they injected the same suspension into the eye cup of E3 (HH stage 20) embryos and observed that the melanoma cells' tumourigenicity was maintained, as invasive melanomas formed, which were entirely comprised of murine cells (Oppitz et al. 2007). This group extended their observation further, after they reasoned that the melanoma cell migration may be due to endogenous BMPs – as normal neural crest cell migration is induced by BMPs and inhibited by noggin, but unlike transplanted neural stem cells (Busch et al. 2006), the melanoma cells did not require pre-treatment with BMP2 to migrate. Aggregates of B16 F1 mouse melanoma cells were cultured with either BMP2, noggin, or left untreated, and then implanted into the chick neural tube. Cells pre-treated with noggin did not migrate, and remained at the graft site. Those untreated and treated with BMP2 migrated through the embryo, but migration was enhanced, in terms of cell number and distance, in those BMP2-treated (Busch et al. 2007). The neural crest-like migration of melanoma cells has also been recapitulated using mouse embryos (Diez-Torre et al. 2009).

The chick-melanoma work was able to conclude, not only that an embryonic environment was capable of ablating the tumourigenicity of aggressive melanoma cells, but that following exposure to the microenvironment of their ancestral cell type, these so-called dedifferentiated cells were capable of responding to the signals they received, and behaved like normal NCCs, effectively going through the process of development a second time, this time differentiating into primitive neural-crest-derived tissues (albeit a small subset of the transplanted cells).

1.9. Hypothesis

Since neuroblastoma can be a highly aggressive disease, and one that is still failing in terms of the treatment of high-risk patients, it is proposed that a similar outcome to the chick melanoma experiments described above could be achieved using neuroblastoma cells. Like malignant melanoma, neuroblastoma cells originate from the neural crest, but unlike melanoma, neuroblastoma is a paediatric cancer, so it is hoped that these comparatively immature cells may be more susceptible to signals within the neural crest embryonic environment. Coupled with the high incidence of spontaneous regression in neuroblastoma, in which cells in these usually young patients have been observed to differentiate and/or apoptose (Koizumi et al. 2006), it is hypothesised that reintroduction into their embryonic site of origin, i.e. the neural crest and its migratory pathways, may allow the neuroblastoma cells to respond to the environmental cues they encounter and behave in a similar manner to the endogenous neural crest cells – in effect, giving the cells a "second chance" at normal development. It is therefore expected that the tumour cells would thrive in an "inappropriate environment", i.e. one in which neural crest developmental cues were absent, and proliferate to form microtumours.

1.9.1. Aims

- Establish a system, using the chick embryo as a model organism, for effective introduction of neuroblastoma cells into an "appropriate" environment (in which neural crest-related developmental cues are present) as well as into an "inappropriate" environment (devoid of neural crest signals).

- Test methods of cell introduction: intra-ocular and intravenous injection.
- Inject various cell lines: SK-N-BE(2)C, B16 F1 (mouse melanoma), SK-N-AS, SH-SY5Y, Kelly, glioblastoma primary line, SH-EP.
- Determine the most effective means of cell labelling.
- Introduce cells at different chick embryonic ages: E3 and E6.

- Determine the consequences of neuroblastoma cell targeting at E10.

  - E3 versus E6 injection.
  - Within neural versus non-neural tissues (E3).

  - Proliferation
  - Differentiation
  - MYCN protein expression

- Test the impact of the chick sympathetic ganglia microenvironment on the "reprogramming" of neuroblastoma cells.

  - Leave cells within the chick until E14.
  - Culture sympathetic ganglia containing Kelly cells *in vitro*: dissociated versus explanted.

Chapter Two:

Materials and Methods

2.1. Cell culture

All experiments were performed using cells from the following cell lines:

Cell line	Sourced from	Culture medium	Primary tumour site	Origin of cell line	NB stage	MYCN status
SK-N-BE(2)C	CRL-2268	DMEM + 10% FCS + 100U/ml penicillin, 100µg/ml streptomycin	Unknown	Bone marrow	IV	MYCN amplified, >150 copies, medium expression
SH-SY5Y	ECACC 94030304	MEM + 10% FCS + 100U/ml penicillin, 100µg/ml streptomycin	Thorax	Bone marrow	IV	MYCN diploid, low expression
SK-N-AS	ECACC 94092302	MEM + 10% FCS + 100U/ml penicillin, 100µg/ml streptomycin	Adrenal gland	Bone marrow	IV	MYCN diploid, no expression
B16 F1 (mouse melanoma)	Gift from Prof Dot Bennett, St George's University of London, UK	RPMI 1640 + 5% FCS + 100U/ml penicillin, 100µg/ml streptomycin	Skin	Skin	N/A	N/A
Kelly	Gift from Dr Louis Chesler, The Institute of Cancer Research, Sutton, UK	RPMI 1640 + 10% FCS + 100U/ml penicillin, 100µg/ml streptomycin	Unknown	Brain	IV	Highly MYCN amplified, >200 copies, high expression
SH-EP	Gift from Dr Louis Chesler, The Institute of Cancer Research, Sutton, UK	DMEM + 10% FCS + 100U/ml penicillin, 100µg/ml streptomycin	Thorax	Bone marrow	IV	MYCN diploid, no expression
SH-EP-MYCN	Gift from Dr Louis Chesler, The Institute of Cancer Research, Sutton, UK	DMEM + 10% FCS + 100U/ml penicillin, 100µg/ml streptomycin	Thorax	Bone marrow	IV	MYCN diploid, medium expression

Table 2.1. Information on the origins and culture conditions of the cell lines used in this project.

2.1.1. Cell line culture

Cell lines were generally cultured as monolayers in 25cm^2 or 75cm^2 culture flasks (Sarstedt), in their appropriate media (see Table 2.1), at 37°C and 5% CO_2, in a humidified incubator. When cells were approaching confluency, Ca^{2+}- and Mg^{2+}-free Hanks Balanced Salt Solution (HBSS) (Sigma-Aldrich) was used to wash the culture surface, following which 1ml 0.05% trypsin EDTA (Gibco) was added per 75cm^2 flask. Following 5 minutes incubation at 37°C, 9ml culture medium containing foetal calf serum (FCS) (Biosera) was added to the flasks to halt the action of the trypsin, and the resulting cell suspension triturated using a 10ml pipette (or blue tip, for the "clumpier" cell lines). Between 1x10^6 and 3x10^6 cells were replated per 75cm^2 flask, and the total volume made up to 12ml with the appropriate medium.

Cell counts were performed by producing a single-cell suspension following trypsinisation, typically in a total volume of 10ml, and pipetting small volumes into a haemocytometer. The average number of cells was calculated from 5 counts, to give (*average)*x10^4 cells/ml.

2.1.2. Primary neuroblastoma cell culture

2.1.2.1. Primary tumour tissue

Neuroblastoma samples termed NB16B, 17, 17B, 2C, 19B*, 20*, 20B*, 21**, 22***, 23*** and 24*** were received as small tissue pieces in a 20ml tube of serum-free medium. These tubes were spun at 1000rpm for 5 minutes, for ease of removal of medium. The samples were then resuspended in 1ml 0.25% trypsin (Gibco), 100µg/ml collagenase (Sigma-Aldrich) and 100µg/ml DNase I (Sigma-Aldrich), and transferred to a 35mm dish. Tissue was cut into small pieces using sterile scalpels (size 10, Swann-Morton), and then incubated in the trypsin at 37°C for 30 minutes. Tissue was washed at least 3 times using HBSS, and then 1-2ml culture medium: RPMI 1640 (Gibco) containing 20% FCS, 1% non-essential amino acids (NEAA) (Gibco), 100U/ml penicillin and 100µg/ml streptomycin (Gibco); was added, following which tissue was minced into yet smaller pieces using the two scalpels. This suspension was triturated using either a blue pipette tip or a glass Pasteur pipette, polished using a Bunsen burner to reduce the bore. The suspension was then filtered through a 40µm cell strainer, and the single cells transferred into one 25cm^2 flask, and the tissue pieces/cell clumps remaining in the sieve transferred to a second flask. Cells were fed with fresh medium every 3 days, and once expanded, were frozen and stored in liquid nitrogen (see section 2.1.4).

* For samples NB19B, 20 and 20B, tissue was minced and filtered without the addition of trypsin, collagenase or DNase I, as this made little difference to the dissociation.

** NB21 was prepared in the same way as tissues NB19B, 20 and 20B, i.e. without trypsin, DNase I or collagenase, but in addition explants of tumour tissue were plated onto 6 well tissue culture plates that had been coated with 10µg/ml Poly-L-lysine in 0.1M sodium borate pH8.3 for 1 hour. These explants, along with the dissociated tumour tissue, was cultured either in RPMI medium as detailed above, or in serum free medium: 3:1 DMEM:F12 (Gibco, Sigma-Aldrich respectively), 100U/ml penicillin and 100µg/ml streptomycin, 2% B27 supplement (Gibco), 40ng/ml bBFGF (Gibco) and 20ng/ml EGF (Sigma-Aldrich) (Hansford et al. 2007).

*** NB22, 23 and 24 were dissociated without trypsin, DNase I or collagenase, and cultured in serum-free medium (detailed above for NB21) – cells mostly grew as non-adherent spheres.

2.1.2.2. Bone marrow samples

Neuroblastoma samples NB22, 23 and 24 were accompanied by bone marrow aspirates, which were taken at the time of biopsy. Universal tubes containing the samples were centrifuged for 5 minutes at 1000rpm and the supernatant removed from the pellet of cells. The pellet was resuspended in serum-free medium (3:1 DMEM:F12, 100U/ml penicillin and 100µg/ml streptomycin, 2% B27 supplement, 40ng/ml bBFGF and 20ng/ml EGF) and then sieved through a 40µm cell strainer. The single cells/smallest clumps that passed through the mesh were transferred to one 25cm^2 flask, and the larger clumps washed from the mesh and cultured in a second 25cm^2 flask.

As the spheres increased in size in culture, they were passaged by mechanical trituration using a reduced bore Pasteur pipette (flamed over a Bunsen burner), and then passed through a 40µm cell strainer, before replating in new flasks.

2.1.3. Thawing of cells

Upon removal from liquid nitrogen store, cryovials were placed in a warm waterbath until just thawed. The now liquid cell suspension (1ml) was transferred to a 10ml plastic tube, kept on ice to limit the damage caused by DMSO, and 1ml of the appropriate unsupplemented base medium (e.g. DMEM/RPMI 1640/etc.) added drop-wise over 30 seconds. A further 8ml medium was added over another 30 seconds, following which the diluted cell suspension was spun using a GLC-4 General Laboratory Centrifuge (Sorvall Instruments) at 1000rpm for 5 minutes to remove the DMSO. The consequential cell pellet was then resuspended in 7ml fresh medium, and seeded in a 25cm^2 flask.

2.1.4. Freezing of cells

Following trypsinisation (see *cell culture*), cells from a 75cm^2 flask were diluted in their appropriate culture medium, up to a volume of 10ml. This cell suspension was then centrifuged at 1000rpm for 5 minutes, and the resulting pellet resuspended, on ice, in 'freezing medium' – a solution of 90% FCS and 10% dimethylsulfoxide (DMSO). 1ml aliquots were transferred into cryovials (Sterilin) – a 75cm^2 flask approaching confluency would typically produce 3 or 4 vials – and these cryovials placed in vapour phase over liquid nitrogen overnight to lower the temperature more slowly, limiting cell damage, and then transferred to the liquid nitrogen store the following day.

2.1.5. Generation of a highly MYCN-expressing SH-EP-MYCN line

In an attempt to produce a more stably MYCN-expressing line, SH-EP-MYCN cells were subcloned (see section 2.2.3.1.1) by plating at a density of one cell per well in a 96 well plate, in a volume of 50µl medium per well. The fastest-growing colonies were expanded and immunofluorescence stained for MYCN (see section 2.4.1.1), and the most consistently MYCN-expressing subclones expanded further into new cell lines.

2.2. Fluorescent cell labelling

2.2.1. GFP cell transfection

2.2.1.1. Plasmids used

The two plasmids used were pEGFP-N1 (Clontech, USA) (Figure 2.1), from which successfully transfected cells could be selected by their resistance to the antibiotic G418, and a pBudCE4.1 vector (Invitrogen, UK) (Figure 2.2) containing GFP, cloned in under control of the human elongation factor 1α (EF-1α) promoter (by Dr Mohammed Akeel (PhD student, University of Liverpool, UK)), and contained a zeocin resistance gene.

This text box is where the unabridged thesis included the following third party copyrighted material:

http://www.human.cornell.edu/dns/qilab/images/pEGFPN11_1.jpg *[plasmid map only]*

Figure 2.1. Vector map for pEGFP–N1. Adapted from http://www.human.cornell.edu/dns/qilab/images/pEGFPN11_1.jpg

This text box is where the unabridged thesis included the following third party copyrighted material:

https://products.invitrogen.com/ivgn/product/V53220 *[a modified form of]*

Figure 2.2. pBudCE4.1 vector map, including GFP that was cloned in (by Dr Mohammed Akeel) under the EF-1α promoter. Adapted from Invitrogen.

2.2.1.2. Killing curves

“Killing curves” were performed as depicted in Figure 2.3, in which varying densities of the cells to be transfected were plated and these were cultured with varying concentrations of the appropriate antibiotic for the transfected plasmid. This was to discover the concentration of antibiotic required to kill the non-GFP-transfected cells at the various densities. Cells were

plated in 24 well plates at the densities shown in Figure 2.3, and 24 hours later, the 6 different concentrations of antibiotic added. Cells were then monitored for survival/death for the following week, and an optimal plating density and antibiotic concentration deduced from these observations.

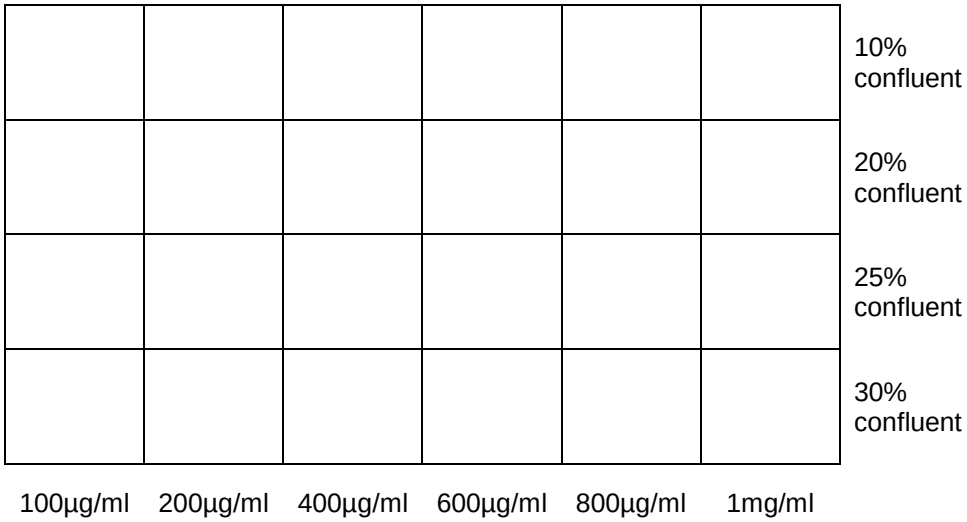

Figure 2.3. Illustration of a "killing curve". Cells were seeded in a 24 well plate at various densities (detailed down the right hand side), and after 24 hours, a range of antibiotic concentrations added to their medium (shown along the bottom).

2.2.1.3. ExGen500

Transfection attempts were made using the pEGFP-N1 plasmid and transfection reagent ExGen500 (Fermentas) on B16 F1 cells. 24 hours after plating of the B16 F1 cells in a 35mm diameter well, 3µg of plasmid DNA was mixed with 10µl ExGen500 in a total volume of 200µl 150mM sodium chloride, and was added to the melanoma cells and incubated for 24 hours.

2.2.1.4. TransIT-LT1

The pEGFP-N1 and pBudCE4.1/EF-1α/EGFP were both transfected into B16 F1 cells, and pBudCE4.1/EF-1α/EGFP only into SK-N-BE(2)Cs, SK-N-AS and SH-SY5Y using TransIT-LT1 (Geneflow). 2.5µg plasmid DNA was added to 7.5µl TransIT-LT1 reagent in 250µl total

volume of serum-free medium. This was added per well of cells that had been seeded on to a 35mm well 24 hours earlier, and incubated for 48 hours.

2.2.1.5. JetPRIME

The JetPRIME (Peqlab) reagent was used to transfect pBudCE4.1/EF-1α/EGFP into SK-N-BE(2)C, SK-N-AS and SH-SY5Y cells. 2µg plasmid DNA was added per 35mm well alongside 4 or 6µl reagent in 200µl total volume of JetPRIME buffer, and incubated for 4 hours.

2.2.2. CFDA-SE labelling

Following trypsinisation, $1x10^6$ Kelly cells per ml of pre-warmed PBS containing 0.1% BSA were incubated with 2µM, 5µM or 10µM CFDA-SE (Invitrogen) for 10 minutes. Cells were washed four times in culture medium, and then plated at 20% confluency in 6 well plates.

2.2.3. Lentiviral cell transduction

2.2.3.1. Kellys

Kelly cells, growing in a monolayer, were transduced with an EGFP-expressing lentivirus by Dr Sokratis Theocharatos (University of Liverpool, UK). EGFP was expressed constitutively under the control of the spleen focus-forming virus (SFFV) promoter (Demaison et al. 2002) (Figure 2.4) and the viral particles were pseudo-coated with a vesicular-stomatitis-virus glycoprotein (VSV-G) envelope (Aiken 1997). The Kellys were cultured in a 24 well plate, and the lentivirus was added to one well's RPMI-based culture medium for 24 hours, after which time it was replaced by fresh, non-virus-containing medium. A proportion (≥80%) of the cells could be seen to be expressing EGFP 48-72 hours subsequent to lentivirus addition. Cells were expanded into a 6 well plate, then into a $25cm^2$ flask, and once thriving in a $75cm^2$ flask, were ready to be subcloned, in order to obtain a homogeneous strongly GFP-expressing cell line from this mixture of cells expressing GFP at varying levels, some not fluorescent at all.

2.2.3.1.1. Subcloning

Cells were removed from their tissue culture flask using 1ml 0.05% trypsin EDTA at 37°C. When cells were seen to have lifted off the culture surface, 9ml of RPMI medium (the 10% FCS was important to counteract the trypsin) was added, and the cell suspension triturated using a blue pipette tip until a single-celled suspension was obtained. Cells could then be counted using a haemocytometer, and sequentially diluted with medium until a suspension of 20 cells/ml was obtained. The suspension was seeded at 50µl per well of a 96 well plate, i.e. an average of 1 cell per well, and fed every 2-3 days, in the hope that fluorescent colonies would form. Subcloning was also attempted a second time, using the same method, except the final cell suspension to be seeded was diluted in half fresh medium and half Kelly cell conditioned medium. The fluorescent colonies that eventually formed were transferred into a 4 well plate, up to a 6 well plate, then expanded into a 25cm^2 and finally a 75cm^2 flask.

2.2.3.2. SH-EPs

SH-EP and SH-EP-MYCN cells were lentivirally transduced in the same way as the Kellys (by Dr Anne Herrmann, University of Liverpool, UK), but instead of subcloning for the brightest GFP cells, they were selected using a FACS cell sorter (by Heba Karosh, MRes student, University of Liverpool, UK).

2.2.4. Culture of GFP-labelled cells

All GFP-expressing cell lines were cultured in the same medium, and using the same methods, as their non-GFP-labelled counterparts (see Table 2.1 and section 2.1.1).

2.3. Chick embryo work

2.3.1. Egg preparation

Batches of (generally 18 or 24) fertilised white leghorn chicken eggs (obtained from Lees Lane Poultry, Wirral, UK) were incubated at 37°C and 35% humidity. The day the eggs were placed in the incubator was “day 0”. On embryonic day 2 (E2) or E3, i.e. Hamburger

Hamilton stage 12-18 (Hamburger and Hamilton, 1951), a small hole was poked in one end of the eggs, and a 19G gauge needle (Terumo) and syringe used to remove 3-4ml of albumin (dependent on the size of the egg), which resulted in the embryo and surrounding vessels being detached from the shell. A Power Craft PKW-160N Combitool was then used to cut a rectangular window (approximately 25x15mm) out of the shell, following which windows were resealed using Scotch Magic adhesive tape. Eggs were then re-incubated until injections at E3 or E6.

2.3.2. Cell preparation

2.3.2.1. For intravenous injections

2.3.2.1.1. GFP-Kelly

Prior to injection, cells were harvested from 75cm^2 culture flasks using 1ml 0.05% trypsin EDTA, and following 5-10 minutes incubation at 37°C, diluted into 10ml total volume with RPMI 1640 medium containing 10% FCS, triturated using a blue pipette tip, and then counted using a haemocytometer. An appropriate number of cells (typically 5x10^6 cells for a batch of 24 eggs, of which 18-20 would be injected) were transferred into a sterile 10ml tube and centrifuged at 1000rpm for 5 minutes. The resulting cell pellet was then resuspended as single cells at a density of 1x10^5 cells/µl in RPMI 1640, containing 100µg/ml DNase I and 0.05% fastgreen (i.e. in 50µl total volume, if preparing 5x10^6 cells).

2.3.2.1.2. GFP-SK-N-BE(2)C

Cells were harvested as above, with the exception that 0.25% trypsin was sometimes used instead of 0.05% trypsin EDTA, DMEM was used instead of RPMI 1640, and 1% collagenase was frequently added along with the 100µg/ml DNase I, to ensure the production of a single cell suspension, as the BE(2)Cs are particularly clumpy, and difficult to triturate.

2.3.2.1.3. GFP-SH-EP and GFP-SH-EP-MYCN

Following trypsinisation, dilution in DMEM medium containing 10% FCS and centrifugation, cells were resuspended at a density of $1x10^5$ cells/µl of DMEM containing 0.05% fastgreen. DNase was not added for these cells, as a single-celled suspension was easily achieved by mechanical trituration.

2.3.2.1.4. GFP-TSIA (glioblastoma)

Cells were prepared as for the Kellys, and following centrifugation, were resuspended at a density of $1x10^5$ cells/µl in DMEM/F12 containing 0.05% fastgreen and 10µg/ml DNase I.

2.3.2.1.5. Non-GFP-labelled cells

In the earliest experiments, non-GFP-labelled SK-N-BE(2)C, SK-N-AS, SH-SY5Y and Kelly cells were all harvested as described for the GFP-Kellys, and following cell counts and subsequent centrifugation, resuspended in a solution of 500µl total volume of 40µM Vybrant DiI (Invitrogen) in the appropriate medium (see Table 2.1). Cells were incubated in the DiI for 30 minutes, centrifuged for 5 minutes at 3000rpm, and then resuspended as single cells at a density of $1x10^5$ cells/µl in the appropriate base medium (no FCS) containing 0.05% fastgreen.

2.3.2.1.6. Fluorescent beads

1µm diameter green fluorescent beads (Invitrogen) were washed in PBS, centrifuged at 1000rpm for 5 minutes, and then suspended in PBS containing 0.05% fastgreen at a density of $1x10^5$ beads/µl.

2.3.2.2. Cells intended for eye cup injections

SK-N-BE(2)C, B16 F1, Kelly (both non-GFP- and GFP-labelled) cells were prepared in the same way as the cells for intravenous injection (including DiI labelling for non-GFP cells), but

for these, resuspended $1x10^6$ cells in a total volume of 50µl – sometimes made up mostly of the appropriate base medium (DMEM, RPMI or MEM, serum-free) with 0.2% fastgreen, and other times 1:1 base medium:matrigel (50µg/ml stock) (BD Biosciences).

2.3.3. Chick injections

Throughout the injection process, cells were kept on ice and occasionally re-triturated either by flicking the eppendorf or pipetting. Borosilicate glass capillary tubing (thin wall with filament, Warner Instruments) was pulled under heat to a thin taper (settings: heat 580, velocity 15, pull 130, time 15, pressure 20; Sutter Instrument Co.), and the resulting needles snapped using dissecting forceps to an appropriate diameter – thin enough for microinjection, but wide enough to allow entry of the cell suspension. Suction was applied via mouth pipette (Sigma-Aldrich) to fill the needle with 2µl of the appropriate cell (or bead) suspension, and this was then injected, under a stereo microscope, into the extra-embryonic vitelline vein of each embryo at E3 (Figure 3.11 B+D) or E6, or, in the earliest experiments, into the E3 eye cup (either left or right, depending on which was up-facing) – as much cell suspension as could be injected, typically less than 0.5µl. Embryos were incubated until E10 or, for some E3 injections, until E14. To assess cell proliferation, typically 1µl of 20mM EdU (Click-iT EdU imaging kits, Invitrogen C10339) – roughly equivalent to a concentration of 10µM, taking the embryo's mass between E9 and E10 to be approximately 2g (Figure 2.4) – was injected into an extra-embryonic blood vessel at E9 for 24 hours (although 0.5 and 2 µl was injected with no appreciable difference in the percentage of cells labelled). 4µl of 20mM EdU was injected at E13. Embryos were then dissected 24 hours later (at E10 or E14), under a Leica M165 FC fluorescence microscope, and locations of GFP-labelled cells noted and photographed using a Leica DFC425C camera and Leica Application Suite V4.0 software. Tissues containing GFP-Kelly cells were then fixed using 4% paraformaldehyde.

Figure 2.4. Average chick embryo masses for each day of gestation. (Taken from http://chickscope.beckman.uiuc.edu/resources/egg_to_chick/development.html. Illustration Copyright © 1998, Jill Hixon and the University of Illinois).

In each experiment, usually 18 eggs (but up to 24) were initially placed into the incubator. A small number of eggs may have been unfertilised, developing embryos were sometimes destroyed during the "windowing" procedure, or were occasionally deformed, and some died for unknown reasons. Therefore between 12 and 18 embryos (in a typical experiment, approximately 15) were injected with malignant cells at E3. On occasion, all of the injected embryos would be alive on the day of analysis (E10 or E14), but usually a few would have died, either as a consequence of excessive bleeding after injection, or often with unknown cause slightly later in development. In a typical batch of 18 eggs, of which 15 had been injected with cells at E3, roughly 11 would have survived to the day of dissection (although this could be as low as 3 or 4 chicks, or as high as 14-15). In addition to the considerable variability described above, further inconsistency could sometimes be observed upon dissection – this would be usually down to a "poor" injections, perhaps because the cell suspension had become particularly clumpy, or the embryo was underdeveloped with smaller blood vessels and lower circulatory volume, both of which would have made it difficult to administer the usual number of cells. However, in a typical experiment, between 7 and 10 embryos would usually contain sufficient numbers of fluorescently labelled cells to allow for analysis (and comparisons) to be performed.

2.3.4. Tissue mounting for morphology studies

Following fixation for the appropriate time (tissue-dependent, but generally 30-90 minutes) in 4% paraformaldehyde, the small tissue pieces were washed in PBS, and then positioned in a drop of Dako fluorescence mountant on a glass slide, and a glass coverslip placed over the top. The sympathetic ganglia and meninges could be laid out and mounted without any problem. The gut was cut in half longitudinally using forceps and mounted luminal surface down. The tail tissue had to be forcibly "squashed" between the slide and coverslip.

2.3.5. Tissue block preparation and frozen sectioning

Tissues of interest were fixed in 4% paraformaldehyde, and then sequentially immersed in 6%, 12%, then 18% sucrose for approximately 1 hour each, or until the tissue sank (this depended on the size of the tissue). The tissues were then mounted on 2cm diameter cork discs in Cryo-M-Bed embedding compound (Bright), orientated so the GFP cells were at the top, near the cutting surface, and frozen in isopentane cooled over liquid nitrogen to ensure more uniform and less rapid freezing through the tissue, thus causing less damage. Blocks were stored at -80°C. 10µm thick tissue sections were cut using a cryostat and collected

onto Menzel Gläser Superfrost Plus glass slides (Thermo Scientific). Those containing GFP-labelled (or DiI-labelled) cells were then stained using the appropriate antibodies.

2.4. Immunofluorescence staining

2.4.1. Pre-fixed staining

2.4.1.1. Cultured cells

Cells that were to be stained for intracellular antigens had to be pre-fixed and permeabilised to allow entry (and exit) of the antibodies. Cells were plated at an appropriate density (typically 25-40%) on 13mm glass coverslips and cultured for 24-48 hours. Immediately following removal from the tissue culture plate, cells were fixed using 100µl 4% paraformaldehyde per coverslip, for 10 minutes at room temperature. Subsequent to paraformaldeyde removal, fixation was quenched with 50µl of 0.1M glycine pH7.4 for 15 minutes at room temperature. Blocking was completed using 1% BSA, 0.1% Triton X100 in 0.12M phosphate pH7.4, and 50µl per coverslip was incubated at room temperature for 15 minutes. 50µl primary antibody (see Table 2.3) diluted in 1% BSA, 0.1% Triton X100 in 0.12M phosphate pH7.4 (or diluent alone for secondary antibody controls) was added per coverslip and incubated at room temperature for 30-60 minutes. Following primary antibody removal, coverslips were dip washed 3 times in PBS ($+Ca^{2+}/Mg^{2+}$). 50µl of the appropriate secondary antibody (see Table 2.4) diluted in 1% BSA, 0.1% Triton X100 in 0.12M phosphate pH7.4, plus 0.1µg/ml DAPI (Sigma-Aldrich), was incubated for 30-60 minutes for each coverslip, at room temperature in the dark. Secondary antibodies were removed, and cells washed 3 times in PBS, once in distilled water, and then left to dry before mounting onto a glass slide with Dako fluorescence mountant.

2.4.1.2. Frozen sections

10µm thick frozen sections were cut, collected onto Superfrost Plus glass slides, and hydrophobic rings were drawn around those sections containing GFP-Kelly cells using a Dako pen, which were then allowed to dry. Tissue had been fixed prior to the production of frozen blocks, therefore the staining procedure began with the addition of 50µl of 0.1M glycine pH7.4 per section, and incubation at room temperature for 15 minutes. The staining

protocol then proceeded exactly as for "cultured cells" above, except for the washing steps, where slides were submerged in PBS ($+Ca^{2+}/Mg^{2+}$) for 10 minutes, before dip washing a further 2 times, and then allowing for drying of the hydrophobic ring before the addition of the next solution. See Table 2.3 for the primary antibodies used to stain frozen sections.

Antibody	Dilution	Species raised in	Clonality	Cross reactivity	Source
Caspase 3	1:10	Rabbit	Polyclonal	Human, mouse, rat	Millipore ab3623
GFP	1:500	Rabbit	Polyclonal	-	Abcam ab290
HMB-45	1:5	Mouse	Monoclonal	Mouse, rat, human	Abcam ab732
Human nuclear antigen	1:50	Mouse	Monoclonal	Human	Chemicon MAB1281
ki67	1:100	Mouse	Monoclonal	Human	Dako F0788
MYCN	1:20	Mouse	Monoclonal	Mouse, human	Abcam ab16898
NB84	1:200	Mouse	Monoclonal	Human	Novocastra NCL-NB84
N-CAM (CD56)*	1:2.5	Mouse	Monoclonal	Human	Diaclone 852.703.020
Nestin	1:200	Rabbit	Polyclonal	Human, mouse, rat, hamster	Abcam ab5968
Phox2b	1:200	Rabbit	Polyclonal	Human, rodent	Sigma-Aldrich P0371
SMA	1:500	Mouse	Monoclonal	Rabbit, mouse, chicken, human, goat, sheep, rat, canine, bovine	Sigma-Aldrich A2547
Sox10	1:100	Goat	Polyclonal	Mouse, rat, human, equine, canine, bovine, porcine	Santa Cruz sc-17342
TH**	1:1000	Sheep	Polyclonal	Mammals	Abcam ab123
TUJ-1 (β-III-tubulin)	1:500	Mouse	Monoclonal	"Multi-species" (including chick, human, rat)	R&D mab1195
Vimentin	1:200	Mouse	Monoclonal	Rat, human, avian, porcine	Santa Cruz sc-6260

Table 2.3. Details of primary antibodies used in pre-fixed staining of cultured cells and/or tissue sections. * Antibodies that detect cell surface antigens, therefore would ordinarily be used in live staining. However, since frozen sections were already fixed, they were used as per the pre-fixed protocol. **Detected (successfully) using goat-specific secondary.

Antibody	Dilution	Source
Goat anti-mouse Alexa Fluor 488 (green)	1:500	Invitrogen, A11001
Goat anti-mouse Alexa Fluor 568 (red)	1:500	Invitrogen, A11004
Goat anti-rabbit Alexa Fluor 488 (green)	1:500	Invitrogen, A11034
Goat anti-rabbit Alexa Fluor 594 (red)	1:500	Invitrogen, A11012
Donkey anti-goat Alexa Fluor 488 (green)	1:500	Invitrogen, A11055
Donkey anti-goat Alexa Fluor 594 (red)	1:500	Invitrogen, A11058

Table 2.4. Details of secondary antibodies used in this project.

2.4.2. Live staining

Cells in culture that were to be stained for cell surface antigens were done so live. Cells were plated on 13mm glass coverslips and cultured for 24-48 hours. Following removal from the culture medium, 50µl primary antibody (see Table 2.5) diluted in 1% BSA in 0.12M phosphate pH 7.4 was added per coverslip and incubated at room temperature for 30 minutes. 50µl diluent alone was added for secondary antibody controls. Coverslips were dip washed 3 times in PBS ($+Ca^{2+}/Mg^{2+}$) and then incubated with 50µl secondary antibody (see Table 2.4) diluted in 1% BSA in 0.12M phosphate pH 7.4 for 30 minutes at room temperature in the dark. Coverslips were dip washed 3 times in PBS, and then fixed using 50µl 4% paraformaldehyde for 10 minutes. Following fixation, coverslips were washed a further 3 times in PBS, once in distilled water, and then left to dry, before mounting on a glass slide with Dako fluorescence mountant.

Antibody	Dilution	Species raised in	Clonality	Cross reactivity	Source
CD133	1:100	Rabbit	Polyclonal	Human	Autogen Bioclear abv-114
CD24	1:50	Mouse	Monoclonal	Human	Abcam ab76514
HNK-1 (CD57)	1:500	Mouse	Monoclonal	Human	Diaclone 853.463.020
N-CAM (CD56)	1:2.5	Mouse	Monoclonal	Human	Diaclone 852.703.020

Table 2.5. Primary antibodies used to live stain cultured cells.

2.4.3. Whole mount/explant staining

Fixed tissue pieces were first placed in 0.25% Triton x100 in PBS (PBST) for 1 hour on a rocker to permeabilise the cells within the tissue, following which they were blocked in 3% BSA in PBST for a further hour. The tissues were then incubated overnight at 4°C in the appropriate primary antibodies, diluted in 3% BSA in PBST (see Table 2.6). The following day, tissues were first washed briefly in PBST to remove the majority of the antibody, and then washed more thoroughly, 3-4 times for at least an hour each in PBST on a rocker. Tissues were once again blocked in 3% BSA in PBST, and then incubated overnight at 4°C with the appropriate secondary antibodies (see Table 2.4) diluted 1:500 in 3% BSA in PBST, plus 0.1µg/ml DAPI. The next day, tissues were washed briefly in PBST, and then washed 3-4 more times for at least an hour each in PBST on a rocker, covered in foil. They were then washed briefly in PBS before mounting between a glass slide and coverslip in Dako fluorescence mountant, ready for viewing.

Antibody	Dilution	Species raised in	Clonality	Cross reactivity	Source
GAP43 (chick-specific)	1:500	Rabbit	Polyclonal	Chick	(Allsopp & Moss 1989)
GAP43 (human-specific)	1:1000	Rabbit	Monoclonal	Mouse, rat, human	Abcam ab75810
GFP	1:500	Rabbit	Polyclonal	-	Abcam ab290
MYCN	1:10	Mouse	Monoclonal	Mouse, human	Abcam ab16898
NF 70kD	1:500	Rabbit	Polyclonal	Human, chick	Dr Diana Moss (University of Liverpool, UK)
TH**	1:1000	Sheep	Polyclonal	Mammals	Abcam ab123
TUJ-1 (β-III-tubulin)	1:500	Mouse	Monoclonal	“Multi-species” (including chick, human, rat)	R&D mab1195

Table 2.6. Primary antibodies used to whole mount stain chick tissue pieces. **Detected (successfully) using goat-specific secondary.

2.5. Cell proliferation detection

2.5.1. ki67

Following successful ki67 staining of cells in culture, yet no positive stain on frozen sections, various techniques were utilised in an attempt to optimise this antibody for use on tissue sections.

2.5.1.1. Antigen retrieval

An E11.5 mouse embryo was fixed in 4% paraformaldehyde for 1 hour, and then mounted as detailed in section 2.3.5, with the head in one block and the body in another, so that saggital sections could be taken. Antigen retrieval techniques were performed in the hope of a successful ki67 stain.

2.5.1.1.1. Sodium dodecyl sulphate (SDS)

Hydrophobic rings were drawn around each mouse tissue section using a Dako pen and allowed to dry. Slides were then washed 3 times for 5 minutes each in PBS ($+Ca^{2+}/Mg^{2+}$). A solution of 1% SDS dissolved in PBS was prepared, and 50µl added to each section and incubated at room temperature for 5 minutes. Following 3 5 minute washes in PBS, 50µl blocking solution (1% BSA, 0.1% Triton X100 in 0.12M phosphate pH7.4) was added per section for 10 minutes, and then 50µl ki67 antibody left on some sections for 1 hour at room temperature, and some sections overnight at 4°C – half at the usual dilution of 1:100 and half 1:50. Staining continued following the protocol in section 2.4.1.2.

2.5.1.1.2. Citrate buffer

Slides containing mouse embryo head or trunk tissue sections were washed 3 times for 5 minutes each in PBS ($+Ca^{2+}/Mg^{2+}$). Citrate buffer was made by dissolving anhydrous citric acid in distilled water to a concentration of 10mM, adjusting the pH to pH6.0 with 1M NaOH, and adding 0.05% Tween 20. The citrate solution was heated inside a beaker, on a hot plate, to 100°C, and the slides were immersed in the boiling buffer for 10, 20 or 40 minutes.

After cooling, slides were washed in PBS 3 times for 5 minutes each. Slides were allowed to dry, and then hydrophobic rings were drawn around each section with a Dako pen. 50µl blocking solution (1% BSA, 0.1% Triton X100 in 0.12M phosphate pH7.4) was added to each section, and antibody staining then proceeded as detailed in section 2.4.1.2, except that the ki67 primary antibody was left on some sections for 1 hour at room temperature and others overnight at 4°C – half at the usual dilution of 1:100 and half at 1:50.

2.5.1.2. Unfixed embryonic rat tissue

Tissues from the brains and intestines of E21 rat embryos were mounted unfixed, i.e. dissected from the rats, washed in PBS, and positioned in the Cryo-M-Bed embedding compound (Bright). Blocks were then frozen as detailed in section 2.3.5. 10µM sections of both tissues were fixed with 4% paraformaldehyde for 10 minutes, which was then quenched with 50µl 0.1M glycine pH7.4. A third of sections were immersed in boiling citrate buffer for 30 minutes, a third were treated with 1% SDS for 5 minutes, and the final third were stained without antigen retrieval. The ki67 antibody was used at a dilution of 1:50 and left on sections overnight.

2.5.2. EdU

The Click-IT EdU Imaging Kit was purchased from Invitrogen (C10339), and their protocol was either followed or adapted.

2.5.2.1. Cells in culture

At least 24 hours after seeding on 13mm glass coverslips, 5µM EdU was added to the culture medium, by producing a 2X (10µM) solution in the appropriate (fresh) medium and replacing half of the cells' culture medium with this solution. 24 hours later, cells were fixed in 4% paraformaldehyde for 10 minutes. Following 2 washes in 3% BSA in PBS, 50µl of 0.5% Triton X100 in PBS (PBST) was added to each coverslip and incubated for 20 minutes at room temperature. Since the Click-IT reaction cocktail used to detect the EdU results in the loss of GFP fluorescence, 50µl of an anti-GFP primary antibody (see Table 2.3) diluted in 3% BSA in PBS was incubated for 30 minutes at room temperature for those coverslips containing GFP-labelled cells. Following 3 washes in PBST, 50µl Click-IT reaction cocktail

(containing Alexa Fluor 594; see Invitrogen protocol) was added per coverslip and incubated for 30 minutes at room temperature in the dark. Following removal of the cocktail, cells were washed 3 times in 3% BSA in PBS. For coverslips containing GFP-labelled cells, the primary anti-GFP antibody was then detected using a goat-anti-rabbit Alexa Fluor 488 secondary (see Table 2.4) diluted in 3% BSA in PBS and incubating at room temperature in the dark for 30 minutes – this step was emitted when testing the system on non-GFP Kellys. Following 2 washes in PBST and 1 wash in PBS, 50µl Hoechst 33342, diluted 1:3000 in PBS, was incubated on each coverslip for 30 minutes at room temperature, protected from light. Each coverslip was then washed 3 times in PBS, once in distilled water, and once dry, mounted onto a glass slide using Dako fluorescence mountant.

2.5.2.2. Frozen sections

For chick tissue sections, EdU had already been injected into the chick embryos 24 hours prior to sacrifice, and tissues had been fixed before frozen blocks were produced. Hydrophobic rings were drawn around sections of interest using a Dako pen and once dry, sections were washed twice in 3% BSA in PBS, and then blocked for 20 minutes with 50µl 0.5% Triton X100 in PBS (PBST). EdU detection then proceeded exactly as for cells in culture (section 2.5.2.1).

2.5.2.3. Tissue pieces/explants

Tissues were fixed in 4% paraformaldehyde and then washed in 3% BSA in PBST 3 times for 5 minutes each. Tissues were permeabilised using 50µl PBST per coverslip, or 500µl per well (of a 24 well plate) containing multiple tissue pieces, which was incubated for 20 minutes at room temperature – each step in this protocol was completed on a rocker for the tissue pieces – before repeating twice more. 50µl anti-GFP primary antibody (see Table 2.3) per coverslip or 500µl per well, diluted in 3% BSA in PBST was incubated overnight at 4°C. Tissues were then washed for 3x1hour in PBST, following which 50µl Click-IT reaction cocktail (containing Alexa Fluor 594; see Invitrogen protocol) was added per coverslip/500µl per well and incubated for 90 minutes at room temperature in the dark. Following removal of the cocktail, cells were washed for 3x30 minutes in PBST. The GFP antibody was then detected using a goat-anti-rabbit Alexa Fluor 488 secondary (see Table 2.4) diluted in 3% BSA in PBST, incubated in the dark overnight. The next day, tissues were washed in PBST 3 times for an hour each, once in PBS for 30 minutes, and once in distilled water for 30

minutes. Hoechst 33342 was not added as the confocal microscope did not have the appropriate filter. The tissues were then mounted onto glass slides using Dako fluorescence mountant.

2.5.2.4. Cell proliferation quantification

Following the detection of EdU incorporation into GFP-Kelly cell nuclei, the proportion of dividing cells was determined by counting EdU-labelled nuclei and calculating this as a percentage of all the GFP-labelled cells. A minimum of 200 cells from at least two experiments, including tissue from at least three embryos per experiment was analysed.

2.6. MYCN fluorescence analysis

10µm frozen sections of E10 chick tissues containing GFP-labelled Kellys that had been immunofluorescence stained for MYCN were photographed using the Leica Application Suite software. Fluorescence intensity was measured using Image J software. In each photograph, the MYCN fluorescence intensity of every Kelly nucleus was measured individually. The “freehand selection” tool was used to demarcate an area that incorporated the majority of one Kelly cell nucleus (aided by the corresponding DAPI photograph), then by selecting “analyze” and “measure”, a mean fluorescence intensity value was obtained. An average background fluorescence value was calculated from the fluorescence intensity measurements for 6 individual chick nuclei per section, and this was subtracted from every single Kelly cell’s fluorescence value in that section. After accounting for background fluorescence, a mean was calculated from all of the individual Kelly values within a particular tissue, to obtain a quantitative MYCN fluorescence intensity value for that tissue.

2.7. Confocal imaging

Tissue pieces mounted onto microscope slides were viewed and photographed on a Zeiss LSM 710 confocal microscope. Images were processed using the Zeiss LSM Image Browser software.

2.8. E10 sympathetic ganglia and tail *in vitro* culture

2.8.1. Dissociated tissue culture

Following dissection of the E10 embryos, sympathetic ganglia and small pieces of tail tissue, both containing GFP-Kelly cells, were incubated for 30min at 37°C in 0.25% trypsin, washed 3 times in Hanks, and then dissociated in 1ml of medium by mechanical trituration using a reduced bore Pasteur pipette (flamed over a Bunsen burner). The single-celled suspensions (chick SG plus the Kelly cells originating within them, and tail cells with their associated Kellys) were plated onto glass coverslips coated for 1 hour with 10µg/ml Poly-L-lysine and 10µg/ml laminin in 0.1M sodium borate pH8.3. The volume of each well was made up to 500µl total with L15 medium (Gibco), containing 0.5% methyl cellulose, 10% FCS, 100U/ml penicillin, 100µg/ml streptomycin, 0.3% glucose and 5ng/ml NGF (Sigma-Aldrich).

2.8.2. Explant culture

Kelly-containing sympathetic ganglia and tail tissues were torn into small pieces of roughly 300-600µm diameter, and following confirmation that they contained GFP-labelled Kelly cells, were plated as explants onto Poly-L-lysine- and laminin-coated coverslips, in L15 medium as described above. 3 or 4 tissue pieces were explanted per well.

Both culture systems were incubated at 37°C in a CO_2-free incubator in order to maintain the correct pH, in accordance with a previously published protocol for sympathetic neuron culture (Mains & Patterso.Ph 1973). After 48 hours, EdU was added to the culture medium in each well to a concentration of 5µM. Cells were then incubated for a further 24 hours before fixation in 4% paraformaldehyde. Dissociated cells were stained for MYCN as detailed in section 2.4.1.1 and EdU incorporation was detected as in section 2.5.2.1. Explants were stained for MYCN using the whole mount method detailed in section 2.4.3 and EdU detected using the method detailed in section 2.5.2.3.

Chapter Three:
Results I – Optimisation of the chick embryo model system for neuroblastoma injection

3.1. Introduction

Neuroblastoma, like melanoma, is a neural-crest-derived malignancy, and also resembles melanoma in that it has unusually high rates of spontaneous regression. Therefore it was reasoned that neuroblastoma was a prime candidate on which to test the previously published chick embryo model detailed in Chapter One.

The chick embryo has long been used as a model system, in a multitude of different ways, to investigate phenomena such as neural crest development and diseases such as cancer. Although humans are closer to mice in the phylogenetic tree than chickens, embryonic development – particularly the early stages – is well conserved amongst all vertebrates. The chick embryo also has certain advantages over the mouse, in that it is significantly cheaper, and one has "easy access" to the developing embryo, for both manipulation and viewing, since it grows *in ovo* rather than *in utero*. In addition, chick development proceeds much more quickly than a mouse in its initial stages, as illustrated in Table 3.1.

Table 3.1. A comparison between the development of human, chicken and mouse embryos. Adapted from Butler & Juurlink 1987.

Chick embryonic development has been well studied and well documented. Although aging the embryos according to their number of days of incubation is a perfectly acceptable and indeed useful developmental assessment throughout most of their gestation, for the first few days, further breakdown into more detailed developmental stages is needed. In a batch of eggs that all go into the incubator at the same time, there can be a huge variation in developmental stages between individual embryos, which is generally most pronounced up to E3/4. In 1951, Hamburger and Hamilton published a universal staging system for chick embryos, which is still used today and is detailed in Figure 3.1 and Table 3.2.

This text box is where the unabridged thesis included the following third party copyrighted material:

http://www.docstoc.com/docs/91438835/HAMBURGER-POSTER

Figure 3.1. Series of photographs documenting Hamburger Hamilton stages 1-35 of chick embryonic development. Adapted from http://www.docstoc.com/docs/91438835/HAMBURGER-POSTER, courtesy of Wiley Developmental Dynamics.

HH stage	Time post fertilisation	Brief description
1		
2	6-7 h	
3	12-13 h	
4	18-19 h	Primitive streak at maximum length
5	19-22 h	Head process visible
6	23-25 h	
7	23-26 h	1 pair somites; neural folds in head
8	26-29 h	4 pairs somites; neural folds meet at midbrain level; foregut formation begins; blood islands over yolk sac, dorsal aorta forming
9	29-33 h	7 pairs somites; heart formation begins
10	33-38 h	10 pairs somites; 3 primary brain vesicles; pronephric kidney formation begins
11	40-45 h	13 pairs somites; anterior neuropore closing
12	45-49 h	16 pairs somites; anterior neuropore closing; heart S-shaped, blood circulation begins; liver primordium visible
13	48-52 h	19 pairs somites; neural tube closed down to posterior neuropore
14	50-53 h	22 pairs somites; pharyngeal arches 1+2 distinct; hindgut present as simple tube
15	50-55 h	24-27 pairs somites; optic cup completely formed
16	51-56 h	26-28 pairs somites; tail bud present; extra-embryonic vasculature formation complete
17	52-64 h	29-32 pairs somites; limb buds present; pancreas formation begins
18	65-69 h	30-36 pairs somites; amnion closed, allantois obvious; gall bladder formation begins; tongue swellings appear
19	68-72 h	37-40 pairs somites, extending into tail; eyes unpigmented
20	70-72 h	40-43 pairs somites; body rotation complete, faint eye pigmentation
21	3.5 d	43-44 pairs somites; primary sympathetic ganglia present
22	3.5 d	Somites extend almost to tip of tail; eye pigmentation distinct
23	4 d	Adrenal masses begin to form
24	4 d	
25	4.5-5 d	Elbow and knee joints distinct
26	5 d	Secondary sympathetic ganglia (“proper”) forms
27	5-5.5 d	
28	5.5-6 d	Beak outgrowth visible; future divisions of intestine recognisable
29	6-6.5 d	
30	6.5-7 d	Feather germs begin to form; chromaffin cells start to differentiate
31	7-7.5 d	
32	7.5 d	
33	7.5-8 d	
34	8 d	
35	8-9 d	Adrenal glands fully formed
36	10 d	Skull begins to ossify
37	11 d	
38	12 d	
39	13 d	Eyelids almost fully formed
40	14 d	
41	15 d	Metanephric kidneys fully functional
42	16 d	
43	17 d	Herniated intestine begins to be drawn back into abdomen
44	18 d	
45	19-20 d	

Table 3.2. Table linking Hamburger Hamilton stages with incubation time.

Dhanya Mullassery (PhD thesis) injected a single-cell suspension of DiI-labelled SK-N-BE(2)C neuroblastoma cells into the E2 neural tube, and found that after 48hr, the cells had segmented into clusters roughly at the levels of the intersomitic clefts, as was reported with the melanoma cells (Oppitz et al. 2007), and some were beginning to migrate with the host neural crest cells (Mullassery 2011). The neuroblastoma cells were behaving in a similar way to the melanoma cells and responding to their ancestral embryonic environment. Therefore the starting point for the project detailed in this thesis was effectively the positive control – do neuroblastoma cells proliferate to form a tumour in an inappropriate embryonic environment? Since the eye cup was a structure in which the injected cells could be nicely contained, yet would still have ample opportunity to invade, and an environment where the developmental signals found in the neural crest microenvironment would not be present, cell injections into this structure were attempted first.

3.2. Aims

To establish and optimise a new model system in which to study the effects of an embryonic microenvironment on neuroblastoma cells.

- Determine the most appropriate technique for cell administration – test intra-ocular versus intravenous injection.
- Test multiple neuroblastoma cell lines: SK-N-BE(2)C, SK-N-AS, SH-SY5Y, Kelly; and the mouse melanoma line B16 F12.
- Attempt to characterise Kelly cells – the most promising cell line.
- Determine the most effective cell labelling method – test DiI, CFDA-SE, GFP plasmids.
- Analyse the behaviour of neuroblastoma cells within the chick embryo by means of immunofluorescence staining frozen sections.

3.3. Results

3.3.1. SK-N-BE(2)C eye cup injections

Initial experiments used SK-N-BE(2)C neuroblastoma cell line, as it is MYCN-amplified, and therefore among the most aggressive lines. In addition, BE(2)Cs have been documented to

form tumours in nude mice (Gaze, Hamilton & Mairs 1994), so it was assumed they would do the same in the chick. As in the Oppitz (2007) paper, cells were injected into the chick embryo eye on embryonic day 3 (E3), equivalent to HH stage 18, and then dissected at E7. The authors of the melanoma paper did not detail their cell preparation or the number of cells transplanted, but in this investigation <0.5µl was injected (limited to the volume each eye could hold) of a cell suspension of 10^6 cells in 50µl volume per eye. Initially the cells were suspended 1:1 in DMEM medium and ice-cold matrigel, with the idea that the matrigel would begin to polymerise within the 37°C chick eye and hold the cells in place, but it made no difference to whether the cells leaked out of the eye cup or remained inside, compared to DMEM alone. The cell suspension contained around 0.2% fastgreen to enable visualisation of the cell suspension in order to confirm they were being injected into the correct place (Figure 3.2 B, arrow), and the cells themselves were labelled with DiI to allow their identification under a fluorescent microscope (Figure 3.2. A). Intra-ocular BE(2)C injections were successfully performed on approximately 40 embryos (that survived with DiI fluorescence inside the eye), in 9 separate experiments. Upon dissection, clumps of BE(2)C cells were usually found within the retina, attached to the internal surface of the lens and in the space outside the vitreous humor (Figure 3.2 and 3.3). When the DiI-containing tissue pieces were dissected out, fixed in paraformaldehyde and mounted between a glass slide and coverslip, the BE(2)C cells were seen to be intensely fluorescent. This suggested limited cell division within the population, due to the lack of dilution of the fluorescent molecules. 10µm frozen sections of the BE(2)C-containing eyes were stained with the ki67 antibody (Figure 3.3 G-I), and negative results implied that the neuroblastoma cells were not proliferating, however, subsequent experiments led to the conclusion that the ki67 antibody was ineffective when applied to frozen sections (see section 3.4. Discussion). Cells also failed to stain for caspase 3, a protein indicative of apoptosis. BE(2)Cs in culture stained positively for both ki67 and caspase 3, both when grown within matrigel and in normal medium alone (Figure 3.4), therefore at this time, a lack of staining for both of these proteins in the cells *in vivo* suggested that the cells were surviving, but not progressing through the cell cycle – in effect, just "sitting there" – as their rounded morphology made any attempts at differentiation seem unlikely. Sections were also stained with an antibody to the human nuclear antigen, to distinguish the human-derived neuroblastoma cells from the chick tissue, and confirm that the red fluorescence that presumably indicated the presence of DiI labelled cells was indeed the BE(2)C cells (Figure 3.3 A-F). This antibody had an extremely high background, and its results were variable – in some cases, a positive stain could be seen to stand out as more intense from the background (Figure 3.3 B, arrows), yet in other sections, no positive stain could be seen (Figure 3.3 E), even when I was relatively confident of the presence of cells. This antibody was not deemed to be particularly reliable.

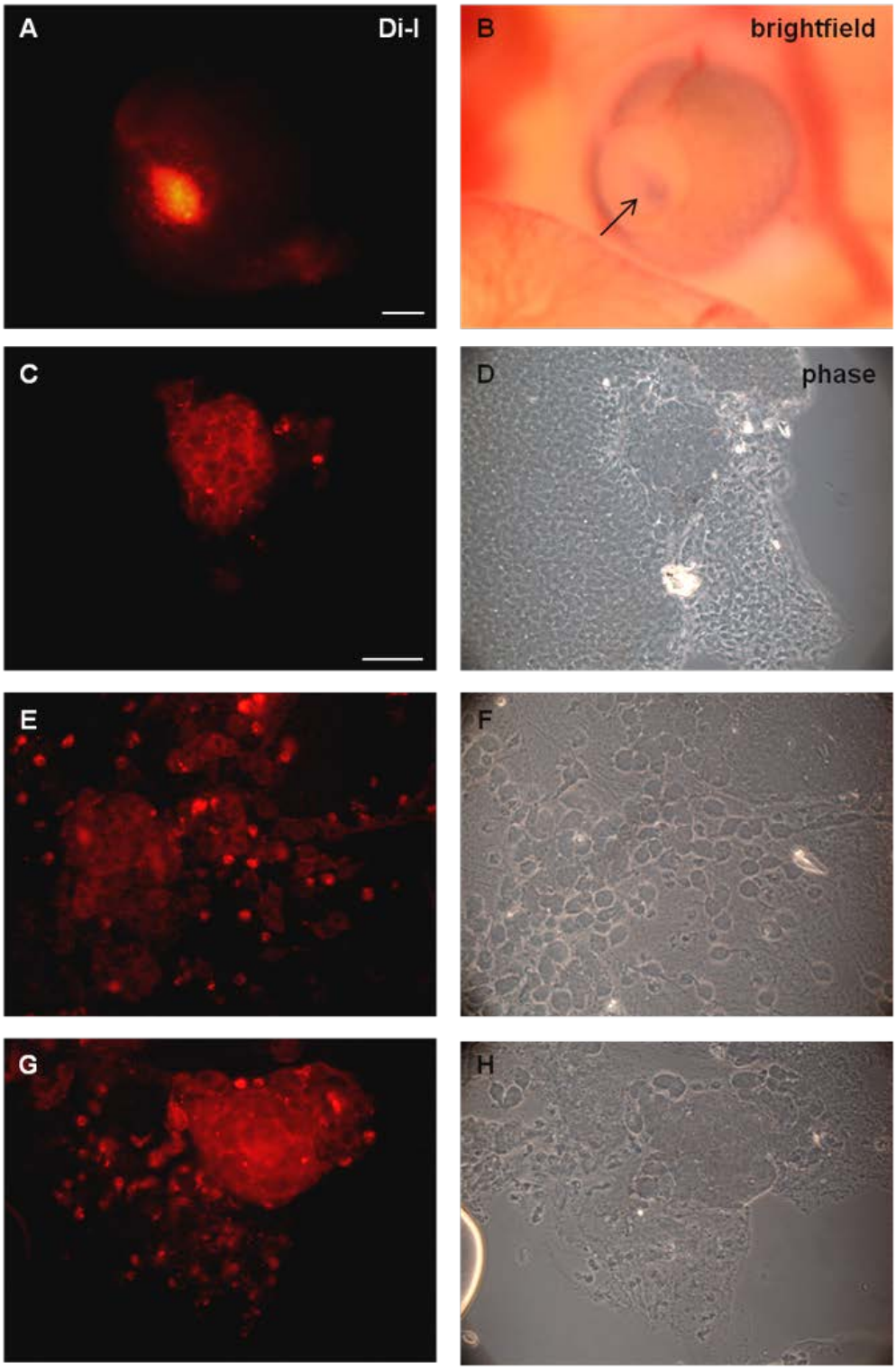

Figure 3.2. <10,000 DiI-labelled BE(2)C cells were injected into the E3 chick eye. A, fluorescence and B, brightfield image of cells shortly after injection. Arrow points to fastgreen-labelled cell suspension. C-H, eye tissues from E7 chicks were dissected, and those containing BE(2)C cells were “squashed” between a slide and coverslip. C,D, retina; E-H lens. Scale bars A-B 100µm, C-H 50µm.

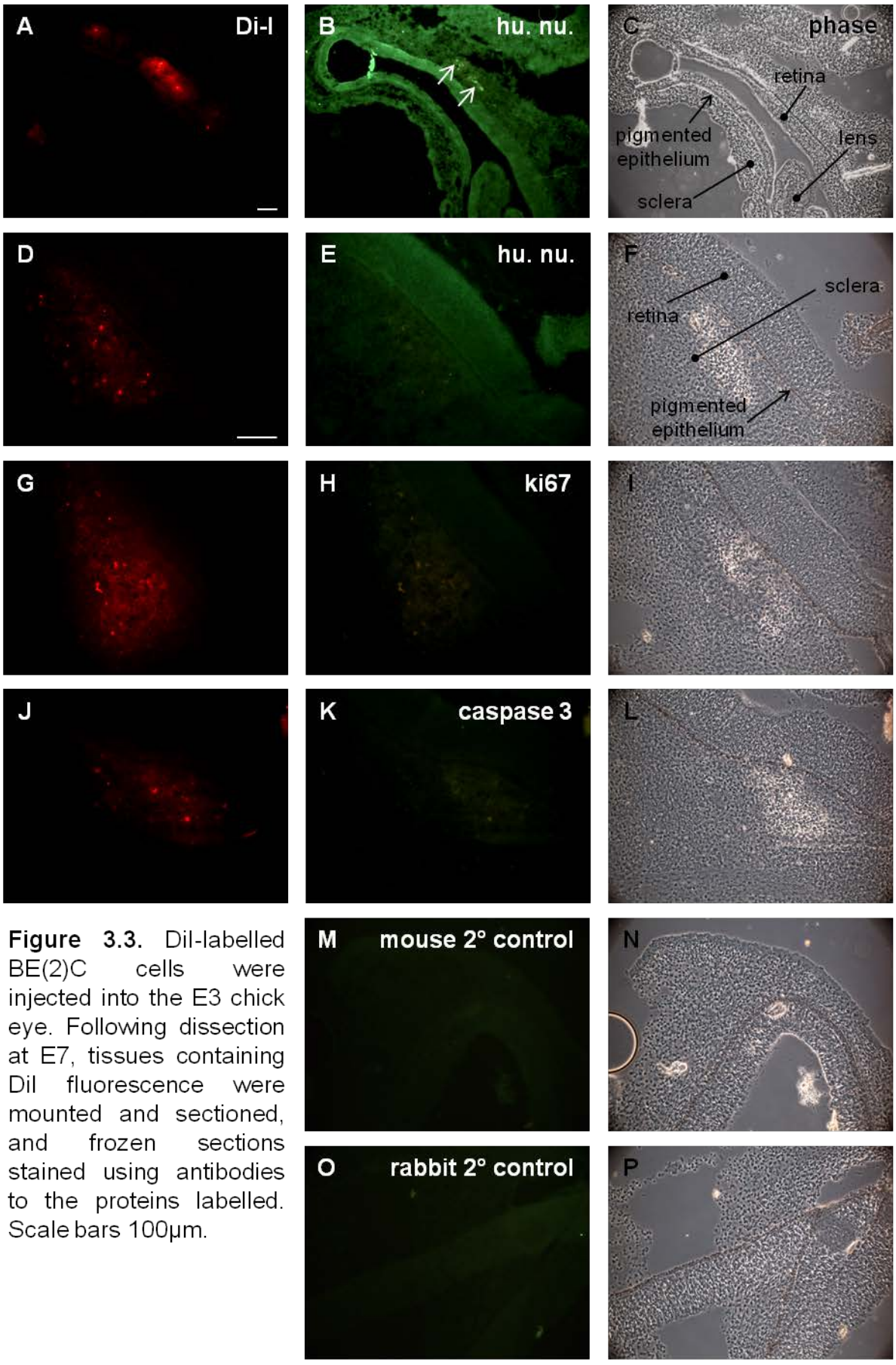

Figure 3.3. DiI-labelled BE(2)C cells were injected into the E3 chick eye. Following dissection at E7, tissues containing DiI fluorescence were mounted and sectioned, and frozen sections stained using antibodies to the proteins labelled. Scale bars 100μm.

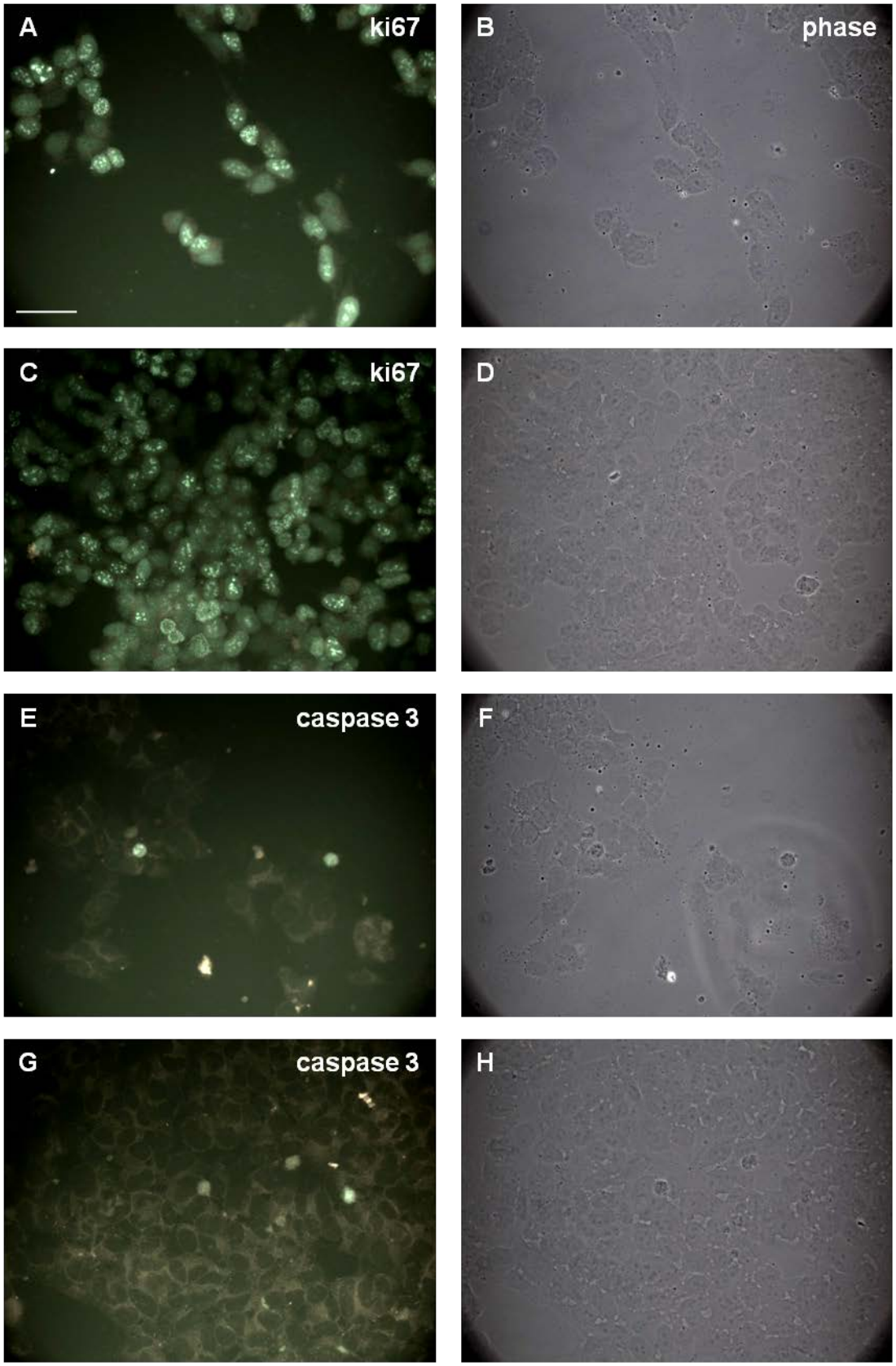

Figure 3.4. In parallel to the chick eye cup injections, DiI-labelled BE(2)C cells were "injected" by mouth pipette on to glass coverslips, grown in culture, then stained using antibodies as labelled. A-B, E-F, cells in a 1:1 matrigel:PBS suspension; C-D, G-H, cells suspended in PBS. Scale bar 50µm.

3.3.2. B16 F1 eye cup injections

As the results of the melanoma eye cup injections had not been reproduced using neuroblastoma cells, the B16 F1 mouse melanoma cell line used by Oppitz et al. (kindly donated by Prof Dot Bennett, St George's University of London, UK) were injected using the same methods as for our BE(2)C eye cup injections (Figure 3.5).

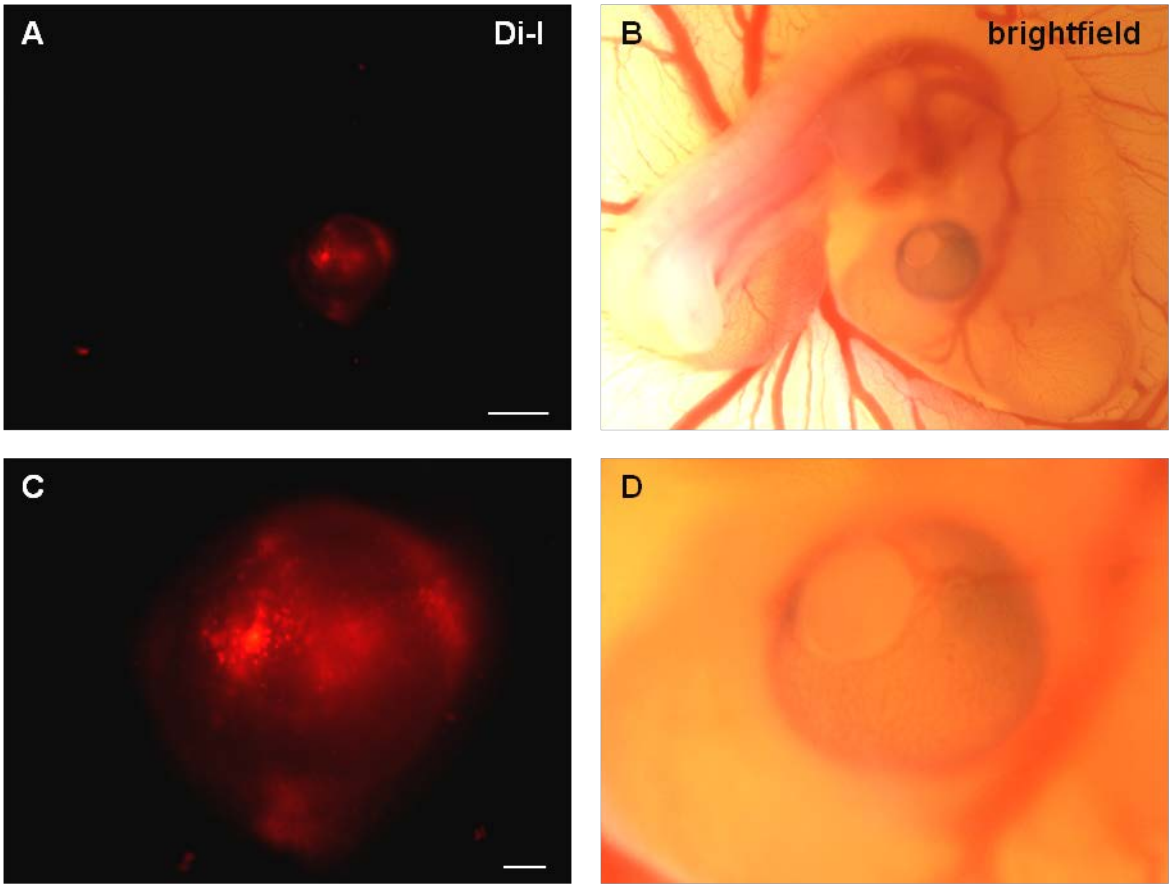

Figure 3.5. <10,000 DiI-labelled B16 F1 mouse melanoma cells were injected into the E3 chick embryo eye. Photographs show cells within the E4 chick eye, 24 hours after injection. Scale bars A-B, 500µm; C-D, 100µm.

Approximately 40 embryos (from 8 separate batches) survived to E7, at which point the eyes were dissected. Upon dissection, the melanoma cells were easily identifiable, even without fluorescence, due to their obvious pigmentation (Figure 3.6). Like the BE(2)Cs, melanoma cells were found within the retina, on the back of the lens, and outside the vitreous humor (Figure 3.6).

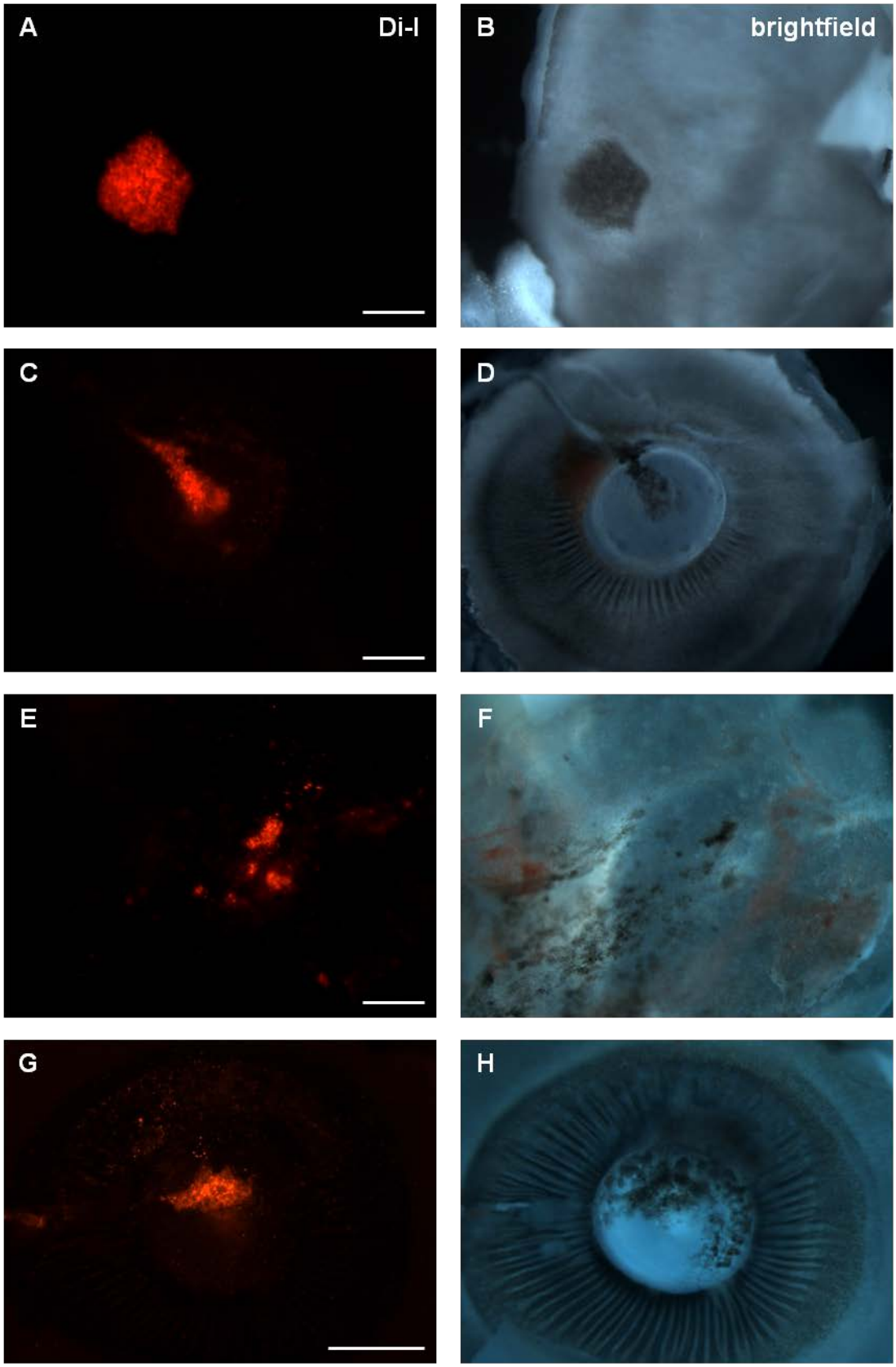

Figure 3.6. Dissected A-D, E7; E-H, E10 chick eye tissues containing DiI-labelled B16 F1 mouse melanoma cells that had been injected at E3. A-B,E-F, retina; C-D,G-H, internal view of the lens. Scale bars A-F, 500µm; G-H, 1mm.

Tissues were then mounted between a glass slide and coverslip and observed under a higher magnification than was permitted by the dissecting microscope. The cells were found to have a similar appearance to the BE(2)Cs, often residing in clumps and usually retaining their DiI fluorescence (Figure 3.7). In frozen sections, confirmation that the red DiI fluorescence belonged to B16 F1 cells was achieved by staining with the Human Melanoma Black antibody, HMB-45 (Figure 3.8 A-C). However, cell division was not detected with the ki67 antibody (Figure 3.8 D-F), again despite the fact that the B16 F1 cells in culture all stained brightly for this protein, when cultured with and without matrigel (Figure 3.9 E-H). Since caspase 3 is a protein involved in the apoptotic pathway, those cells that had already undergone the process may not have been identified by this antibody, plus even those that stained positively had an altered cell morphology, so although we were fairly confident of a tiny proportion of positively staining B16 F1 cells in culture (Figure 3.9 I-L), it was not clear whether the odd stained cell in the sections was authentic caspase 3 staining or an artefact (Figure 3.8 H, arrow). Nevertheless, it was clear that there were not vast numbers of these cells undergoing apoptosis. The apparent lack of cell proliferation was still a mystery, as the sheer size and appearance of the “tumours” seen in the Oppitz (2007) work suggested this to be the case. Further sections stained for HMB-45, showed corresponding green HMB-45 melanoma-specific fluorescence over a clump of DiI fluorescent cells in the retina, but also identified an extension of this clump deeper into the tissue, which had lost most, if not all, of its DiI red fluorescence (Figure 3.10 A-D). This suggested that the cells had been proliferating, which had resulted in a dilution of the DiI (unfortunately these sections were not stained for ki67). Proliferation had been assessed using ki67 staining in early experiments, however subsequent results revealed that ki67 failed to stain frozen sections unlike cultured cells (see section 3.4. Discussion). The staining in Figure 3.10 A-D also implied that the cells had invaded further into the tissue (although this could not be confirmed, as it may well have been the route of injection at E3, and so the cells could have been deposited here as the needle was removed). The invasive nature of these cells when placed in the eye cup was substantiated by the finding of chains of single cells stained with HMB-45 (Figure 3.10 E-H), that were further along the section than the clump mentioned above, and appeared to be migrating through the chick tissue. This was deemed to be a somewhat successful replication of the published melanoma experiments, therefore focus was returned to the neuroblastoma cells.

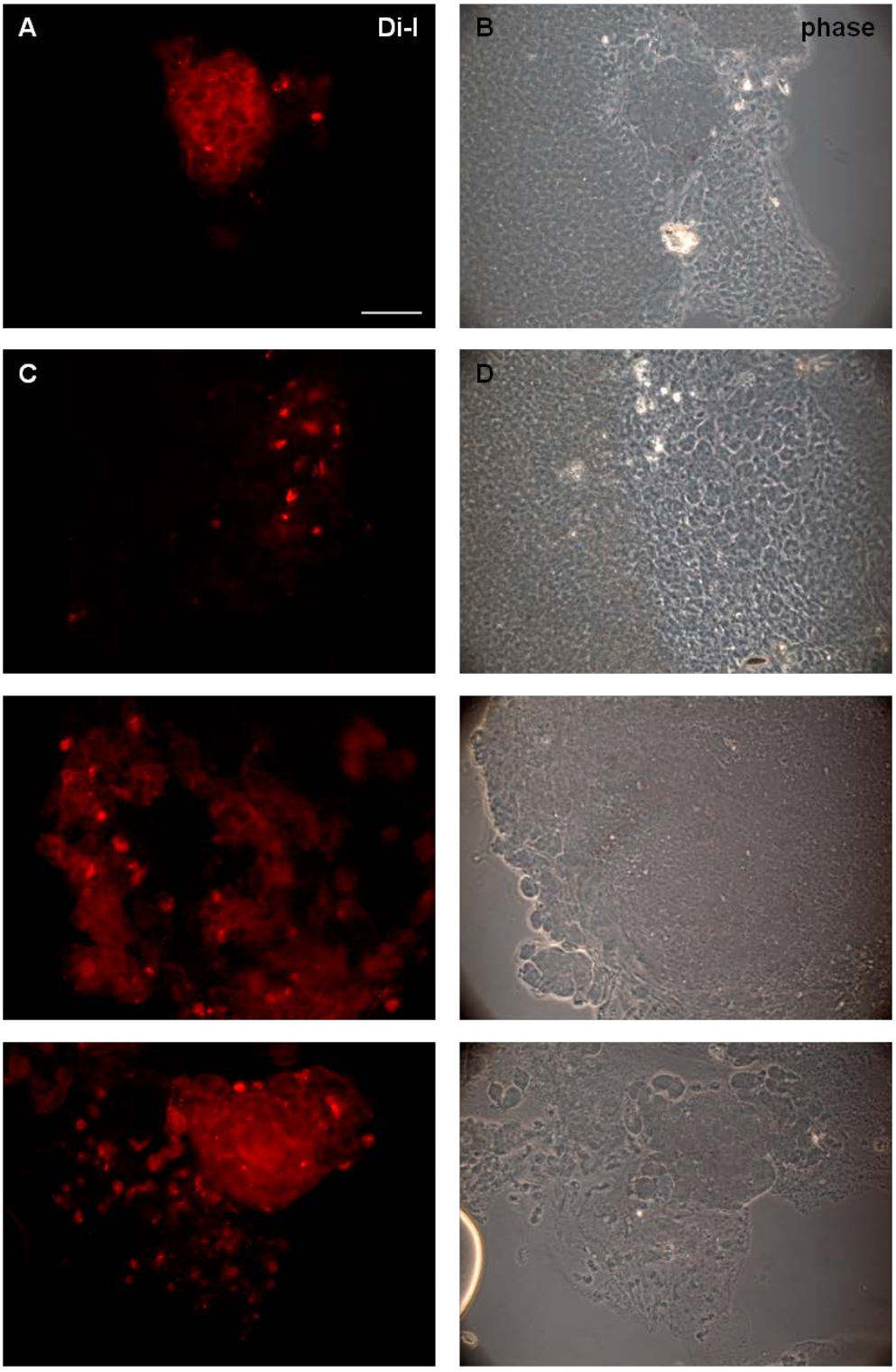

Figure 3.7. Following injection at E3, DiI-labelled B16 F1 mouse melanoma cells were left to reside in the chick embryo eye until dissection at E7. Tissues found to contain DiI fluorescence were mounted between a glass slide and coverslip. A-D, retina; E-H, lens. Scale bar 50µm.

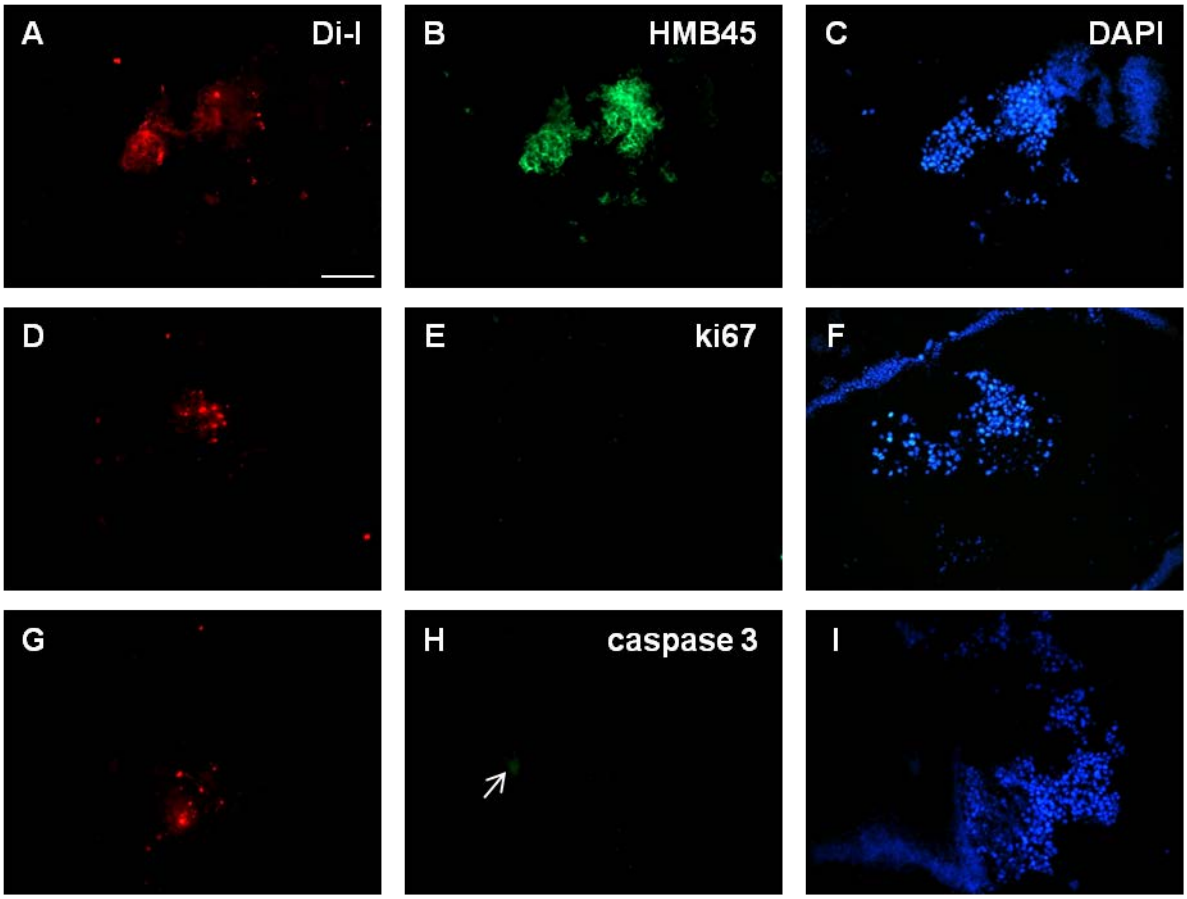

Figure 3.8. Following intra-ocular injection of DiI-labelled B16 F1 mouse melanoma cells at E3 and dissection at E7, E7 chick eye tissues containing DiI fluorescence were frozen and sectioned. 10µm sections were then stained using antibodies to the proteins as labelled. Scale bar 100µm.

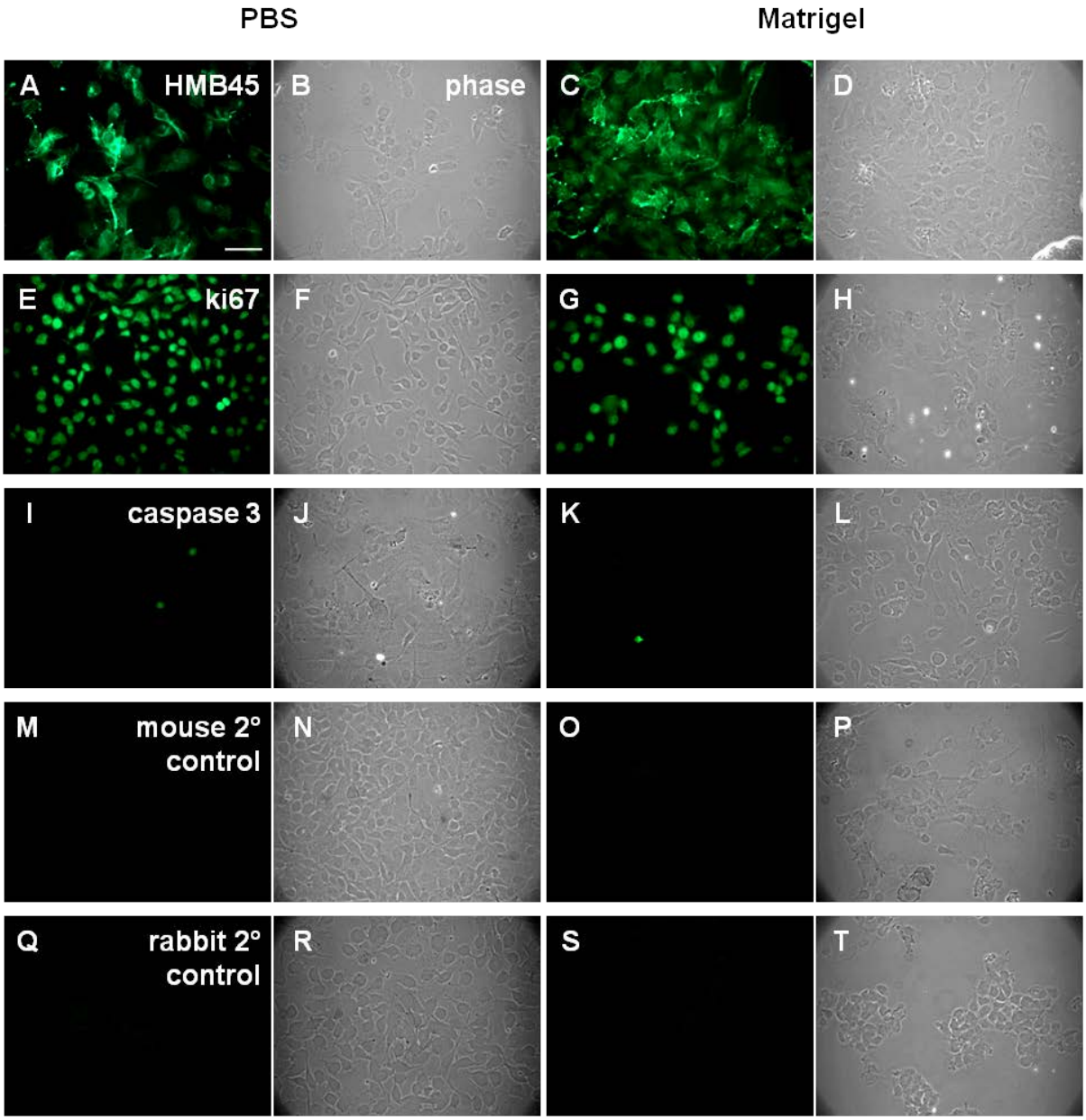

Figure 3.9. B16 F1 mouse melanoma cells were plated within a cell suspension of PBS (left column) or matrigel (right column), cultured in appropriate medium for 24 hours, and then stained with antibodies as labelled. Scale bar 50µm.

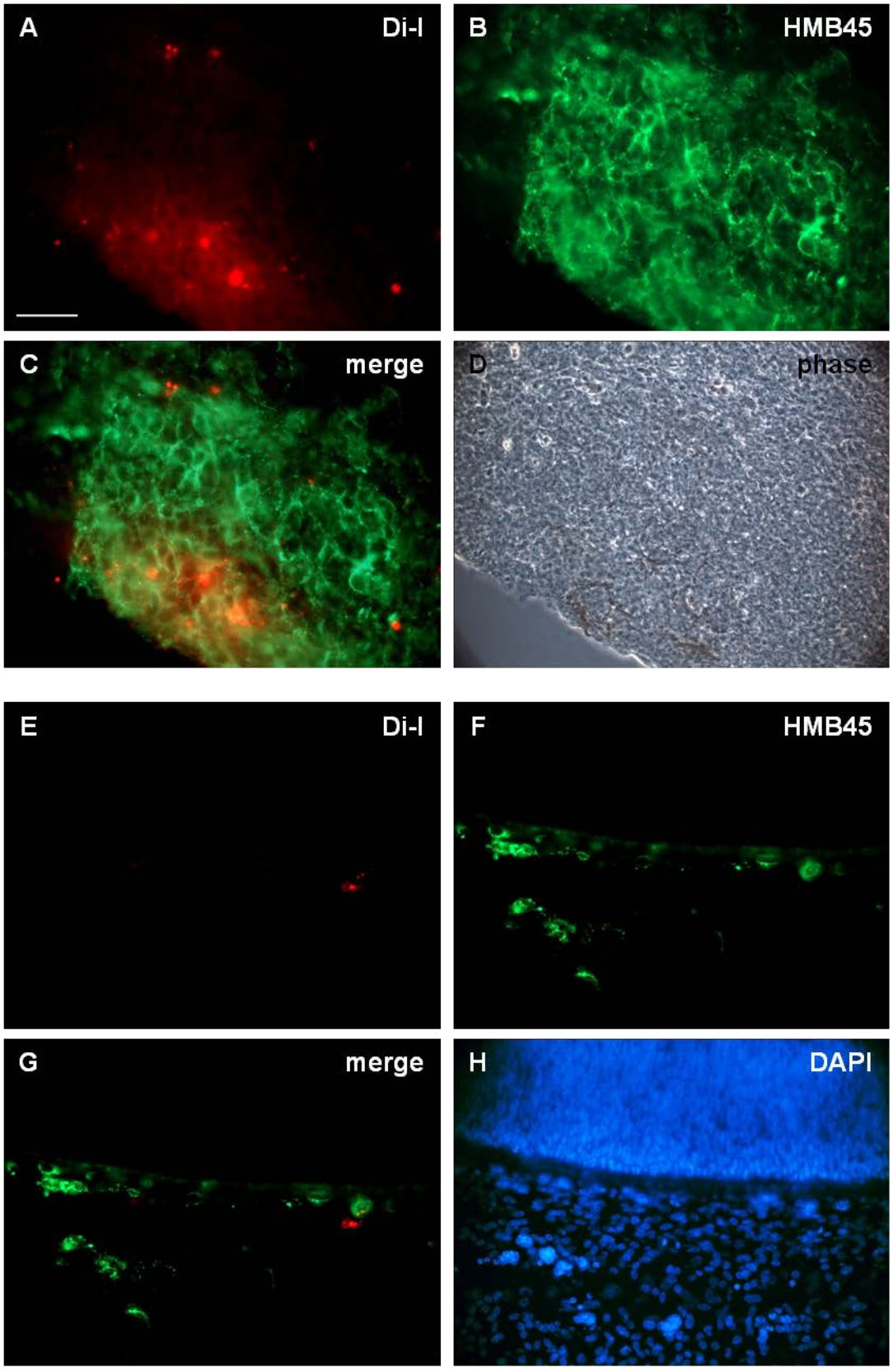

Figure 3.10. Following intra-ocular injection of DiI-labelled B16 F1 mouse melanoma cells at E3 and dissection at E10, 10µm frozen sections of E10 eye tissues were stained with an antibody to HMB45 in order to conclusively identify the melanoma cells. Scale bar 50µm.

When additional BE(2)C eye cup injections failed to reproduce the melanoma results, the distinct possibility that the eye cup environment was not a suitable one to facilitate neuroblastoma growth led to a change in strategy. In accordance to the seed and soil hypothesis proposed by Stephen Paget in 1889, it was hoped that by introducing the cells by intravenous injection, the “seeds”, i.e. the cancer cells, would be carried around the chick embryo vasculature and locate to the appropriate “soil” – chick tissue microenvironment – in which conditions were favourable for said neuroblastoma cells to thrive.

3.3.3. SK-N-BE(2)C intravenous injections

Intravenous injections were carried out at E3 because this is the earliest point at which a complete circulatory system is present. This new method of administration meant that significantly more neuroblastoma cells could be introduced into the embryos. The volume that the E3 circulation is capable of holding was the limiting factor, and after several attempts, and depending on the stage of development of the embryo (E3 chicks can vary from around HH stage 16-20, but are usually around HH stage 18), it was concluded that the optimum injectable volume was around 2µl, generally not more than 3µl. A single-celled suspension of 100,000 DiI-labelled cells per microlitre was prepared, and injected into the E3 extra-embryonic vitelline vein (Figure 3.11 B, D, arrows). The fastgreen allowed visualisation of the cell suspension being carried away by the chick circulation, straight into the heart and then around the body, and sometimes, as in Figure 3.11 D, the entire chick embryo turned green. Under fluorescence, the red BE(2)C cells could be seen throughout the entire chick embryos and in the extra-embryonic blood vessels (Figure 3.11 A, C), and as demonstrated in Figure 3.11 E-F and G-H, cells were passing through even the thinnest intersomitic vessels and those in the brain.

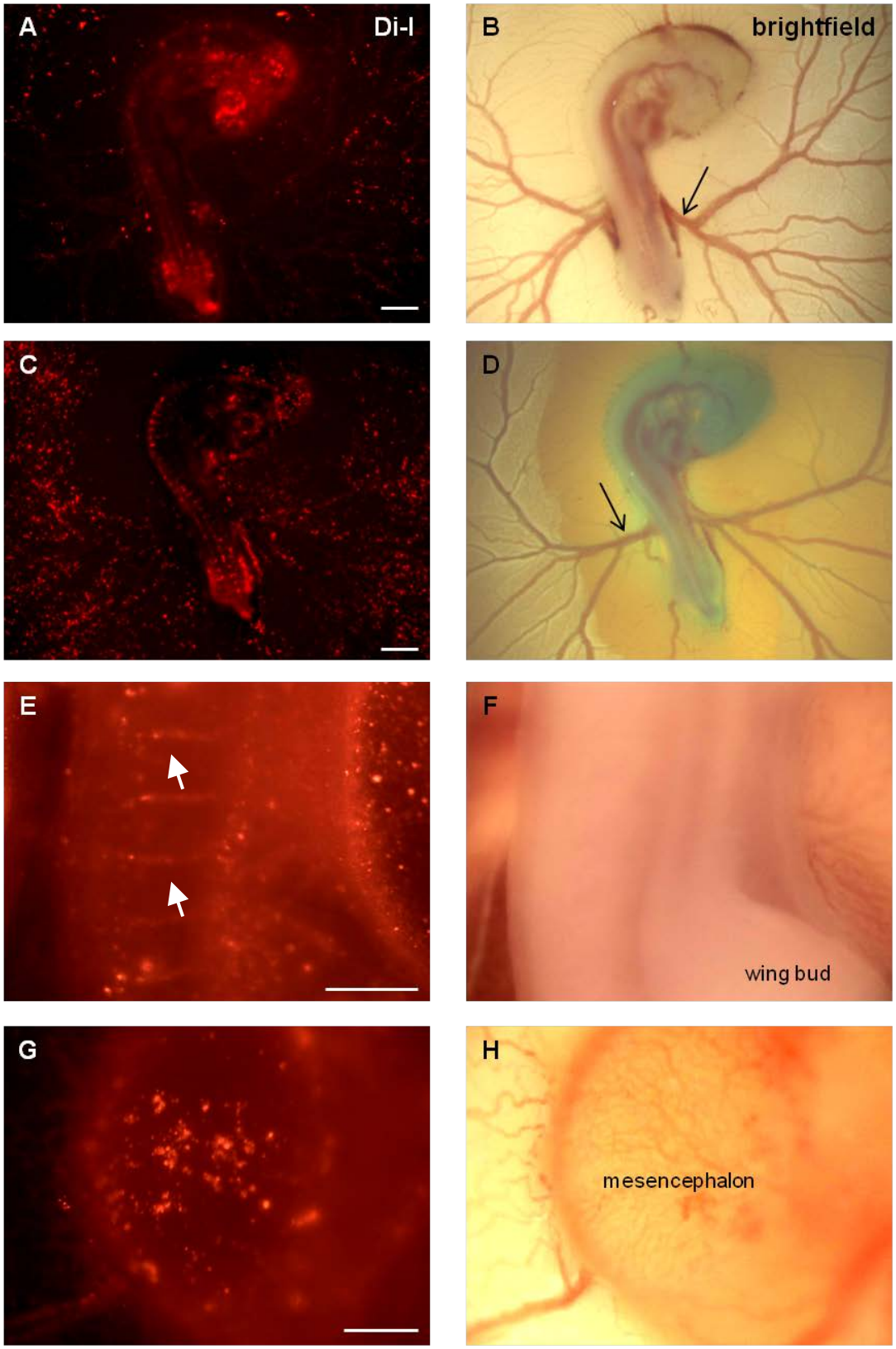

Figure 3.11. 200,000 DiI-labelled BE(2)C cells were injected into the extra-embryonic vitelline vein at E3. Chicks were photographed soon after injection. Some cells had settled within embryonic tissues, whereas others were still circulating. A-D, whole chick, open arrows (black) indicate sites of injection; E-F, DiI-labelled cells within the horizontal intersomitic vessels (closed arrowheads, white); G-H, brain. Scale bars A-D, 1mm; E-G, 500µm.

These cells could still be visualised 24 hours later, at E4. However from E5/6 onwards, the increasing size of the embryos hence greater density of body tissues, as well as the overlying allantois, made it impossible to observe the DiI-labelled cells anywhere other than the extra-embryonic blood vessels and external body parts such as the eyes (when the embryos positioned themselves so that these came into view). The embryos were therefore left in a humidified incubator until E9 or E10, at which point they were dissected and the locations of fluorescence noted. Following 6 (E9) or 7 (E10) days *in vivo*, DiI fluorescence was observed throughout the majority of the embryonic tissues in every successfully-injected embryo (n = approximately 35 surviving embryos, 9 separate experiments). Interestingly, fluorescence (which was presumed to be an indicator of BE(2)C cells) was found within the sympathetic ganglia of almost all embryos, a structure in which neuroblastoma develops in humans. This fluorescence was present in two forms – as small "speckles" (Figure 3.12 A+E), which may possibly have been DiI molecule incorporation into individual cells, and as larger patches of fluorescence that were somewhat "hazy" in appearance (Figure 3.12 C+G), it was considered that these may be small tumour-like masses of neuroblastoma cells. DiI fluorescence was also found in the gut – from the oesophagus down to the cloaca, including the gizzard (an organ unique to avians and known as the mechanical stomach) (Figure 3.13 A-B), small intestine, caeca and colon. See Figure 3.14 for overview of the chicken's digestive system. This DiI appeared more like flecks of fluorescence, as opposed to the clumps sometimes seen in the sympathetic ganglia. In the meninges, the DiI occurred both as tiny speckles – which may have been within the plasma membranes of individual cells, or may have been DiI molecules that had precipitated out of the cells – and as larger clumps of cells, roughly 25-100µm in diameter (Figure 3.13 C-F).

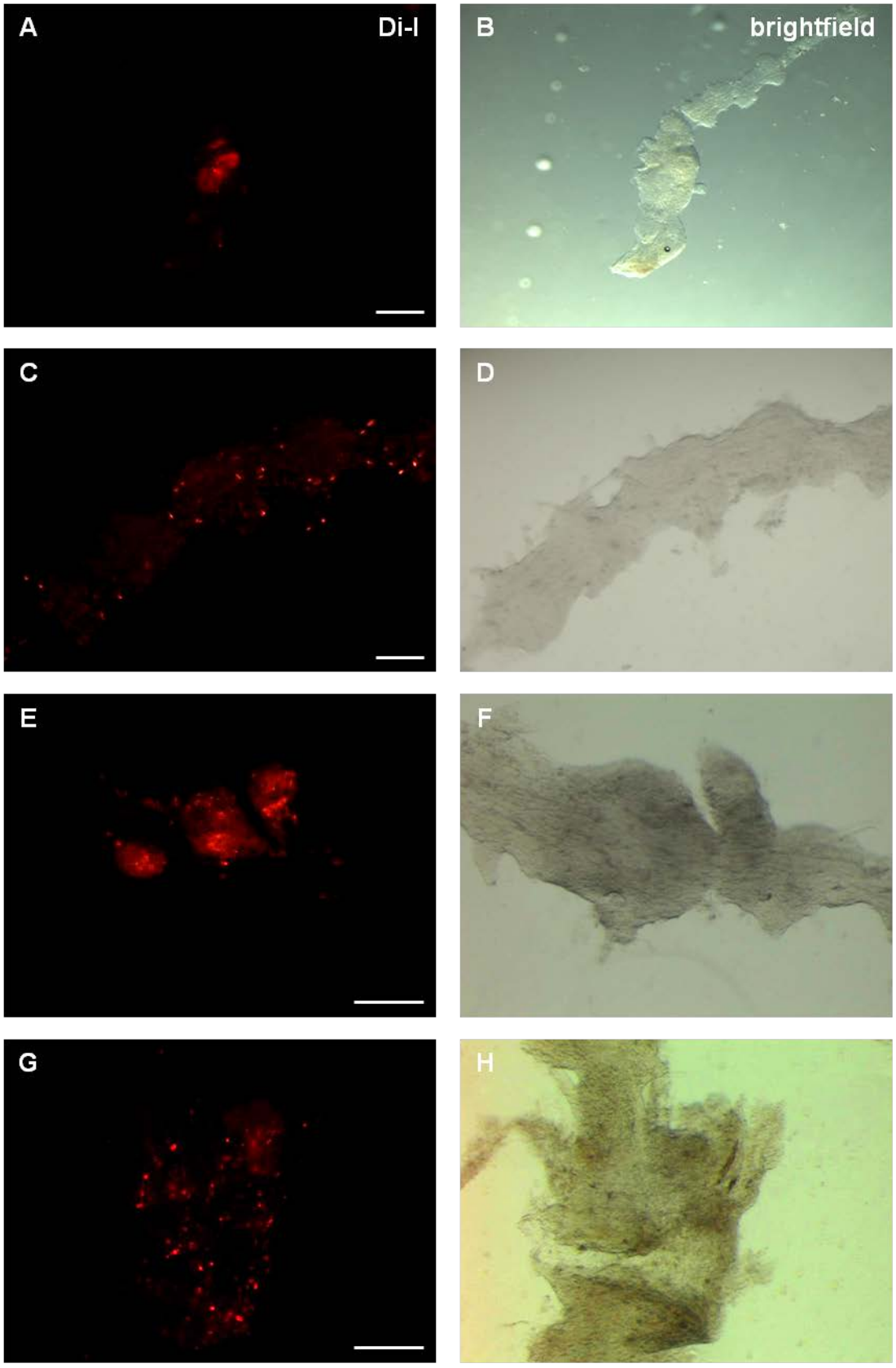

Figure 3.12. DiI-labelled BE(2)C cells within the chick sympathetic ganglia. Following intravenous injection at E3, chicks were dissected and photographed at A-D, E9; E-H, E10. Scale bars A-B, 500µm; C-H, 200µm.

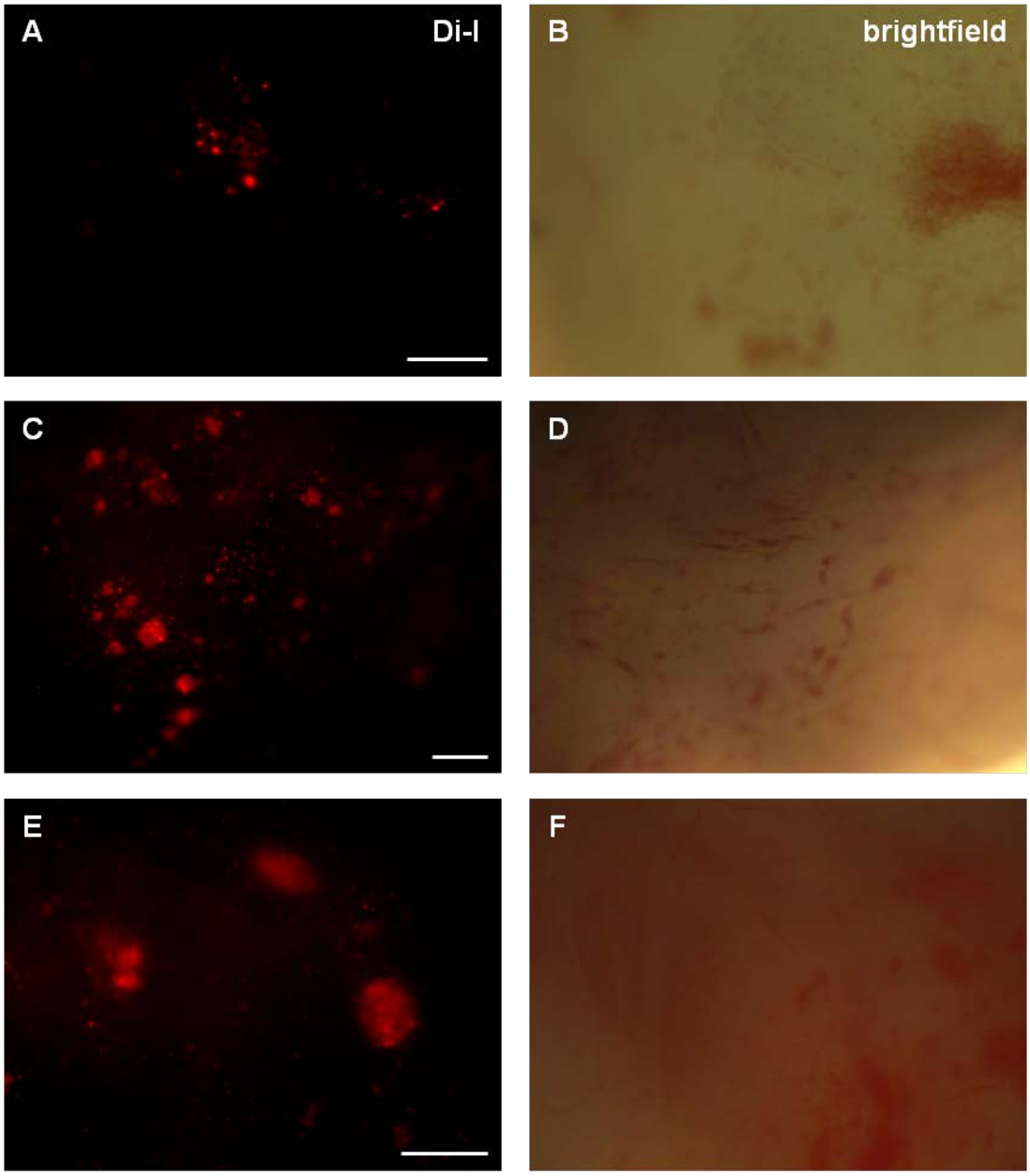

Figure 3.13. DiI-labelled BE(2)C cells within the A-B, E10 gizzard; C-D, E9 meninges; E-F, E10 meninges. Cells were injected intravenously at E3, and chicks dissected and photographed when specified. Scale bars A-B, 200µm; C-F, 500µm.

This text box is where the unabridged thesis included the following third party copyrighted material:

http://www.ca.uky.edu/poultryprofitability/Production_manual/Chapter3_Anatomy_and_Physiology/Chapter3_digestive.html *[Figure 3.2]*

Figure 3.14. Digestive system of adult chicken, dissected and laid out as organised *in vivo*. Photograph taken from http://www.ca.uky.edu/poultryprofitability/Production_manual/Chapter3_Anatomy_and_Physiology/Chapter3_digestive.html

Particularly large clumps of cells were consistently observed in the tail regions of the embryos (Figure 3.15 A-B), ranging from around 30-300µm in diameter. Other organs, such as the heart (Figure 3.15 C-D), liver (Figure 3.15 E-F), kidneys (Figure 3.15 G-H), lungs and spleen had speckles of fluorescence throughout, which in the heart was always more concentrated in the conotruncal region (i.e. in the vicinity of the great vessels) and often at the apex, but in the other organs, was much more dispersed.

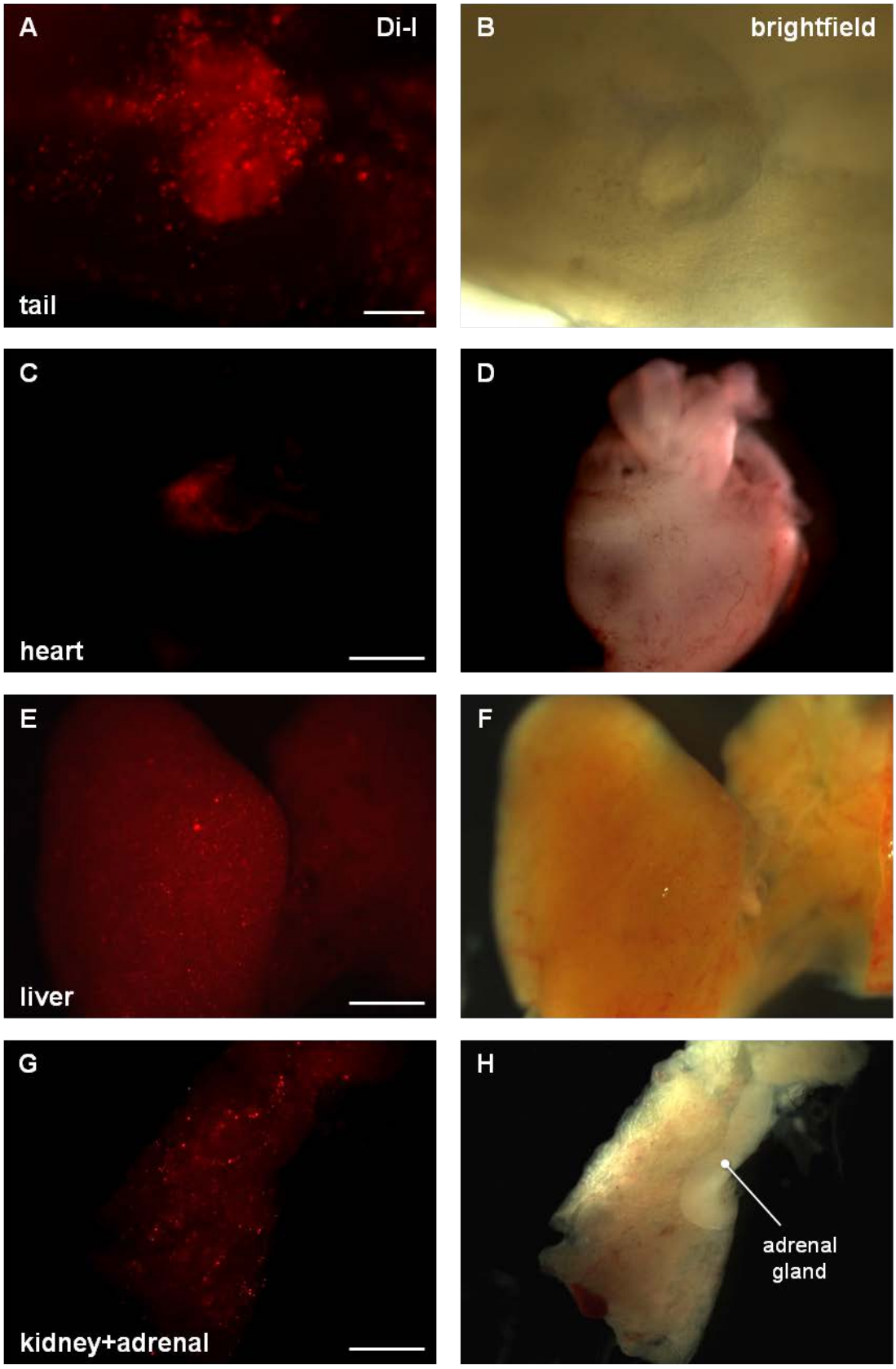

Figure 3.15. DiI-labelled BE(2)C cells were injected intravenously into E3 chick embryos. Upon dissection at E10, DiI fluorescence was observed within the A-B, tail; C-D, heart; E-F, liver; G-H, kidney. Minimal fluorescence was found in the adrenal glands (G-H). Scale bars A-B, 200µm; C-H, 1mm.

Following 6-7 days in the embryo, it was extremely difficult to confirm whether the fluorescence observed was due to the presence of BE(2)C cells, or molecules of DiI that had left the neuroblastoma cells and incorporated into the chick tissues. Therefore, two thin (hence easy to mount) tissues were chosen for increased scrutiny – the sympathetic ganglia and meninges – which both had speckles and clumps of fluorescence. The tissues were fixed and then "squashed" between a glass slide and coverslip within Dako fluorescence mountant, following which they could be observed under a x40 oil magnification lens. As shown in Figure 3.16 A, in certain areas of the sympathetic ganglia, speckles could be seen to define the outline of a small number of cells – seemingly the BE(2)C cells incorporated into the SG tissue. Upon inspection of the fluorescent clumps within the SG, although less clear, cellular outlines were still perceived, particularly within the area defined by the dashed lines in Figure 3.16 C. These areas were similar in appearance to those in the meninges, (Figure 3.16 E, G), which themselves were of various sizes.

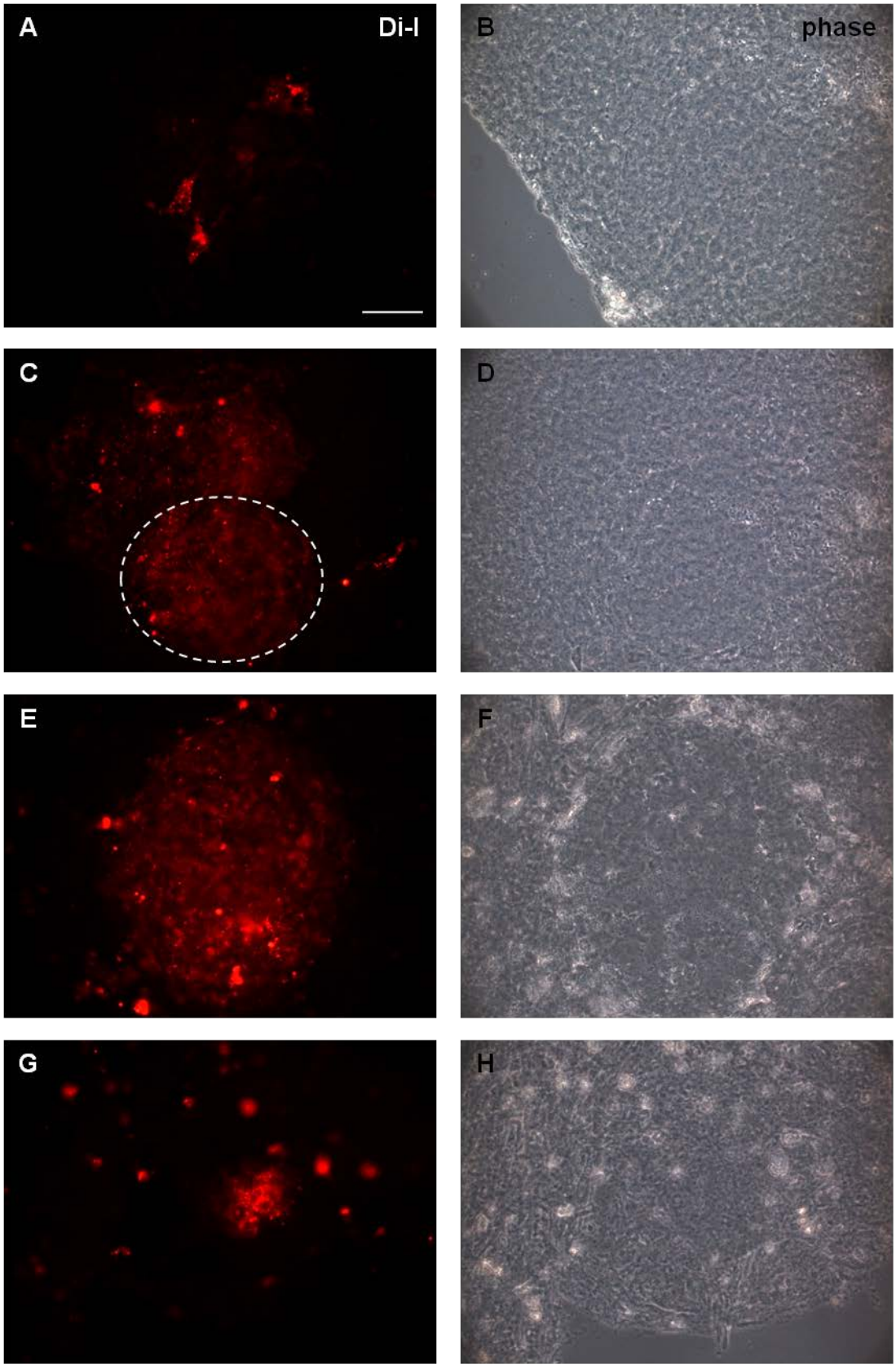

Figure 3.16. Following E3 intravenous injection of DiI-labelled BE(2)C cells, chicks were dissected at E10, and tissues containing DiI fluorescence were mounted between a glass coverslip and slide. A-D, sympathetic ganglia; E-H meninges. Scale bar 50µm.

Being relatively confident that at least some of the fluorescence observed within embryonic tissues was incorporated into the external membranes of cells, the next task was to conclusively identify that these were the human neuroblastoma cells and not chick cells. In histopathology laboratories, identification of neuroblastoma is aided by a positive stain for the proteins NB84 and N-CAM (CD56). Frozen sections of chick tissues containing DiI-labelled areas were stained for these human-specific antibodies, and a positive result led to the presence of BE(2)C cells being confirmed (Figure 3.17).

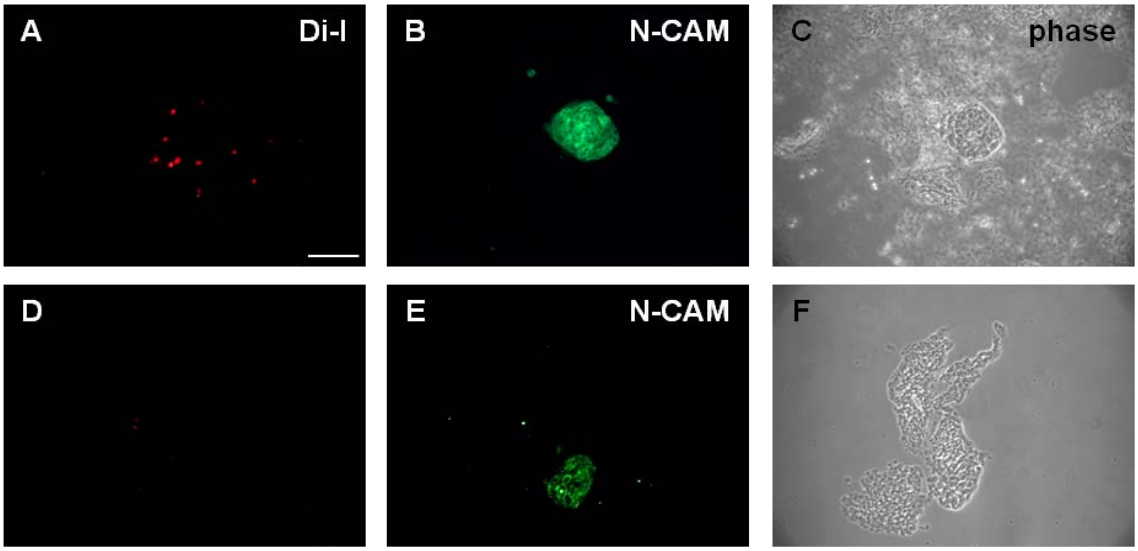

Figure 3.17. DiI-labelled BE(2)C cells were intravenously injected into E3 chicks, which were then dissected at E10. A-C, meninges; and D-F, sympathetic ganglia containing DiI fluorescence were frozen and sectioned. 10µm sections were stained using antibodies as labelled, to aid in the identification of neuroblastoma cells. Scale bar 100µm.

3.3.4. SK-N-AS and SH-SY5Y intravenous injections

DiI labelled cells from the SK-N-AS and SH-SY5Y neuroblastoma cell lines were also (separately) injected into the chick bloodstream at E3, using the same method as for the BE(2)C cells, and then dissected at E10. Around 10 embryos containing DiI fluorescence, from 2 separate experiments, were dissected at E10 for each cell line. Both SK-N-AS and SY5Y cells have a single copy of the MYCN gene and very low MYCN protein expression, in contrast to the MYCN-amplified BE(2)Cs. However, results were very similar to those obtained with DiI-labelled BE(2)Cs – for example, with speckles and clumps in the sympathetic ganglia and meninges, clumps in the tail, speckles around the great vessels of the heart, speckles in the liver, kidneys and spleen – observations were consistent in all embryos. A representation of these dissections can be seen in Figures 3.18 (SK-N-AS) and 3.19 (SH-SY5Y).

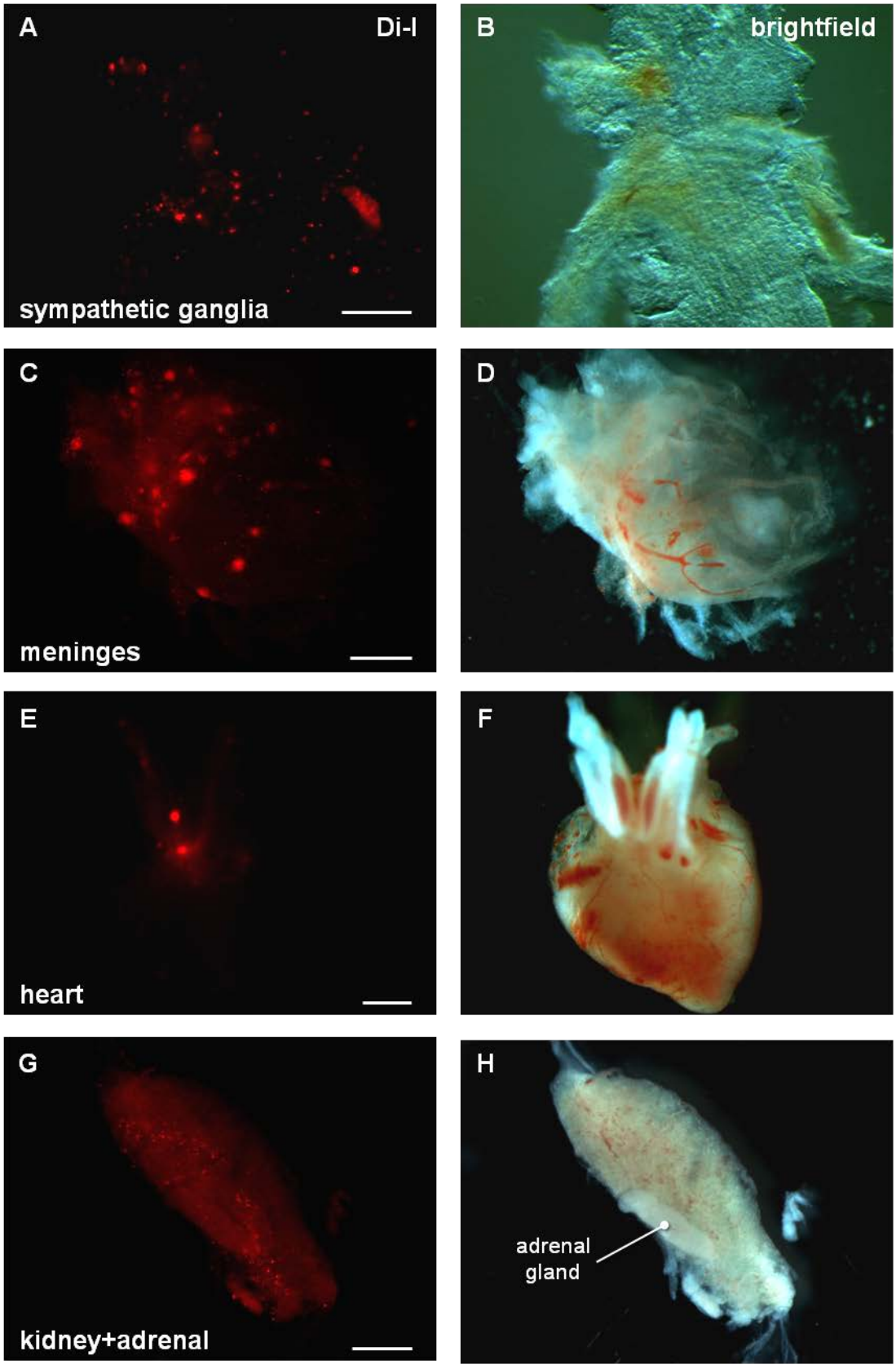

Figure 3.18. DiI-labelled SK-N-AS cells were injected intravenously at E3, and then dissected and photographed at E10. DiI fluorescence was observed in the sympathetic ganglia, meninges, heart and kidney, as indicated. Scale bars A-B, 200µm; C-H, 1mm.

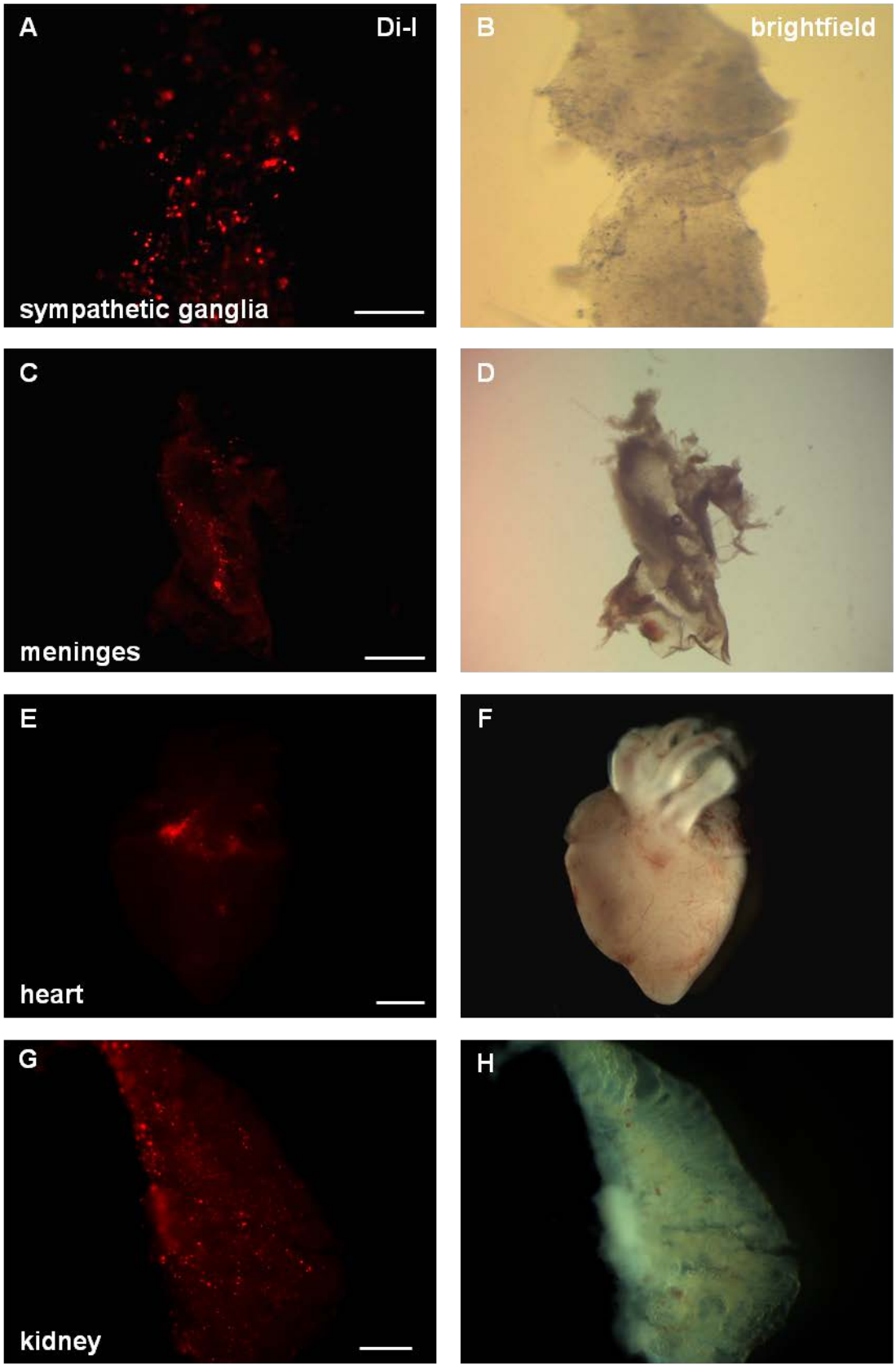

Figure 3.19. Following intravenous injection at E3 and dissection at E10, DiI-labelled SH-SY5Y cells were discovered within the chick sympathetic ganglia, meninges, heart and kidneys, as labelled. Scale bars A-B, 200µm; C-H, 1mm.

3.3.5. Protein markers within SK-N-BE(2)C-injected cells

To characterise the injected cells, in one E10 BE(2)C-injected chick heart, a large patch of DiI fluorescence was sectioned and stained for a variety of antibodies. DiI fluorescence sometimes (Figure 3.20 A+B), but not always (Figure 3.20 D+E) coincided with the presence of BE(2)C cells. Their presence was confirmed by a positive membranous stain for N-CAM (CD56) (Figure 3.20 A-C) and a nuclear staining for human nuclear antigen (Figure 3.20 D-F). The vast majority of cells in the fluorescent heart patch stained positively for the proliferation indicator ki67 (Figure 3.20 G-I), and a small proportion stained for the intermediate filament protein vimentin (Figure 3.20 J-L). The most encouraging result from this experiment was the identification of a population of dividing neuroblastoma cells within the chick, as judged by successful ki67 (nuclear) staining, which had failed up until this point.

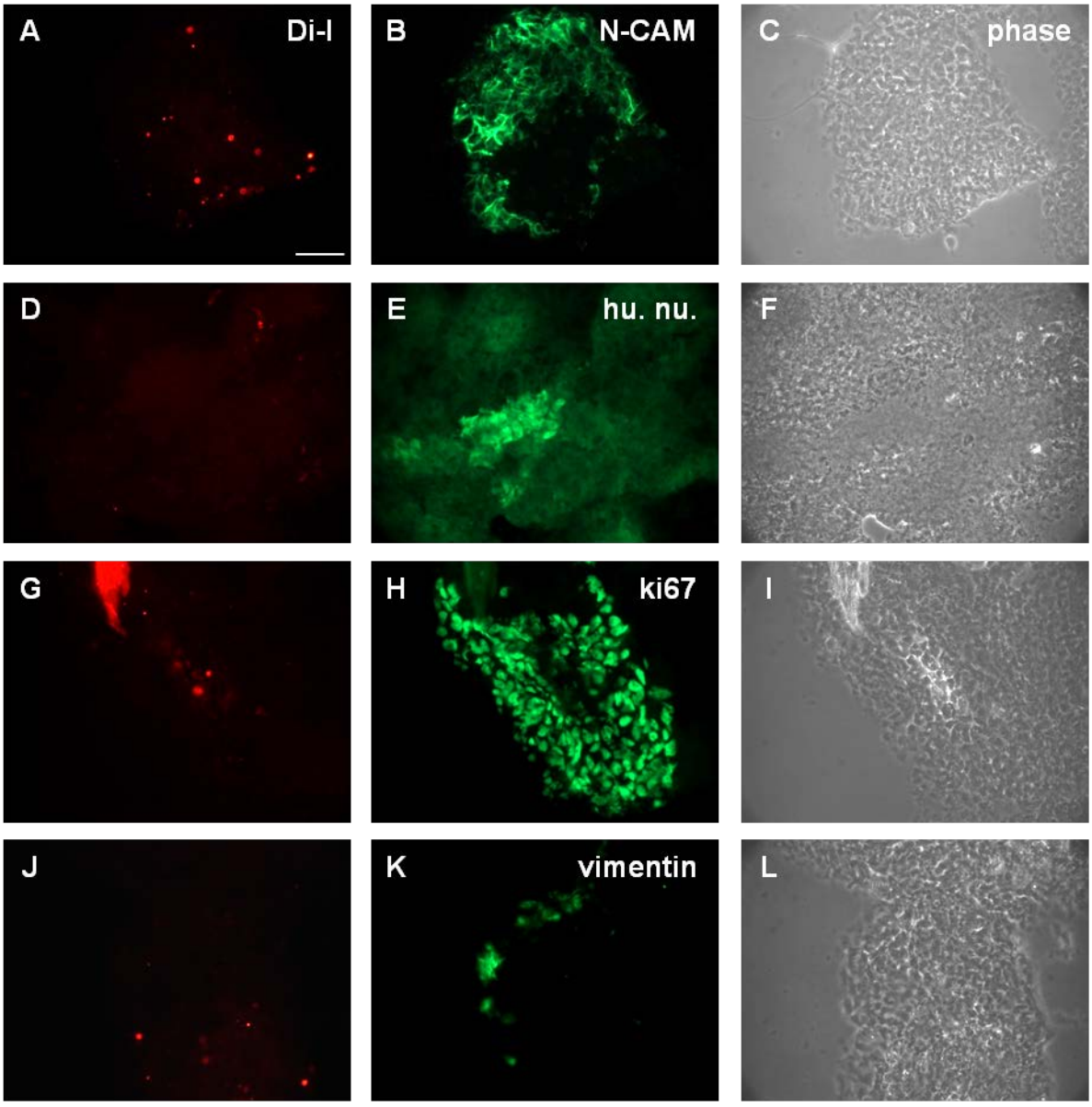

Figure 3.20. Following E3 intravenous injection and dissection at E10, frozen sections were taken of an E10 chick heart containing DiI fluorescence. 10µm sections were stained with antibodies to the proteins as labelled. hu. nu., human nuclear antigen. Scale bar 50µm.

3.3.6. Kelly cells

Kelly cells were received as a kind donation from Dr Louis Chesler (The Institute of Cancer Research, Sutton, UK). Kellys are a MYCN-amplified and highly MYCN-expressing neuroblastoma cell line, with over 200 copies of the MYCN gene. They have been shown to form tumours in mouse xenograft models (Fichtner et al. 1997; Valentiner, Valentiner & Schumacher 2008). It was perceived that the BE(2)Cs had not been growing well in the embryos, therefore a more aggressive cell line was required. The Kelly cell line possesses the ALK^{F1174L} mutation, is p53 mutated (suggesting the tumour of origin was a relapse), has chromosome 11q deletion (which is rare to occur alongside MYCN amplification), 9p deletion (which includes the tumour suppressor, and CDK inhibitor, p16), as well as 3p deletion (which includes receptor protein tyrosine phosphatase (PTPRD), a candidate tumour suppressor) – all suggestive of an aggressive tumour with poor patient prognosis (Akudugu et al. 2004; Caren et al. 2008; Caren et al. 2010; George et al. 2008). It was hoped that the Kelly cells would fulfil this criterion and form tumours in the chick embryos, which the BE(2)Cs did not seem to do.

3.3.6.1. Kelly cell characterisation

To characterise the Kelly cell line, cells were stained using a panel of antibodies. The first and most obvious immunofluorescence analysis needed was for the MYCN protein. Although individual cells expressed different levels of the protein, some considerably brighter than others (Figure 3.21, A-D), MYCN was detected in all of the Kelly cells. So although a heterogeneous population in terms of protein levels, their multiple copies of the gene meant that there was expression in every cell. In terms of neural crest markers, almost all of the cells (94%, n=240) displayed a membranous stain for HNK-1 (Figure 3.21 E-F), yet no staining whatsoever was found for Sox10 (Figure 3.21 G-H). The Phox2b protein, which is normally expressed in the sympathetic ganglia and adrenal and chromaffin cells, was detected in around 2% of Kelly cells (n=307), and although not so obvious in the photograph in Figure 3.22 A, the nuclei that stained positively were generally ones in which the chromatin stained most brightly, and appeared as if the cells were preparing to undergo mitosis. All of the Kelly cells stained for tyrosine hydroxylase (Figure 3.22 C-D), which is not surprising considering the increased catecholamine production and secretion found in neuroblastoma tumours. All of the cells also stained positively for CD24 (Figure 3.22 E-F), a cell surface protein expressed on differentiating neuroblasts. CD133 is a protein that has been documented as a marker of cancer stem cell in some malignancies (Baba et al. 2009;

Singh et al. 2004), and is expressed on the surface of various non-cancerous tissue-specific progenitor cells (Corbeil et al. 2000; Yin et al. 1997). Publications of expression in neuroblastoma have varied: aggressive bone marrow derived tumour initiating cell (TIC) spheres do not express CD133 (Hansford et al. 2007), whereas CD133 has been detected in some neuroblastoma cell lines, where it has been shown to regulate proliferation and repress differentiation (Takenobu et al. 2011). A positive stain was observed in 17% of Kelly cells (n=264). Two proteins indicative of neuronal differentiation were also tested: the growth associated protein GAP43 (Figure 3.23 A-B) and NF70 (Figure 3.23 C-D), the lightest neurofilament subunit. Unsurprisingly, neither of these proteins were expressed in any of the cells – neuronal differentiation would mean that cells had dropped out of the cell cycle, hence were no longer contributing to the aggressive malignant nature of the tumour. Vimentin is an intermediate filament found in mesenchymally-derived cells, as well as those undergoing EMT, and was found to stain 22% of the Kelly cells (n=255) (Figure 3.23 E-F). Since neuroblastoma develops from neural crest cells, which undergo EMT in order to migrate, a lack of vimentin staining, particularly alongside a lack of neurofilament expression, suggests a possible de-differentiation in the majority of these cells, which would probably contribute to their aggressive phenotype. Smooth muscle actin (SMA) is documented as a marker for cancer-associated fibroblasts, which have a critical supporting role in the progression of tumours (Kalluri & Zeisberg 2006), and was seen to stain all of the Kelly cells (Figure 3.23 G-H).

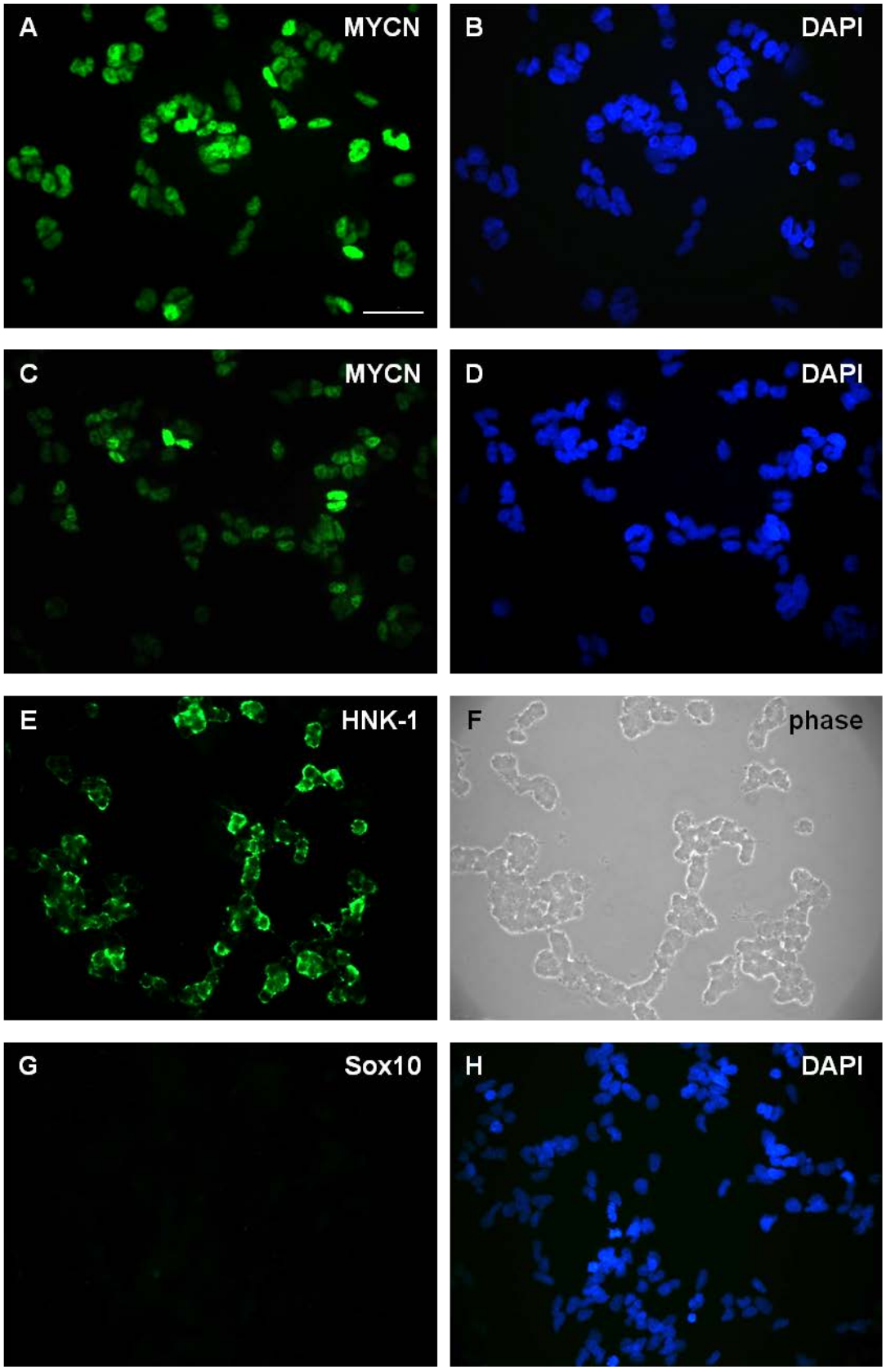

Figure 3.21. Kelly cells in culture stained using antibodies as labelled. A-D, G-H, pre-fixed stain; E-F, live stain. Scale bar 50µm for all.

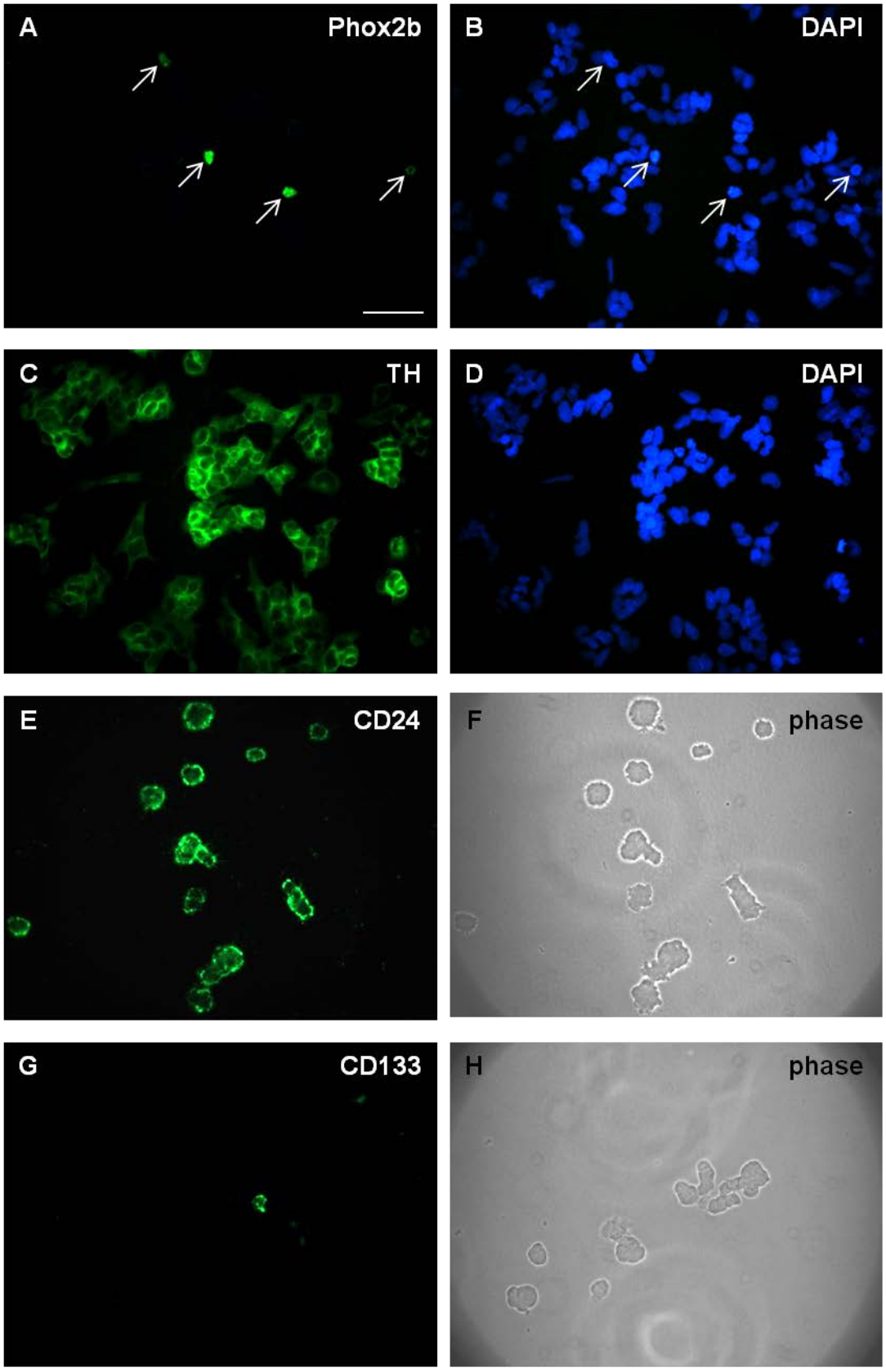

Figure 3.22. Kelly cells in culture stained with antibodies as labelled. A-D, pre-fixed stain; E-H, live stain. Arrows identify Phox2b stained cells. Scale bar 50µm.

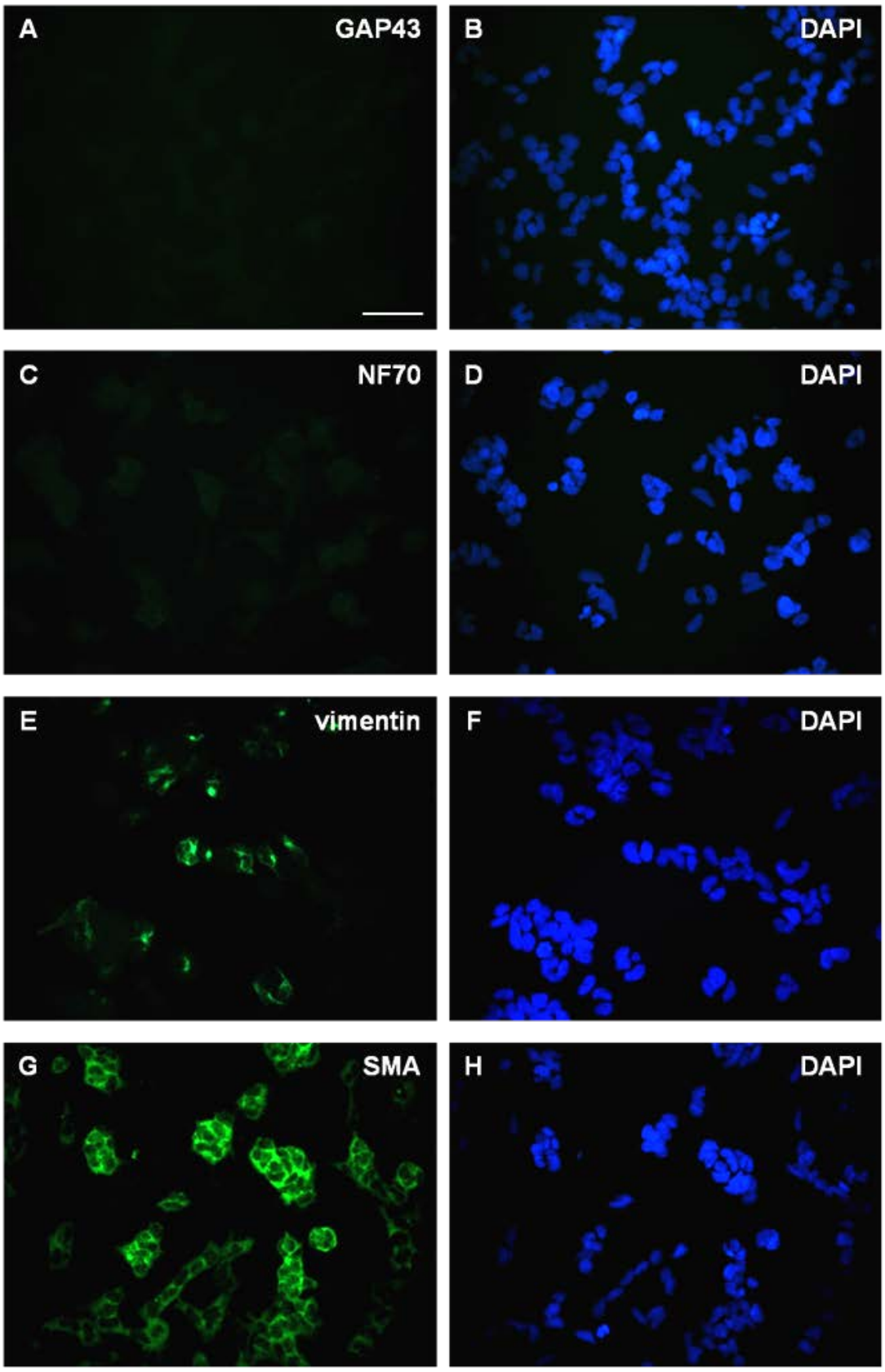

Figure 3.23. A-D, Kelly cells in culture stained with antibodies as labelled. All fixed prior to staining. Scale bar 50µm for all.

3.3.6.2. Kelly eye cup injections

Kelly cells were injected into the E3 eye cup (Figure 3.24 A+B) to discover whether they would behave more aggressively than the BE(2)Cs – this was a distinct possibility, owing to their increased levels of MYCN protein. Successfully-injected eyes from 9 embryos, from 2 separate batches were then dissected at E7. DiI fluorescence was observed on the posterior surface of the lens (Figure 3.24 C), attached to the vitreous humor and on the retina in the vast majority of eyes; all like the BE(2)Cs (Figure 3.2) and B16 F1s (Figure 3.6). In addition, speckles of DiI fluorescence were seen forming linear patterns along the folds of the ciliary muscle (Figure 3.24 E) – interestingly, a structure that is innervated by both the sympathetic and parasympathetic divisions of the autonomic nervous system.

Sections of chick eyes containing DiI fluorescence were then stained successfully for N-CAM and NB84 (Figure 3.25 A-C and D-F, respectively), which confirmed that this fluorescence was definitely incorporated into the Kelly cells. However, even though a successful ki67 stain had been detected in BE(2)Cs within the E10 chick heart (Figure 3.20 H), this was not observed within the Kellys in the eye cup (Figure 3.25 G-I). A couple of Kellys seemed to stain for caspase 3 (Figure 3.25 J-L), but as the large nuclei of the Kelly cells can easily be distinguished from those of the surrounding chick cells via DAPI staining, it was clear that apoptosing cells were in the minority.

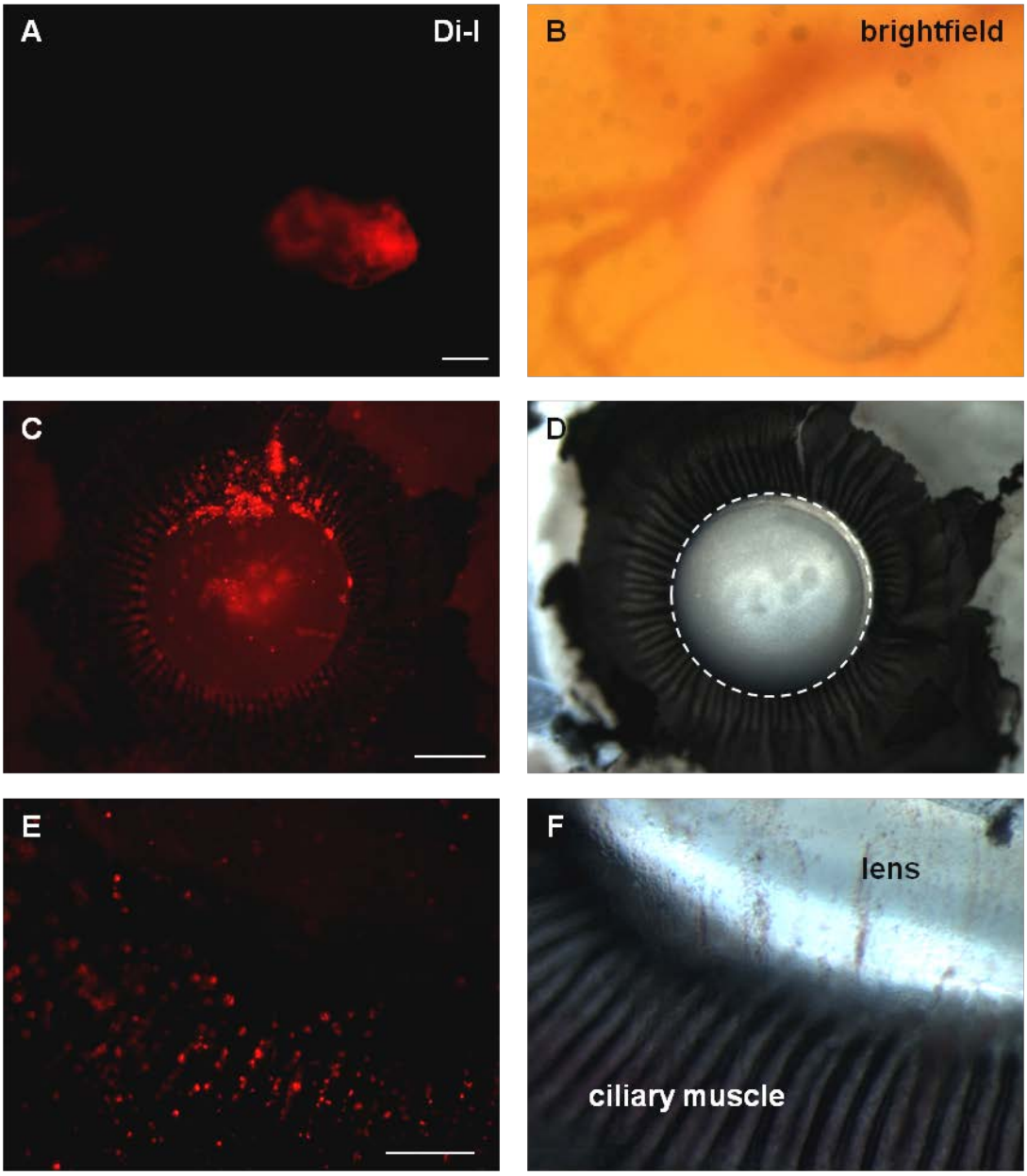

Figure 3.24. DiI-labelled Kelly cells were injected into chick eyes at E3. A-B, E4 eye, 24 hours post injection, scale bar 100µm. Eyes were then dissected at E7, and any DiI observed was photographed. C-D, anterior half of E7 eye, viewed from interior, area inside white dashed line is the lens, scale bar 500µm; E-F, interior of E7 eye, DiI "speckles" – possibly cells – radiating along ciliary muscle, scale bar 200µm.

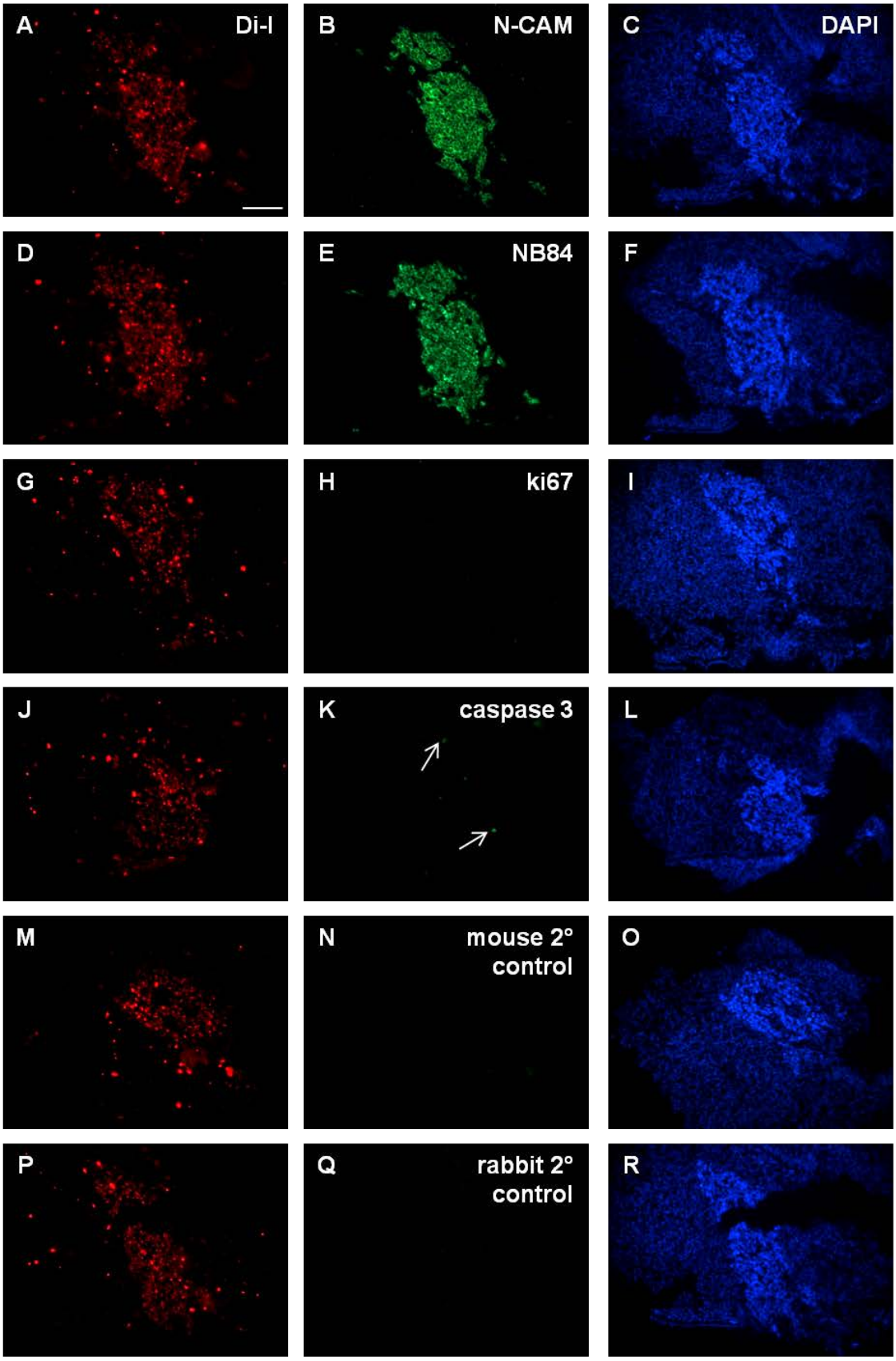

Figure 3.25. Following intra-ocular injection of DiI-labelled at E3, eyes were dissected at E7, and DiI-containing tissues mounted. 10µm frozen sections were taken of said DiI fluorescence, and stained with antibodies to the proteins as labelled. Arrows indicate single caspase 3-stained cells. Scale bar 100µm.

3.3.6.3. Kelly intravenous injections

Intravenous injections of the DiI-labelled Kellys were also performed at E3, following which approximately 25 successfully-injected embryos from 4 separate experiments were dissected at E10. Results were very similar to the BE(2)C line – fluorescence was found throughout most regions of all embryos, including the sympathetic ganglia, in both speckles and clumpier-looking patches (Figure 3.26 A-D), the gut (Figure 3.26 E+F), meninges (Figure 3.26 G+H), spleen (Figure 3.27 A+B), heart (Figure 3.27 C+D), liver (Figure 3.27 E+F) and kidneys (Figure 3.27 G+H)[1]. Overall, these results were almost indistinguishable from those of the BE(2)C cells. Kellys grown in culture had been shown to stain for the human-specific antibodies NB84 and N-CAM (Figure 3.28, A-D), and indeed when fluorescent patches in the E10 sympathetic ganglia were stained using these antibodies (Figure 3.28 E-H), it was confirmed that the DiI fluorescence was an indicator of the presence of Kelly cells.

[1] It should be noted that the brightfield images in Figures 3.26 and 3.27 are not as clear as usual, as they were taken when the goose neck light source was broken, therefore a backlight had to be used for illumination.

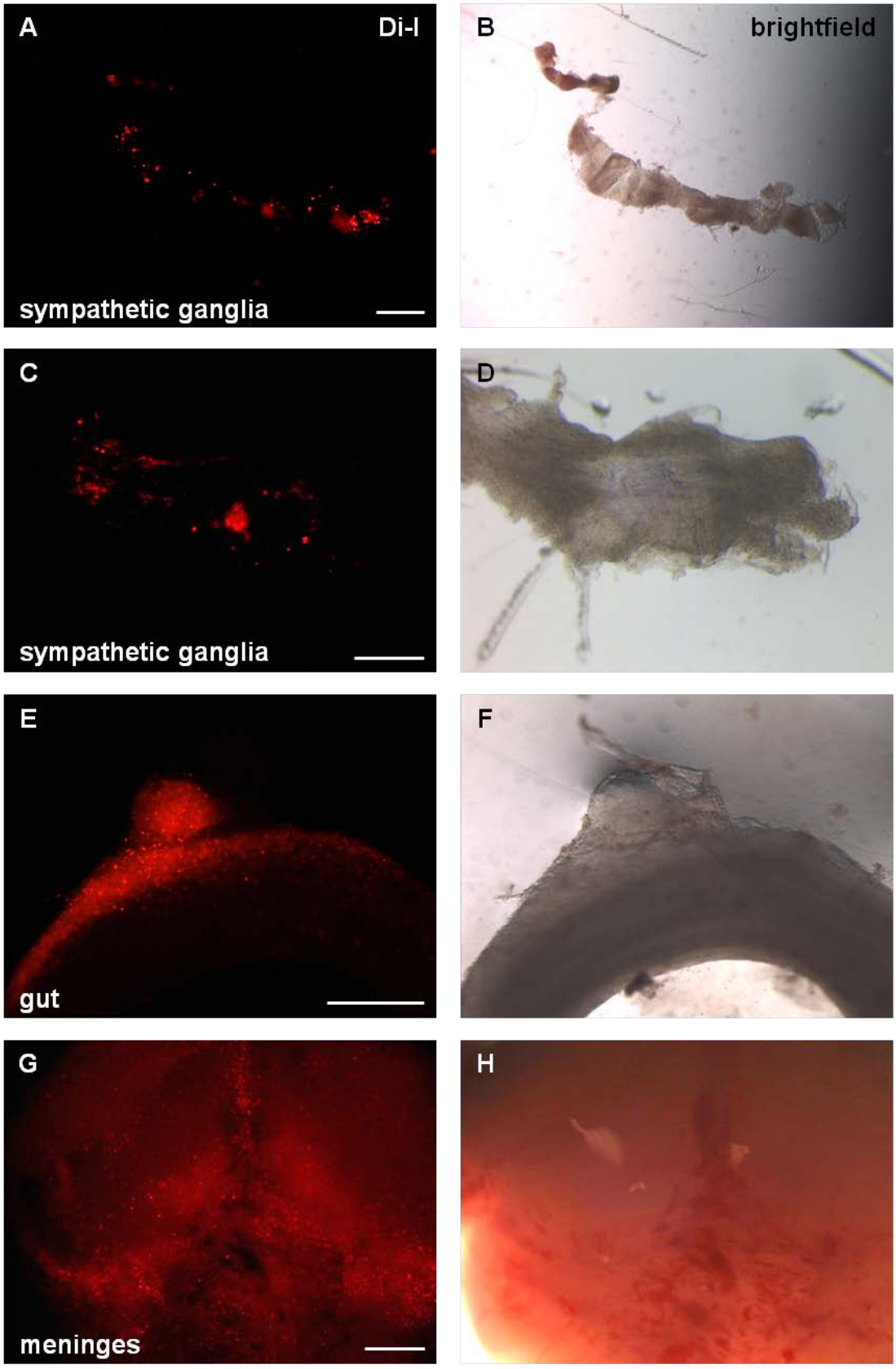

Figure 3.26. DiI-labelled Kelly cells were injected intravenously at E3, and embryos incubated until E10. Upon dissection, DiI fluorescence was observed within chick tissues as labelled. Scale bars A-B, E-F, 500µm; C-D, 200µm; G-H, 1mm.

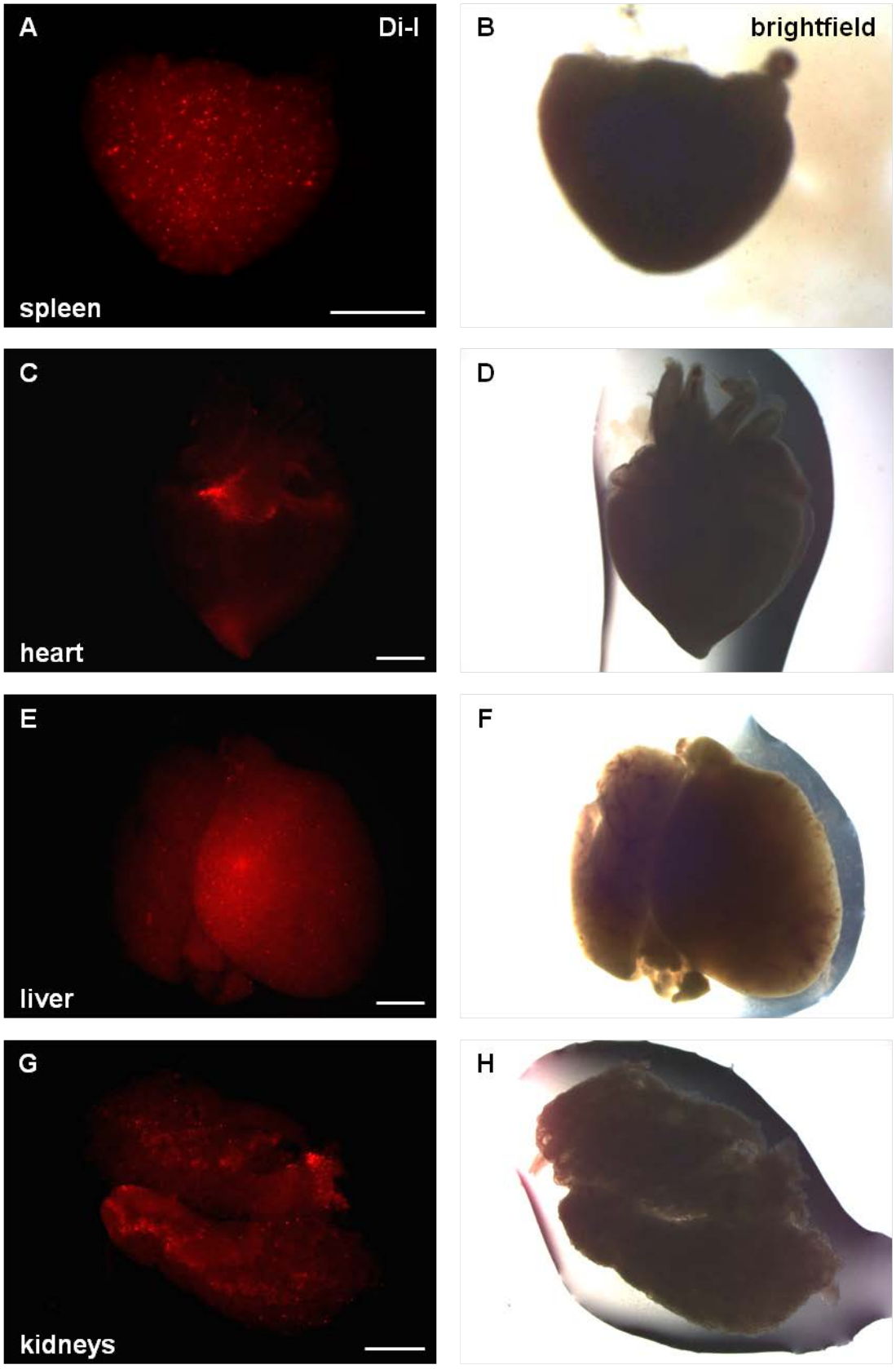

Figure 3.27. Following intravenous injection of DiI-labelled Kellys at E3 and dissection at E10, DiI fluorescence was observed within the chick tissues labelled. Scale bars A-B, 500µm; C-H, 1mm.

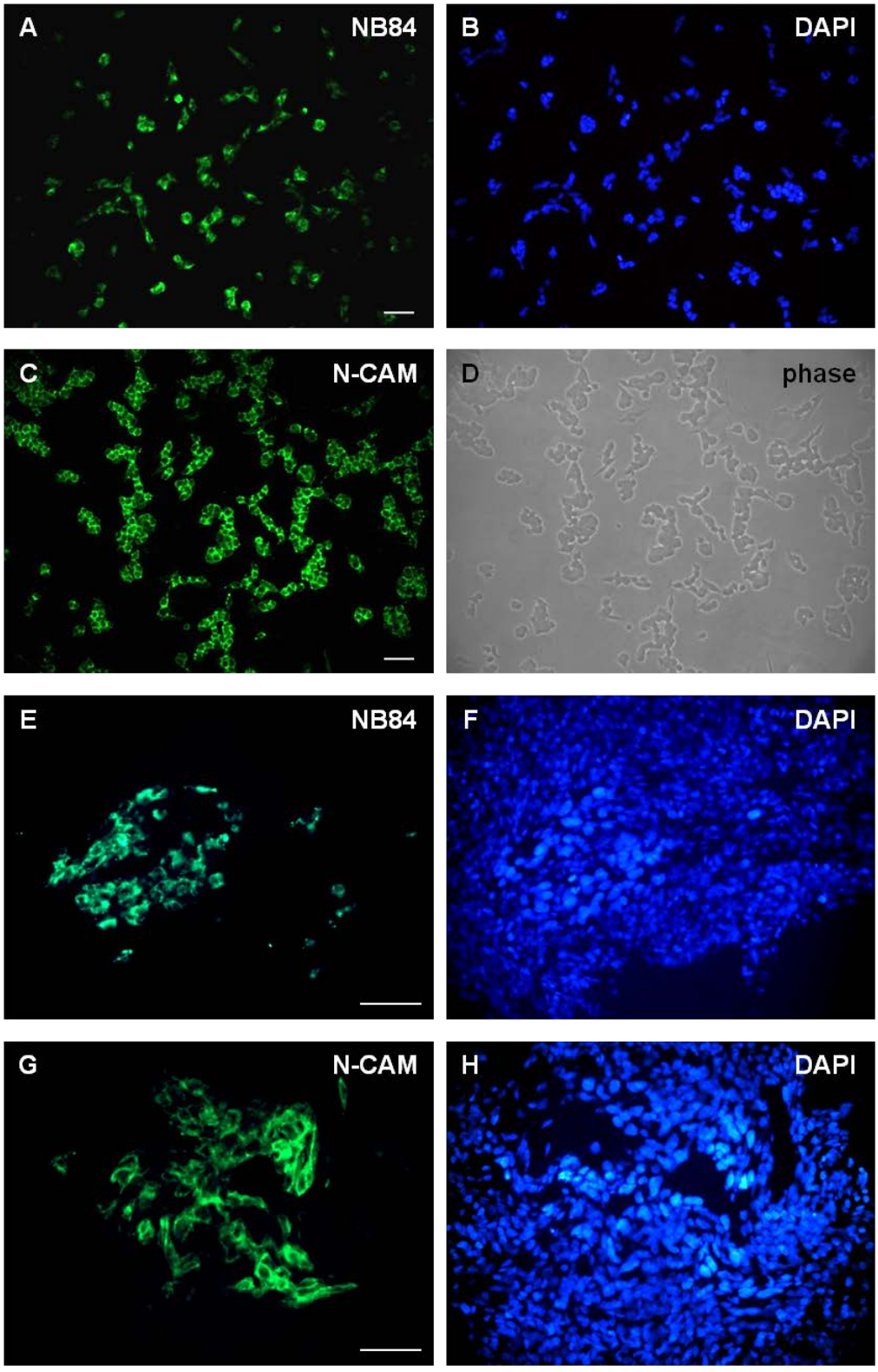

Figure 3.28. A-D, Kellys in culture stained for A-B, NB84 (pre-fixed); C-D, N-CAM (live stained). E-H, frozen sections of DiI-labelled Kelly cells within E10 chick sympathetic ganglia, that had been intravenously injected at E3. Kellys can be identified by their large nuclei in the DAPI staining (B,D) and their corresponding immunofluorescence staining for NB84 (A) and N-CAM (C). Scale bars 50µm.

3.3.6.4. Kelly cell labelling

3.3.6.4.1. Previous neuroblastoma cell line GFP transfection attempts

Thus far a recurring problem had been the difficulty to be able to absolutely confirm the presence of neuroblastoma cells within both the dissected chick embryo tissues and the frozen sections without additional staining, due to the limitations of DiI described above. Several attempts were therefore made to transfect a GFP plasmid into various neuroblastoma cells, with the aim of producing a stable fluorescent line.

Two different plasmids were transfected, using three different reagents, into four different cell lines. Killing curves were performed on each of the cell lines, using the antibiotic appropriate to the plasmid being transfected, to determine the concentration of antibiotic required to kill the non-GFP-transfected (therefore non-antibiotic-resistant) cells at various densities. In general, the higher the antibiotic concentration, the greater the cell death, but the higher the cell density, the more cells survive. This needed to be balanced out, so that the minimum possible concentration of antibiotic could be used (specific to each cell line), that would successfully kill the non-transfected cells, but not too quickly, as they play an important supporting role to those cells that incorporate the plasmid DNA, particularly in the initial stages.

Transfection of the B16 F1 cells using pEGFP-N1 and the reagents ExGen500 and TransIT-LT1 yielded initial transfection efficiencies of 5-30%, and over the following days, this reduced to much less than 5%, with only a couple of fluorescent cells in each well. Transfection of pBudCE4.1/EF-1α/EGFP proved this plasmid was far superior in terms of generating fluorescent cells.

Since the main focus was on neuroblastoma cells, BE(2)C, SK-N-AS and SY5Y cells were transfected with pBudCE4.1/EF-1α/EGFP using TransIT-LT1 and jetPRIME (using various reagent:plasmid ratios), resulting in transfection efficiencies of between 15 and 40%. The SY5Y cells did not survive well following transfection with either reagent, even when the antibiotic concentration was reduced. Although the BE(2)C and SK-N-AS initially looked promising, with increasing time it was clear that the GFP-transfected cells would not form colonies – they were simply not dividing, yet not dying either.

3.3.6.4.2. CFDA-SE

Lack of success with GFP plasmid transfection into neuroblastoma cell lines (section 3.3.6.) led to the consideration of an alternative fluorescent labelling technique. To be effective, this dye had to remain visible after multiple cell divisions, in order to be visible in the embryos. CFDA-SE (also known as CSFE) was added to Kelly cells in culture in 3 concentrations: 2, 5 and 10µM, and subsequently observed alongside cells labelled with DiI. The 5 and 10µM concentrations of CFDA-SE were toxic to the neuroblastoma cells, and although the cells labelled with a 2µM concentration were almost all initially fluorescent, this label rapidly faded, even more rapidly than the DiI.

3.3.6.4.3. GFP lentiviral transduction

Neuroblastoma cells are notoriously difficult to transfect (Dr Louis Chesler, personal communication), but administration of plasmids using lentiviral transmission has been proven to be effective (De, Lewis & Gambhir 2003). The Kelly cells were infected with a lentivirus in which enhanced GFP (EGFP) was constitutively expressed under a spleen focus-forming virus (SFFV) promoter (kindly carried out by Dr Sokratis Theocharatos, University of Liverpool, UK). The lentiviral construct was added to the RPMI medium in one well of a 4 well plate containing Kelly cells at around 40% confluency. This virus-containing medium was removed after 24 hours, and a further 24-48 hours subsequent to this, more than 80% of the cells were seen to express the GFP protein. These cells were eventually subcloned at a density of average 1 cell per well of a 96 well plate, and after the first attempt it was feared that the fluorescent cells were not going to divide. However, since the non-fluorescent cells were not dividing either, a second subcloning attempt was made, this time using half conditioned medium and half fresh medium, and in this case, a brightly fluorescent stable cell line was produced from subclone D4.

3.3.6.5. GFP-Kelly eye cup injections

Once a stable GFP-expressing Kelly cell line had been established, the cells were injected into the E3 chick eye cup to recapitulate the melanoma experiments, and to validate that what had been observed with DiI was in fact neuroblastoma/melanoma cells. These eyes were left to develop until E9 or E10, and upon dissection of 14 embryos from 3 different batches, it was discovered that the DiI that had been seen within the retina, lens (Figure 3.29 A+B) and vitreous humor (Figure 3.29 C+D) was reproduced by the GFP Kelly cells (in which no fluorescent molecules would have been able to precipitate out of the cells). However, the speckles of DiI radiating out along the ciliary muscle (Figure 3.24) was not observed to the same extent when the Kellys were GFP-labelled (Figure 3.29 E+F), indicating that the DiI seen here previously may not have been integrated into neuroblastoma cells. The GFP Kellys within the eye stained positively for N-CAM, NB84 and the neural crest marker HNK-1 (Figure 3.30).

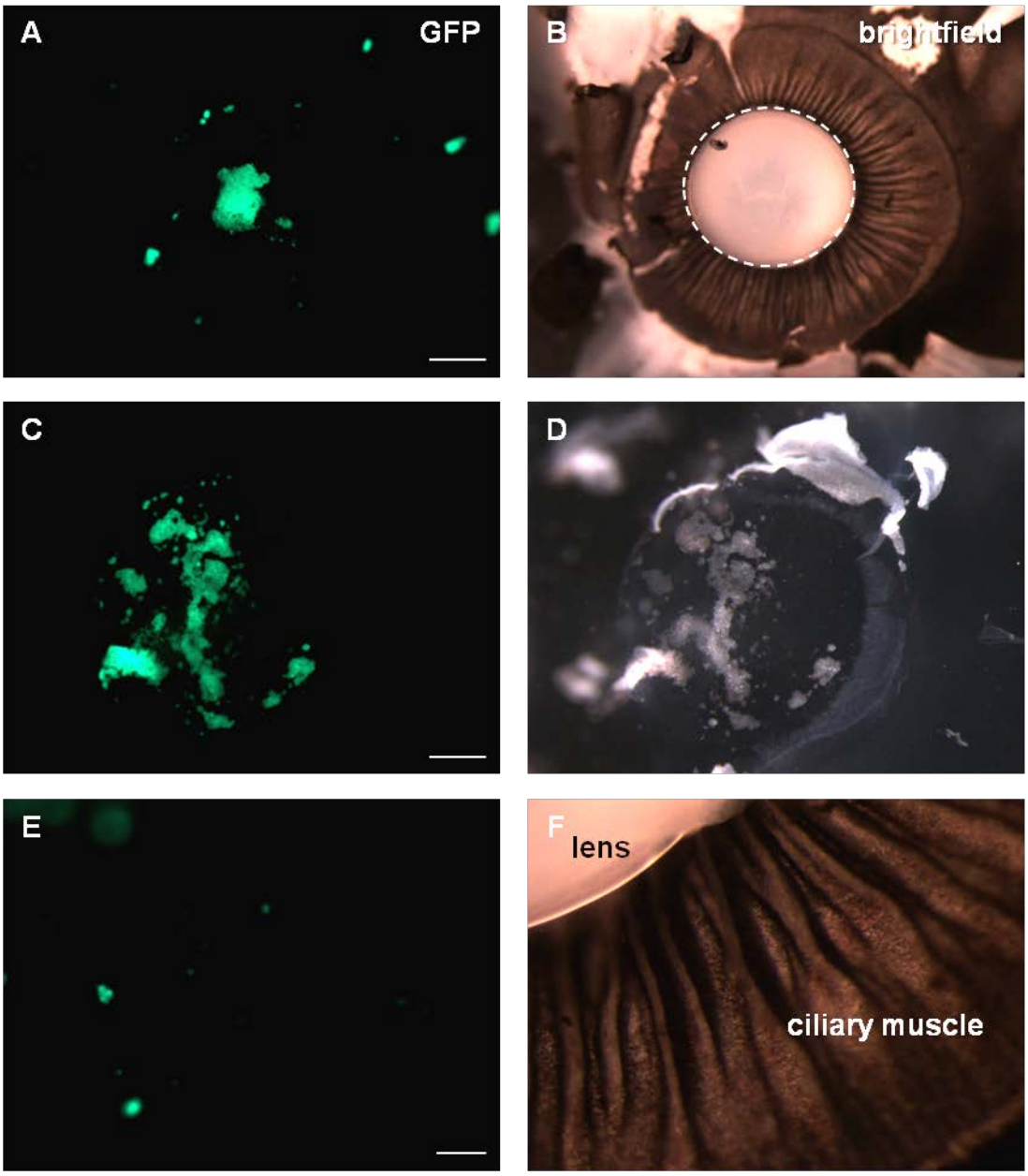

Figure 3.29. GFP-labelled Kelly cells were intra-ocularly injected at E3, and following 7 days incubation, chick eyes dissected at E10, when any GFP fluorescence was documented. A-B, anterior half of eye, viewed from interior, area inside white dashed line is the lens, scale bar 500µm; C-D, vitreous humor “bag”, cells attached to outside, scale bar 500µm; E-F, interior of eye, cells within ciliary muscle, scale bar 100µm.

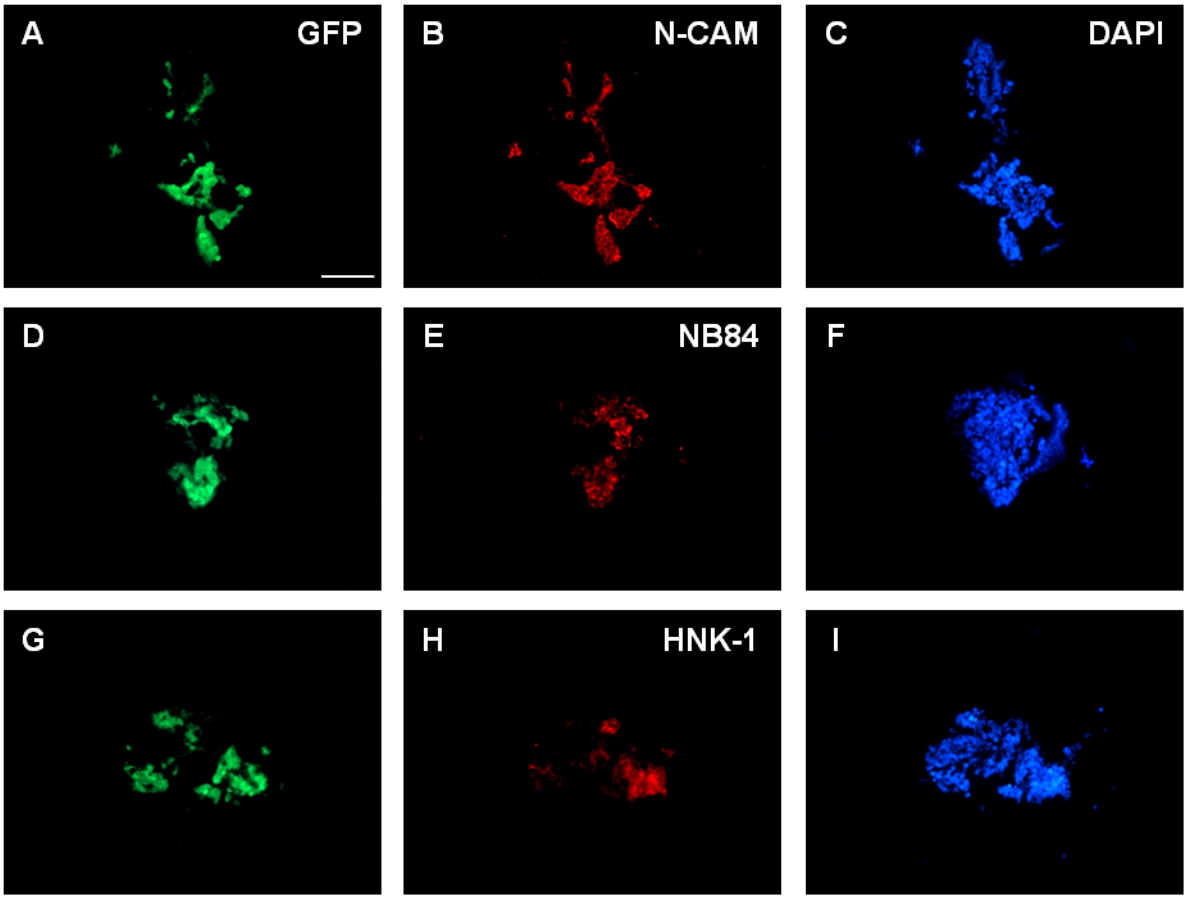

Figure 3.30. Frozen sections of GFP-labelled Kelly cells within the chick eye, following intra-ocular injection at E3 and dissection at E9. 10µm sections were stained using antibodies to the proteins labelled. Scale bar 100µm.

3.3.6.6. GFP-Kelly intravenous injections

The GFP Kellys were DiI-labelled prior to E3 intravenous injections, so that a true comparison between the red DiI and green GFP fluorescence could be made. Figure 3.31 shows the results of this one experiment, following dissection of 7 embryos at E10. On the whole, DiI fluorescence was a good indicator of the neuroblastoma cells – the areas with the most dense regions of red fluorescence in the sympathetic ganglia and gut were generally indicative of GFP Kellys, although, as expected, there were many red "speckles" that did not correspond to Kelly cells. In the meninges, however, many areas of DiI that had been assumed to be clumps of Kelly cells, were in fact merely DiI molecules that had dissociated from the cells – in the field shown in Figure 3.31 J-L, there was only one group of Kelly cells indicated by the GFP fluorescence, but looking at the DiI, one would have assumed there were several clumps. In the tail and heart, the DiI generally corresponded to GFP Kellys, although the cells were slightly more focussed than was suggested by the DiI. However, in organs such as the liver, kidneys and spleen that had previously been shown to have tiny speckles of DiI throughout the entire tissue (Figure 3.15 and 3.27), no GFP Kellys could be found, implying either that cells has initially located here and then died, leaving their DiI behind, or that DiI molecules had escaped from (either living, proliferating or dying) cells and then travelled to these organs via the bloodstream.

Figure 3.31. ***(Over the page).*** GFP-labelled Kelly cells were also labelled with DiI, in order to distinguish where within the DiI "speckles" in chick tissues Kelly cells were really present. Cells were injected intravenously at E3, and chicks dissected at E10. Comparisons between the DiI and GFP fluorescence were noted in a number of dissected tissues. SG, sympathetic ganglia. Scale bars A-C,G-I,M-R, 500µm; D-F,J-L, 200µm.

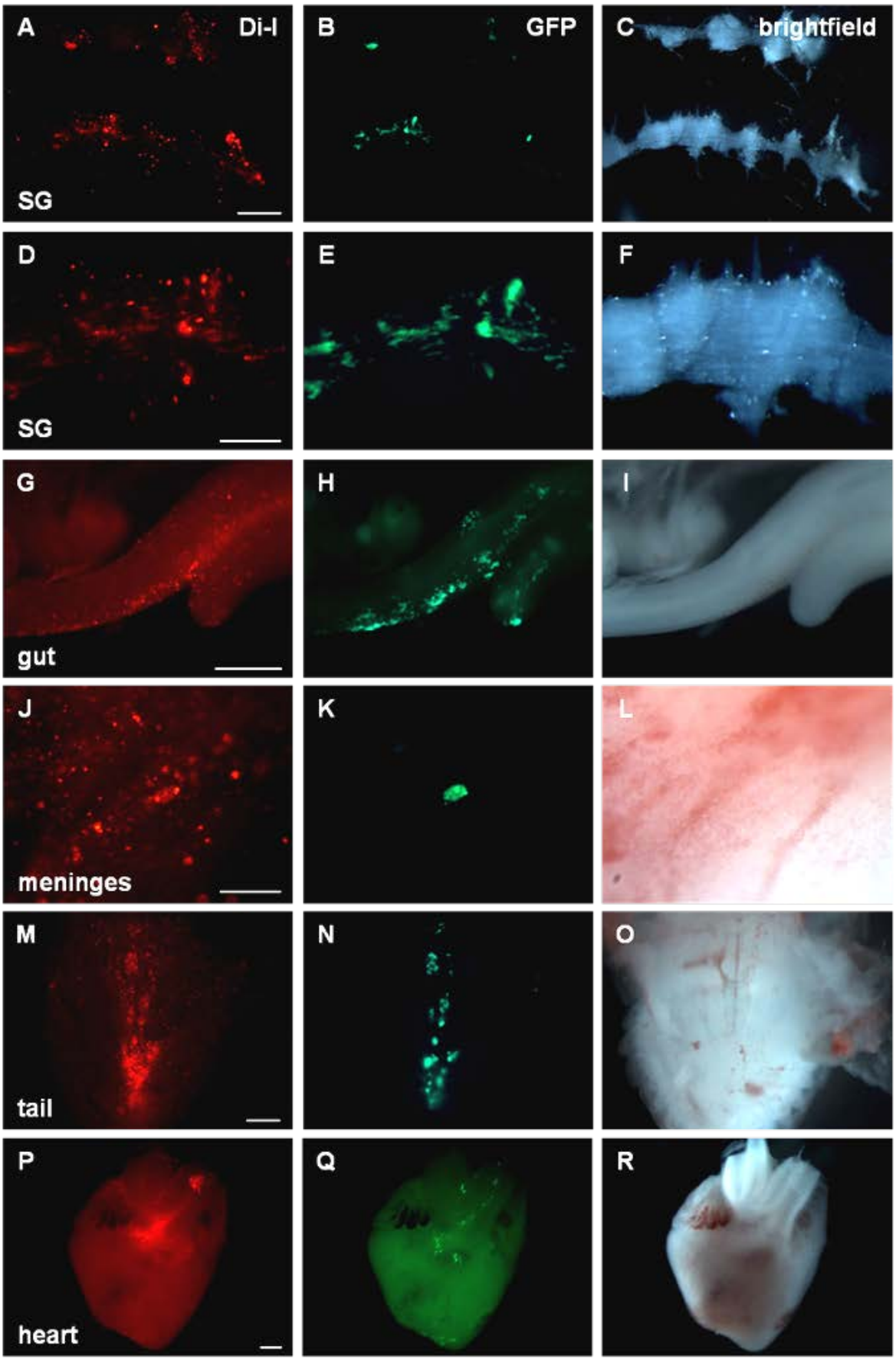
A
Di-I
SG
B
GFP
C
brightfield
D
SG
E
F
G
gut
H
I
J
meninges
K
L
M
tail
N
O
P
heart
Q
R

3.4. Discussion

The generation of a GFP-labelled Kelly cell line is ideal for identification of neuroblastoma cells upon dissection of the embryos. Although DiI labelling was a good tool for preliminary experiments in establishing the model system, a GFP line is preferable regarding long term behavioural studies of cells within the embryos, as no matter how many cell divisions are completed, the cells will continue to express the fluorescent protein. DiI, in contrast, is a lipophilic dye that inserts into the lipid fraction of the cell membrane, therefore its fluorescence is progressively diluted as a cell divides, and each of its daughters receives approximately half of the DiI molecules. An additional problem was that following dissection of chick tissues, a strong red speckled appearance to the surrounding tissue was noted where GFP-labelled cells were not present. This may have been due to one/a combination of: free DiI molecules being injected in the original cell suspension (washing will not have removed all excess dye); DiI molecules having precipitated out of the neuroblastoma cell membranes they labelled; or phagocytosis of DiI-labelled apoptotic fragments into neighbouring chick cells. Structurally, apoptosis begins with nuclear and cytoplasmic condensation, and is followed by fragmentation of the cell into membrane-bound apoptotic bodies (Kerr, Wyllie & Currie 1972). These may enter neighbouring cells by phagocytosis, and subsequently be degraded – in this scenario, transferring their fluorescent DiI molecules to the chick cells. The speckled appearance (when viewed under fluorescence) of almost the entire embryo made it difficult to identify the neuroblastoma cells within the chick tissues without immunofluorescence staining or prior GFP labelling. This was particularly evident in the liver, however, no GFP cells were ever seen there, so the abundance of DiI speckles here may have been due to rogue circulating DiI molecules that had been transported to the liver during blood detoxification.

Assessment of cell proliferation was an ongoing problem. The ki67 antigen is present at all stages of the cell cycle, except from in resting cells (G0). Although the ki67 antibody worked well on cells in culture, it did not seem to work on frozen tissue sections. This was complicated by a positive nuclear stain of BE(2)C cells in the heart, which although never obtained in any other sections, implied that a successful stain of cells within tissues was possible. It was unknown whether cells simply did not proliferate within the chick embryo, or if there was a problem with the ki67 antibody. The combination of the DiI and HMB-45 stain of B16 F1 cells in chick eye sections made the latter possibility more likely. Therefore numerous methods of optimising conditions to lead to a positive ki67 stain were trialled, the most simple of which was using a different ki67 antibody. Fixation with agents such as paraformaldehyde preserve cell structure, but can form cross-links that obstruct the antibody

binding sites. Therefore antigen retrieval was performed using citrate buffer or 1% SDS on embryonic mouse heads. In addition, embryonic rat tissue was mounted without prior fixation to prevent cross-linking, and paraformaldehyde was added to the sections for 10 minutes, as was the case for the cultured cells. However no success was gained with any of the above mentioned techniques.

From the outset, cells were “injected” into wells containing medium, and successful culture subsequent to this indicated that cells were entering (and leaving) the needle and surviving the injection process. Therefore any lack of survival should be as a result of the embryonic environment.

A basic model system had now been established, in which neuroblastoma cells had been seen to localise to certain chick tissues and not others. Further investigation was necessary to assess their behaviour, and discover whether proliferating tumours were forming *in vivo*.

Chapter Four:

Results II – Neuroblastoma cell behaviour in the chick embryo

4.1. Introduction

As a result of the preliminary work detailed in Chapter Three, the basic tools were now in place to begin to truly test the effects of an embryonic environment on the neuroblastoma cells. The DiI labelling used thus far was not ideal because as described previously, the DiI molecules had a tendency to leak out of the cells they had labelled, so locations of cells could not be irrefutably verified. However, following the establishment of a stably GFP-transfected Kelly cell line, it would be possible to identify exactly where the neuroblastoma cells were locating to following intravenous injection, and make assessments from their morphology and protein markers as to their behaviour in various tissues.

4.2. Aims

To optimise the model system established in Chapter Three to be able to analyse the effects of different chick embryonic environments on the behaviour of MYCN-amplified Kelly cells.

- Inject GFP-labelled Kellys into chick embryos, intravenously at different timepoints: specifically E3 and E6.
- Confirm specific targeting by injecting fluorescent beads and a primary glioblastoma line (for contrast), as well as SK-N-BE(2)C cells (for comparison).
- Analyse behaviour of Kellys within chick tissues, in terms of morphology, differentiation, proliferation and MYCN expression.

4.3. Results

4.3.1. Cell targeting

4.3.1.1. GFP Kelly E3 intravenous injections

The first objective was to assess the distribution of Kelly cells following E3 injection and obtain a more conclusive result via the GFP-labelled cells, compared to the DiI used in Chapter Three. Kellys were prepared as in section 2.3.2.1.1 (Chapter Two), and as for the DiI-labelled cells, approximately $2x10^5$ were injected into the extra-embryonic vitelline veins (Figure 3.11 B+D). Embryos were incubated for a further 7 days and dissected at E10 – this

was conducted on approximately 35 batches of eggs (i.e. 35 independent experiments), with Kelly cell incorporation analysed in an excess of 250 dissected embryos in total. Within the E10 embryos, GFP Kelly cells were found in a number of body tissues. Kellys were routinely found in the sympathetic ganglia (Figure 4.1). As long as an embryo's cell injection had been an efficient one, with a considerable number of cells observed within its dissected tissues, SG incorporation was evident almost every time – in approximately a quarter of embryos, confined to a few individual (neighbouring) ganglia within the chain, but more often extending along most of the length. Injection of DiI-labelled cells had led to the conclusion that neuroblastoma cells often formed clumps in the sympathetic ganglia, reminiscent of micro-tumours, however scrutiny of the GFP-Kellys revealed that the they frequently resided as single cells, sometimes grouped in slightly more dense patches, but there was little evidence of the neuroblastoma "tumours" that were suspected from the DiI experiments. Morphological observations were restricted, but the Kellys seemed to display a lengthened appearance, with chains of cells often orientated longitudinally along the length of the ganglia (Figure 4.1 E, G). Each sympathetic chain usually contained at least 50 Kelly cells, with some incorporating several hundred.

GFP Kellys were also found within the chick digestive system (for overview of digestive tract, see Figure 3.14), where they appeared to be located relatively superficially. Kellys were rarely observed along the oesophagus or in the stomach, in around 10% of embryos were on the external surface of the gizzard (although relatively few cells), but were mostly concentrated along the small intestine (Figure 4.2 E-H), and to an even greater extent, the caeca and colon (Figure 4.2 A-D). This incorporation into the caeca/colon was observed in greater than 90% of surviving, efficiently-injected embryos, and cells were observed in the small intestine of around 80%. Their predominance in the hindgut suggests considerable migration by the Kellys, which must have entered the most rostral part of the gut mesenchyme, and followed the endogenous NCCs in their rostrocaudal along the length of the gut. Kellys appeared to be located mostly as single cells, although like in the sympathetic ganglia, they were often in patches of a few collective cells. But in neither of the formerly mentioned tissues did the fluorescent cells give the impression of a proliferating population – more that they were integrating into the chick tissues.

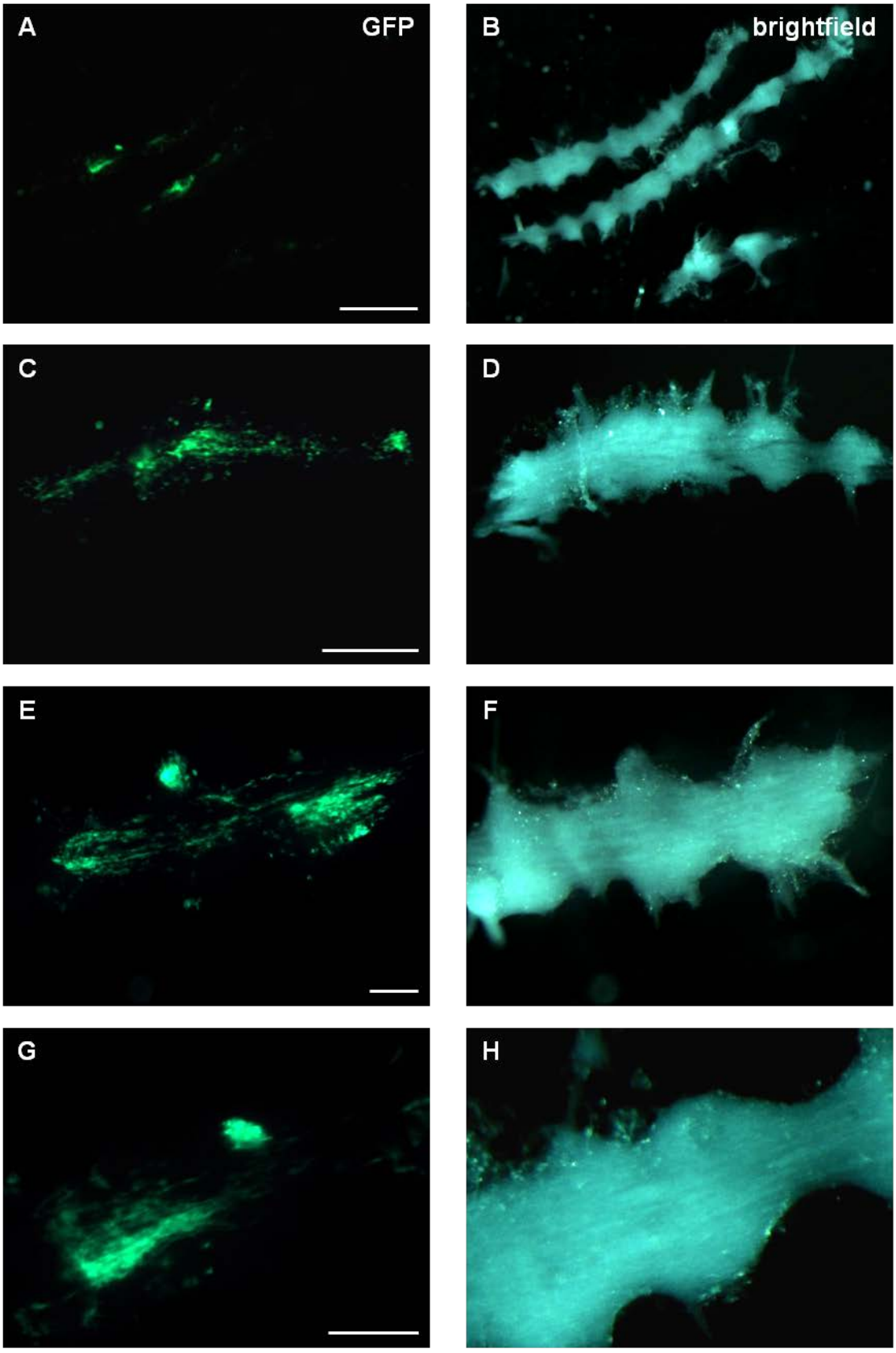

Figure 4.1. GFP-labelled Kelly cells were injected intravenously into E3 chick embryos, which were then dissected at E10. Cells were found to have incorporated into the sympathetic ganglia. Scale bars A-B, 1mm; C-D, 500µm; E-H, 200µm.

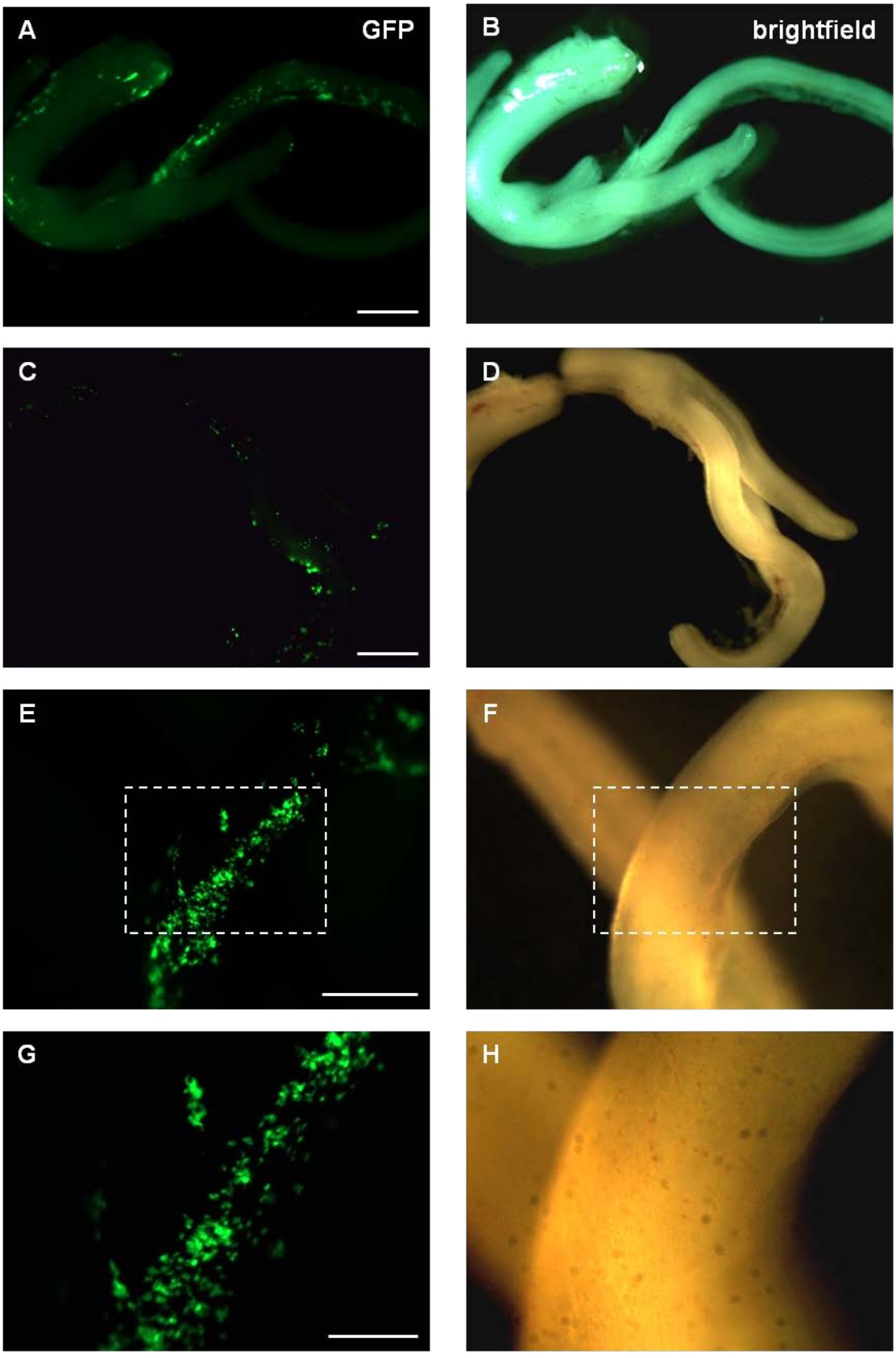

Figure 4.2. GFP-labelled Kelly cells were intravenously injected at E3 and dissected at E10. Cells were observed within the gut. E-F are a higher magnification of the area within the dashed boxes in C-D. Scale bars A-D, 1mm; E-F, 500µm; G-H, 200µm.

Posterior and slightly caudal to the colon, clumps of cells were found in the tail regions of almost all of the embryos (Figure 4.3). There were typically multiple clumps per embryo, which were of various sizes and often distributed down the length of the tail (Figure 4.3 E). In this region, the Kellys were not so incorporated into the chick tissue, instead forming clusters of cells that may well have been the tumour-like masses that were the original aim when the injection strategy was changed to an intravenous route.

Upon dissection of the head, although GFP Kellys were never found within the brain tissue, they were always observed in the meninges (Figure 4.4 A-F). They appeared as numerous (at least 10, often up to 100 or more) “balls” of cells that were remarkably regular in size, at around 30-35µm in diameter, and spherical in appearance. Also in the head, cell clumps of similar spherical shapes were frequently witnessed inside the mouth – most often on the ventral surface of the tongue (Figure 4.4 G-H) and sometimes within the muscle forming the floor of the oral cavity.

Injected neuroblastoma cells also targeted the heart – in a typical experiment, if 12 embryos had survived following successful injections (i.e. a sufficient number of cells had entered the embryos at E3), at least 10 would show cardiac incorporation of GFP Kellys. Of these, cells were almost always found in the conotruncal region (the area of the great vessels) (Figure 4.5 A, E, G), often near the apex (Figure 4.5 A, E) and less often but still repeatedly (1 or 2 embryos out of 12), along the interventricular septum on the posterior surface (Figure 4.5 C). Like those cells that located to the sympathetic ganglia and gut, the cells in the heart appeared to be integrated into the tissue rather than forming clumps of cells.

Cells were usually found within the eyes – either in the sclera or uvea, but not the (internal) retina (Figure 4.6 E-F). In addition, they were found in around half of the parasympathetic ciliary ganglia examined (situated posterior to the eye, near the optic nerve) (n = approximately 45 ganglia from roughly 30 embryos), and within these structures the cells were seen to integrate into the tissue and extended processes, possibly indicative of neuronal differentiation (Figure 4.6 G).

There were numerous areas of the embryos in which no cells were found to have invaded, such as the lungs, spleen, skin, liver (Figure 4.6 A-B), rarely to the kidneys, and surprisingly, never to the adrenal glands (Figure 4.6 C-D).

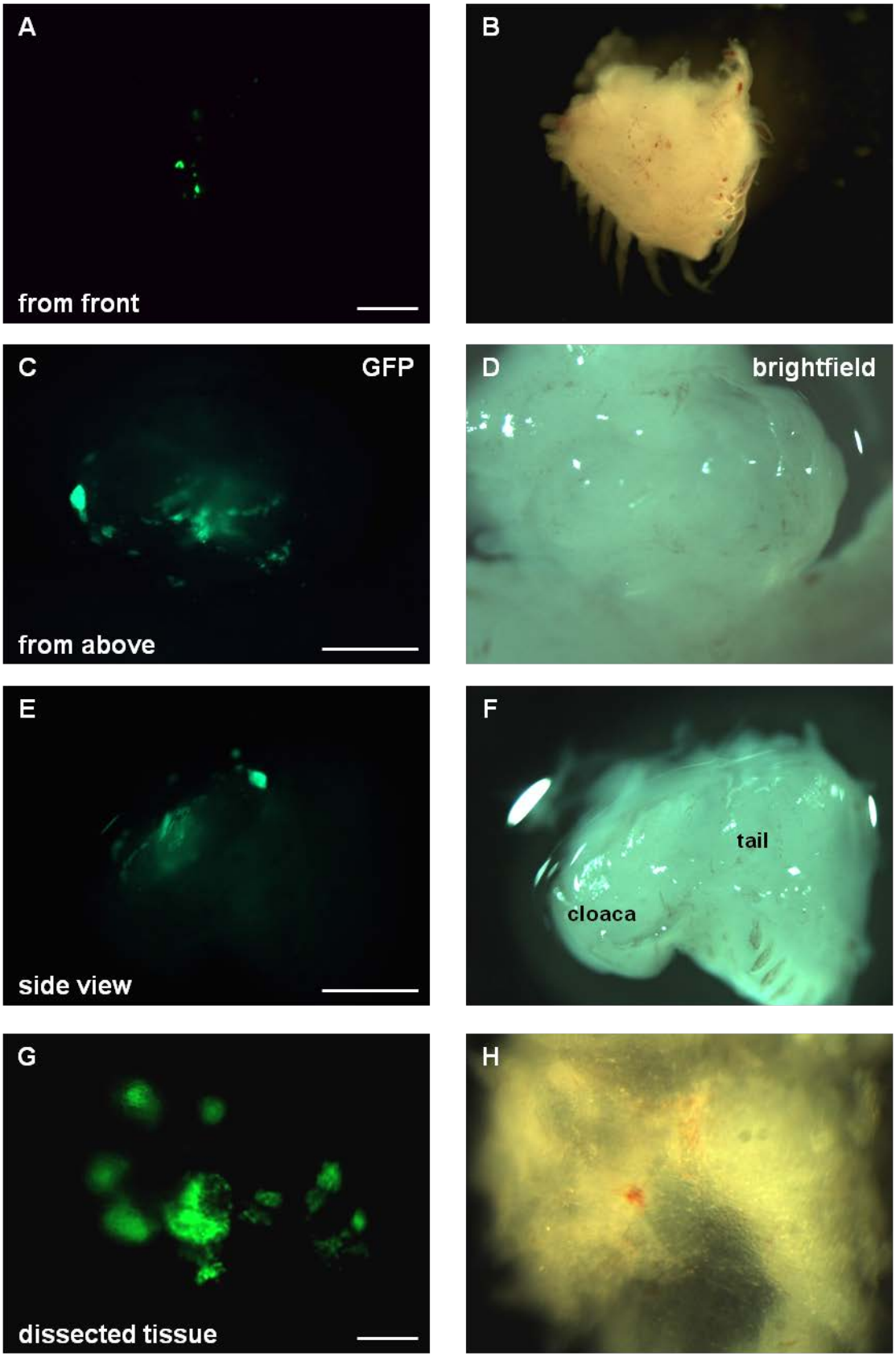

Figure 4.3. GFP-labelled Kelly cells were injected intravenously into E3 chick embryos. Following dissection at E10, cells were observed within the tail tissue. Scale bars A-F, 1mm; G-H, 200µm.

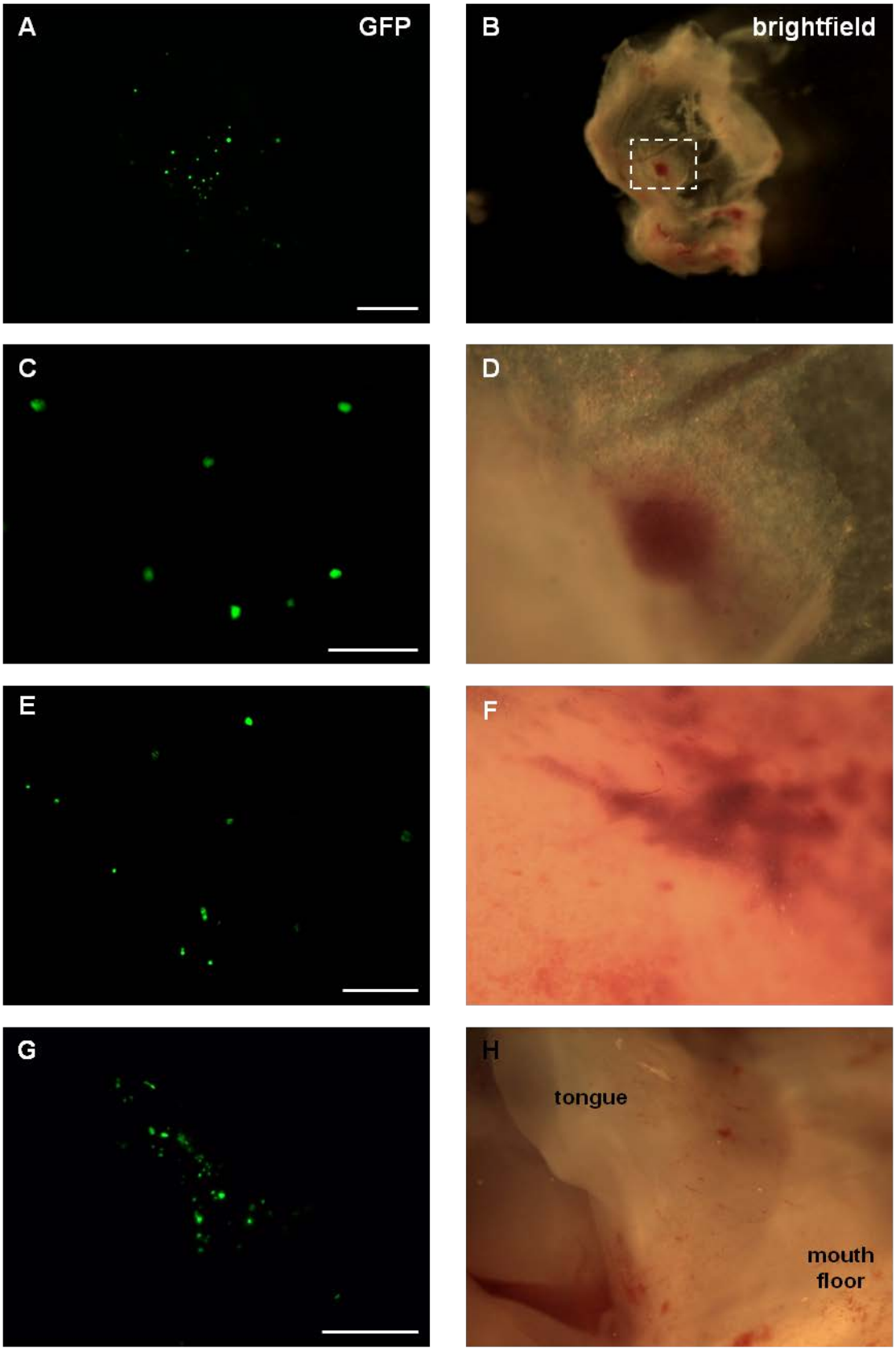

Figure 4.4. GFP-labelled Kelly cells were injected intravenously at E3, and chicks dissected at E10. Cells were observed within the A-F, meninges; G-H, tongue. C-D is a higher magnification of the area within the dashed box in B. Scale bars A-B, G-H, 1mm; C-D, 200µm; E-F, 500µm.

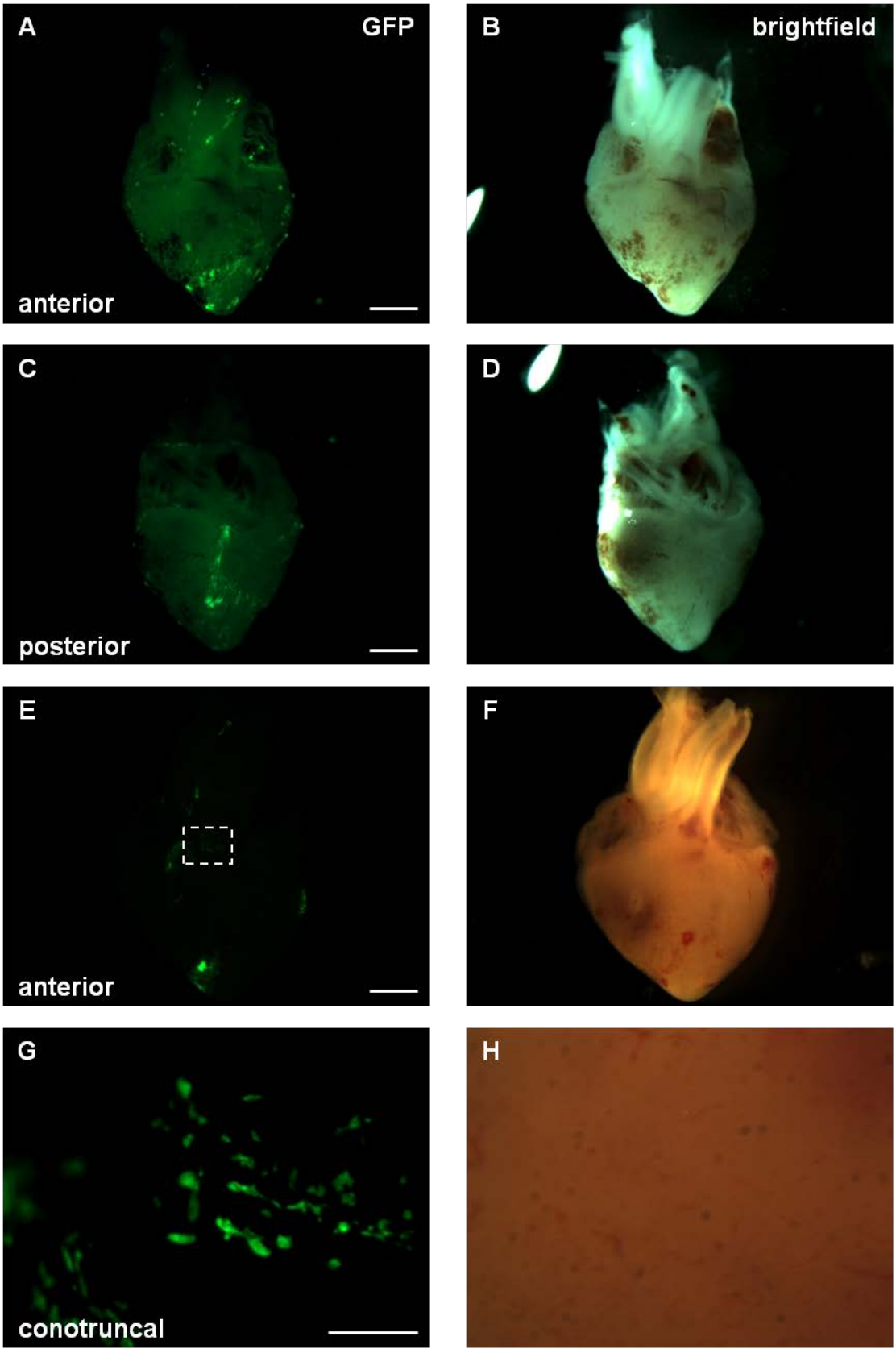

Figure 4.5. GFP-labelled Kelly cells were injected intravenously at E3, and upon dissection at E10, were observed within the chick hearts. G-H is a higher magnification of area within dashed box in E. Scale bars A-F, 1mm; G-H, 200µm.

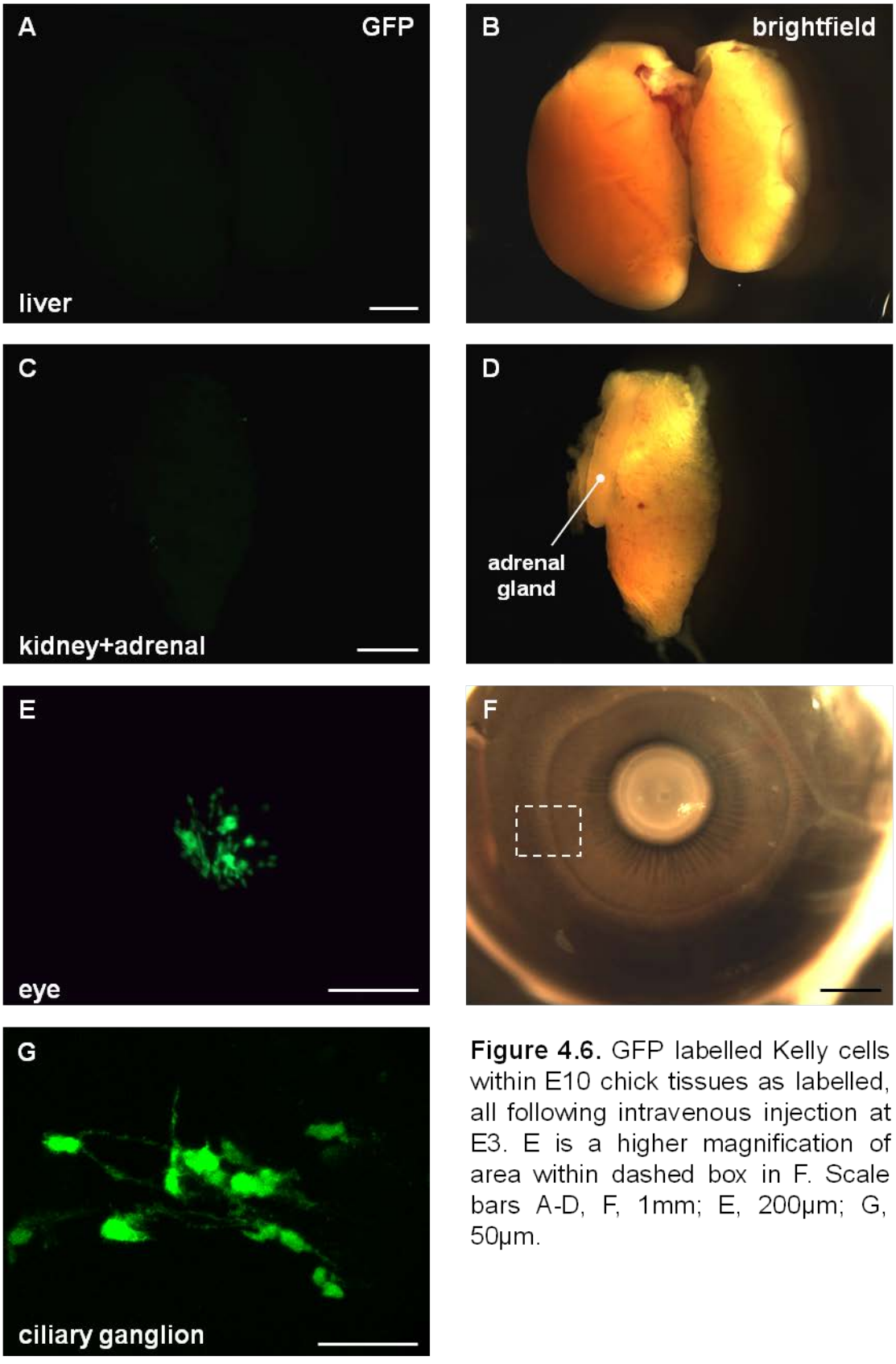

Figure 4.6. GFP labelled Kelly cells within E10 chick tissues as labelled, all following intravenous injection at E3. E is a higher magnification of area within dashed box in F. Scale bars A-D, F, 1mm; E, 200µm; G, 50µm.

It was deduced that the tissues to which the Kelly cells located were either wholly neural crest-derived, or at least had a neural crest component to them. As discussed in Chapter 1, the sympathetic ganglia are formed entirely by cells that have migrated from the neural crest, whereas in the gut, the neural crest contribution is via the enteric nervous system (ENS). More puzzling was the recurrent appearance of GFP Kellys in the tail regions of the embryos. However, staining of frozen sections of tail tissue for the neuronal marker TUJ-1 (which detects the protein β-III-tubulin) revealed a fine network of parasympathetic neurons (Figure 4.7) which are themselves derived from the neural crest. An additional parasympathetic structure targeted by the Kelly cells was the ciliary ganglion (Figure 4.4 G).

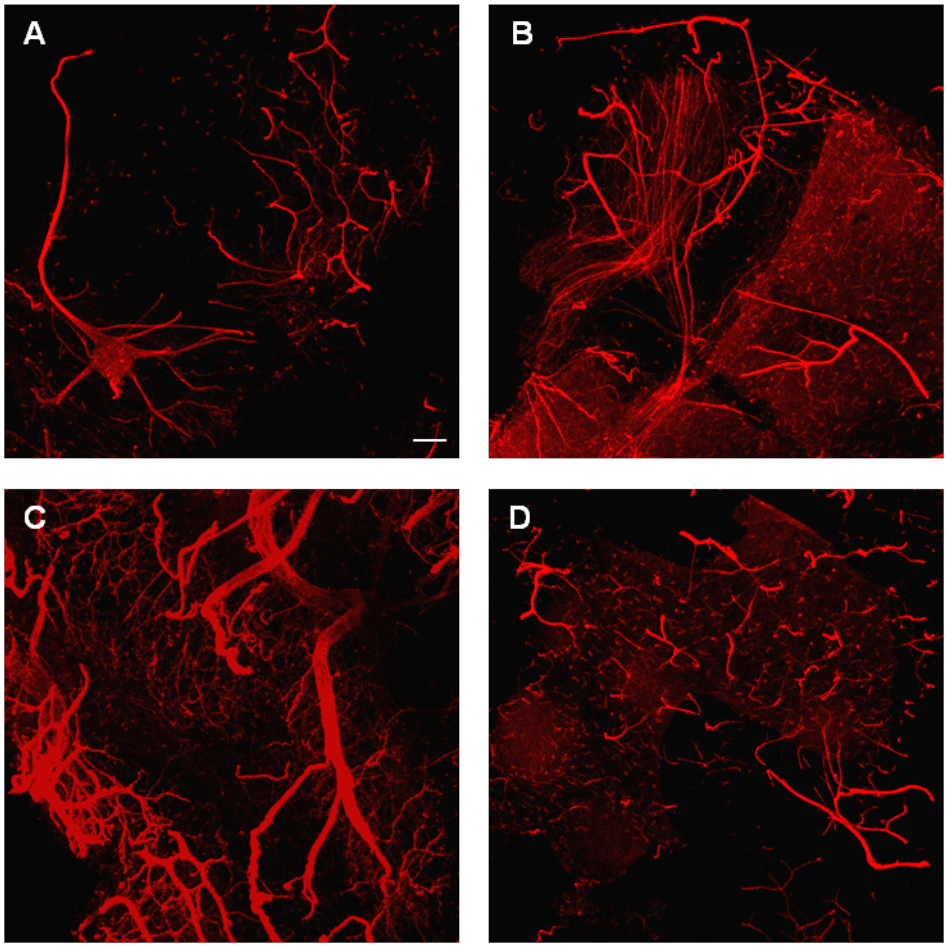

Figure 4.7. E10 chicks (no previous injections) had their tails dissected, and the resulting tissues were whole mount stained with a TUJ-1 antibody (detecting β-III-tubulin). Confocal images were taken of the nervous tissues that had been revealed – those shown are compressed Z stacks. Scale bar 100µm.

4.3.1.2. GFP Kelly E6 intravenous injections

For comparison, Kelly cells were injected at E6, when neural crest migration had been completed and neural crest-derived structures such as the sympathetic ganglia and adrenal glands had been formed, at least in a primordial form. An identical method of cell preparation and intravenous injection was employed to that utilised at E3, with approximately 200,000 cells being introduced into each embryo. At E10, GFP cell location was markedly different to that following E3 injection (n = >70 embryos, 14 separate experiments). Cells were distributed more widely throughout the embryo, but were discovered predominantly as clusters of cells within the liver (Figure 4.8 A-D) and kidneys (Figure 4.8 E-H) in almost every embryo examined. The meninges continued to be a regular site of Kelly cell incorporation – like at E3, in small "balls" of cells (Figure 4.9). Again, these were somewhat regular in size, although understandably smaller than when cells were injected at E3, generally between 15 and 20µm in diameter, likely owing to their reduced time within the embryo (4 days as opposed to 7). Cells were found in other locations such as the heart and lungs, and also in the gut – although the latter tissue contained considerably fewer neuroblastoma cells than the embryos injected at E3. Those cells within the gut may have colonised this structure along with the sacral component of the neural crest contributing to the formation of the ENS (Burns & Le Douarin 1998).

In general, the Kellys discovered within chick tissues following E6 administration resided within small clumps of neuroblastoma cells, rather than fully integrating into the tissues as some of the cells injected at E3 had appeared to do in the sympathetic ganglia and gut.

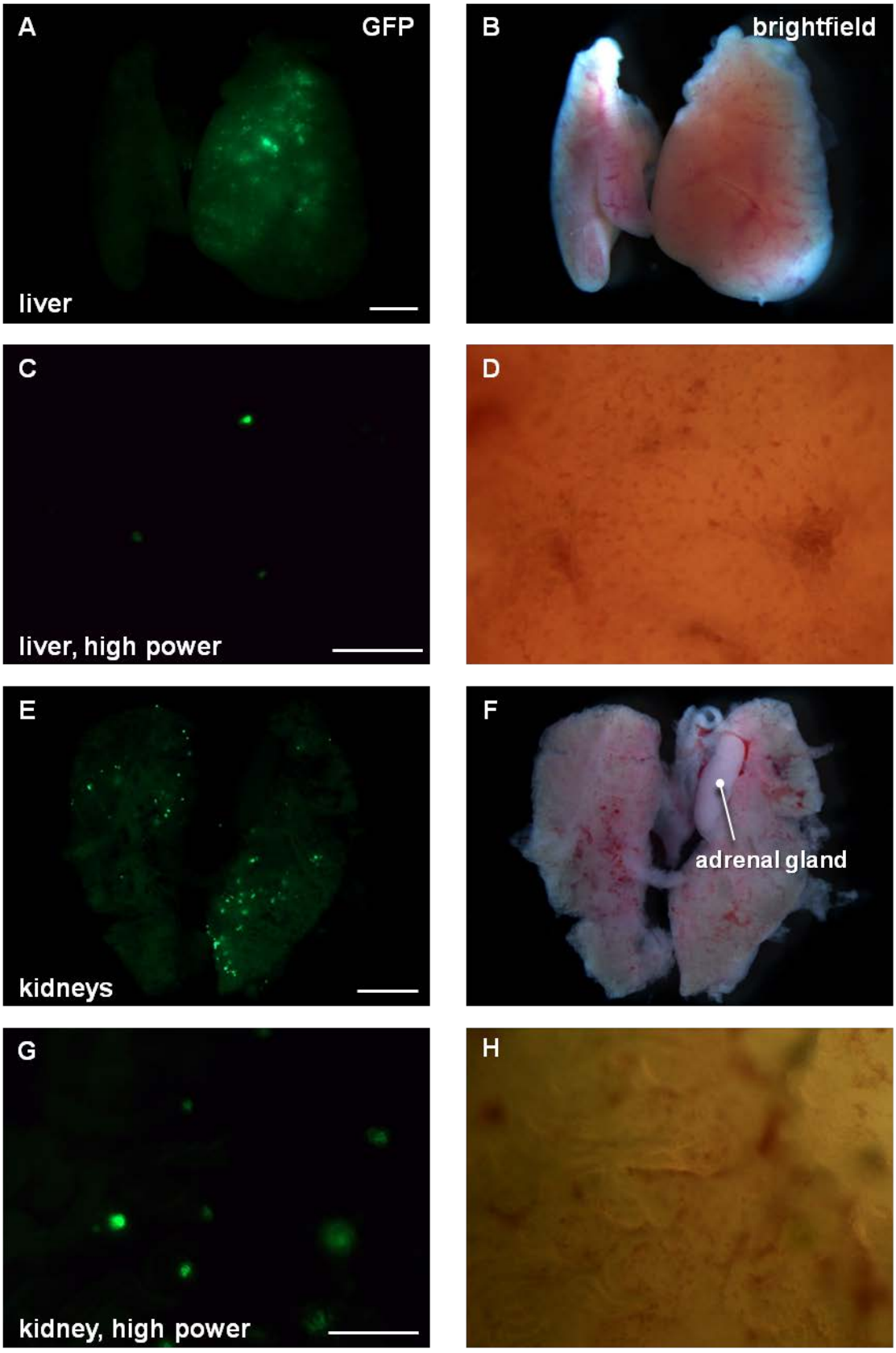

Figure 4.8. GFP-labelled Kelly cells were intravenously injected into E6 chick embryos. Upon dissection at E10, small clumps of cells were observed within the livers and kidneys. Scale bars A-B, E-F, 1mm; C-D, G-H, 200µm.

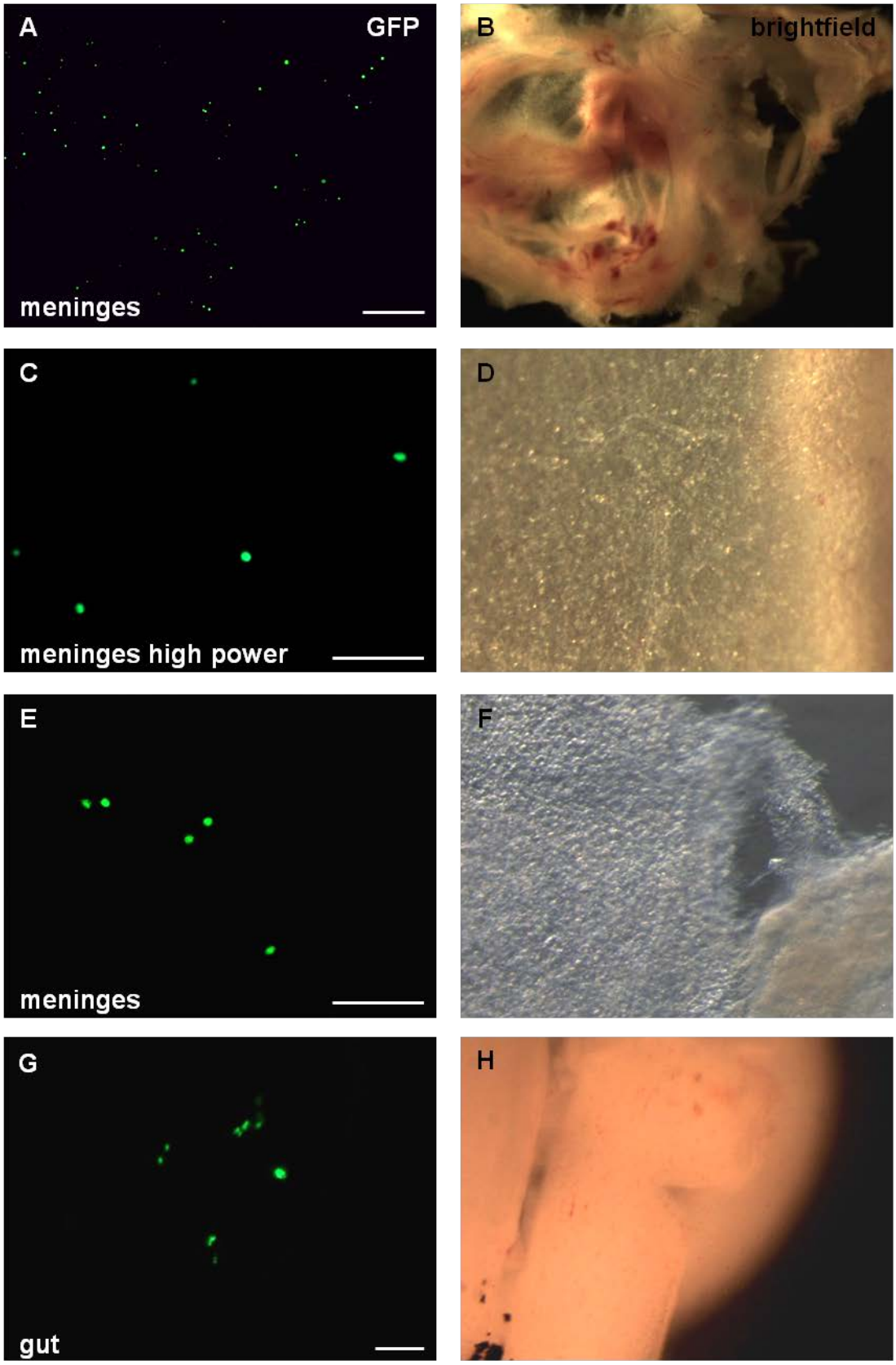

Figure 4.9. GFP-labelled Kelly cells were intravenously injected at E6, and chicks dissected at E10. Cells were discovered within the meninges and gut, as labelled. Scale bars A-B, 1mm; C-H, 200µm.

4.3.1.3. Fluorescent bead injections at E3 and E6

To assess whether the differences in neuroblastoma cell targeting between E3 and E6 intravenous injection could be attributed to changes in blood flow in the developing circulatory system between the two time points, 1µm diameter fluorescent beads were injected at both E3 and E6 and their locations noted at E10. The beads were diluted in PBS to a density of $1x10^5$/µl, and as with the Kelly cells, 2µl of the suspension was injected into the extra-embryonic circulation either at E3 (n=10 surviving embryos) or E6 (n=11 surviving embryos). Upon dissection of the embryos at E10, beads were widespread throughout the entirety of the embryos, regardless of their time of injection (Figures 4.10, 4.11 and 4.12). The relative quantities of beads in each tissue were estimated very approximately: a value of 1 equated to the presence of a small number of beads relative to the whole tissue, similar to that observed in the sympathetic ganglia (Figure 4.10 A), a value of 2 was given to the spleen (Figure 4.12 A), and a value of 3 meant there was an abundance of beads, such as in the meninges (Figure 4.10 G). Figure 4.12 E shows a graph summarising the beads' locations at E3 and E6.

It was concluded that the differences in cellular integration observed between the Kellys injected at E3 and at E6 were due to tissue-specific targeting of the neuroblastoma cells. This was later substantiated by differential targeting of alternate cell types (Figures 4.13, 4.14, 4.15, and summarised in Table 4.1).

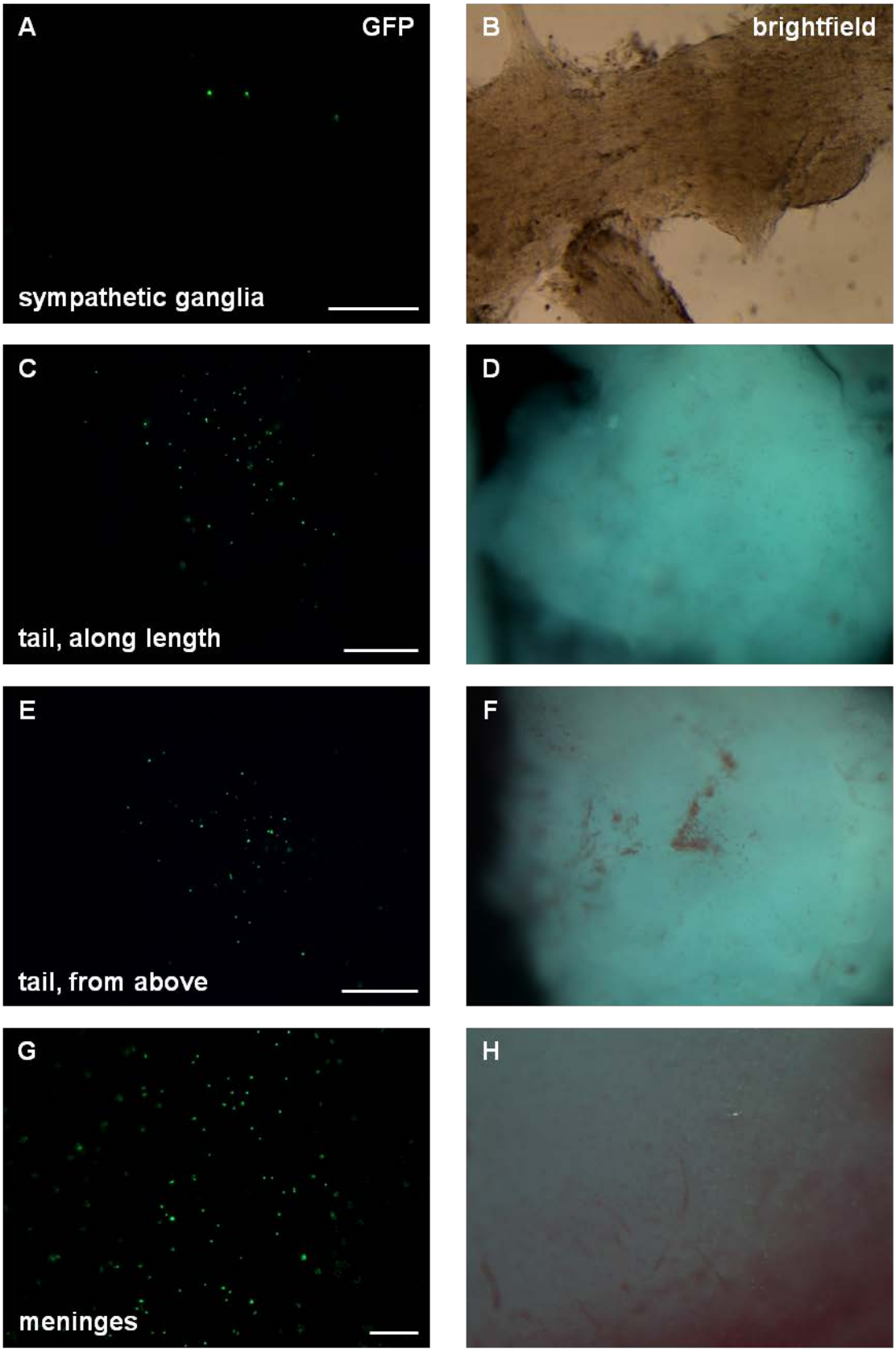

Figure 4.10. 1µm diameter green fluorescent beads were injected intravenously into E3 chick embryos. Upon dissection at E10, beads were observed within most chick tissues, including the sympathetic ganglia, tail and meninges. Scale bars A-B, G-H, 200µm; C-F, 500µm.

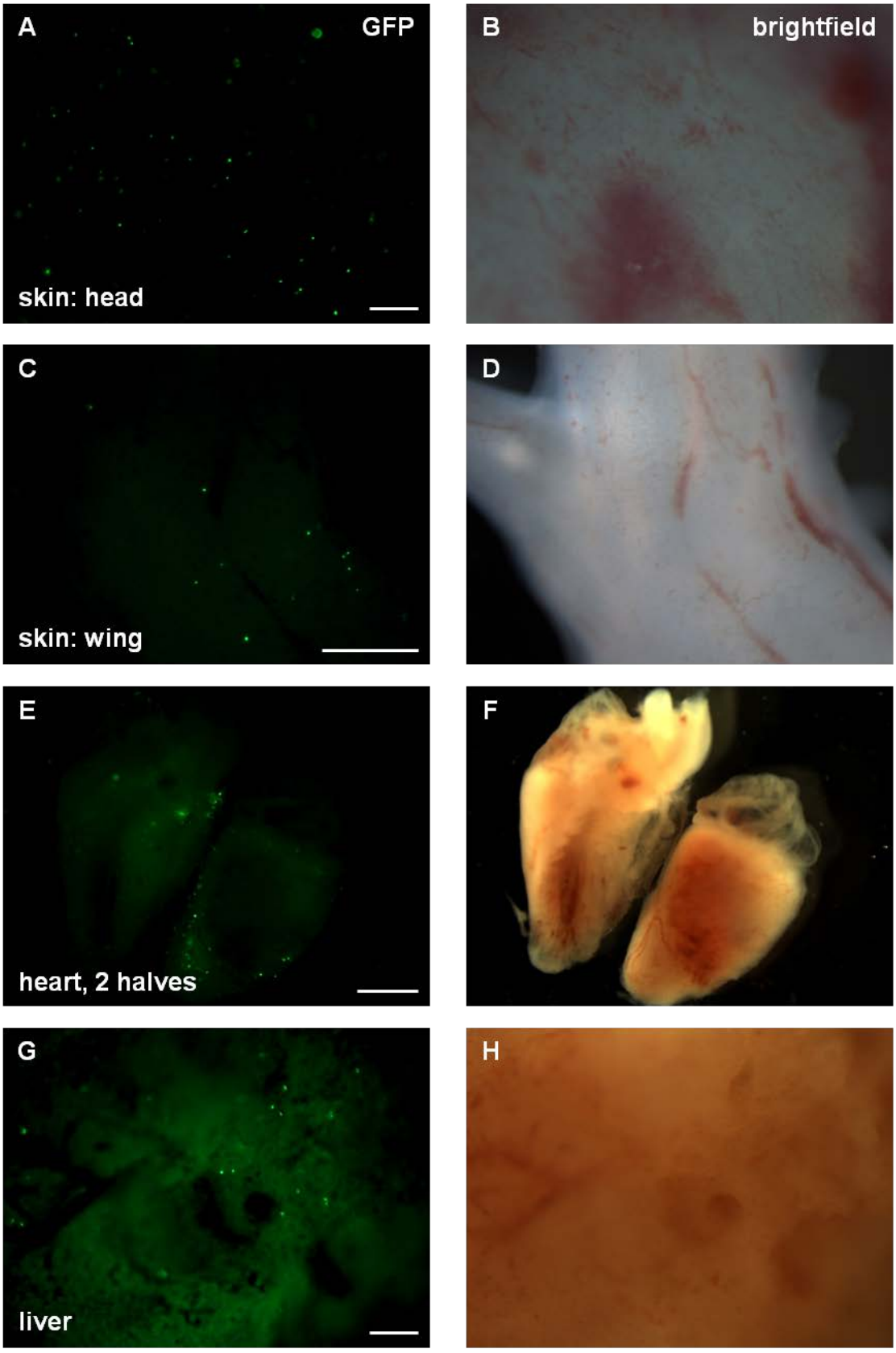

Figure 4.11. 1µm diameter green fluorescent beads were injected intravenously into E3 chick embryos. Upon dissection at E10, beads were observed within most chick tissues, including the skin, heart and liver. Scale bars A-B, G-H, 200µm; C-D, 500µm; E-F, 1mm.

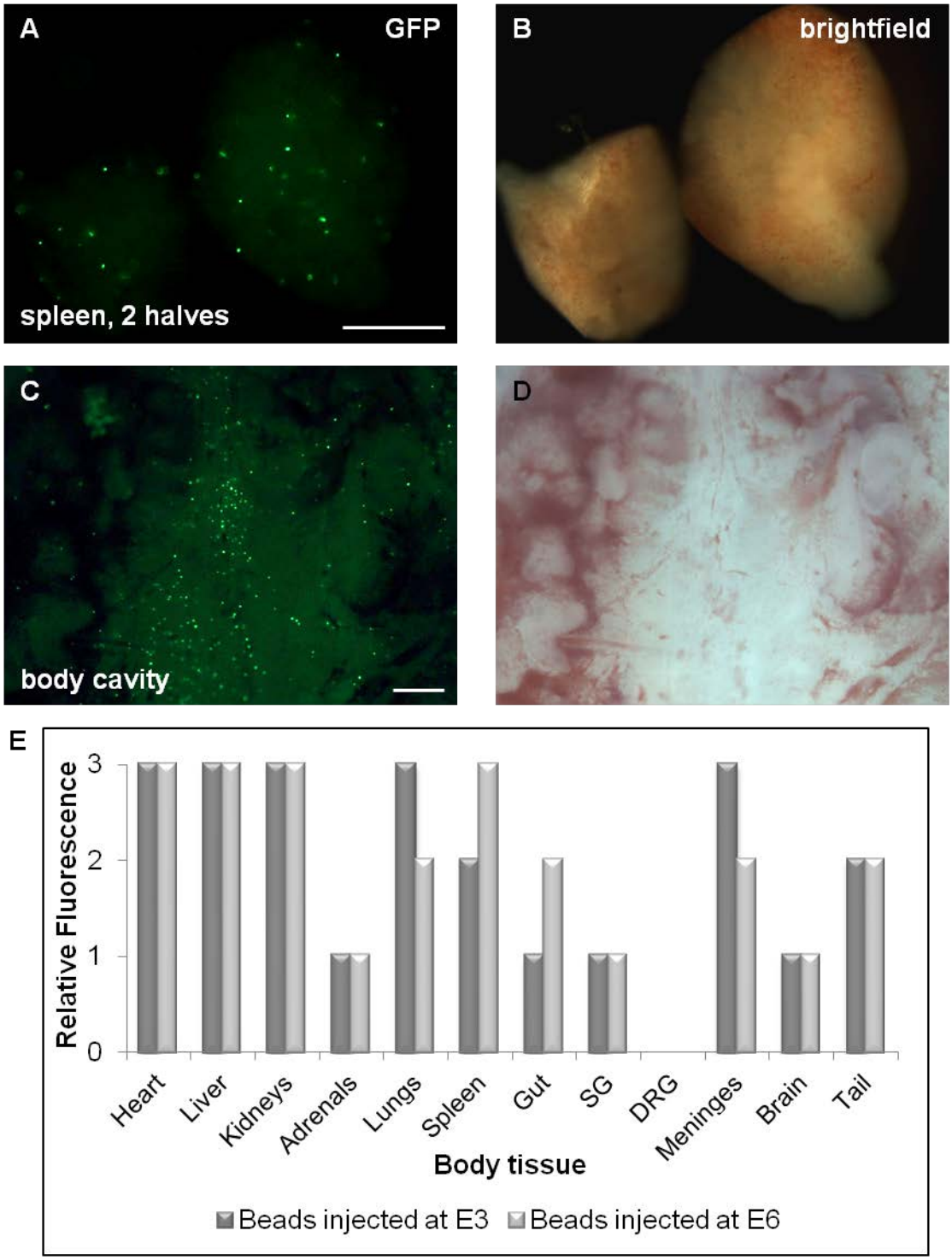

Figure 4.12. Following the intravenous injection of 1µm green fluorescent beads into E3 chick embryos, and subsequent dissection at E10, beads were observed within the majority of chick tissues, including the A-B, spleen; and C-D, mesenchyme within the body cavity. Scale bars 500µm. E, histogram to illustrate the distribution of fluorescent beads throughout the E10 chick embryos, following injection of beads at E3 (n=10) versus injection at E6 (n=11). Relative fluorescence was quantified very approximately, by comparing all tissues with one another and assigning values of 0, 1, 2 or 3 to each structure.

4.3.1.4. GFP BE(2)C intravenous injections at E3 and E6

Establishment of a GFP-labelled BE(2)C line by Dr Anne Herrmann (University of Liverpool, UK), meant that a second MYCN-amplified cell line could be injected intravenously at E3 and E6, to discover whether the targeting of neural crest derived tissues observed following E3 injection was a phenomenon unique to Kelly cells or a feature common to multiple neuroblastoma cells. Dissection at E10 of roughly 35 embryos from 5 separate experiments revealed that the BE(2)C cells injected at E3 targeted exactly the same neural crest derived structures as the Kellys, including the sympathetic ganglia, gut, tail and meninges (Figure 4.13), and like the Kellys, the BE(2)Cs were not observed in the chick adrenal glands. Similarly, following E6 injections, there was a total lack of neural crest specific targeting, with cells locating to tissues such as the liver, kidney and meninges (Figure 4.14), but never to the sympathetic ganglia (n = 14 embryos, from 3 separate batches).

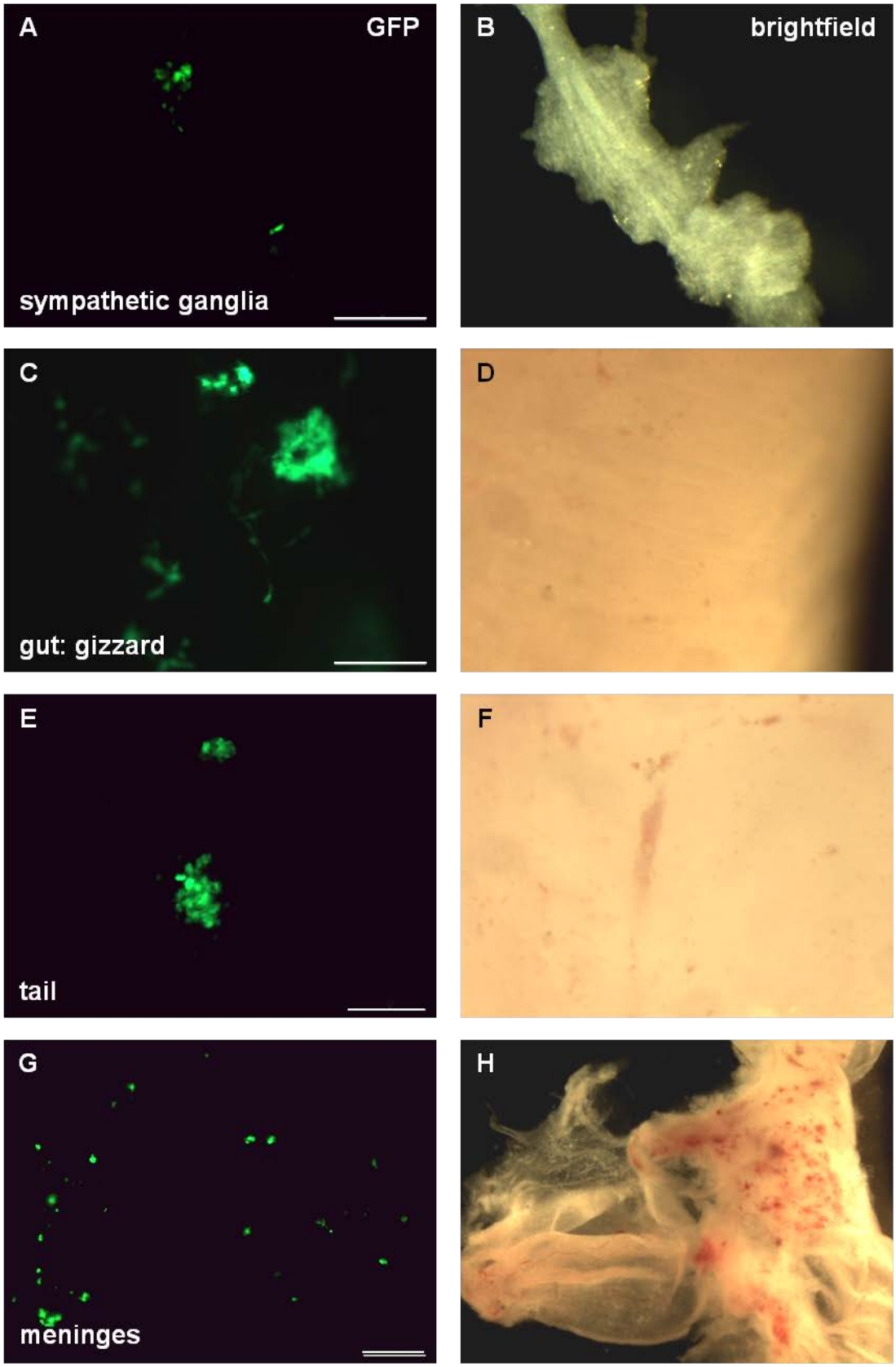

Figure 4.13. GFP-labelled BE(2)C cells were intravenously injected at E3. Upon dissection at E10, cells were observed primarily within the sympathetic ganglia, gut, tail and meninges, as labelled. Scale bars: A-F, 200µm; G-H, 1mm.

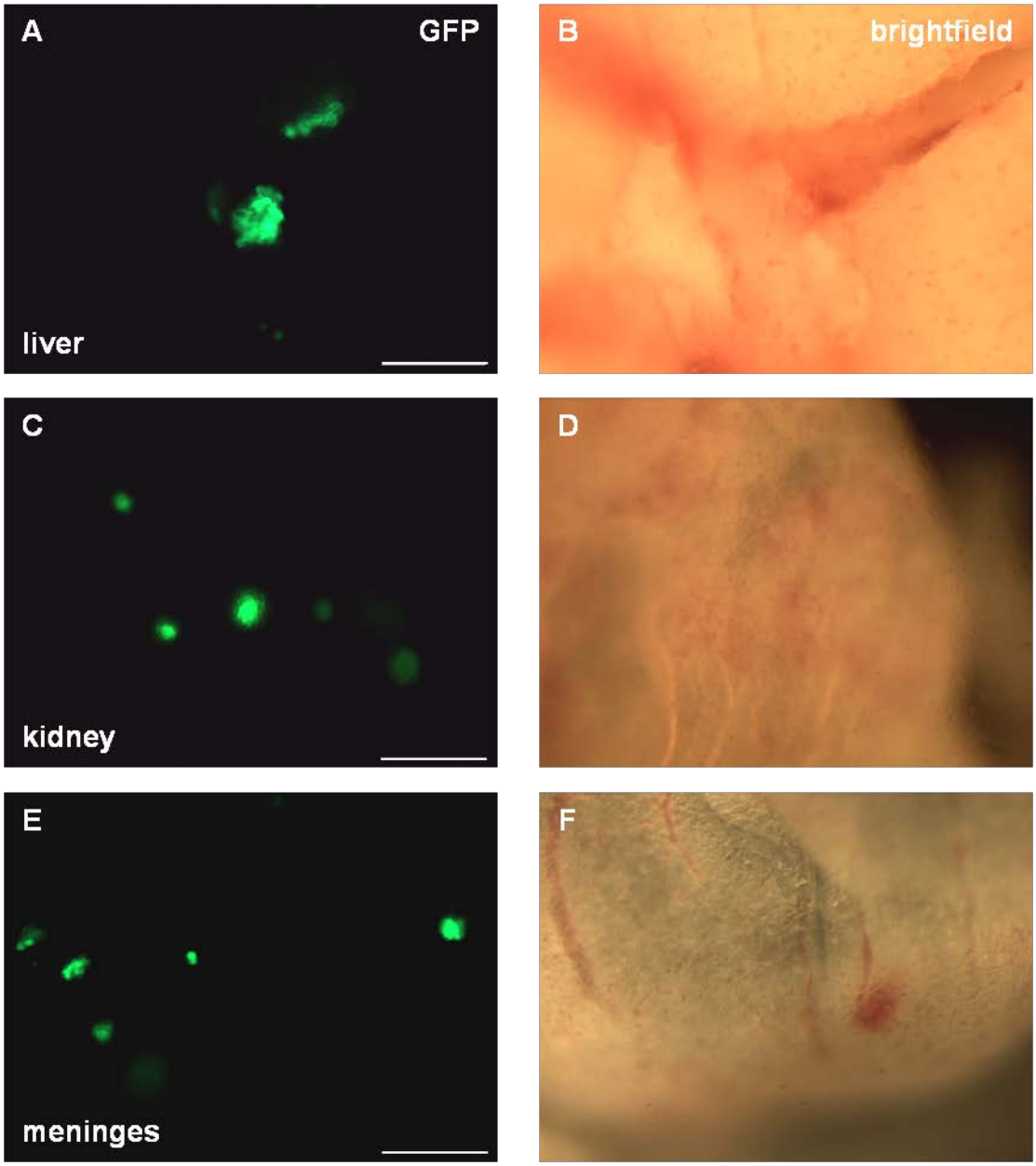

Figure 4.14. Following intravenous injection at E6, and chick embryo dissection at E10, GFP-labelled BE(2)C cells were observed within the liver, kidney and meninges, as labelled. Scale bars 200µm.

4.3.1.5. GFP glioblastoma intravenous injections at E3 and E6

The MYCN-amplified neuroblastoma cell lines had shown specific time-dependent targeting to neural crest derived structures. Therefore a different cancer line, from a glioblastoma tumour, was injected (in collaboration with Omar Pathmanaban, University of Manchester, UK) to determine whether it would also show patterns of targeting, and whether this would be similar to neuroblastoma or specific to its nature as a brain tumour. Glioblastoma multiforme is a brain malignancy, usually occurring in adults from a dedifferentiation of the cranial glial cells (typically astrocytes) and in which distant metastases are rare (Jellinger 1978). It was anticipated that targeting would be different, as in stark contrast to neuroblastoma being an embryonic tumour of the PNS, glioblastoma is an adult cancer occurring in the CNS.

GFP TSIA cells, a glioblastoma line derived from a primary tumour (by Omar Pathmanaban), were injected at the established E3 (n= 12 surviving embryos, 2 experiments) and E6 (n= 7 surviving embryos, 1 experiment) time points and dissected at E10, both for comparison to the neuroblastoma cell lines. Although roughly $2x10^5$ cells were injected per embryo, very few cells (difficult to quantify, but less than 100) were found to have survived in each embryo by E10, regardless of their injection time. Those cells that were alive were almost all found in CNS tissues – mostly the brain and sometimes the spinal cord - with a very small proportion also being discovered in peripheral neural tissues such as the dorsal root ganglia and sympathetic ganglia. This was the case for each one of the (albeit limited number of) surviving embryos. It may be hypothesised that survival was correlated with the cells' invasiveness, in that only those able to extravasate and migrate into CNS tissue were able to sustain themselves within the embryo. As demonstrated in Figure 4.15, the GFP labelled glioblastoma cells observed within chick neural tissues had extended extremely long processes, strongly suggestive of them being neuronally differentiating cells – although they perhaps could have been astrocytic, but nevertheless were differentiating. This was surprising particularly in those cells injected at E6 (Figure 4.15 H-K), considering their short time within the chick embryos (4 days).

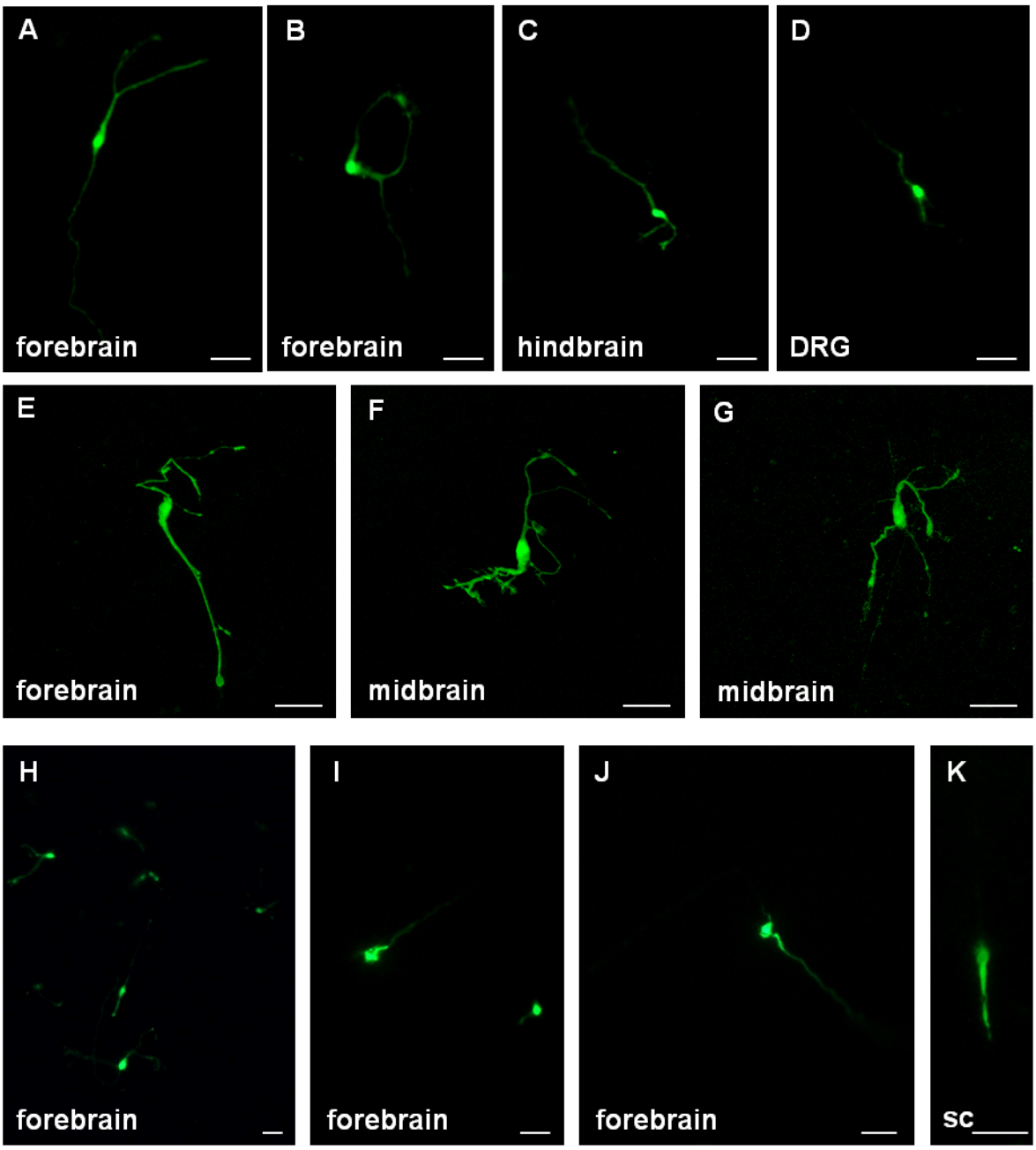

Figure 4.15. GFP-labelled glioblastoma cells within dissected E10 chick tissues as labelled, following intravenous injection at A-G, E3; H-K, E6. A-D, H-K, Images taken on Leica dissecting microscope; E-G, confocal microscopy, compressed Z stack images. sc, spinal cord. Scale bars A-D, H-K, 50µm; E-G, 20µm.

The targeting of the glioblastoma cells was substantially different from that of the Kellys, BE(2)Cs and fluorescent beads (Table 4.1), thus neural crest cell targeting was deemed to be a trait compatible with neuroblastoma being a neural crest derived tumour.

Chick tissue	Kelly E3	Kelly E6	Fluo. beads E3	Fluo. beads E6	BE(2)C E3	BE(2)C E6	Glio-blastoma E3, E6
Sympathetic ganglia	+++	-	+	+	+++	-	+
Gut	+++	+	+	++	++	+	-
Tail	+++	+	++	++	+++	+	-
Meninges	+++	++	+++	++	+++	++	+
Heart	++	+	+++	+++	++	+	-
Eye	++	+	++	+	++	+	-
Adrenals	-	-	+	+	-	-	-
Dorsal root ganglia	+	-	-	-	+	-	+
Lungs	-	+	+++	++	-	-	-
Spleen	-	-	++	+++	-	-	-
Brain	-	+	+	+	+	++	++
Spinal cord	-	-	-	-	-	-	+
Liver	-	+++	+++	+++	-	+++	-
Kidneys	+	+++	+++	+++	+	+++	-

Table 4.1. Summary table of relative numbers of cells/beads discovered in various chick embryo tissues following intravenous injection at E3 or E6 and dissection at E10. Targeting was strikingly different, when neuroblastoma cells (Kelly, BE(2)C) were compared to fluorescent beads and glioblastoma. Quantification was subjective: **-**, no cells incorporated; **+**, contained cells, but very few and/or rarely; **++**, usually contained a reasonable number of cells; **+++**, almost always possessed a relatively large number of injected cells. Shaded rows draw attention to those tissues with significant differences in targeting of neuroblastoma cells between E3 and E6 injections – the sympathetic ganglia, gut and tail displayed considerably more NB cell integration following E3 injection, and the liver and kidneys contained more cells when chicks were injected at E6.

4.3.2. GFP cells observed within E10 chick embryos were human neuroblastoma cells

In order to ascertain that the GFP fluorescence detected within the E10 chick tissues could be attributed only to the GFP-labelled Kelly cells injected at E3/E6 and was not derived for example from chick macrophages that had ingested the Kelly cells, frozen sections of sympathetic ganglia, gut, meninges and tail containing GFP fluorescence were stained with antibodies to the proteins N-CAM (CD56) and NB84, which have been shown to stain the Kelly cells in culture (Figure 3.28) and are human specific. As shown in Figures 4.16 and 4.17, there was a direct correlation between the GFP and the antibody staining, indicating that these were Kelly cells surviving within the various chick tissues. In addition, a lack of staining of the Kelly cells within the sympathetic ganglia, gut and ciliary ganglia, as well as the non-neural tail and meninges with a chick-specific antibody to GAP43 (Figure 4.18), demonstrated that the human neuroblastoma cells had not fused with chick cell nuclei. Histology of the GFP-containing livers, in addition to N-CAM staining (Figure 4.19, thanks to Andrew Dodson, University of Liverpool, UK) confirmed the lack of cell fusion and phagocytosis in tissues derived from E6-injected embryos. Cell clusters in the liver were usually located close to blood vessels/sinusoids, and their appearance following H&E staining was reminiscent of the small round blue cells observed in malignant primary neuroblastomas.

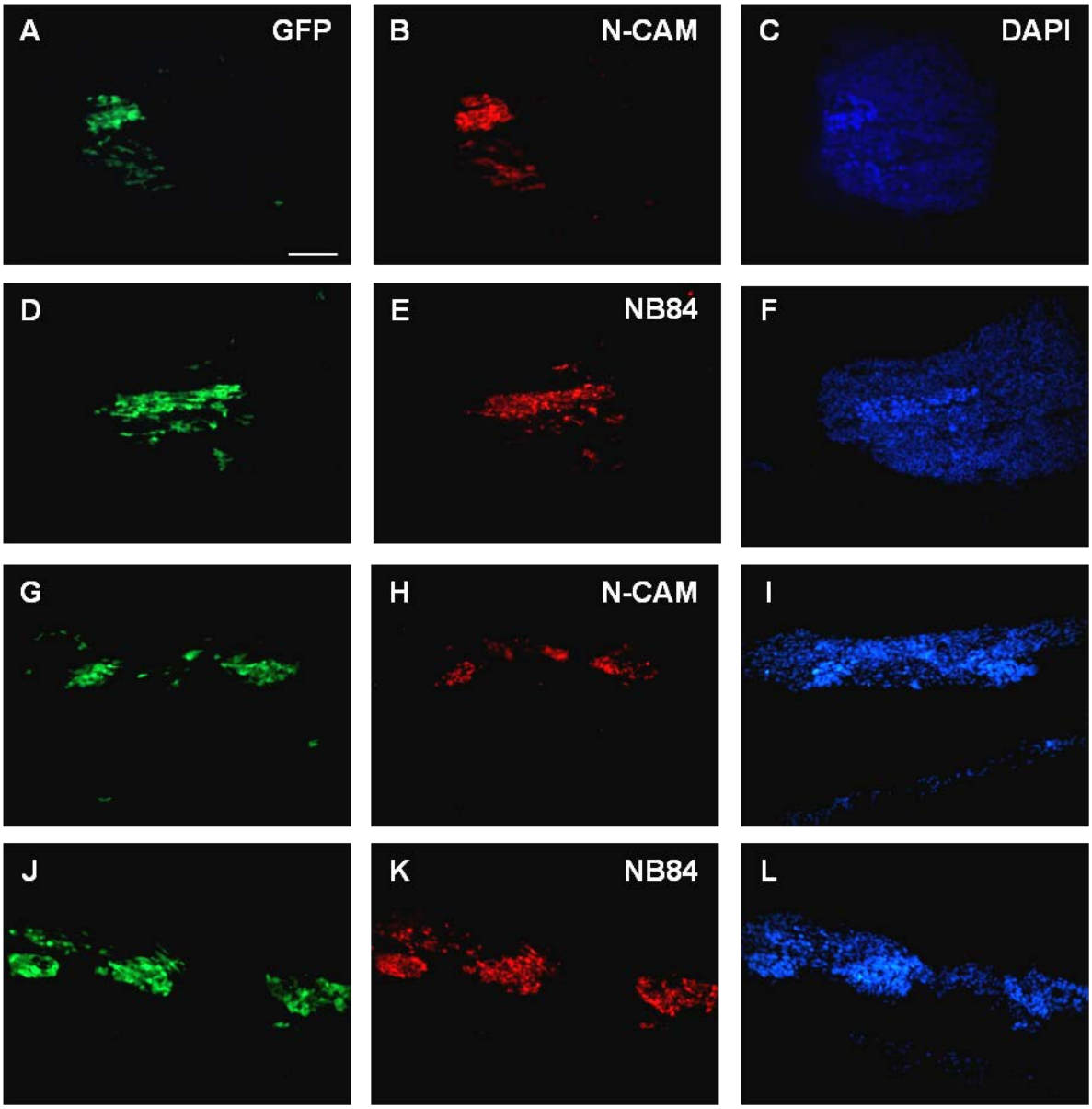

Figure 4.16. Frozen sections of GFP-Kelly cells within E10 chick A-F, sympathetic ganglia; G-L, gut; following intravenous injection at E3. Sections were stained for N-CAM and NB84 as labelled. Scale bar 50µm.

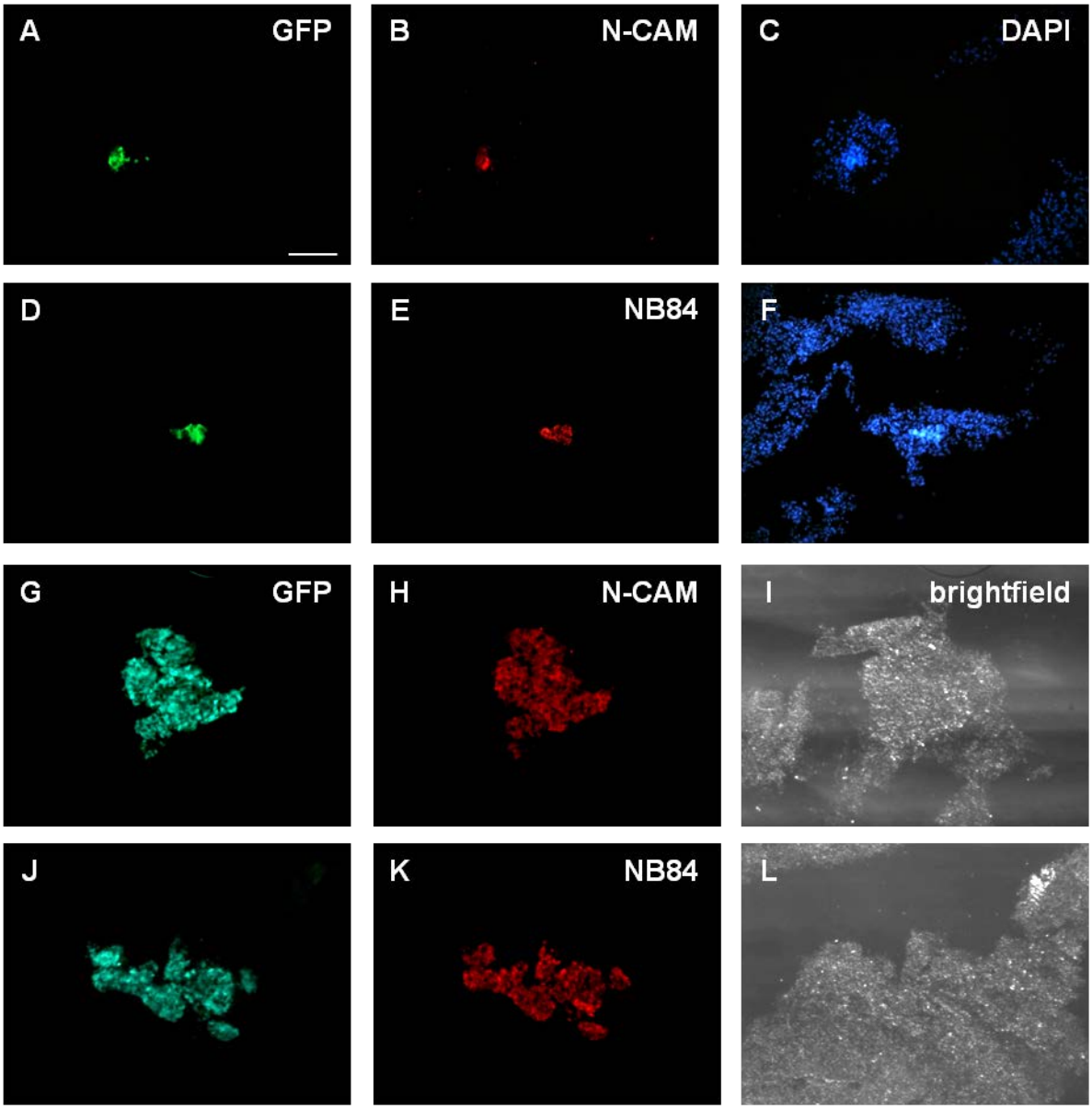

Figure 4.17. Frozen sections of GFP-Kelly cells within E10 chick A-F, meninges; G-L, tail; following intravenous injection at E3. Sections stained for N-CAM and NB84 as labelled. Scale bar 50µm.

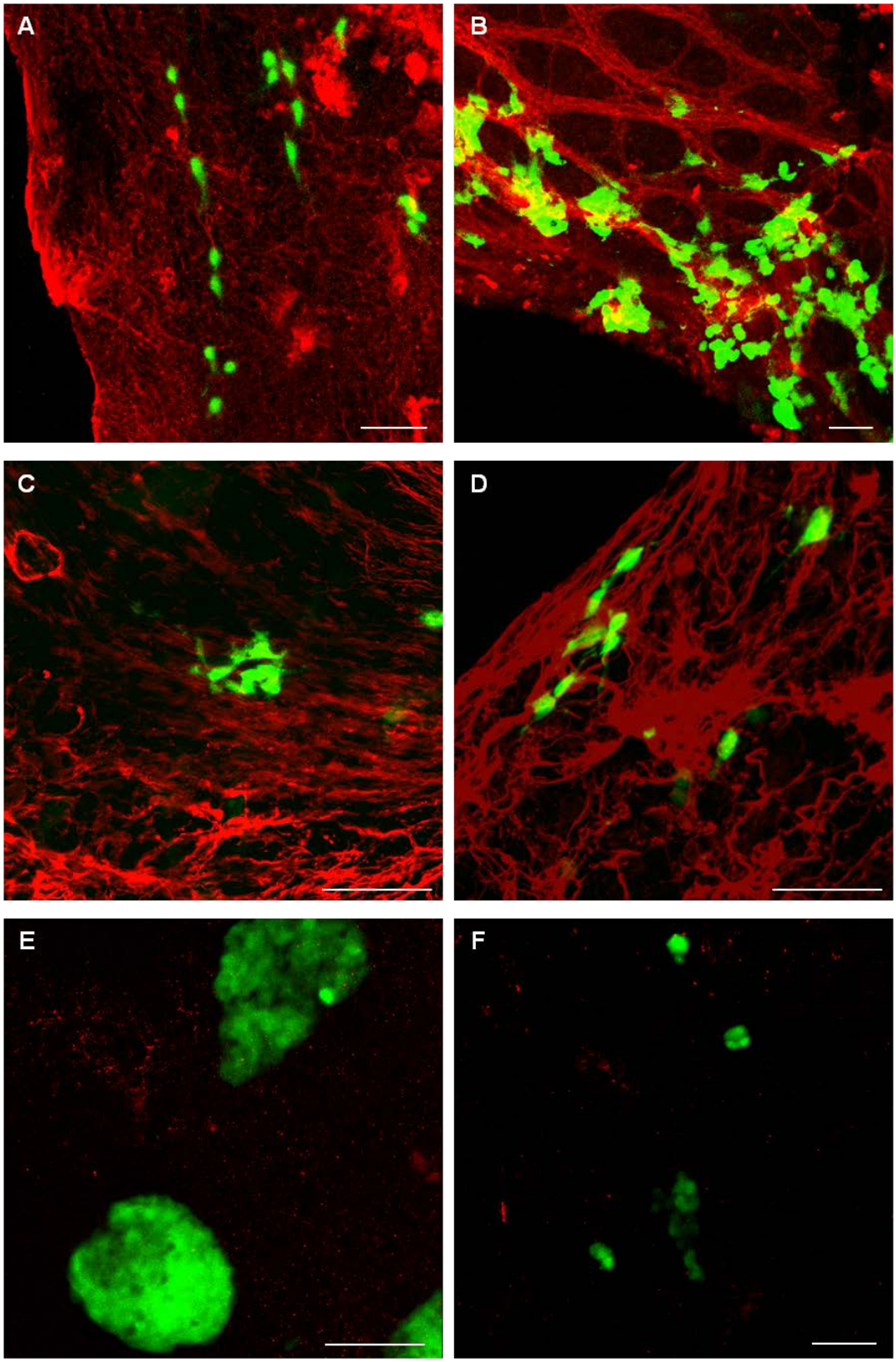

Figure 4.18. Confocal images, compressed from Z stacks, of GFP-labelled Kelly cells (green) within dissected E10 chick tissues, following intravenous injection at E3. Tissues were whole mount stained with chick-specific GAP43 antibody (red). A, sympathetic ganglia; B, gut; C,D, ciliary ganglia; E, tail; F, meninges. Scale bars 50µm.

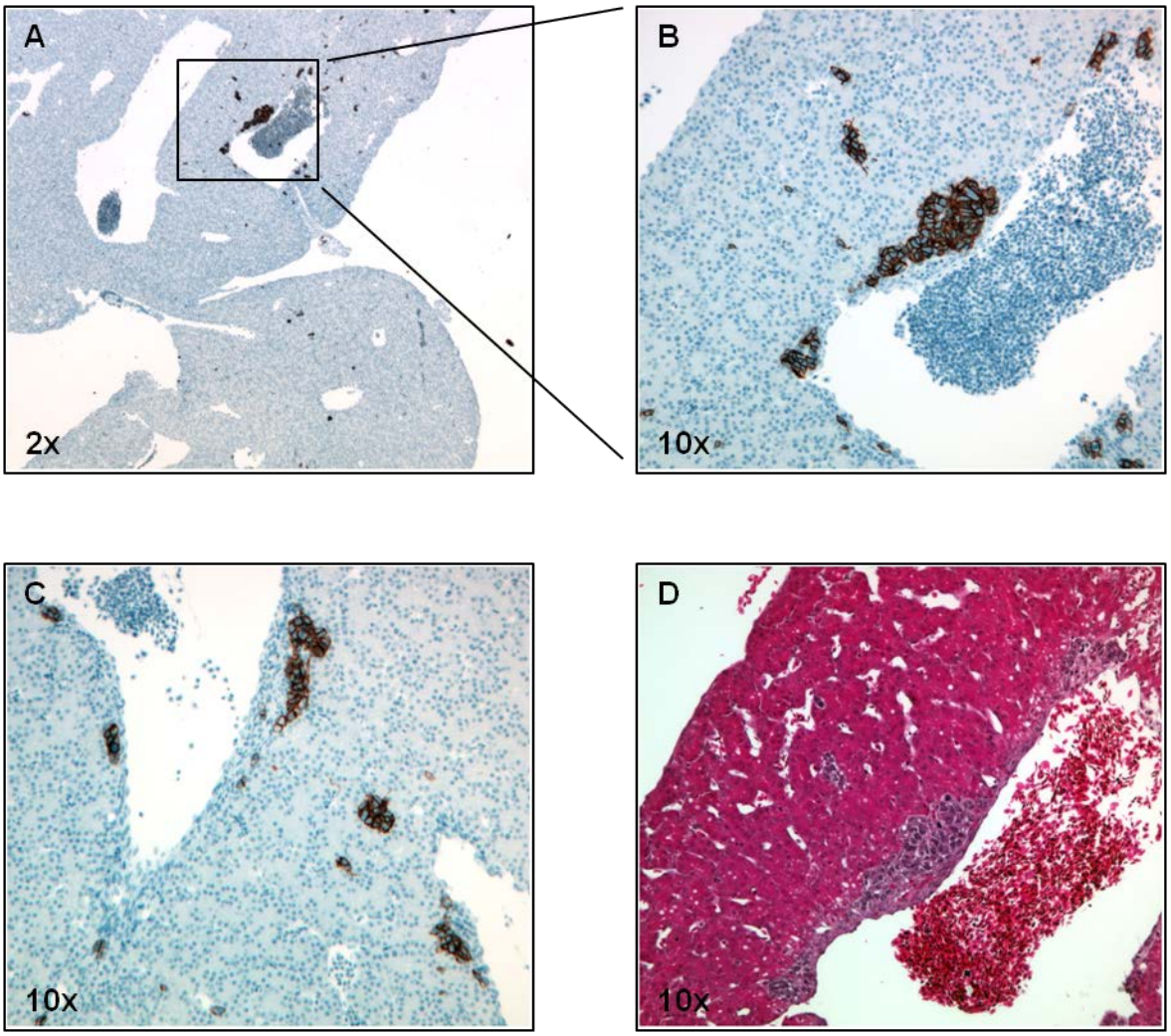

Figure 4.19. Following E6 intravenous injection of GFP-labelled Kelly cells, a dissected E10 liver was mounted in a paraffin block and sectioned. A-C, N-CAM (CD56) staining of liver paraffin sections identifies the Kelly cells (brown); D, H&E stain shows the histology of the liver containing Kelly cells.

4.3.3. GFP Kelly cell behaviour within chick tissues

4.3.3.1. Morphology and differentiation

Confocal microscopy of the GFP Kelly-containing E10 chick tissues revealed differing morphologies of the neuroblastoma cells depending on their environment. In neural tissues such as the sympathetic ganglia and gut (Figure 4.20 A and B, respectively), the Kellys were elongated in appearance and extended short processes, suggestive of cell migration or the beginnings of neuronal differentiation. In contrast to what was interpreted during dissection of the gut, cells were not located on the external surface, but were situated deeper within the tissue, integrated in two separate layers – the myenteric and submucosal plexuses of the

enteric nervous system (Figure 4.20 C). The Kellys in the two aforementioned tissues typically resided as single cells, or sometimes in groups of 2-5 loosely associated cells. This was in contrast to the appearance of Kellys in non-neural tissues such as the tail and meninges (Figure 4.20 D and E, respectively), where they were more rounded and tended to exist as clumps, which in the meninges were particularly tightly packed. This morphological state implied limited or no migration and/or cells undergoing proliferation.

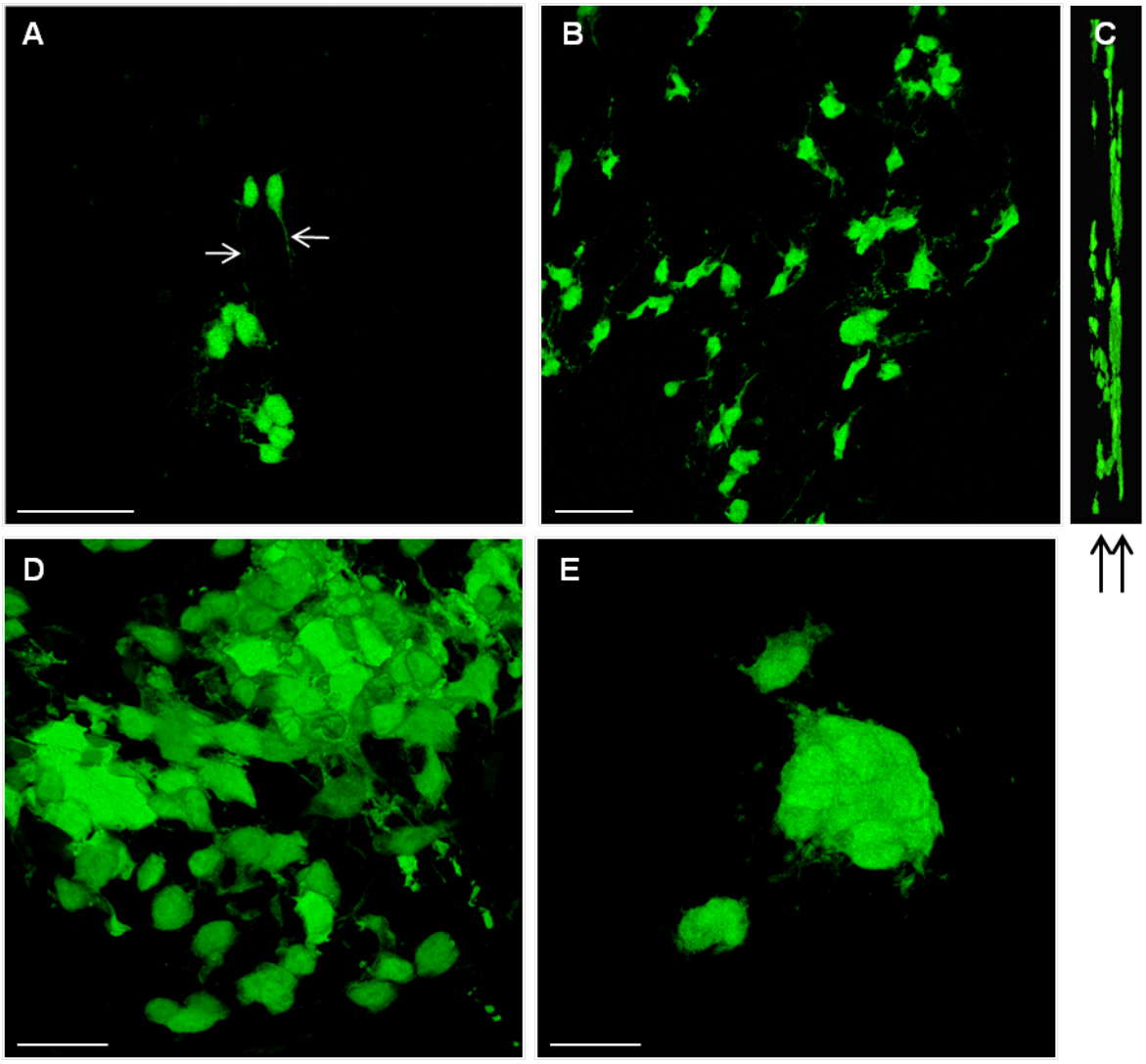

Figure 4.20. Confocal images, compressed from Z stacks, of GFP-labelled Kelly cells within E10 chick tissues. Kellys were intravenously injected at E3, chicks were dissected at E10, and tissues containing GFP cells were fixed and "squashed" between a glass slide and coverslip. A, sympathetic ganglia, white arrows indicate processes; B, gut ('looking down' onto the two layers of Kelly cells within the ENS); C, gut (image in B rotated though 90°, revealing the two plexuses of the ENS, identified by black arrows); D, tail; E, meninges. Scale bars A-C, 50µm; D-E, 20µm.

The morphologies observed for the Kellys were recapitulated using the BE(2)C cells; with cells extending processes in the sympathetic ganglia and gut and integrating into the two plexuses of the ENS, but forming more dense clumps in the tail and meninges (Figure 4.21).

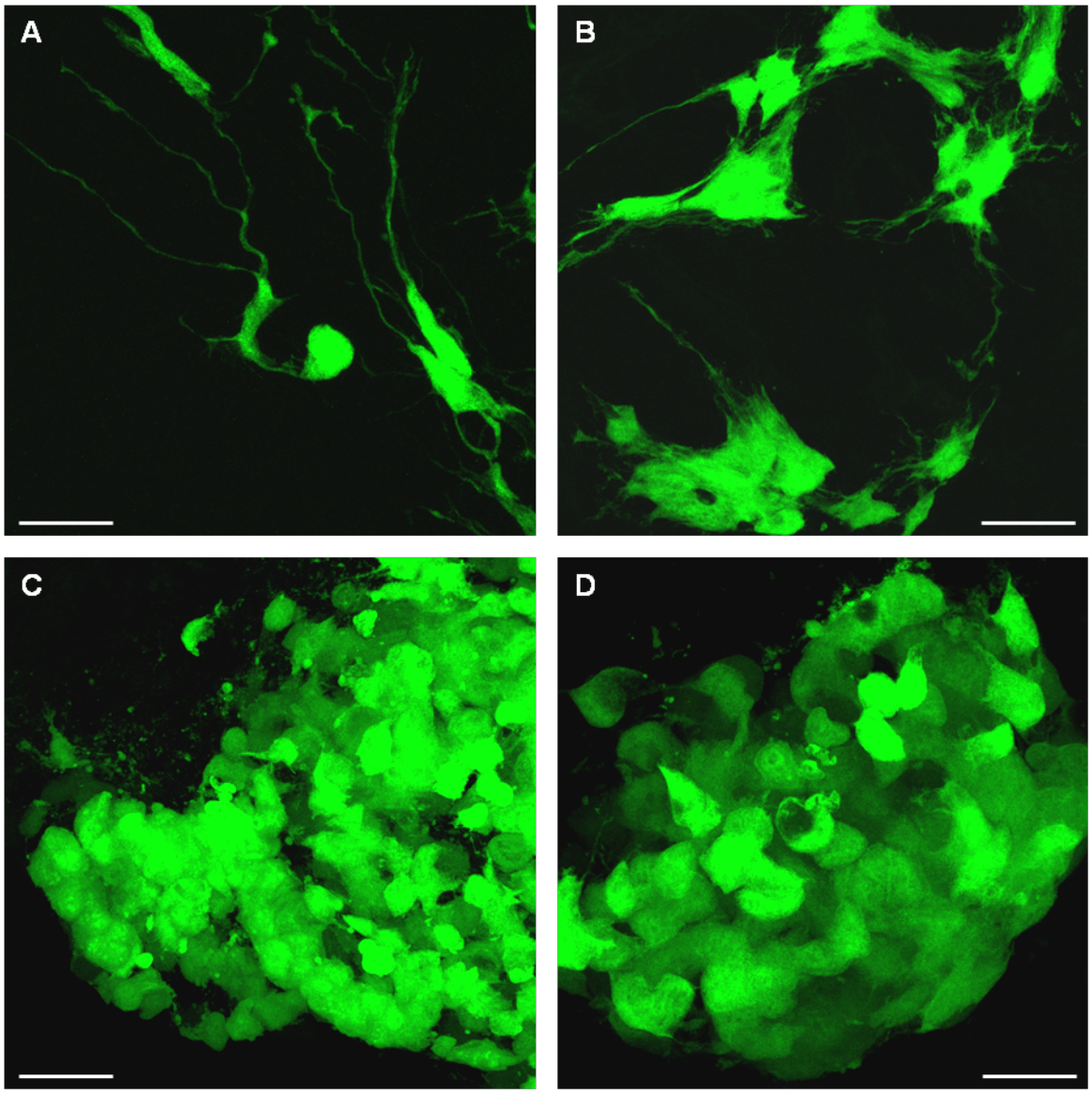

Figure 4.21. Confocal images of GFP-labelled BE(2)C cells within E10 chick tissues. BE(2)Cs were intravenously injected at E3, chicks were dissected at E10, and tissues containing GFP cells were fixed and "squashed" between a glass slide and coverslip. Images are compressed from Z stacks. A, sympathetic ganglia; B, gut ('looking down' onto the two layers of BE(2)C cells within the ENS); C, tail; D, meninges. Scale bars 25µm.

E10 chick tissues containing GFP Kellys were whole mount stained for the neurofilament 70kD subunit, and the antibody was able to detect both chick and human antigens. Although none of the Kellys stained positively for this neuronal marker (Figure 4.22), the staining, along with the immunofluorescence for GAP43, revealed that the neuroblastoma cells had integrated well into the neuronal tissues and were closely associated with the chick neurons (Figure 4.18 A-D and 4.22 A-D), particularly in the ENS. In the tail the Kellys remained distinct from the chick tissue and its limited neuronal network (Figure 4.22 E). Similarly in the meninges, where no neural tissue exists, the Kellys existed as discrete clumps (Figure 4.22 F). In all tissues, Kelly cells continued to stain positively for tyrosine hydroxylase, regardless of their morphology (Figure 4.23).

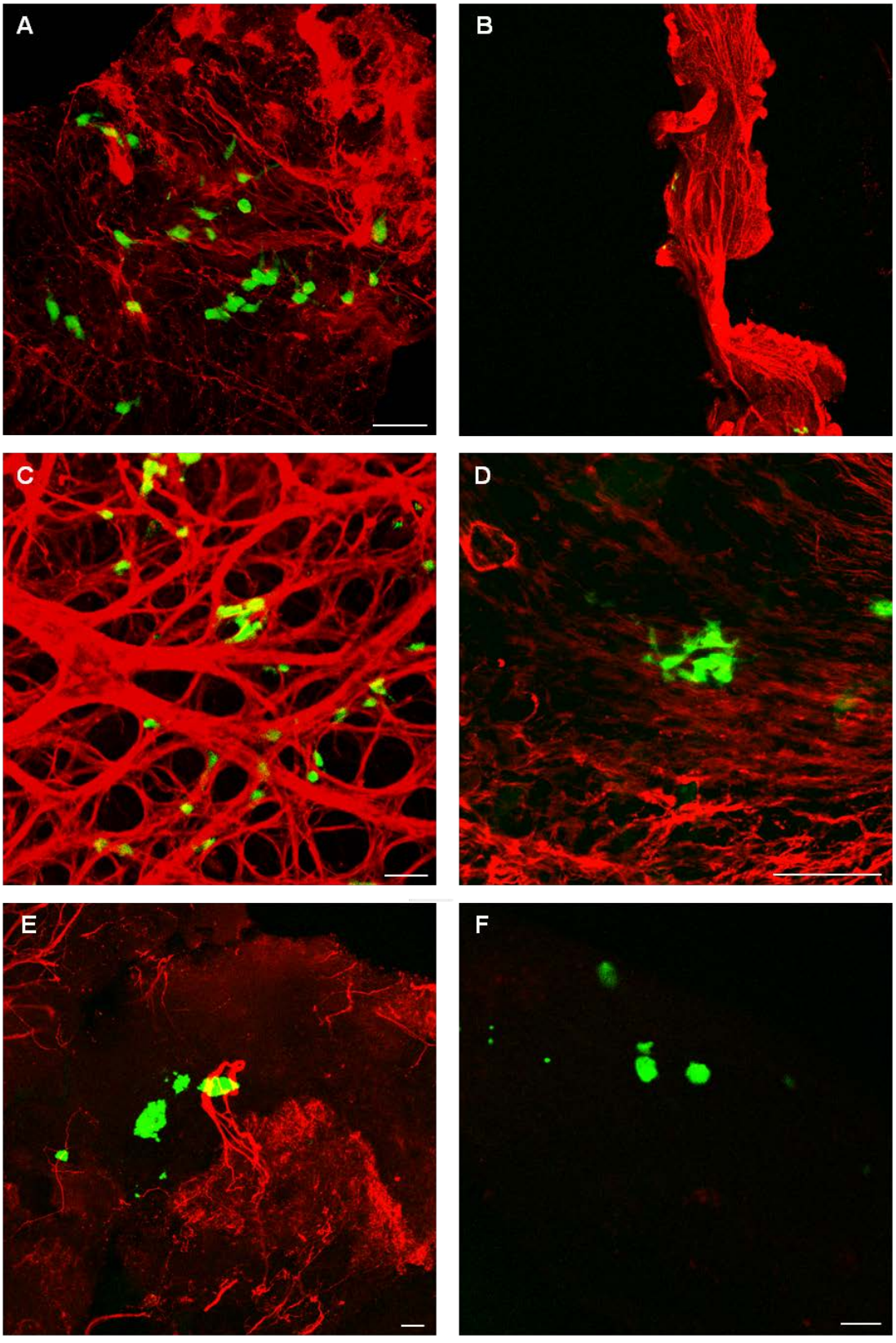

Figure 4.22. Confocal images, compressed from Z stacks, of GFP-Kellys (green) within dissected E10 chick tissues following intravenous injection at E3, and whole mount staining with an antibody to the neurofilament 70kD subunit (red). A-B, sympathetic ganglia; C, gut; D, ciliary ganglion; E, tail; F, meninges. Scale bars 50µm.

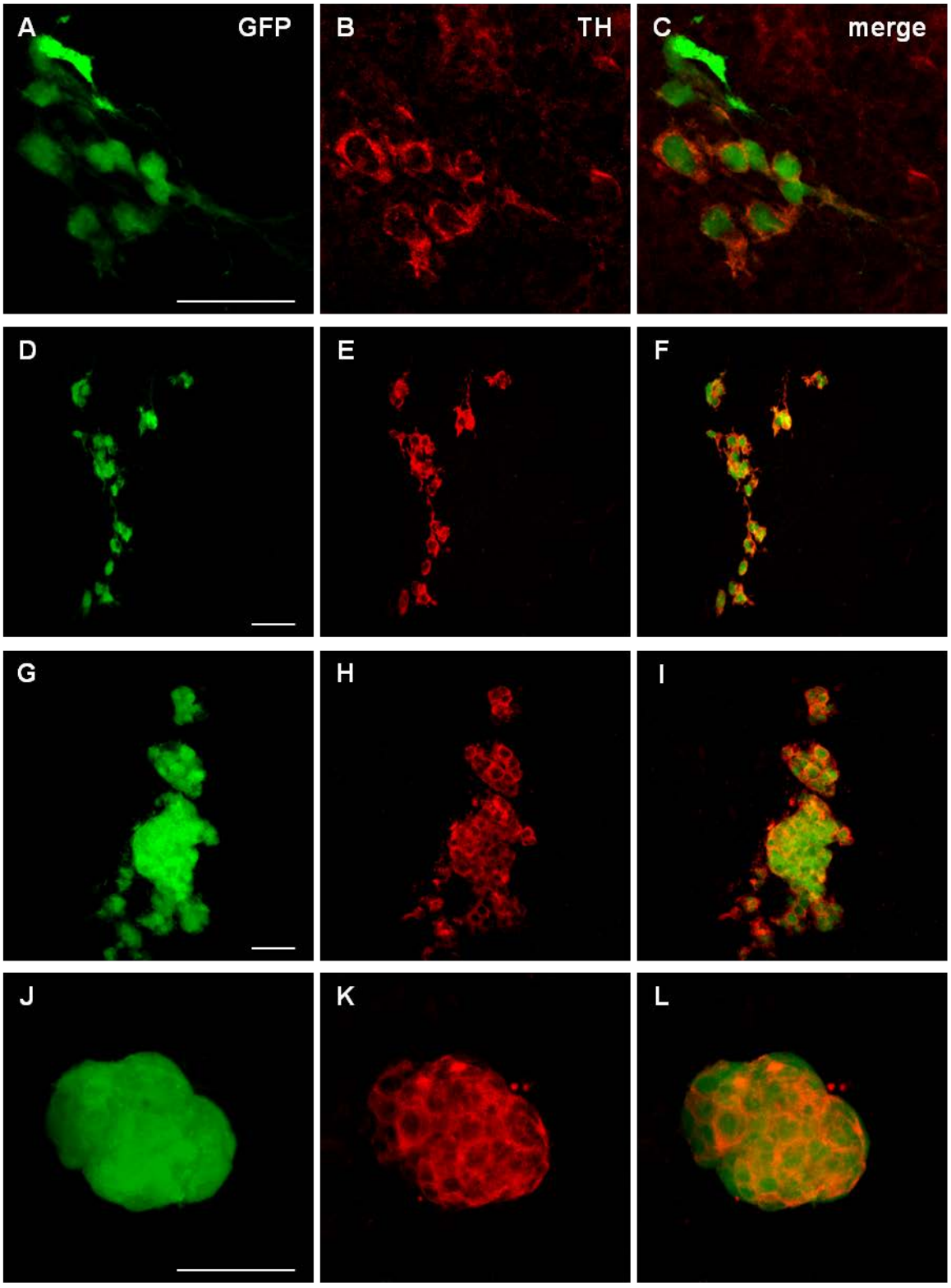

Figure 4.23. Confocal images, compressed from Z stacks, of GFP-Kellys (green) within the E10 chick A-C, sympathetic ganglia; D-F, gut: G-I, tail; J-L, meninges; all following intravenous injection at E3. Cells were whole mount stained for human-specific tyrosine hydroxylase (red). C,F,I,L are merged images. Scale bars 50µm.

Confocal analysis of E10 tissues of chick embryos injected at E6 confirmed the presence of small masses of rounded cells (Figure 4.24), which were of various sizes, particularly in the liver, where they could range from only a few cells, up to irregularly-shaped clumps with diameters of 300µm or more. Clumps in the kidneys were more regular in both shape and size; roughly 50µm in diameter, and those in the meninges were also regularly sized, at 15-20µm. The morphologies of the cells within the tissues of E6-injected embryos were indicative of cells undergoing proliferation.

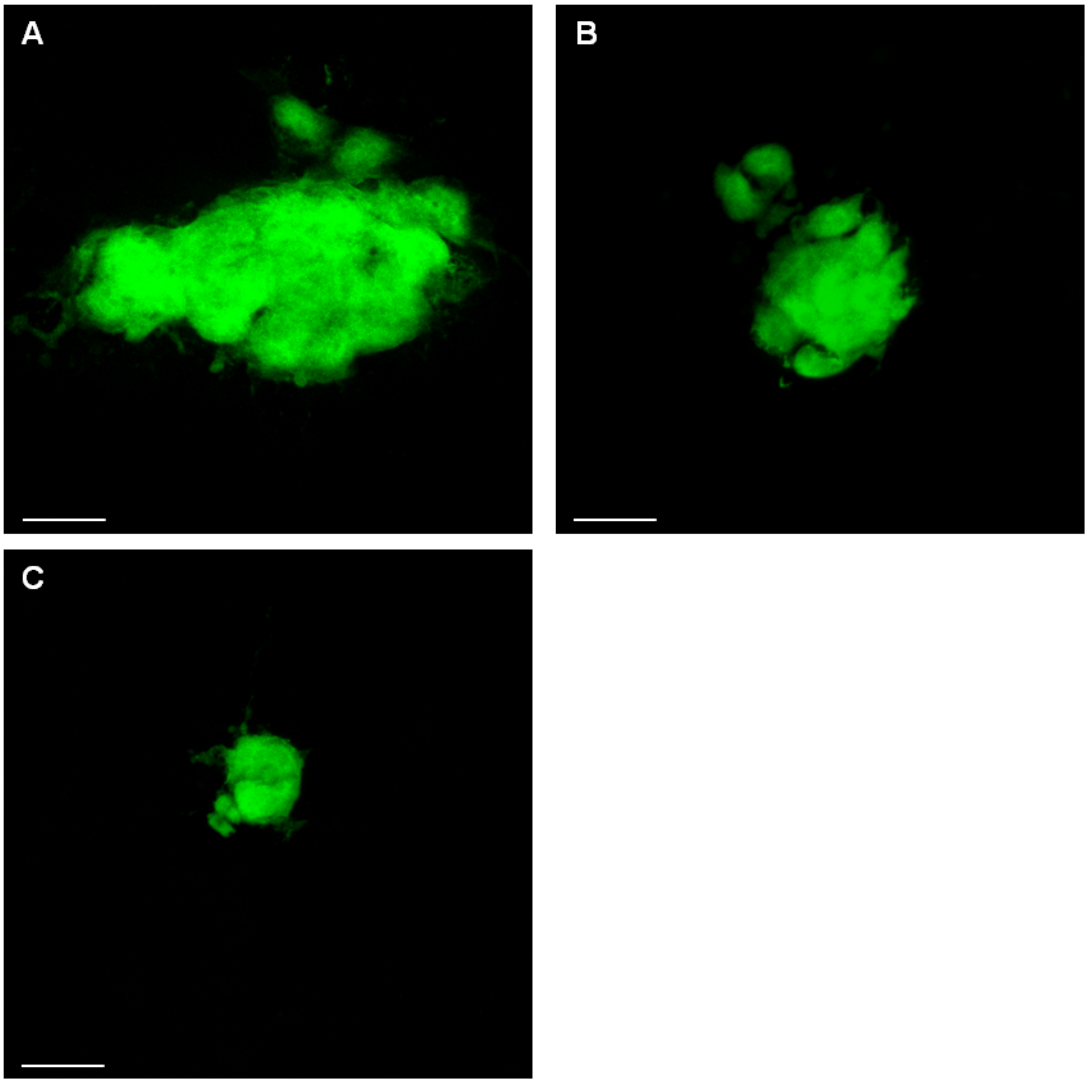

Figure 4.24. Confocal images of GFP-labelled Kelly cells within dissected E10 chick tissues. Kellys were intravenously injected at E6, chicks were dissected at E10, and tissues containing GFP cells were fixed and "squashed" between a glass slide and coverslip. Images shown are compressed from Z stacks. A, liver; B, kidney; C, meninges. Scale bars 20µm.

4.3.3.2. Proliferation

Assessment of cell proliferation was crucial in determining the behaviour of the neuroblastoma cells within the chick tissues. However, as detailed in Chapter Three, the opportunity to quantify this had remained elusive, due to a lack of success with the ki67 antibody on frozen sections. An alternative method was therefore tested. EdU (5-ethynyl-2'-deoxyuridine) is a thymidine analogue that is incorporated into cellular DNA during the synthesis stage of the cell cycle, and can then be detected within cells that have divided, in these experiments using an Alexa Fluor 594 label. The EdU kit was initially trialled on Kelly cells in culture; adding concentrations of 15, 10 or 5µM to the culture medium and then uptake detected 24 hours later. The fluorescence emitted by the EdU-containing cells was of varying intensities, but was in general stunningly bright regardless of the concentration and was incorporated by almost all of the cells (Figure 4.25). Hence 5µM was deemed sufficient to label all cells in culture for a 24 hour time period.

To test EdU within the chick "whole animal" model system, 0.5µl of a 20mM solution was calculated to be roughly equivalent to a concentration of 5µM within the embryo, taking its mass between E9 and E10 to be approximately 2g (Figure 2.4). Initially 0.5µl of the 20mM stock solution was injected into each E9 embryo, and this was subsequently changed to 1µl, roughly equivalent to 10µM, to ensure the amount of available EdU was not a limiting factor in the assessment of cell division. Cell proliferation rates were similar between the two EdU concentrations, but 10µM (i.e. 1µl injections) were routinely used, as an excess of EdU was preferable to a deficit.

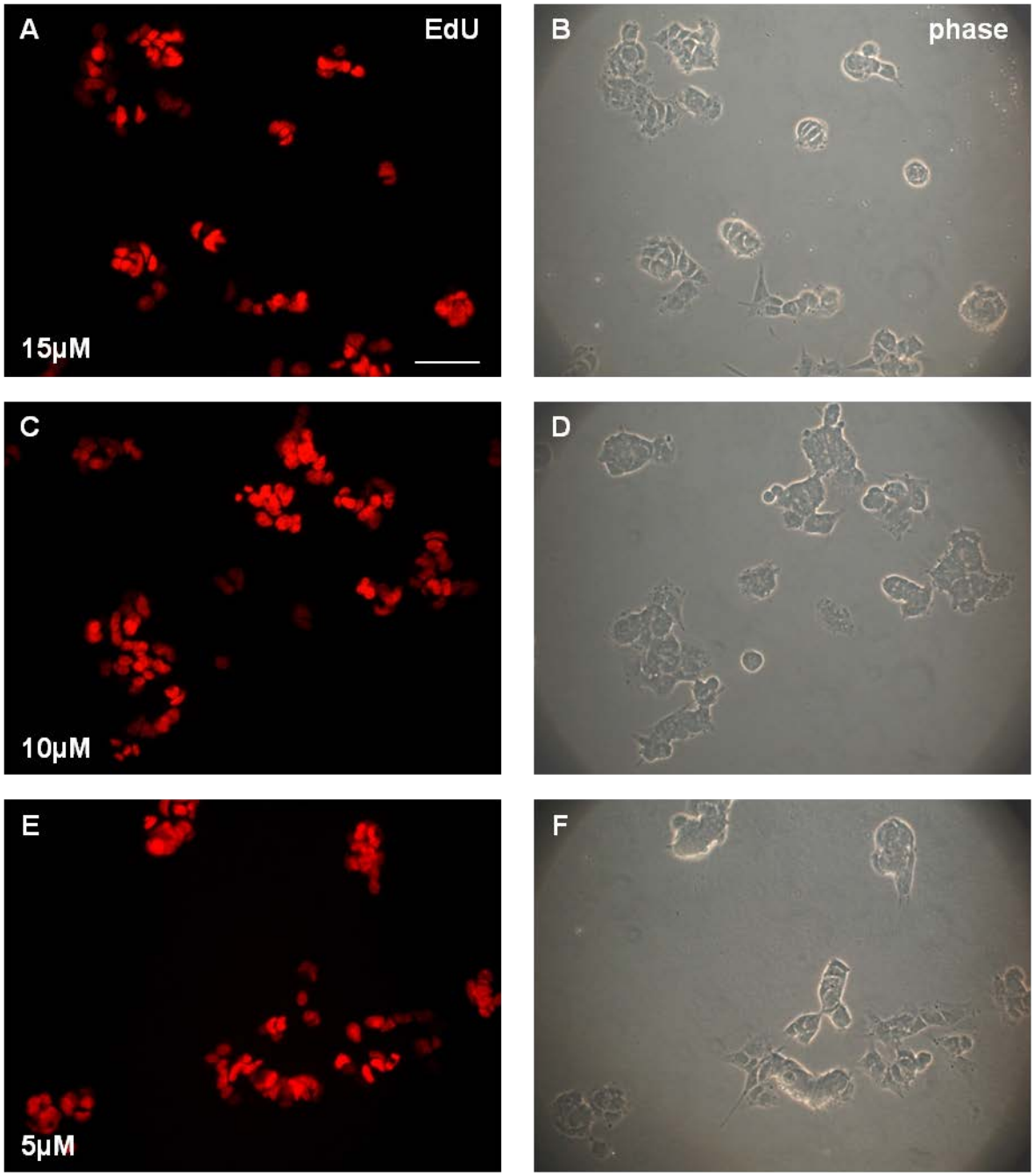

Figure 4.25. EdU incorporation into cultured Kelly cells, following addition of 15, 10 or 5µM concentrations (as labelled) to the culture medium 24 hours prior to detection. Scale bar 50µm.

EdU integration was successfully detected in frozen sections of E10 tissues from EdU-injected chicks. In all tissues tested, a significant proportion of cells had incorporated EdU, thus had divided within the 24 hours previous to sacrifice (Figure 4.26).

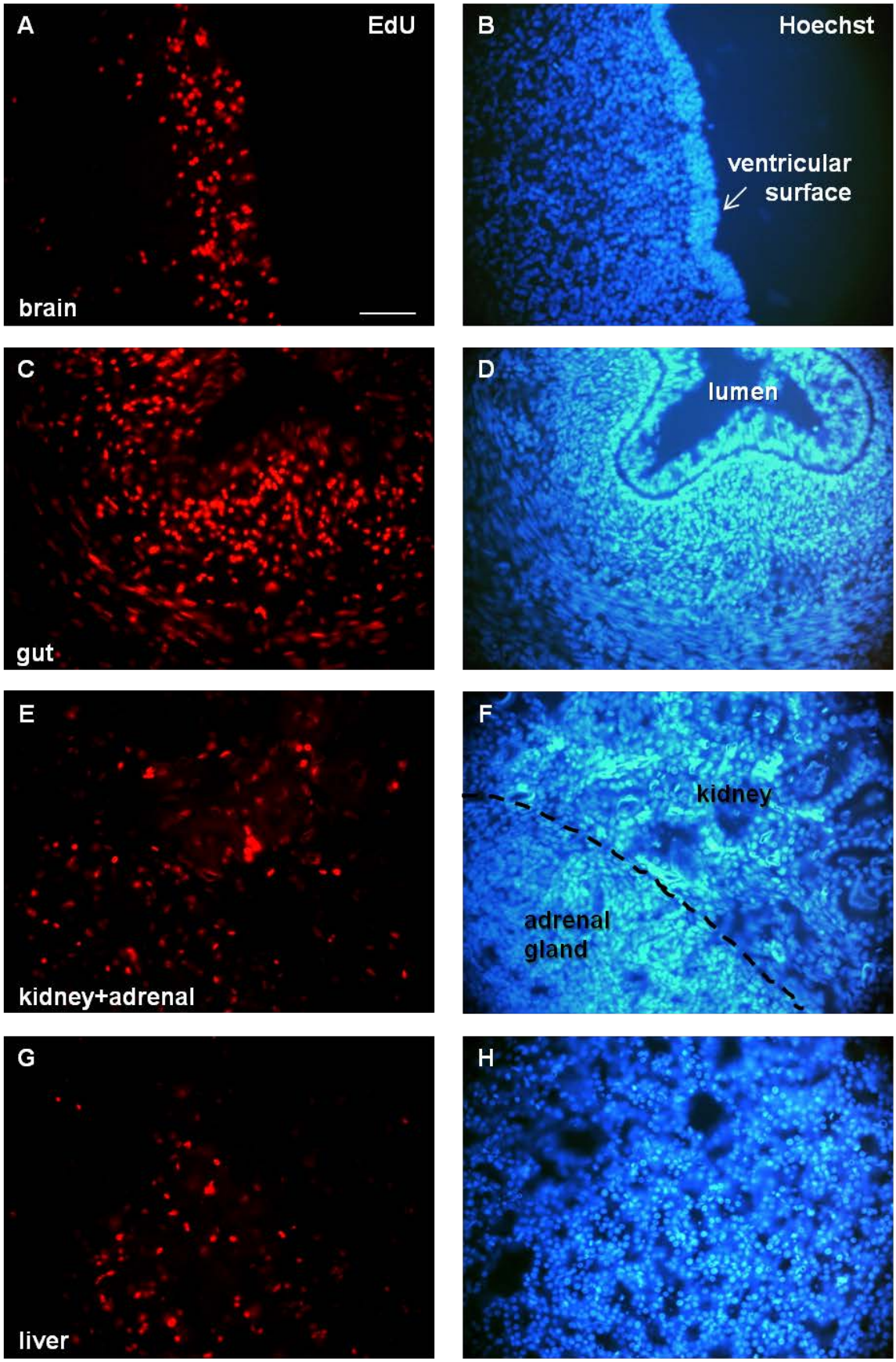

Figure 4.26. The equivalent of approximately 5µM EdU was intravenously injected into E9 chick embryos. Following dissection at E10, EdU incorporation was detected in frozen sections of the tissues indicated. Scale bar 50µm.

To discover the extent of Kelly cell proliferation within the various embryonic locations, 1µl of 20mM EdU solution was injected into each E3- or E6-injected embryo at E9 (roughly equivalent to a 10µM concentration). Results are summarised in Figure 4.27, from a total of 9 different embryos, from 3 separate experiments: tissues analysed from 3 chicks per batch. In the sympathetic ganglia, only 15% of Kelly cells had divided between E9 and E10 (n=215 cells). Host ganglion cells were also dividing, indicating proliferation as a normal physiological event in this tissue at this point in development (Figure 4.28). A similar result was observed in the gut, with the chick cells proliferating, but few EdU-labelled nuclei for the GFP Kelly cells (15%, n=210) (Figure 4.29). In contrast, within the clumps of Kellys in the tail and meninges, 50% and 53% respectively (n=534 and n=204, respectively) of the neuroblastoma cells had undergone division between E9 and E10 (Figure 4.30 and data not shown). Following E6 injection, 46% of Kelly cells within clumps in the liver (n=1008) (Figure 4.31), 37% of Kellys in the kidney (n=307) (Figure 4.32) and 38% of Kellys in the meninges (n=209) (Figure 4.33) were seen to be actively proliferating within a 24 hour window.

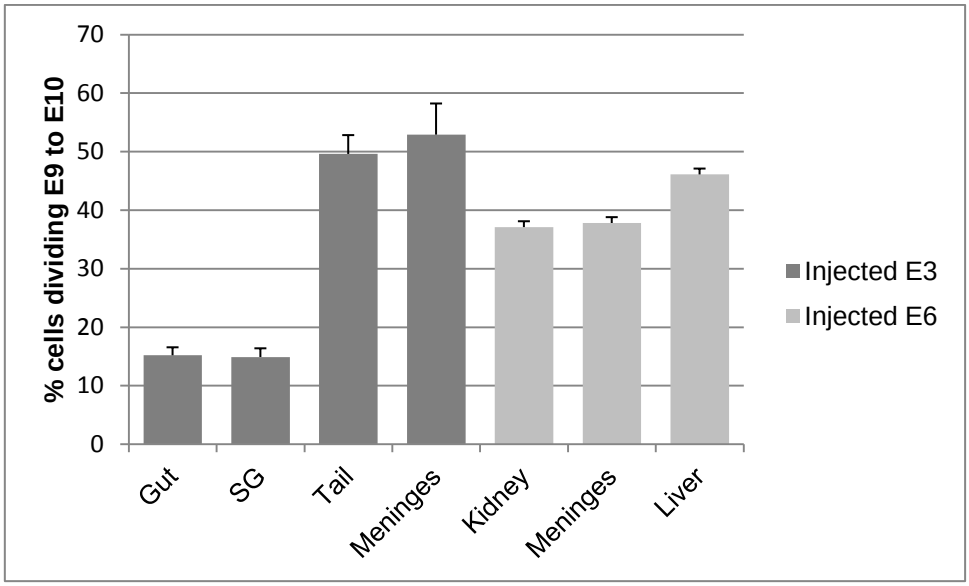

Figure 4.27. Summary of EdU incorporation into Kelly cells within E10 chick tissues, following cell injection at E3 or E6 as specified, and EdU injected to a concentration of approximately 10µM at E9. Error bars display standard deviation from the mean.

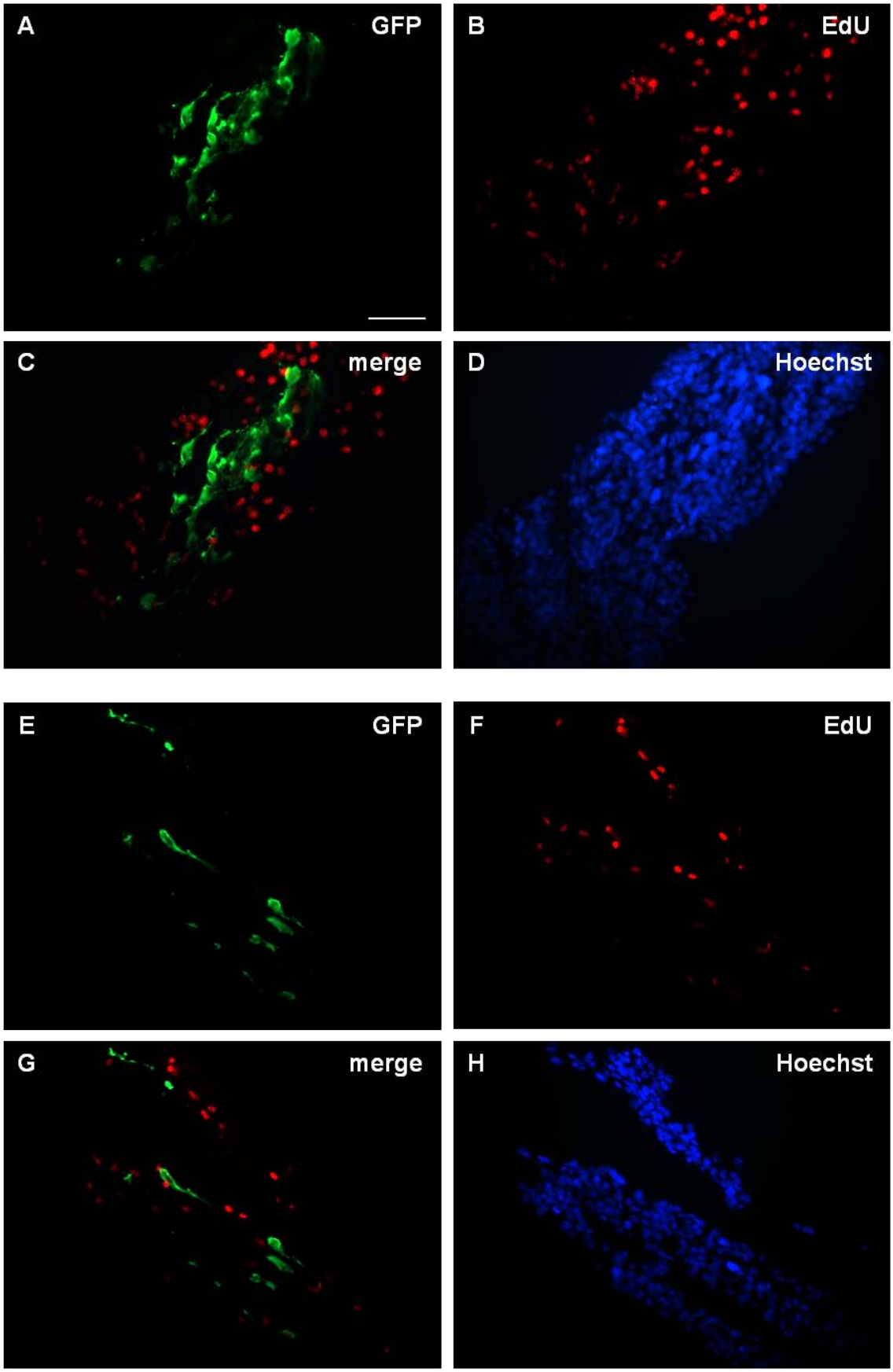

Figure 4.28. EdU incorporation into E10 sympathetic ganglia, containing GFP Kellys injected intravenously at E3. EdU was injected at E9, chicks dissected at E10, and detection performed on frozen sections. Scale bar 50µm.

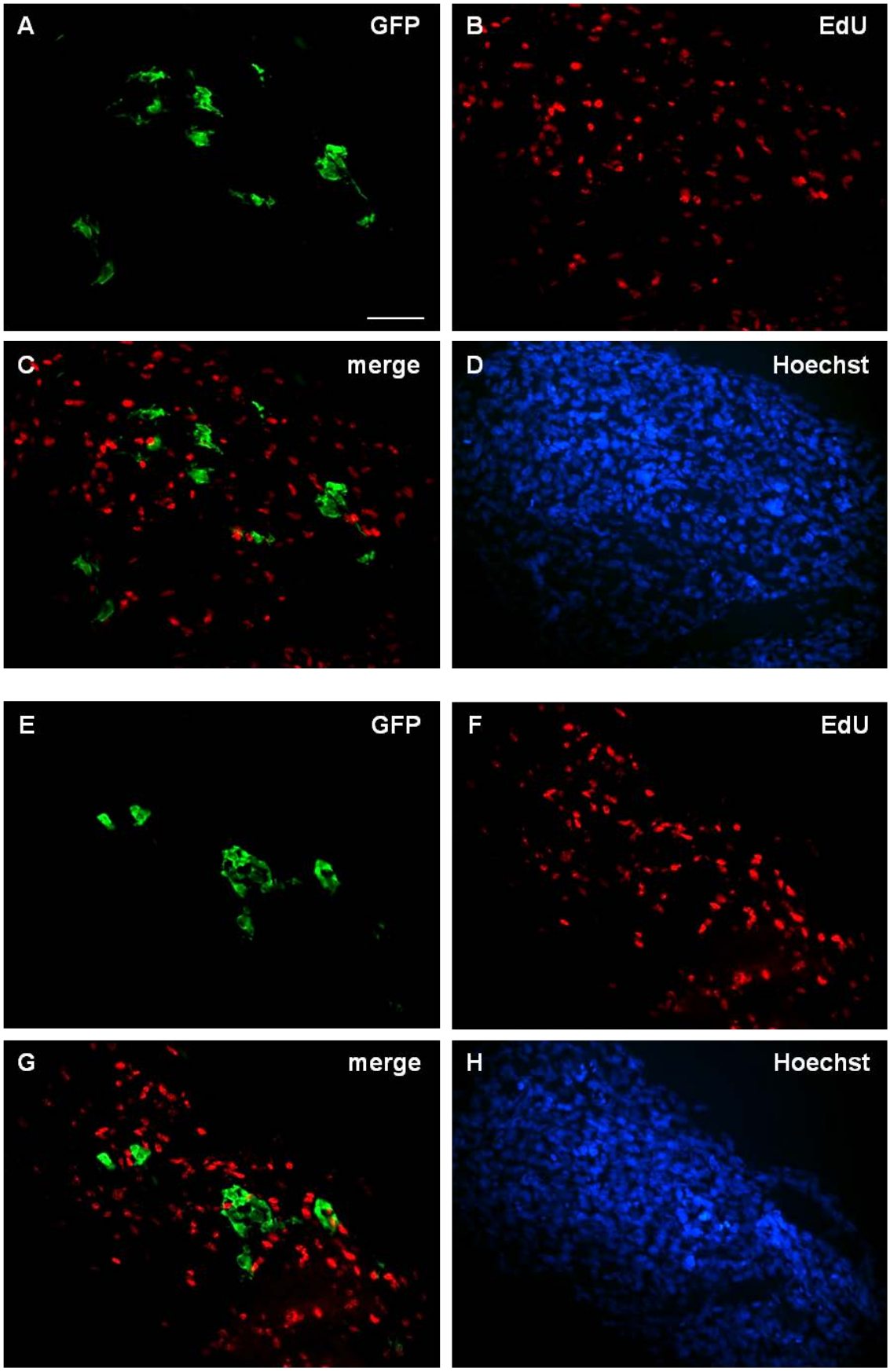

Figure 4.29. EdU incorporation into E10 gut tissue, containing GFP Kellys injected intravenously at E3. EdU was injected at E9, chicks dissected at E10, and detection performed on frozen sections. Scale bar 50µm.

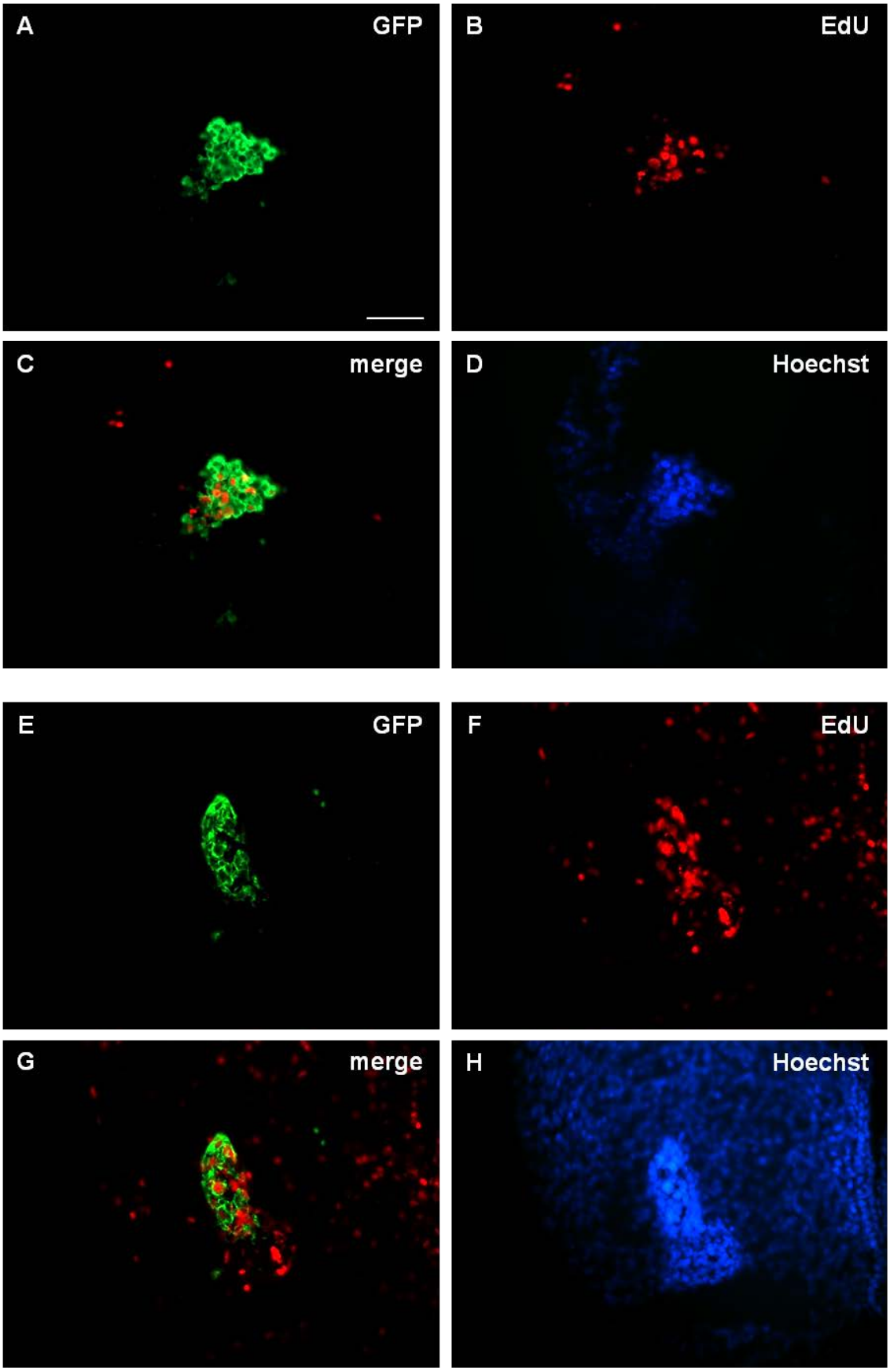

Figure 4.30. EdU incorporation into E10 tail, containing GFP Kellys injected intravenously at E3. EdU was injected at E9, chicks dissected at E10, and detection performed on frozen sections. Scale bar 50µm.

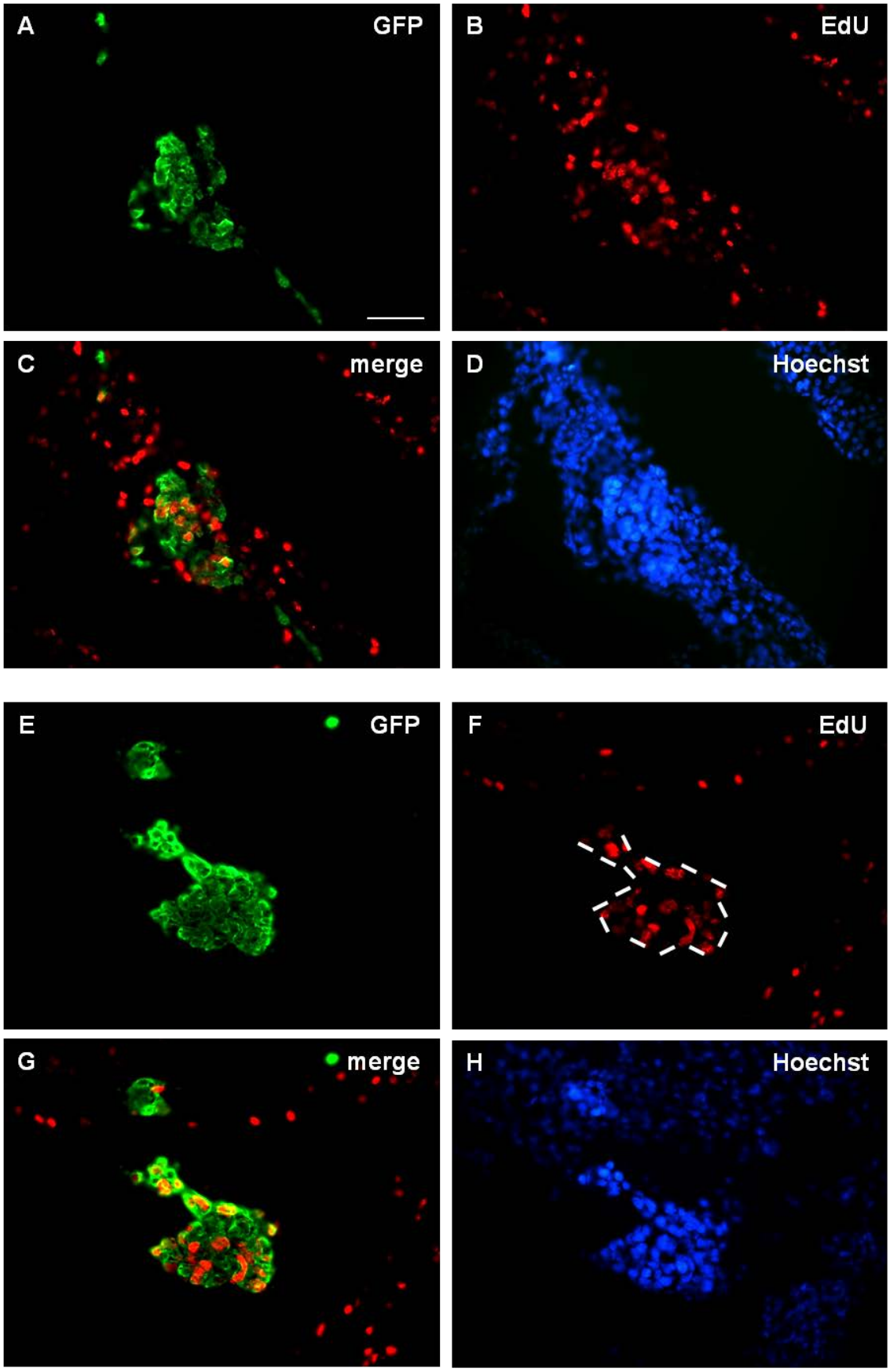

Figure 4.31. EdU incorporation into E10 liver, containing GFP Kellys injected intravenously at E6. EdU was injected at E9, chicks dissected at E10, and detection performed on frozen sections. Dashed lines in F roughly outline the clump of GFP Kelly cells. Scale bar 50µm.

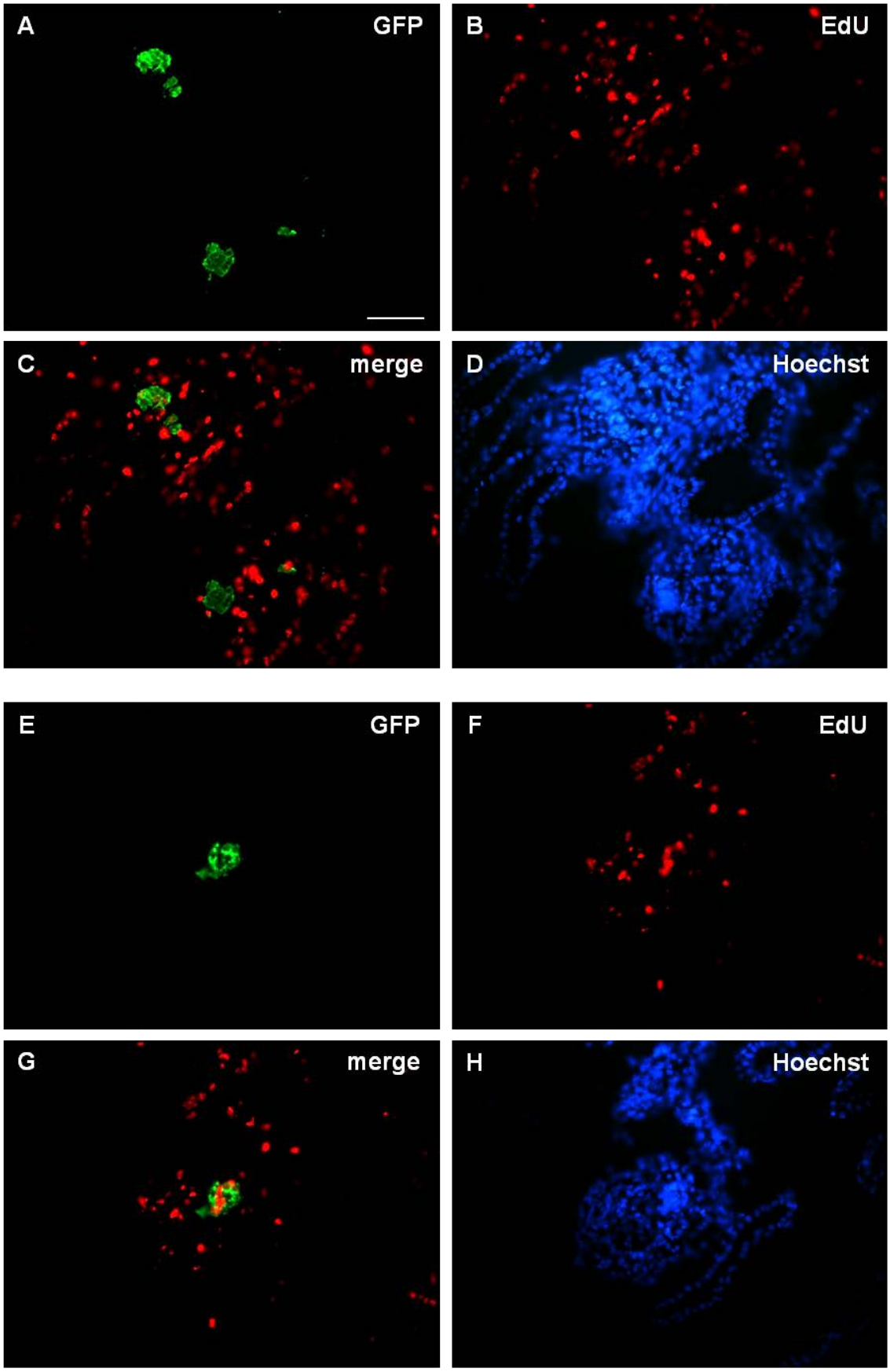

Figure 4.32. EdU incorporation into E10 kidney, containing GFP Kellys injected intravenously at E6. EdU was injected at E9, chicks dissected at E10, and detection performed on frozen sections. Scale bar 50µm.

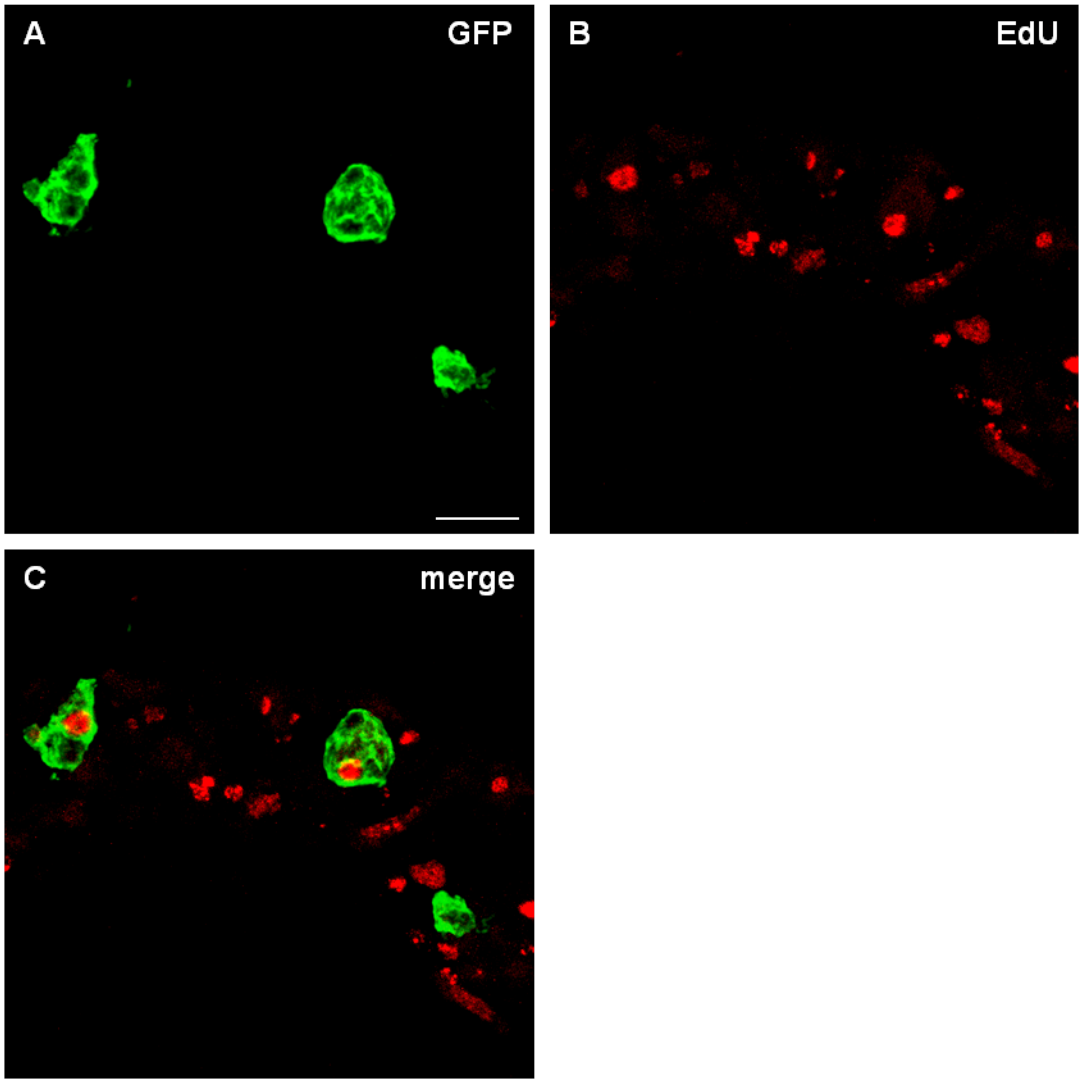

Figure 4.33. Confocal image, compressed Z stack, of EdU incorporation into E10 meninges, containing GFP Kelly cells injected intravenously at E6. EdU was injected at E9, chicks dissected at E10, and detection performed as a whole mount stain on meningeal tissue. Scale bar 20µm.

4.3.3.3. MYCN expression

Kellys are a MYCN-amplified cell line and have been shown to express high levels of the protein in culture (Figure 3.22). MYCN amplification is a feature associated with high risk neuroblastoma tumours, with the protein encouraging progression of cells through the cell cycle and resulting in a population of aggressively dividing cells. Therefore, taking into consideration the differences in both morphology and proliferation between Kelly cells within neural crest-derived neural tissues (SG, ENS) and those in non-neural (tail, meninges) and non-neural crest-derived (liver, meninges) tissues, an investigation into whether the levels of MYCN had changed within the Kelly cells was deemed to be particularly interesting.

The sympathetic ganglia and tail were selected as two contrasting regions in terms of Kelly cell incorporation, which could be tested in parallel with tissues having been derived from the same embryos, having experienced the same incubation conditions. Frozen sections were cut from each of the two tissues and stained with a monoclonal antibody to detect the MYCN protein. Looking down the microscope, it appeared that unsurprisingly, the cells in the tail had maintained their high MYCN levels (Figure 4.34 A-D and Figure 4.35 A-D), whereas in those in the sympathetic ganglia, no MYCN immunofluorescence could be detected by eye in any of the Kelly cells above the background fluorescence (Figure 4.34 E-H and Figure 4.35 E-H). To confirm these observations, intensity of the red MYCN stain was measured within the GFP Kellys in both tissues (n=41 for SG, n=104 for tail), using Image J software. An average background fluorescence intensity measurement was taken from n=6 host nuclei per section, and subtracted from each Kelly cell's measured fluorescence value in that frozen section. As shown by the graph in Figure 4.36, the mean fluorescence intensity of the MYCN stain in GFP Kelly cells within the E10 tail was quantified at 4.330 (standard deviation 2.138), compared to 0.027 (standard deviation 0.397) for those in the sympathetic ganglia. This result reflected what had been seen by eye and conclusively proved that levels of the MYCN protein had been dramatically reduced to below detectable levels in the Kellys in the sympathetic ganglia compared to those in the tail. This was observed in all of the Kelly cells incorporated into the ganglia of at least 8 chicks in total, taken from 3 separate experiments.

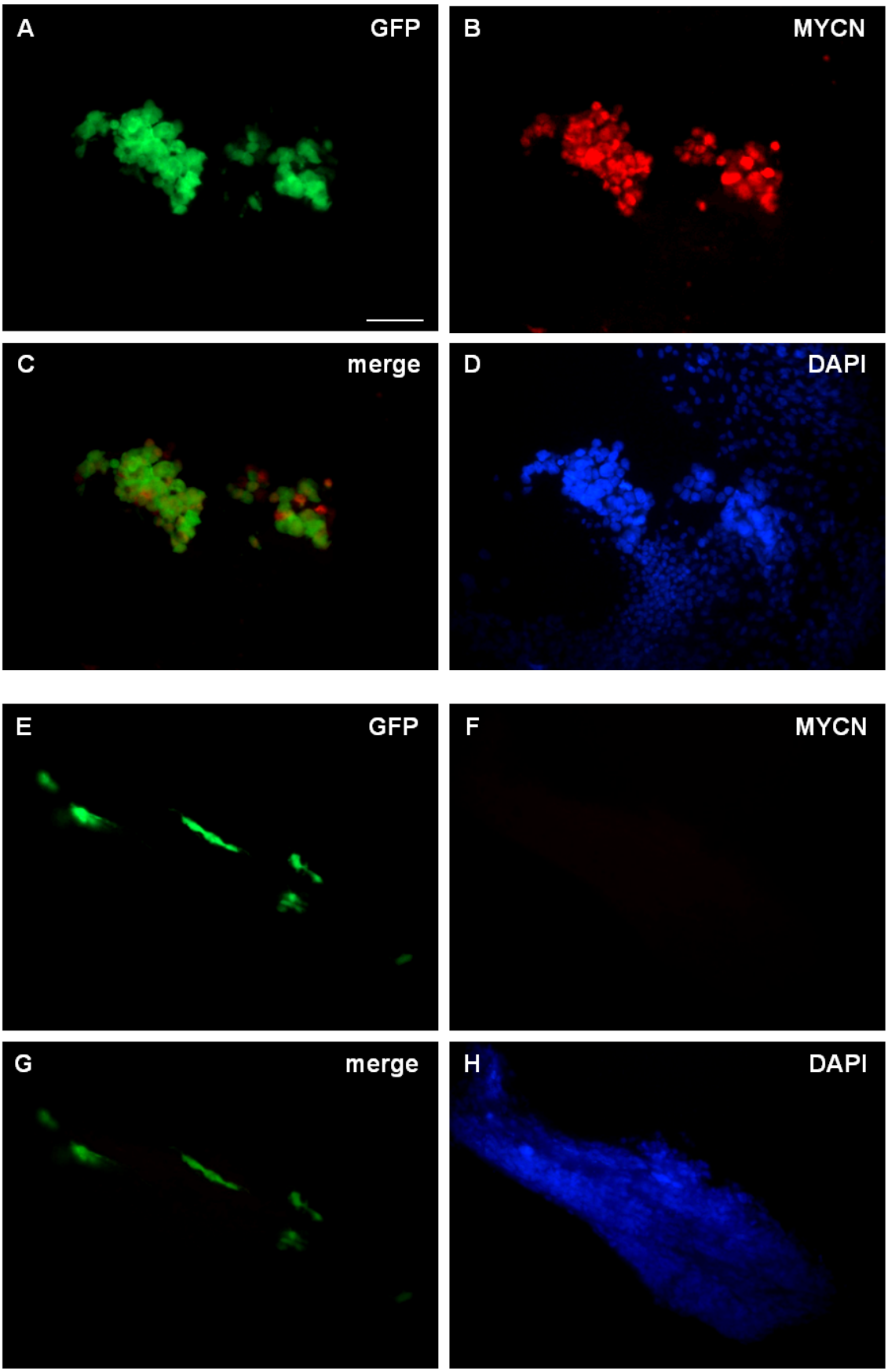

Figure 4.34. MYCN expression (red, human-specific) in GFP Kellys (green) within frozen sections of the E10 A-D, tail; E-H, sympathetic ganglia, following intravenous injection at E3. Scale bar 50µm.

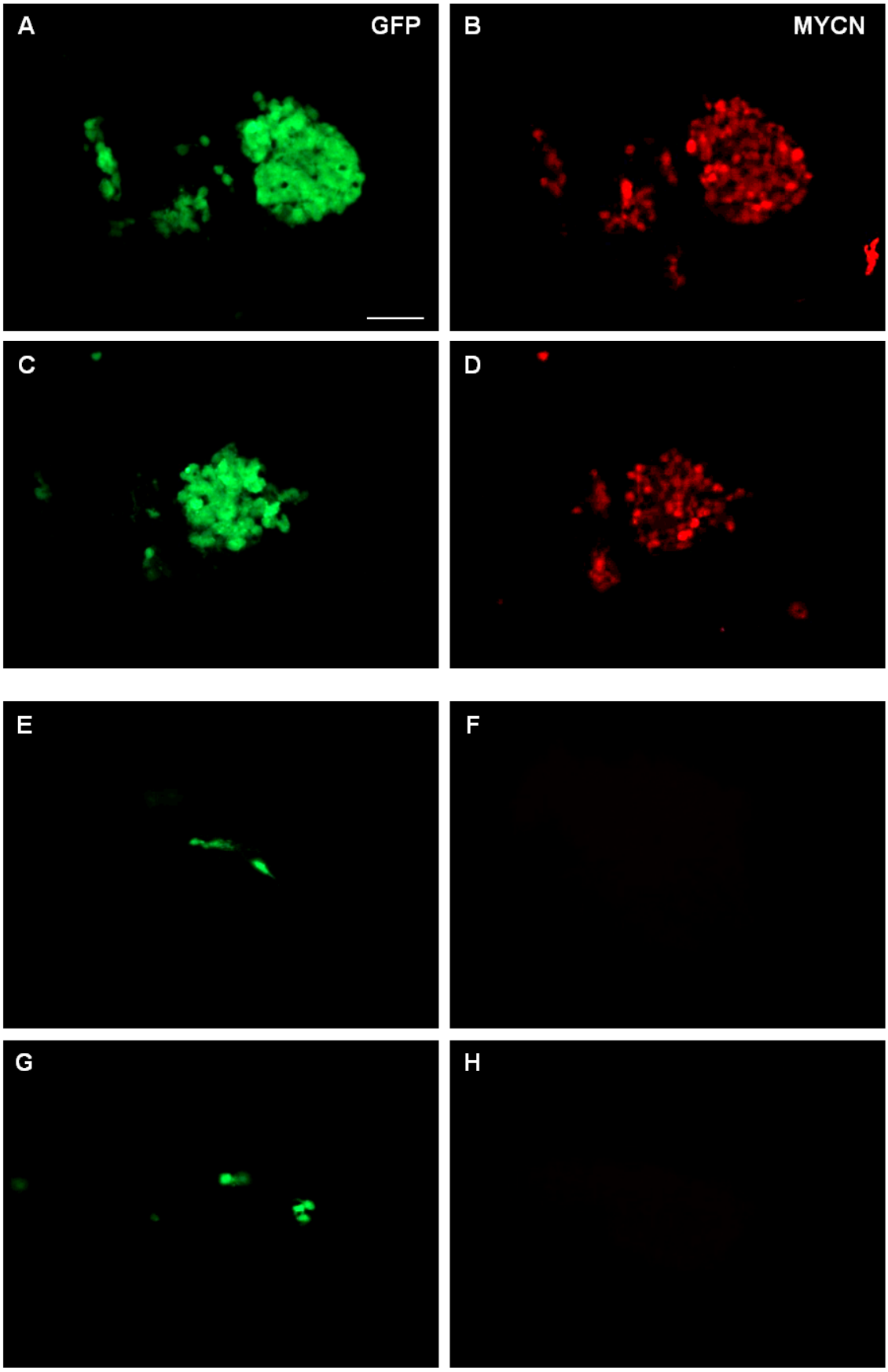

Figure 4.35. MYCN expression (red, human-specific) in GFP Kellys (green) within frozen sections of the E10 A-D, tail; E-H, sympathetic ganglia, following intravenous injection at E3. Scale bar 50µm.

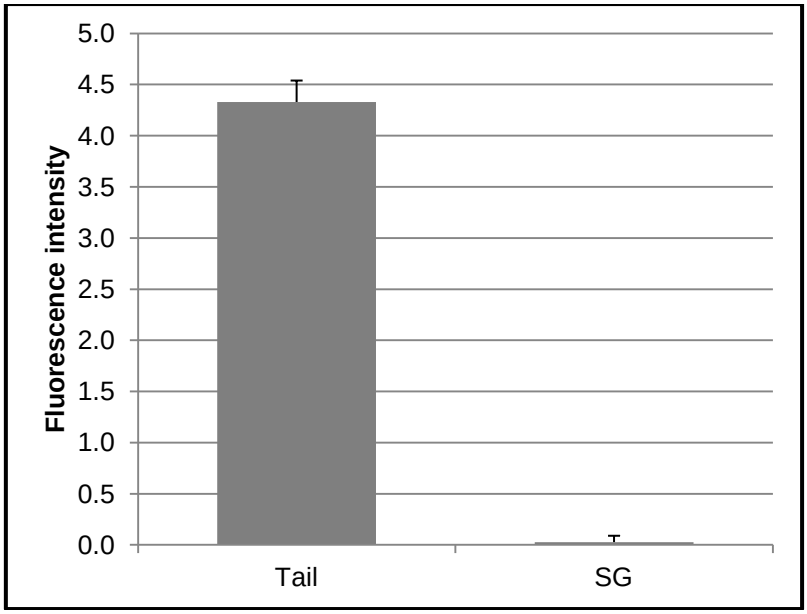

Figure 4.36. Histogram displaying the average fluorescence intensity of MYCN staining in the nuclei of Kelly cells intravenously injected into E3 embryos, dissected at E10, and found to have located to the tail and sympathetic ganglia. Error bars display the standard error of the mean, calculated by dividing the standard deviation by the square root of the sample size.

4.4. Discussion

Prior to completing the intravenous injections, it had been expected that the neuroblastoma cells would locate to regions of the embryo where they would both survive and thrive, hence it was assumed that small proliferating tumour masses would be discovered upon E10 dissection. It was essential to terminate experiments by E10.5 (halfway through gestation) according to Home Office guidelines, as a license to prolong these experiments was not possessed. Cells were injected at E3 because it is the earliest point in development that a fully-formed circulatory system is present, and having to dissect at E10, meant the cells could be left within the embryos for the maximum possible length of time. Unexpectedly, the cells responded to the guidance cues that direct neural crest cells along their migratory pathways, and following extravasation, incorporated largely into neural crest-derived tissues. This was a feature found consistently within the >250 embryos dissected, where cell integration was consistent in terms of both the organs targeted and cellular appearance. It had been presumed that targeting would occur following neuroblastoma implantation into the neural tube, but was surprising due to their ectopic site of introduction. Any uncertainty over whether cells had located to most tissues throughout the embryos, and apoptosed in some yet survived in others, was abated following the dissection of embryos at E7 (data not

shown), where Kellys were only observed in those structures found to contain the cells at E10.

The targeting of cells to the parasympathetic ciliary ganglion and parasympathetic neuron-containing tail, as well as non-neural tissues such as the meninges, indicated that the cells were not merely following the sympathetic nervous system developmental route, but the numerous different neural crest pathways. In the embryo, trunk neural crest cells migrate along two different pathways: the ventromedial route, which gives rise to cells of the DRG and SG; and the dorsolateral pathway, the cells from which form melanocytes (Henion & Weston 1997). Delamination and hence cell migration along the dorsolateral pathway is at least one day later than the NCCs travelling ventromedially (Erickson & Perris 1993; Henion & Weston 1997). Interestingly, the neuroblastoma cells seemed only to target the ventral neural crest migratory path, as cells were not found in the skin – even though neural crest delamination of cells destined to become melanocytes occurs at around HH17-18 in the chick (Kitamura et al. 1992), therefore migration would have been underway at the time of neuroblastoma cell injection. Perhaps the neuroblastoma cells have some kind of intrinsic epigenetic memory that resulted in them responding to factors along the neural crest pathway they would have originally followed in their pre-oncogenic state as neural crest cells.

The formation of the primary sympathetic ganglia at HH21 (E3.5) in the chick embryo (Lallier & Bronnerfraser 1988), is near perfect timing to allow the neuroblastoma cells injected at E3 to coalesce with the endogenous chick NCCs and participate in the formation of sympathoadrenal structures. This may be why the cells are fully integrated into the SG tissue. The earliest NCCs migrate between the neural tube and somites, and follow the routes of the intersomitic blood vessels (Kulesa & Gammill 2010), and immediately following injection, neuroblastoma cells are seen within these narrow vessels – therefore it may be postulated that the cells are attracted out of these small vessels to then aggregate with the sympathoadrenal precursors. However, this makes it even more intriguing that neither the Kellys nor BE(2)Cs were observed in the chick adrenal glands. Neuroblastoma tumours primarily occur in the sympathetic ganglia and the adrenal medulla, and both tissues are said to be derived from the same initial pool of sympathoadrenal precursors (Langley & Grant 1999). It has been published that in mouse tail vein injections, neuroblastoma cells do locate to the mature adrenal glands (Engler et al. 2001), therefore targeting of the chick adrenal glands may be strictly time- and spatially-dependent – for example, by cells originating from a particular somitic level (18-24), in an embryo of a very specific age. It is also conceivable that the neuroblastoma cells locate to the primary sympathetic ganglia that form at around

E3.5, but do not migrate with the primitive adrenal cells (around E4); instead remaining with the cells that will go on to form the sympathetic ganglia at E5. It has been reported that neuroblastomas do not express phenylethanolamine-*N*-methyl transferase (PNMT), the enzyme involved in the conversion of noradrenaline to adrenaline which is expressed in the adrenal chromaffin cells (Hoehner et al. 1996). It has therefore been hypothesised that neuroblastomas occurring in the adrenal glands may arise from misplaced sympathetic ganglion cells rather than cells of the adrenal medulla (Pahlman et al. 2004), particularly as pheochromocytoma, a tumour derived exclusively from the adrenal chromaffin cells does express PNMT. If true, this would be a plausible explanation for neuroblastoma cells not targeting the chick adrenal glands following E3 intravenous injection.

The targeting of the Kelly (and BE(2)C) cells to the gut following E3 injection may be explained by the contribution of chick neural crest cells to the enteric nervous system, which arises mostly from the vagal NCCs (at the level of somites 1-7). The endogenous NCCs collect in the caudal branchial arches, before entering the pharyngeal gut mesenchyme at around HH20 in the chick (Burns & Le Douarin 1998). The neuroblastoma cells injected at approximately HH18-20 may likely have located to the branchial arches along with the chick NCCs, and then followed them into the gut tissue at HH20. The neuroblastoma cells then presumably migrated rostrocaudally with the chick NCCs, which colonise the entire length of the gastrointestinal tract (Burns & Le Douarin 1998; Sasselli, Pachnis & Burns 2012).

The ENS – specifically within the hindgut – has a sacral contribution from NCCs caudal to somite 28, which initially form the nerve of Remak, adjacent to the gut wall, from which the NCCs enter the hindgut upon arrival of the vagal NCCs at this region of the gut (Kapur 2000). In the chick, sacral NCCs have been observed in the hindgut from E7 and colonisation is completed by E8.5 (Burns & Le Douarin 1998), and this may explain why a small number of Kelly cells injected at E6 are observed in the gut – the cells may have resided along with the endogenous NCCs in the nerve of Remak, before following them into the gut at E7.5.

The meninges – particularly overlying the forebrain – have a neural crest contribution (Couly & Ledouarin 1987), and incidentally, it was primarily the forebrain meninges in which the Kelly cells were observed following E3 injection. Similarly in the eye, the cornea, sclera and uvea (consisting of the iris, ciliary muscle and choroid) all have a neural crest component (Johnston et al. 1979), and Kelly cells have been observed specifically in these locations.

In the heart, neuroblastoma cells displayed very specific homing to areas of cardiac tissue rather than the vasculature. One may have expected that, as the first organ the cells encountered following injection and the "key player" in the circulatory system the cells were initially contained within, the cells may have incorporated into the internal atrial/ventricular walls – these tissues being in the closest proximity. However, perhaps in part due to the magnitude of the contractional force, or maybe wholly due to the lack of neural crest contribution to this tissue, neuroblastoma cells were not observed in the inner heart muscle. They were instead discovered primarily in the conotruncal region and in the septa between the great vessels – it may be no coincidence that during development cranial neural crest cells have been demonstrated to contribute to the conotruncus and the septation of the outflow tract (Farrell et al. 1999; Jiang et al. 2000).

The targeting of Kellys to the tongue seemed to be the exception to the rule, as this has no neural crest contribution, being derived from the somites and branchial arches (Bellairs & Osmond 1998). However, one possible explanation could be that if some NCCs did in fact locate to the branchial arches prior to gut colonisation (see above), there may have been a residual population that did not migrate with the prospective ENS, but remained in the branchial arches and incorporated into the tissue of the developing tongue from E4.

The consistent appearance of neuroblastoma cells within the embryos' tails was originally a mystery, but following immunofluorescence staining for TUJ-1 where they were shown to be loosely associated with the parasympathetic network of neurons, it was proposed that the cells followed the routes of neural crest cells destined to form parasympathetic structures, but once in the tail regions, the lack of dense nervous tissue for them to integrate into and be influenced by led to the formation of proliferating clumps of cells.

Following injection at E3, cells were never/rarely found in structures such as the liver, lungs and spleen, which are not derived from neural crest cells.

The targeting shown at E3 was in stark contrast to that seen following E6 injection, when the neural crest migratory cues were absent and the primordia of the resultant structures had already formed – very few cells were found in neural crest derived structures. Targeting was also considerably different following E3 injection of an alternative tumour line, glioblastoma, where the primary target for GFP cells was the CNS. In addition, when GFP-labelled SK-N-AS neuroblastoma cells with a single copy of the MYCN gene were injected at E3 by Dr Anne Herrmann (University of Liverpool, UK), considerably fewer were observed within the E10 embryos than with the MYCN-amplified Kellys and BE(2)Cs. When GFP SH-EP

neuroblastoma cells, containing a single MYCN copy and negligible expression of the oncogene, were injected at E3 (by myself and Heba Karosh), no cells were found to have survived up to E10 within the embryos. A medulloblastoma cell line, D283, was injected by Haleh Shahidipour (technician, University of Liverpool, UK), and like the SH-EP, very few cells were observed in embryonic tissues at E10. Not only did neural crest targeting seem to be a feature compatible with neural crest derived neuroblastoma cells, but cell survival may possibly be confined to MYCN-amplified cells – particularly as MYCN amplification has been documented in medulloblastoma (Korshunov et al. 2012), but D283 are a non-MYCN-amplified, non-MYCN-expressing cell line (Andrae et al. 2002). However more cell lines need to be tested before a firm conclusion can be reached. However, the observed differences in targeting meant that a useful model system had been established, in which the effects of various embryonic environments on tumour cells could be tested.

The Kelly cells within chick tissues behaved differently depending on the site of incorporation. In neural tissues, the predominantly single cells displayed an elongated or "spread" appearance, which contrasted with the spherical, clumped appearances of Kellys within the tail, meninges, liver and kidneys. The clumps may have been a result of either clonal expansion (for example, in the relatively small, regularly-sized "balls" in the meninges) or aggregation and proliferation (one example may be the larger clumps of cells in the tail). In fact, observations on the various morphologies of the Kelly cells corresponded to the proliferation quantification data. For the generally single cells that extended processes within neural tissues, proliferation was restricted compared to the rounded cells residing in clusters within non-neural tissues, which were dividing more rapidly. The fact that a small proportion of Kellys in the sympathetic ganglia and ENS were dividing was less extraordinary, when it was taken into account that the endogenous chick cells in each of these structures were proliferating. For the sympathetic ganglia, particularly in Figure 4.29 A-D, there is a large blank space in the EdU photograph where the Kelly cells are located, with the surrounding chick SG cells showing evidence of proliferation. However in the tail and liver, the EdU-containing nuclei are most abundant in the region of the Kelly cells, with what appears to be a much lower proportion of cells in the surrounding chick tissue dividing. This contrast between levels of proliferation in the Kellys and the surrounding chick cells in various locations, suggests that the Kelly cells do not seem to be influenced by the host tissue, in terms of reflecting the levels of proliferation of their surrounding cells.

During ventromedial NCC migration, MYCN is expressed uniformly across the whole cell population. However, following aggregation at the primordial sympathetic ganglia, MYCN is switched off in all cells except those destined to become neurons (Wakamatsu et al. 1997).

The MYCN may have been downregulated in the Kellys soon after colonisation of the SG, in line with the non-neuronal host cells. It was not possible to detect MYCN levels in the chick SG cells as a chick-specific MYCN antibody is not commercially available. Regardless, the loss of MYCN expression in the Kellys implies that the cells are able to respond to the cues that downregulate MYCN during normal development.

The fact that Kellys continued to express tyrosine hydroxylase in all tissues tested is perhaps unsurprising, as this enzyme is habitually expressed in normal developing neuroblasts, neuroblastoma tumours (which may be recapitulated to an extent by the MYCN-expressing, rapidly proliferating “microtumours” in the tail) and in sympathetic neurons (which the Kellys extending processes in the SG and ENS are reminiscent of). However, the cells in neural tissues did not appear to express the neuronal marker NF70 following analysis at E10, which may have been expected, thus left the fate of these cells slightly more unclear.

When the morphological, proliferative and MYCN data were combined, it strongly implied that in the sympathetic ganglia the Kellys had been reprogrammed to a less aggressive phenotype. However, the reduction in MYCN expression made it intriguing that some of the cells within the sympathetic ganglia were still dividing.

Chapter Five:

Results III – Extending the model system

5.1. Introduction

The discovery that neuroblastoma cells were being influenced by the sympathetic ganglia environment in a favourable way (in the context of patient prognosis) was hugely exciting. It appeared that the majority of cells were being reprogrammed to a more benign phenotype, in that they had reduced rates of proliferation compared to those in non-neural regions such as the tail, and even more significantly, had lost any detectable MYCN expression. This was observed following 7 days in the embryos. MYCN immunofluorescence was not detected in any of the Kelly cells analysed, therefore it was surprising that 15% of the cell population continued to divide. A Home Office licence was obtained to allow incubation of the embryos past the previous restriction of E10.5. It was speculated that by leaving the GFP Kellys to survive within the chick tissues until E14, i.e. for 11 days in total, the proliferating fraction of Kelly cells in the sympathetic ganglia may decrease or disappear, presumably in parallel with those cells in the host tissue and also possibly as a result of the loss of MYCN in the whole cell population.

5.2. Aims

- To extend the duration of the Kelly cells' subsistence within the different chick embryo environments *in vivo*, primarily to discover the effects on the Kellys following prolonged contact with and influence by the cells of the sympathetic ganglia.
- To inject two SH-EP neuroblastoma cell lines: one with no MYCN expression and one with constitutive expression; to compare cell behaviour with the highly MYCN-expressing Kelly cells.
- To amass a selection of primary neuroblastoma cell lines, cultured from biopsies/resections of neuroblastoma tissue, for potential intravenous injection into the established chick embryo model system.
- To establish an *in vitro* system in which to investigate the reliance of the Kelly cells on the sympathetic ganglia microenvironment for MYCN downregulation, and allow the identification of possible responsible factors.

5.3. Results

5.3.1. GFP Kelly cells survive within chick embryos until E14

5.3.1.1. Locations and morphology

With the intention of investigating the behaviour of Kelly cells within E14 chick tissues compared to the results obtained at E10, GFP-labelled cells were injected intravenously at E3, as for the experiments detailed in Chapter Four; with $2x10^5$ cells injected into the bloodstream of each embryo. Embryos were then incubated until E14, at which point experiments were terminated using a Schedule One procedure: decapitation. A total of approximately 45 chicks survived to E14, from 7 independent experiments. Dissection of the embryos showed that Kelly cell location was similar to that at E10, revealing that cells continued to survive in all locations. In the sympathetic ganglia (in all successfully injected embryos) and gut (at least 80-90% of embryos), Kellys remained elongated in appearance and existed mostly as single cells or in small loosely associated groups (Figure 5.1 A-B and C-D, respectively). Clumps of cells were still almost always found in the tail tissue (Figure 5.1 E-H), and in this region, were also observed between the cloaca and cloacal bursa in almost every embryo (Figure 5.1 G-H), the latter being a structure which is a site of haematopoiesis, is considerably more pronounced at E14 than E10, and atrophies around 6 months after hatching. The tightly packed groups of cells in the meninges were still present in large numbers in greater than 90% of E14 embryos (Figure 5.2 A-D) and were usually at least 50μm, often reaching 100μm in diameter. They were often located near to blood vessels (Figure 5.2 C-D), suggesting limited migration into the meningeal tissue following extravasation, possibly favouring proliferation. Cells remained integrated into predominantly the conotruncal region of the heart (Figure 5.2 E-F) in at least 6 or 7 of a typical batch of 10 surviving embryos, and in the outer layers of the eye (Figure 5.2 G-H) in more than half. Kellys were also observed as clumps on the ventral surface of the E14 tongue (Figure 5.3 A-B) in roughly a quarter of embryos dissected, and in 20-30% of cases were observed in major peripheral nerves, such as the sciatic, imaged in Figure 5.3 C-D. Like in the SG and ENS, cells appeared to be fully integrated into the nervous tissue and presented with an elongated morphology, reminiscent of cells undergoing neuronal differentiation. Interestingly, a small number of Kelly cell clumps were observed in the kidneys (Figure 5.3 E-F) of at least three quarters of the embryos. It was not unknown for a very small number of cells to appear in the kidneys at E10 (Table 4.1), but this was not found consistently enough, neither were there large enough numbers of cells in the organs, to be deemed particularly relevant compared to the other chick tissues. However, the appearance of groups of more than 1-3

cells at E14, suggested that the odd cells present at E10 had proliferated into small clusters. Once again, Kellys were not observed in the adrenal glands.

Confocal microscopy revealed the Kellys' morphology to be similar to, but a more exaggerated version of those in the E10 tissues – presumably owing to the prolonged influence of the various chick tissue microenvironments. In the E14 sympathetic ganglia, the majority of the Kellys had extended processes of roughly 30-70µm in length (Figure 5.4 A). A small proportion of the cells had processes in excess of 100µm (Figure 5.4 B, arrow), irrefutably representative of neuronal differentiation and axonal growth. Confocal imaging confirmed the observations made upon dissection, that the cells were often solitary within the ganglia, but also resided in small groups (Figure 5.4 B, arrow head). In the gut, like at E10, some cells existed singly, whereas many resided in ganglion-type groups (Figure 5.4 C+D, arrow heads). Most of the cells extended processes, generally shorter than those from the Kellys in the sympathetic ganglia, but some more than 60µm long (Figure 5.4 C+D, arrows). It was once again confirmed that the neuroblastoma cells were integrated into the gut tissue in two separate layers, assumed to be the myenteric and submucosal plexuses of the enteric nervous system. In the tail, the cells were located in masses that were often more numerous and almost always of an increased size compared to those observed at E10, presumably due to the rapid cell proliferation by the cells in this region over the additional 4 days. The cell clumps varied in size, but were often in excess of 200µm in diameter (Figure 5.5 A+B). Similarly in the meninges the cells remained within compact clusters (Figure 5.5 C+D), which were bigger in size than those witnessed within the E10 meninges. A notable increase in number of these clumps was not apparent.

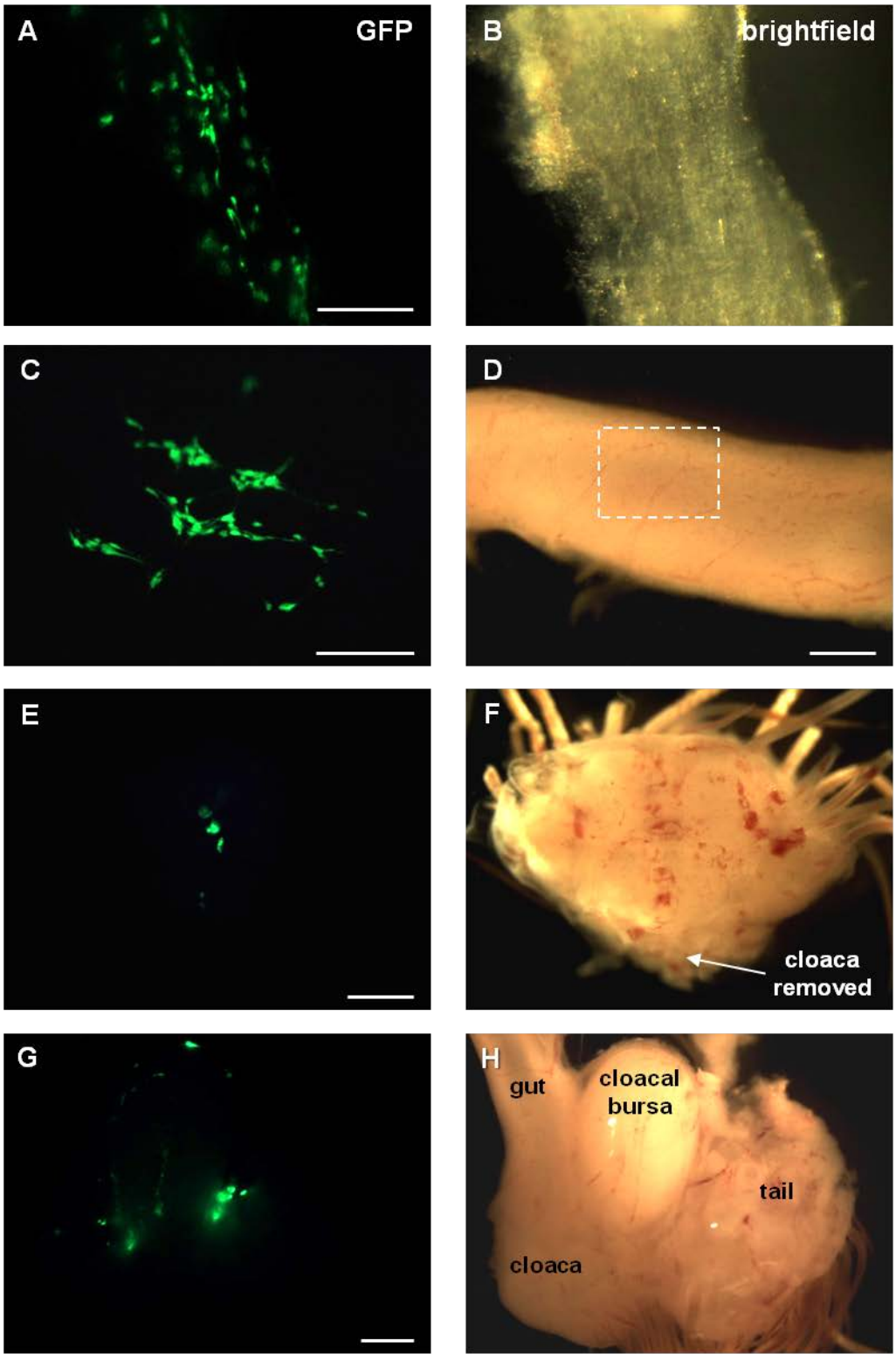

Figure 5.1. GFP-labelled Kelly cells, following intravenous injection at E3 and incubation for a further 11 days prior to dissection, were found integrated into the E14 chick A-B, sympathetic ganglia; C-D, gut (C is a higher magnification image of the area within the dashed box in D); E-F, tail; G-H, caudal region (as labelled). Scale bars A-C, 200µm; D, 500µm; E-H, 1mm.

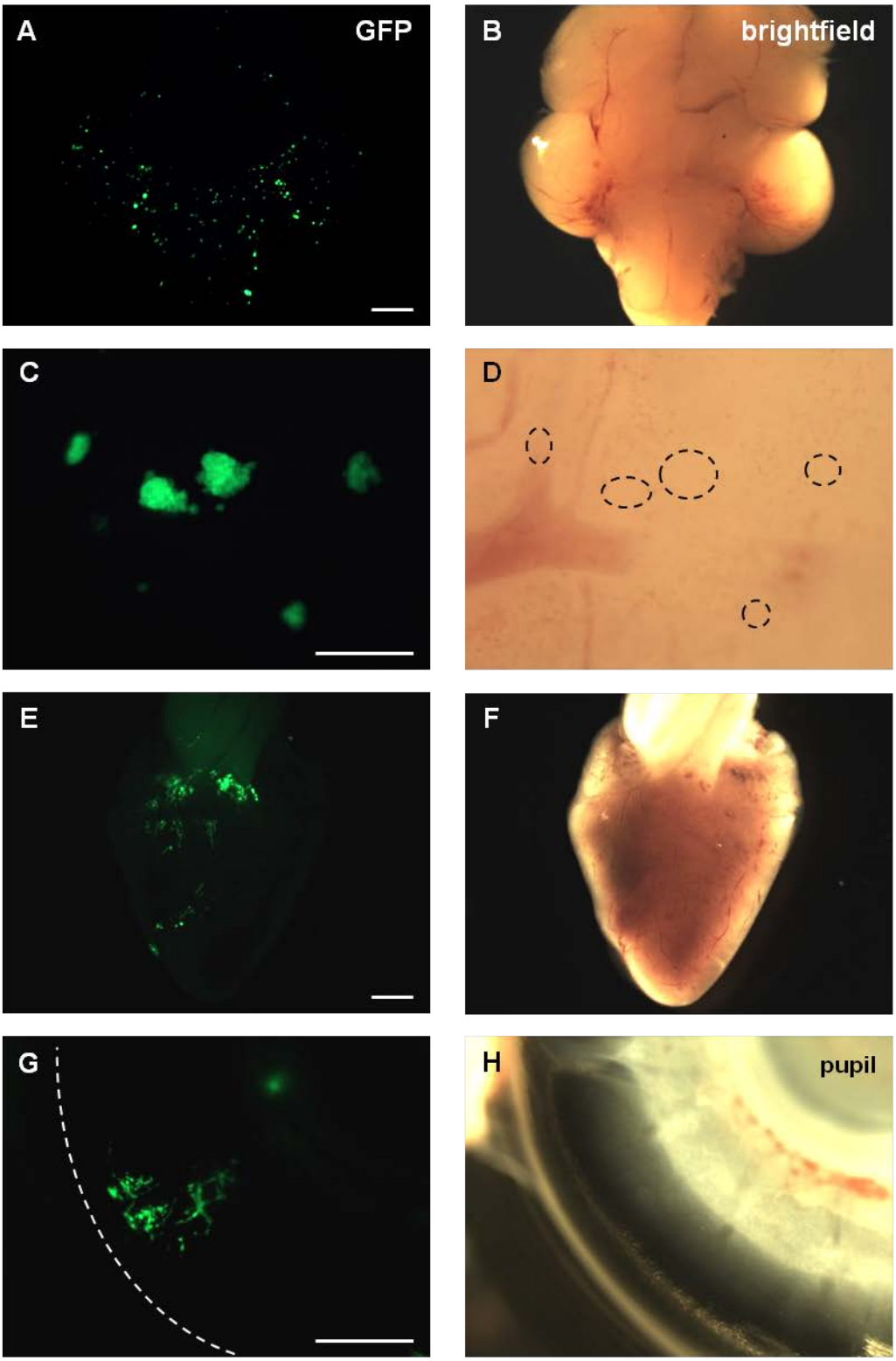

Figure 5.2. GFP-labelled Kelly cells were intravenously injected into E3 chick embryos. Following dissection at E14, cells were discovered within the A-B, meninges *in situ*, over surface of brain; C-D, magnified area of the meninges, dashed lines in D indicate the positions of the clumps of Kelly cells in relation to the blood vessels; E-F, heart; G-H, eye, dashed line in G indicates the outer boundary of the eyeball. Scale bars A-B, E-H, 1mm; C-D, 200µm.

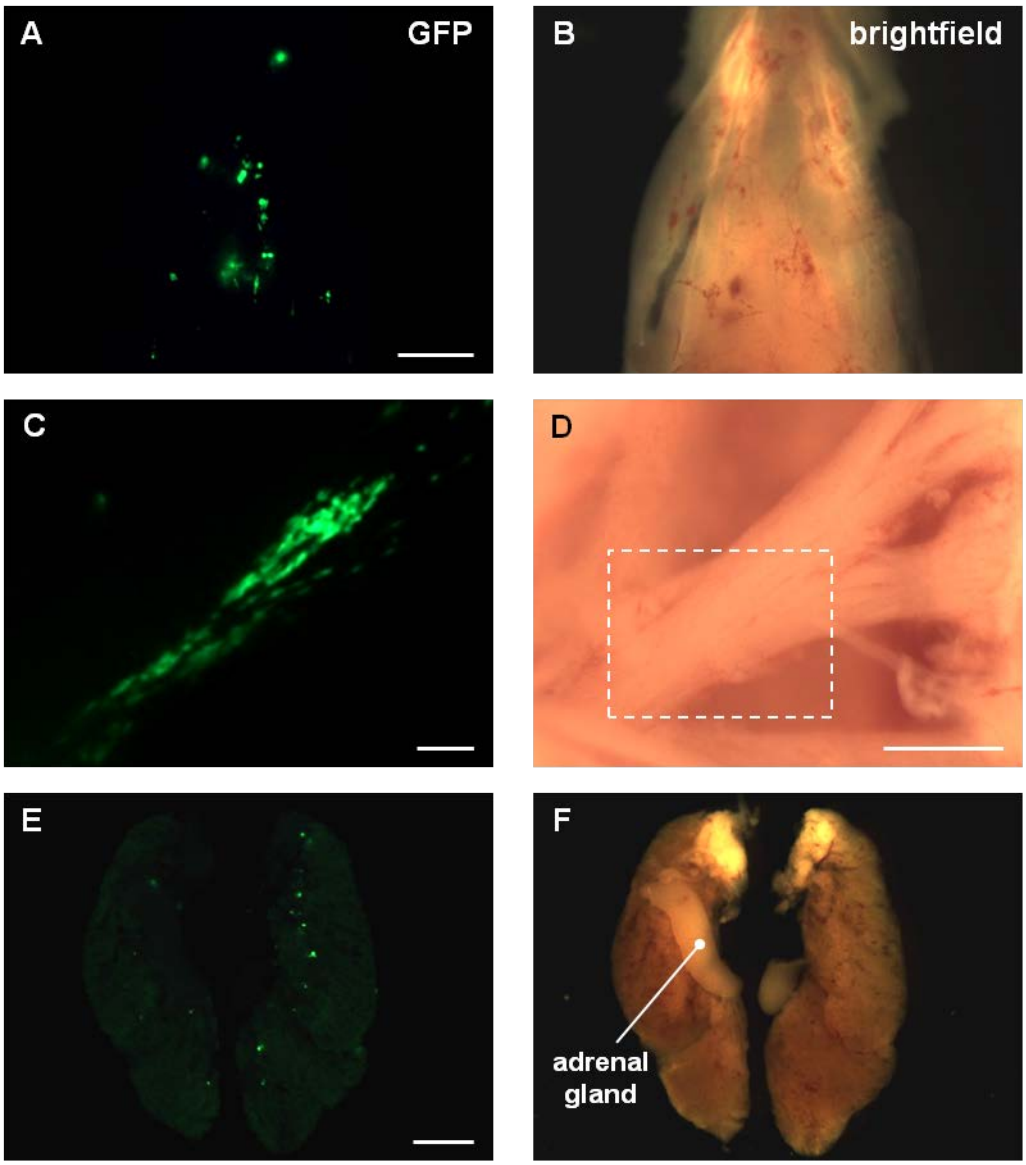

Figure 5.3. GFP-labelled Kelly cells were injected intravenously into E3 chick embryos, and following dissection at E14, were found within the A-B, tongue, ventral surface; C-D, spinal nerve, possibly the sciatic, C is a magnified image of the area within the dashed box in D; E-F, kidneys, but were not seen in the adrenal glands. Scale bars A-B, E-F, 1mm; C-D, 500µm.

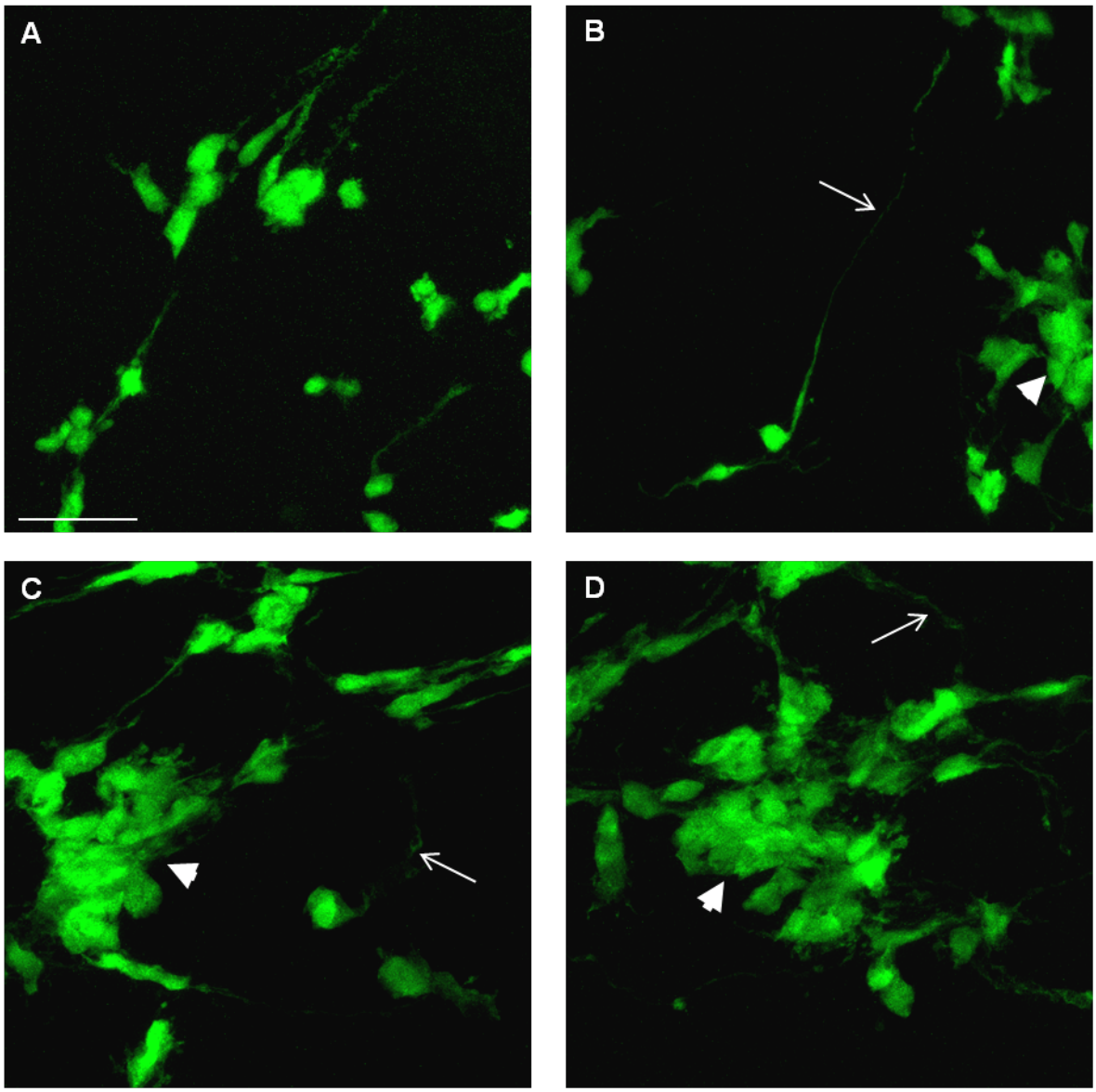

Figure 5.4. Compressed Z stack confocal images of GFP-Kelly cells within neuronal E14 chick tissues, having been intravenously injected at E3. A-B, sympathetic ganglia; C-D, gut (ENS). Scale bar 50µm. Arrows identify long processes extended by the Kelly cells; arrow heads point to clumps of cells.

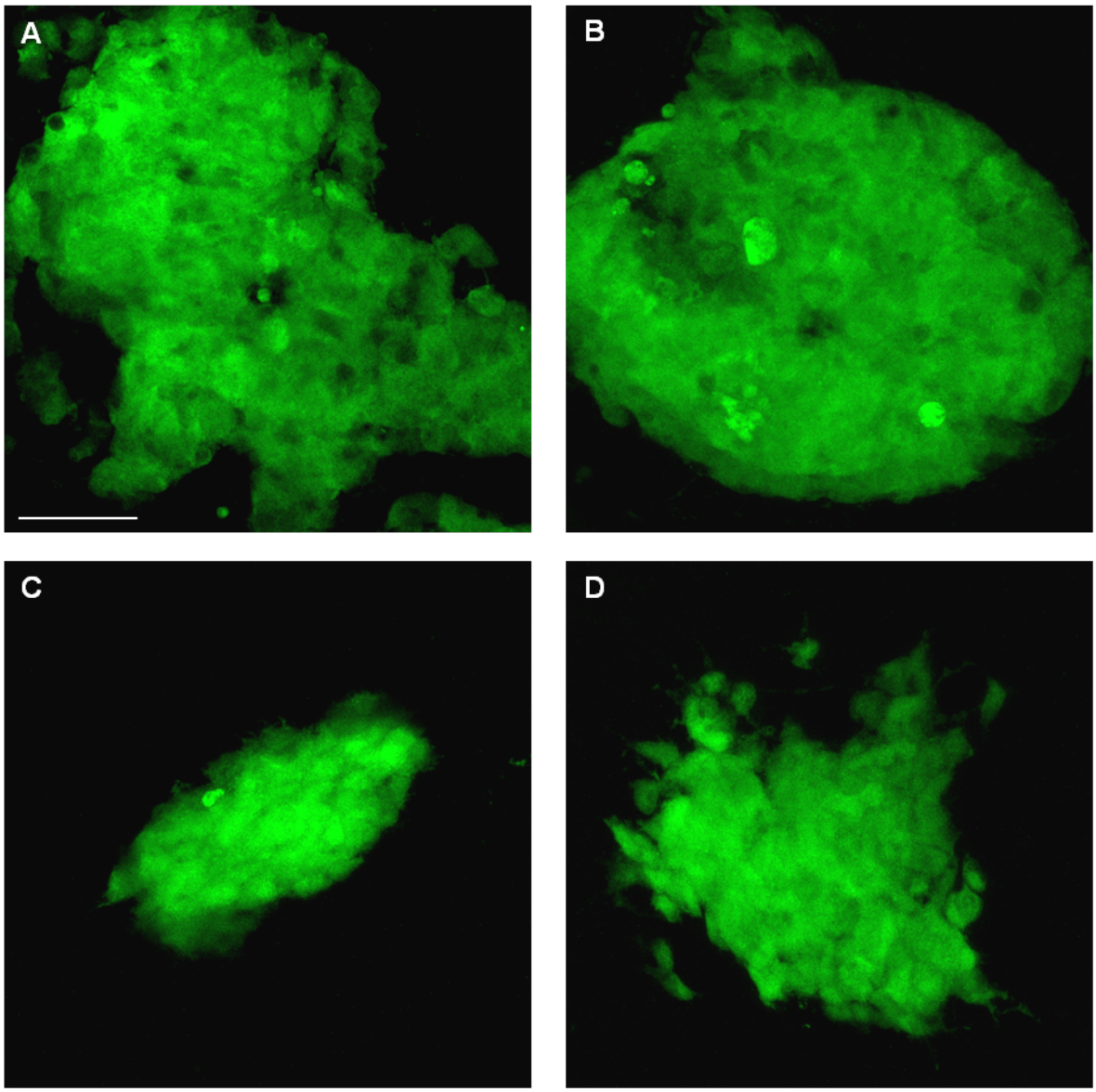

Figure 5.5. Confocal images (compressed Z stacks) of GFP-labelled Kelly cells that were injected intravenously into E3 chick embryos, and upon E14 dissection, were discovered within non-neuronal tissues, residing in clumps. A-B, tail; C-D, meninges. Scale bar 50µm.

The meninges data was analysed further, being the only tissue in which approximately regularly-sized “balls” of cells were consistently observed. Only meninges containing GFP-labelled cells from the Kelly line were studied because data was available for all three injection/dissection time points. The BE(2)Cs were not included in the E3-E10 bracket because their meningeal clumps were considerably larger and much more variable in size compared to the Kellys – many reaching, and some exceeding, 100µm in diameter. As shown in Figure 5.6, the clumps in the embryos injected at E6 and dissected at E10 were the smallest in size, on average 15-20µm, having only been in the embryos for 4 days. Those embryos injected at E3 and dissected at E10 possessed meningeal clumps of Kelly cells that were intermediate in size, roughly 30-35µm in diameter. In comparison, those cells that had survived within the embryos for 11 days, from E3 to E14, were in by far the largest cell masses, generally between 50 and 100µm in diameter. Thus the size of the Kelly clumps increased with increasing time in the embryos and this, along with their relatively rounded form and regular size, suggested they had originated from single cells rather than aggregation and were actively proliferating, i.e. could be regarded as neuroblastoma micro-tumours.

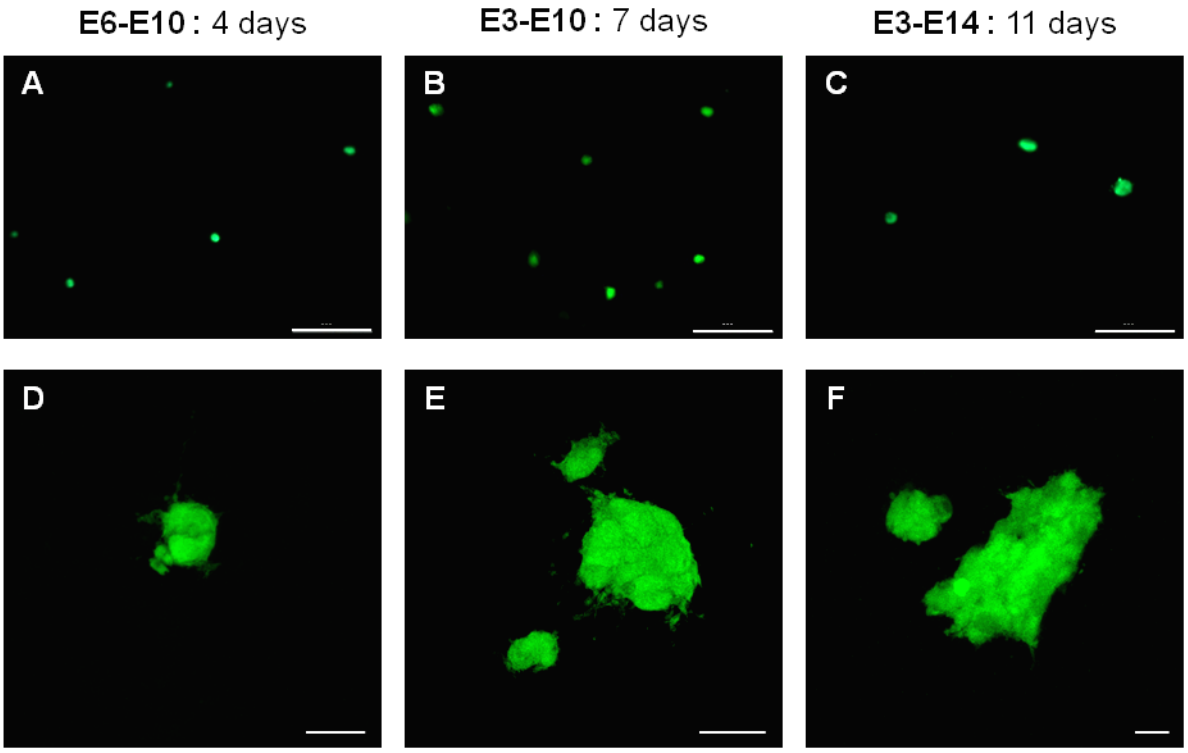

Figure 5.6. GFP-Kelly cells within chick meninges; A+D, following intravenous injection at E6 and dissection at E10; B+E, E3 injection, E10 dissection; C+F, E3 injection, E14 dissection. Note the difference in the length of the scale bar for F, showing a cell clump considerably larger than in D and E. Scale bars A-C, 200µm; D-F, 20µm.

5.3.1.2. Proliferation

EdU was used to quantitatively assess the extent of proliferation of the Kellys in each of the four embryonic tissues analysed at E10: the sympathetic ganglia, ENS, tail and meninges. EdU was intravenously injected at E13, thus proliferation was measured over the 24 hours prior to sacrifice. The increased mass of the embryos was accounted for (see Figure 2.4), and 4µl of a 20mM solution was administered, roughly equivalent to a concentration of 10µM in an 8g embryo. Results are summarised in Figure 5.7, from Kellys within tissues from 6 embryos, taken from 2 separate experiments, i.e. 3 per batch. In the sympathetic ganglia, the proportion of dividing Kelly cells was quantified at 22% (n=241) (Figure 5.8 A-D) – an increase from the 15% witnessed at E10. Of the Kelly incorporated into the enteric nervous system in the gut, 28% (n=200 cells) were proliferating (Figure 5.8 E-H), compared to 15% at E10. However, within the clumps of rounded cells in the tail and meninges, 49% (n=1247 cells) (Figure 5.9 A-D) and 50% (n=660 cells) (Figure 5.9 E-G) respectively had divided between E13 and E14, which was almost identical to the results obtained at E10 – when 50% of Kellys in the tail and 53% in the meninges were dividing.

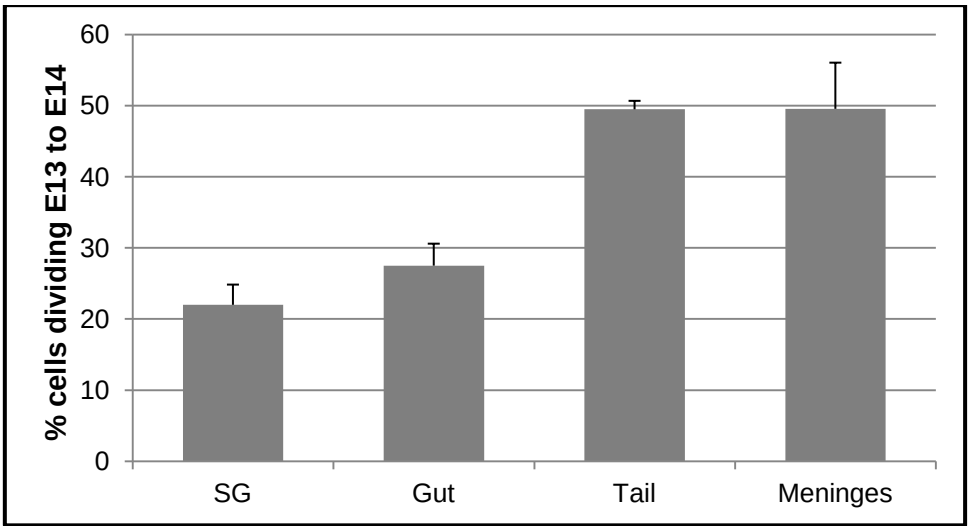

Figure 5.7. Histogram to show the proportions of proliferating Kelly cells between E13 and E14 within chick tissues as labelled. Error bars display the standard deviations from the mean values for each tissue.

Although the increased rated of cell proliferation in the sympathetic ganglia and ENS was unexpected, the endogenous chick cells were still dividing in both of these tissues (Figure 5.8), so perhaps the result was consistent with Kelly cells responding to their environment.

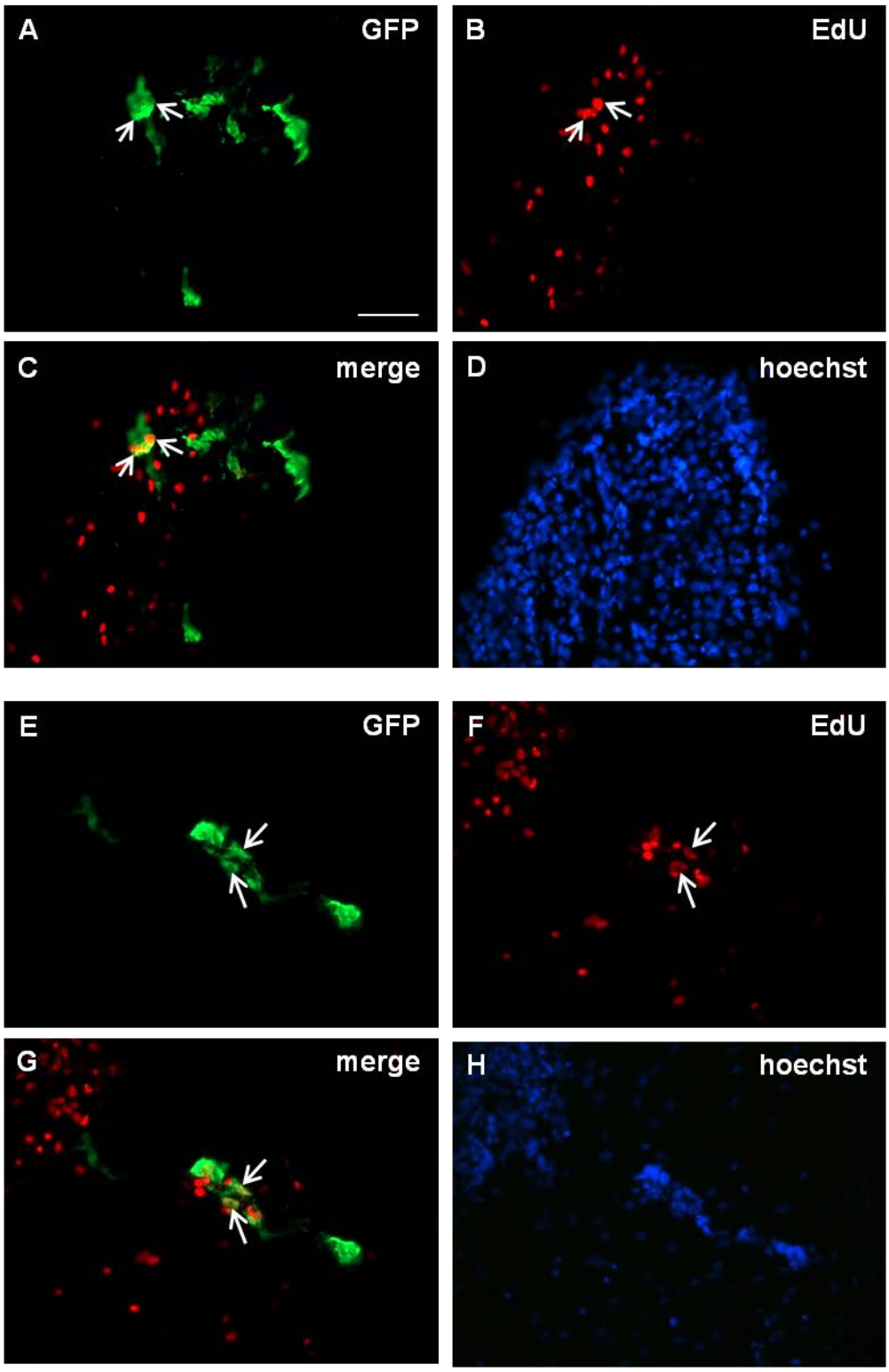

Figure 5.8. GFP-labelled Kellys were intravenously injected into E3 chick embryos. 4µl of a 20mM solution of EdU was injected into E13 embryos, which were sacrificed and dissected 24 hours later. E14 A-D, sympathetic ganglia; E-H, gut (ENS); were sectioned using a cryostat and EdU incorporation could then be detected. Arrows identify Kelly cells with nuclear EdU incorporation. Scale bar 50µm for all.

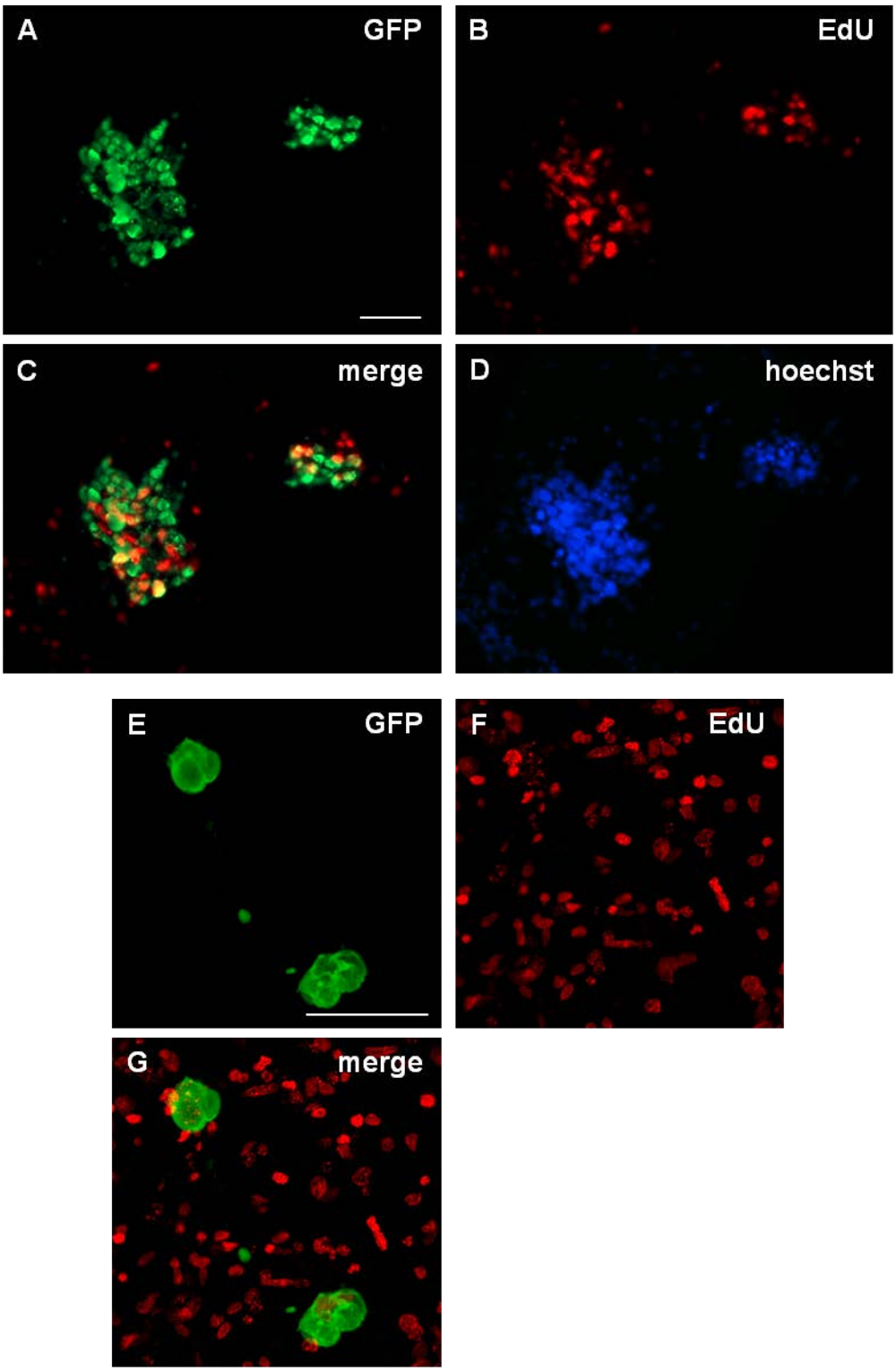

Figure 5.9. EdU incorporation into E14 A-D, tail; E-G, meninges; tissues containing GFP-labelled Kellys that had been intravenously injected at E3. EdU was injected at E13, 24 hours prior to dissection, and incorporates into all dividing cells – human and chick. A-D, frozen sections; E-G, whole mount stain. Scale bars 50µm.

5.3.1.3. MYCN expression

At E10, the proliferating Kelly cells in the tail and meninges had continued to express MYCN at high levels, whereas in the sympathetic ganglia and gut, expression was downregulated; in the SG to below detectable levels in every Kelly cell. When assessed at E14, unsurprisingly, the Kellys in the tail and meninges still maintained their MYCN protein expression (Figure 5.10 and Figure 5.11). In the neural sympathetic ganglia and gut, results are different to those achieved at E10. In the Kellys located as single cells in the sympathetic ganglia, therefore mostly, if not completely, surrounded by chick cells, MYCN expression remained below detectable levels (Figure 5.12). However, there was an increased incidence of clusters of Kelly cells within the tissue, which were to some extent protected by each other from the chick host environment. Within these clusters, many of the Kelly cells had begun to re-express MYCN (Figure 5.13). There may have been very low levels of MYCN in some Kellys within the ENS, but many had undetectable MYCN (Figure 5.14).

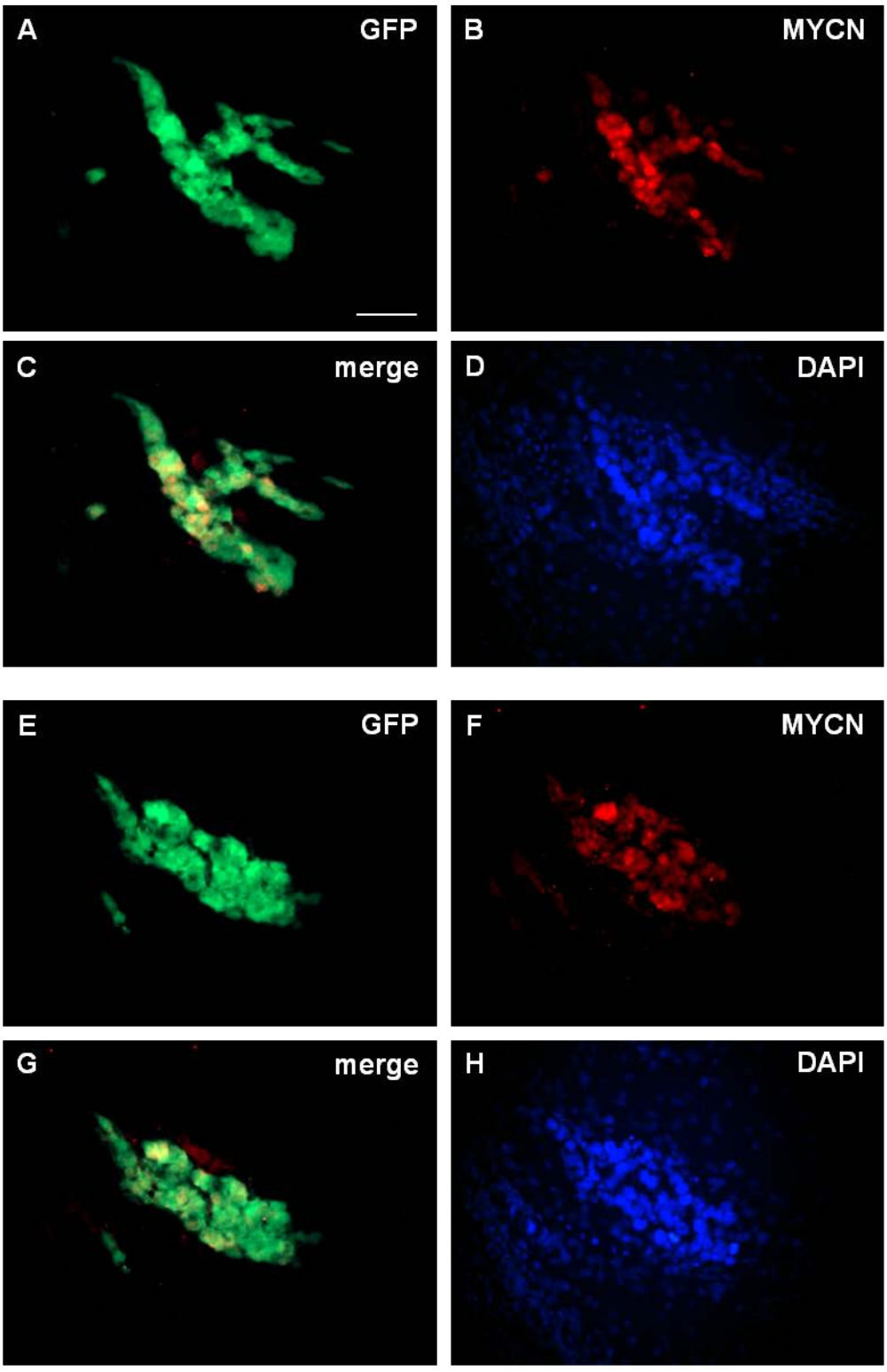

Figure 5.10. MYCN expression in frozen sections of GFP-labelled Kelly cells, residing in clumps within the E14 chick tail. Kellys had been injected intravenously at E3. Scale bar 50µm for all.

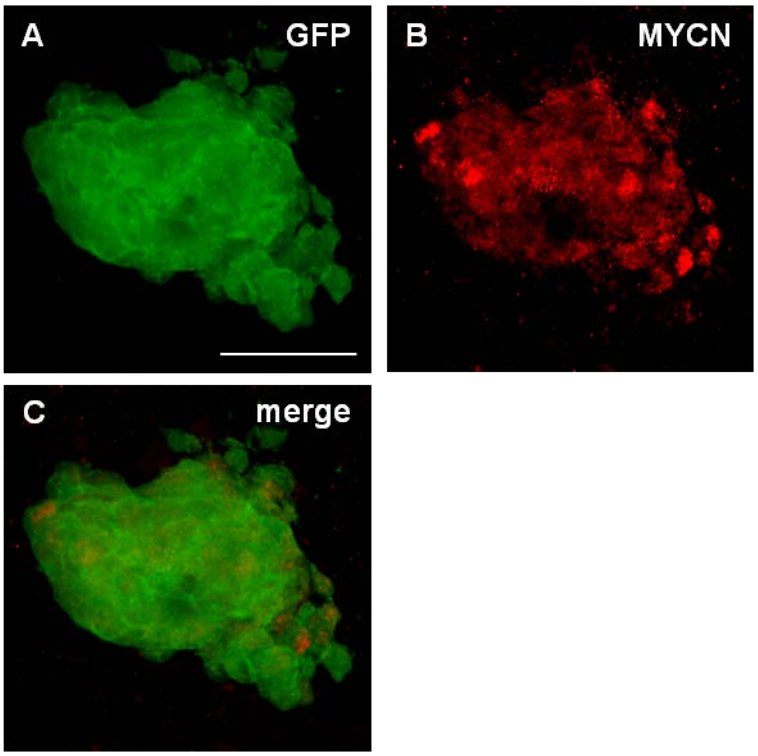

Figure 5.11. Confocal image (compressed Z stack) showing MYCN expression in GFP-labelled Kelly cells in a clump within the E14 chick meninges. Kellys were injected into the chick intravenously at E3. Whole mount tisue stain. Scale bar 50µm.

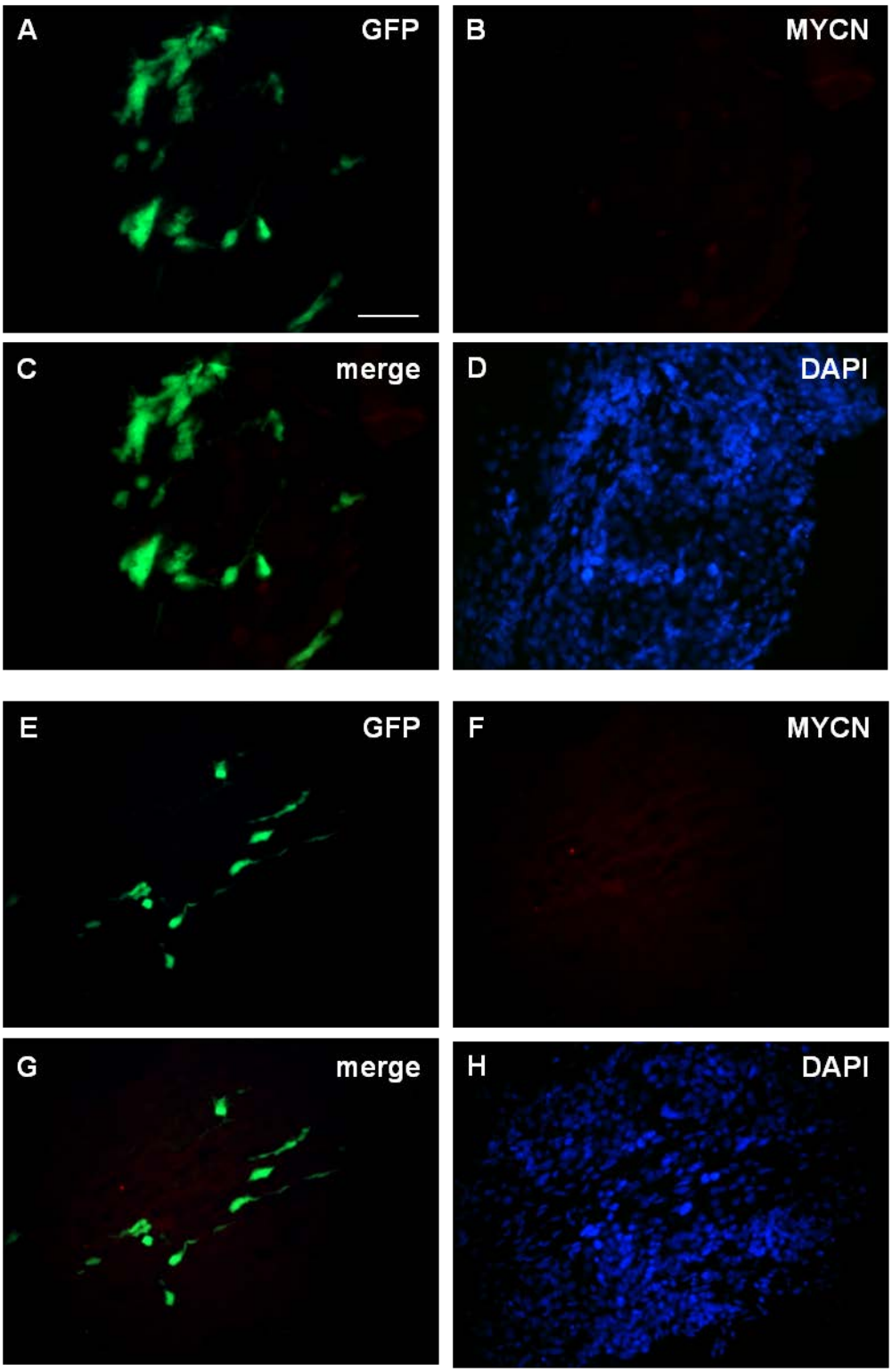

Figure 5.12. GFP-labelled Kelly cells were intravenously injected into the E3 chick, and allowed to survive within the embryo for 11 days, until dissection at E14. Kellys were discovered within the sympathetic ganglia, which were frozen and sectioned. 10µm sections were stained for human-specific MYCN expression. Images shown are of Kellys located either as single cells or in small groups, and these do not express detectable levels of the MYCN protein. Scale bar 50µm for all.

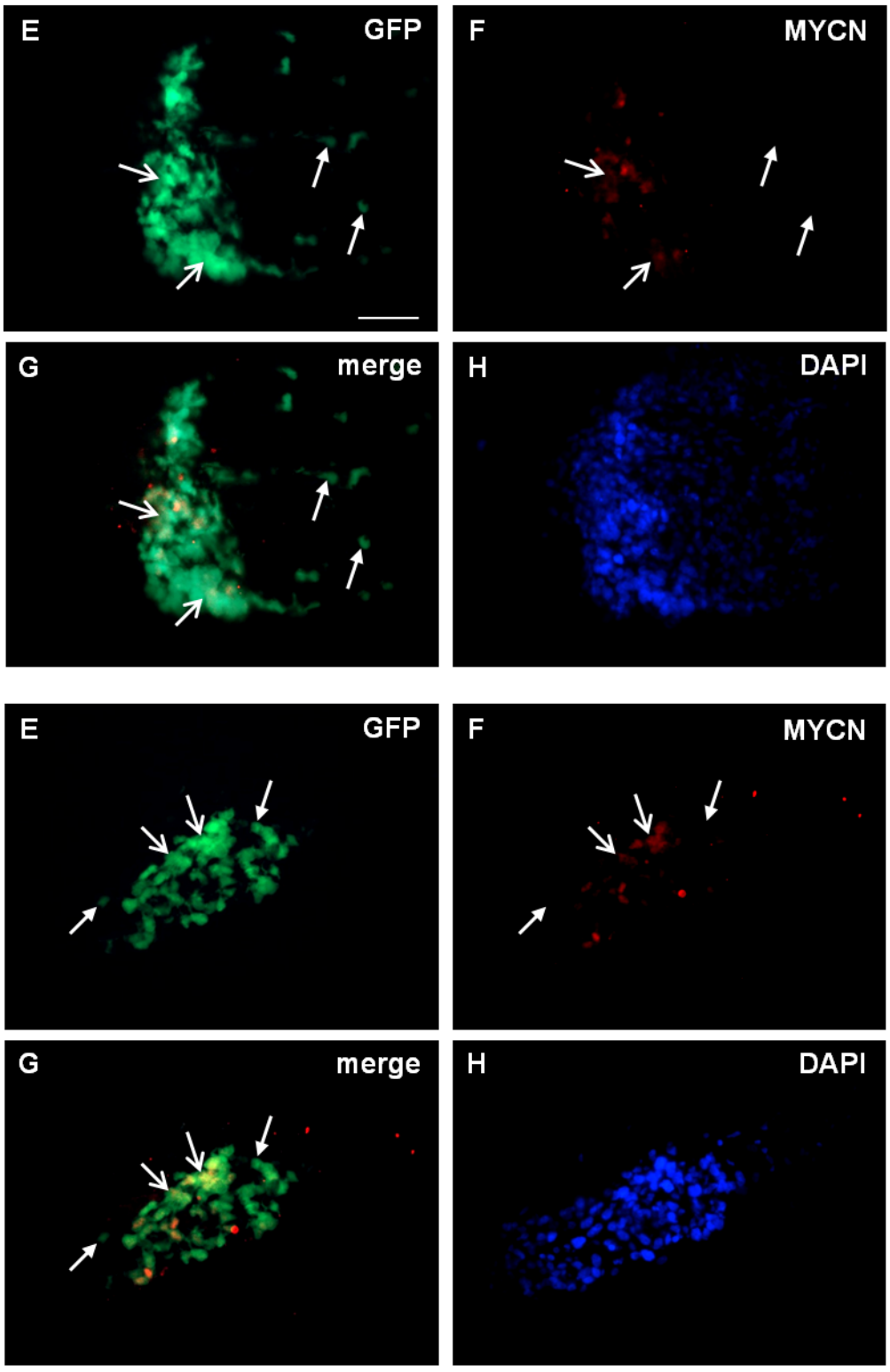

Figure 5.13. GFP-labelled Kelly cells were intravenously injected into the E3 chick, and allowed to survive within the embryo for 11 days, until dissection at E14. Kellys were discovered within the sympathetic ganglia, which were frozen and sectioned. 10µm sections were stained for human-specific MYCN expression. Images shown are of Kellys located in more dense groups, in which some cells – particularly those shielded from the SG microenvironment – have re-expressed MYCN. Open arrows identify GFP-Kellys with MYCN expression, block arrowheads point to more singly-located Kellys with undetectable MYCN expression. Scale bar 50µm for all.

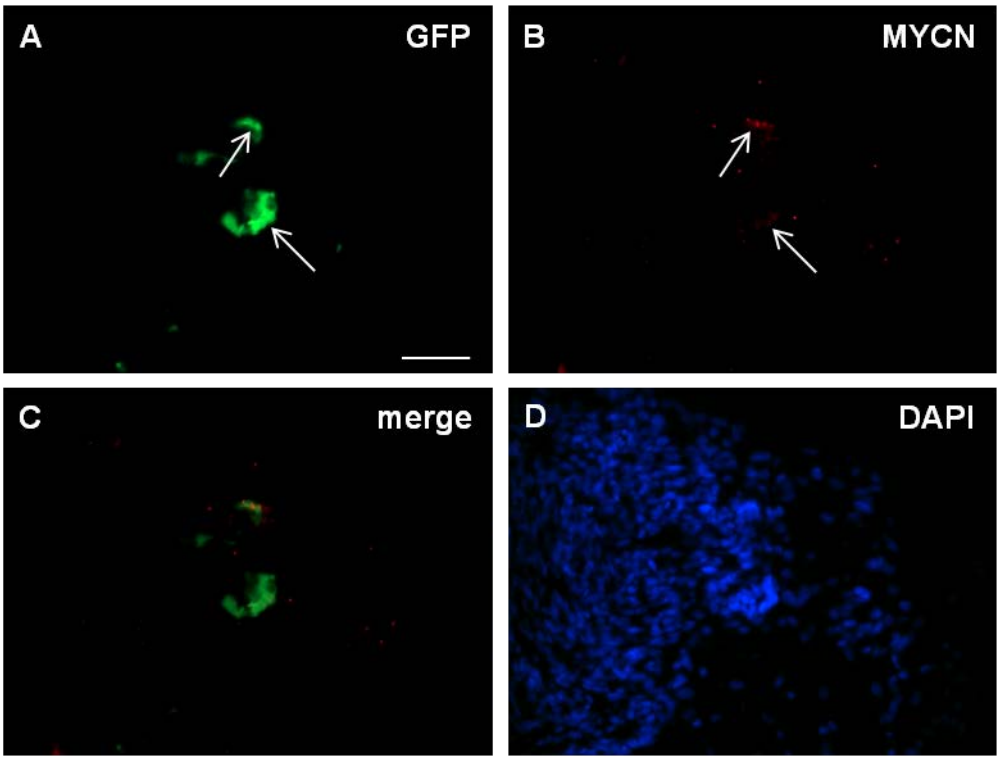

Figure 5.14. MYCN expression in frozen sections of GFP-labelled Kelly cells within the E14 chick gut (ENS). Cells were injected intravenously at E3 and allowed to survive in the embryos for a total of 11 days. Some cells did not show detectable MYCN protein expression, however some may have low levels of expression (arrows). Scale bar 50µm.

5.3.1.4. Differentiation

Although over one fifth of the Kelly cells within the sympathetic ganglia were proliferating, and many of those shielded from the host environment had begun to re-express MYCN, the extension of significantly long processes by a proportion of cells prompted the completion of whole mount staining of the tissue for markers of neuronal differentiation. Tissues were stained using antibodies to the NF 70kD subunit (cross-reacts with both human and chick) and GAP43 (cross-reacts with human only). Although Kellys within the fluorescently neurofilament-stained chick neurons did not themselves stain positively for neurofilament, a small number of cells did express the GAP43 protein (Figure 5.15), revealing that the sympathetic ganglion environment was capable of inducing differentiation and hence a reversal in tumourigenesis of these MYCN-amplified neuroblastoma cells.

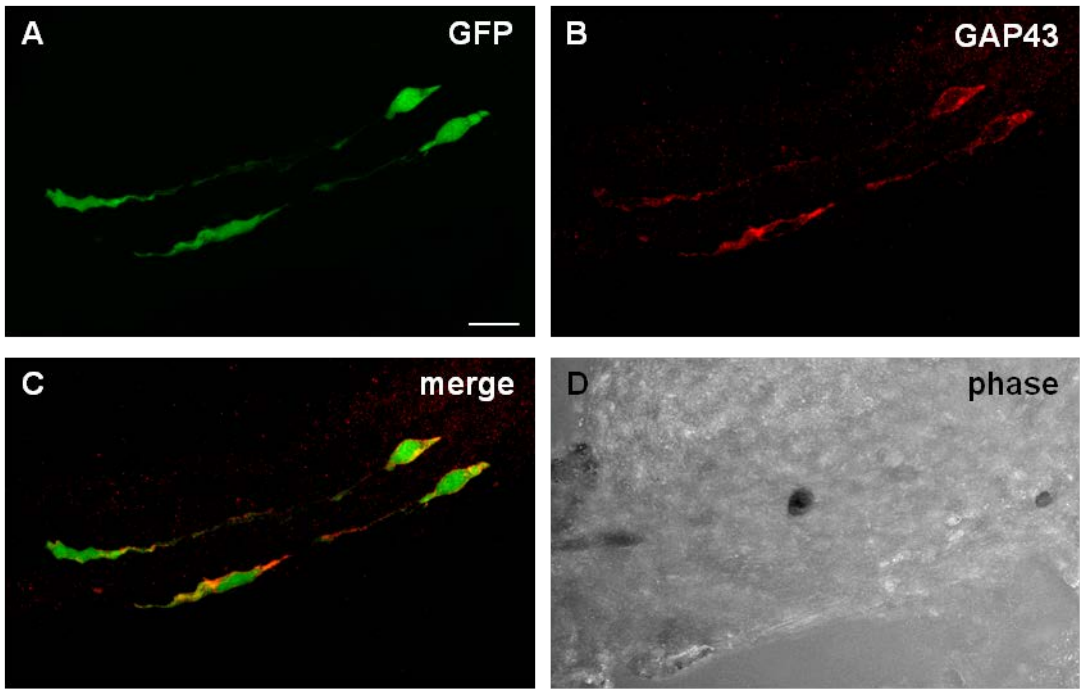

Figure 5.15. Following intravenous injection of GFP-labelled Kellys into E3 chick embryos, E14 sympathetic ganglia containing integrated Kellys were whole mount stained for MYCN protein expression and imaged using a confocal microscope. A small proportion of GFP-labelled Kellys within the ganglia were found to express the neuronal lineage protein GAP43. Scale bar 20µm.

5.3.2. GFP-labelled SH-EP injections

5.3.2.1. SH-EP wildtype

The SH-EP cell line is a non-MYCN-amplified neuroblastoma line, with no/negligible MYCN expression. It was intriguing to discover how these cells would behave in the chick embryos compared to the highly MYCN-expressing Kelly cells. A GFP-labelled SH-EP line was generated (with thanks to Dr Anne Herrmann, University of Liverpool, UK), and $2x10^5$ of these cells were intravenously injected into E3 chick embryos, using exactly the same protocol as for the Kelly cells. As briefly mentioned in the Chapter Four Discussion, when embryos were dissected at E10, no SH-EP cells were found within any chick tissues (n=11 embryos, 2 experiments). Following E3 injection, embryos had been examined under fluorescence, and GFP-labelled cells were observed throughout the circulation and within embryonic tissues, therefore cells must have undergone apoptosis at some point between E3 and E10.

5.3.2.2. SH-EP-MYCN

The SH-EP-MYCN cell line (kindly donated (and produced) by Dr Louis Chesler, The Institute of Cancer Research, Sutton, UK) is one in which MYCN expression is driven by a human cytomegalovirus (CMV) promoter, resulting in the MYCN oncogene being constitutively expressed. Although this expression would probably not be as high as that in the Kelly cells, which have over 200 copies of the MYCN gene (Murphy et al. 2009), in theory, being under the CMV promoter, the MYCN would not be able to be turned off/downregulated in those cells within the sympathetic ganglia microenvironment. MYCN strongly induces cell proliferation, and rat embryo cells transfected with MYCN derived from Kelly cells have been shown to proliferate for at least 200 generations (Schwab & Bishop 1988). Therefore it was considered to be of great interest how the cells would behave particularly in the sympathetic ganglia, where the stable MYCN expression could not be repressed by the as yet unidentified factor(s). Would SH-EP-MYCN cells form microtumours reminiscent of those occurring in the embryonic chick tail and meninges?

The SH-EP-MYCN cells were stained in culture by Heba Karosh (MRes student, University of Liverpool, UK) to assess the MYCN protein levels. In this supposedly highly MYCN-expressing line, only around half of the cells stained positively for the MYCN protein, therefore efforts had to be made to produce a more consistently MYCN-expressing line. After subcloning, although MYCN staining intensities still varied slightly, the subclones were initially much more uniform in terms of their expression than the original cell line. The most consistently highly MYCN-expressing subclone was GFP labelled by Dr Anne Herrmann (University of Liverpool, UK), and from the masterclone of cells with varying GFP fluorescence intensities, the brightest cells were selected by Heba Karosh using a FACS cell sorter. Thus a brightly GFP-expressing, constitutively highly MYCN-expressing SH-EP cell line was thought to have been produced. However, when this was later stained using a MYCN antibody, only 60-70% of cells stained positively, which although improved on the original cell line, was not favourable.

The GFP-labelled SH-EP-MYCN subcloned cells were nevertheless injected intravenously: $2x10^5$ cells per E3 chick embryo. When these embryos were dissected at E10 (n=12 embryos, 2 experiments), they were either completely devoid of neuroblastoma cells or found to contain less than 10 isolated SH-EP cells. The embryos had been examined under fluorescence at E3, 0-3 hours after injection, and every one had an abundance of cells within the chick tissues and travelling through the circulation, comparable in numbers to those typically seen following Kelly cell injection. When E3-injected embryos were then dissected

at E7 (n=4 embryos, 1 experiment), a greater number of SH-EP-MYCN cells were found, but this was still relatively few; less than 100 cells per embryo. These were mostly located in the internal heart tissue, plus single-figured numbers of cells were isolated in the gut (gizzard, intestine, colon), tail, meninges, eyes and body cavity – similar locations to the Kellys. In the four E7 embryos dissected, cells were not observed in the sympathetic ganglia, or adrenal glands.

5.3.3. Moving forward with the chick intravenous injection model system

Following the results obtained with the E3-injected Kelly cells, there are inevitably a multitude of questions to be answered and opportunity to pursue various routes of further investigation. Two different approaches on which work has commenced are the culture of primary neuroblastoma tissues, in the hope that these cells can be injected into the chick embryo, and *in vitro* culture of chick tissues containing neuroblastoma cells, to examine the dependence of the Kelly cells on chick tissues for maintenance of their phenotypes.

5.3.3.1. Primary neuroblastoma cell culture

Neuroblastoma primary tumour tissue was received from Alder Hey Children's Hospital, Liverpool, UK – either from a biopsy at diagnosis or from a surgical resection. Eleven samples were received, and for the latter three (all biopsy tissues), they were accompanied by bone marrow aspirates. Images of cultured tissues are shown in Figures 5.16, 5.17 and 5.20: those labelled with digits only (e.g. NB17) are from biopsy samples, i.e. pre-treatment, those labelled "B" (e.g. NB16B) are resected tissues, i.e. post-chemotherapy, and NB2C is from a relapse.

Initially, for samples NB16B to 20B, tissue was dissociated as far as possible, and the single cells cultured along with small tissue pieces in serum-containing medium. The cells grew adherent to the culture surface, were usually large and flat displaying varying morphologies (Figure 5.16 A-D). However, some extended long processes (Figure 5.16 E and Figure 5.17 C). All tumours behaved differently – some growing rapidly, and others taking weeks to expand. In general, the attachment of tissue pieces to the culture surface, as in Figure 5.16 H and Figure 5.17 E, generally resulted in outgrowth of a large number of cells. However, for

many tumours, the tissue would not adhere, even if the culture surface was coated with Poly-L-lysine and/or laminin.

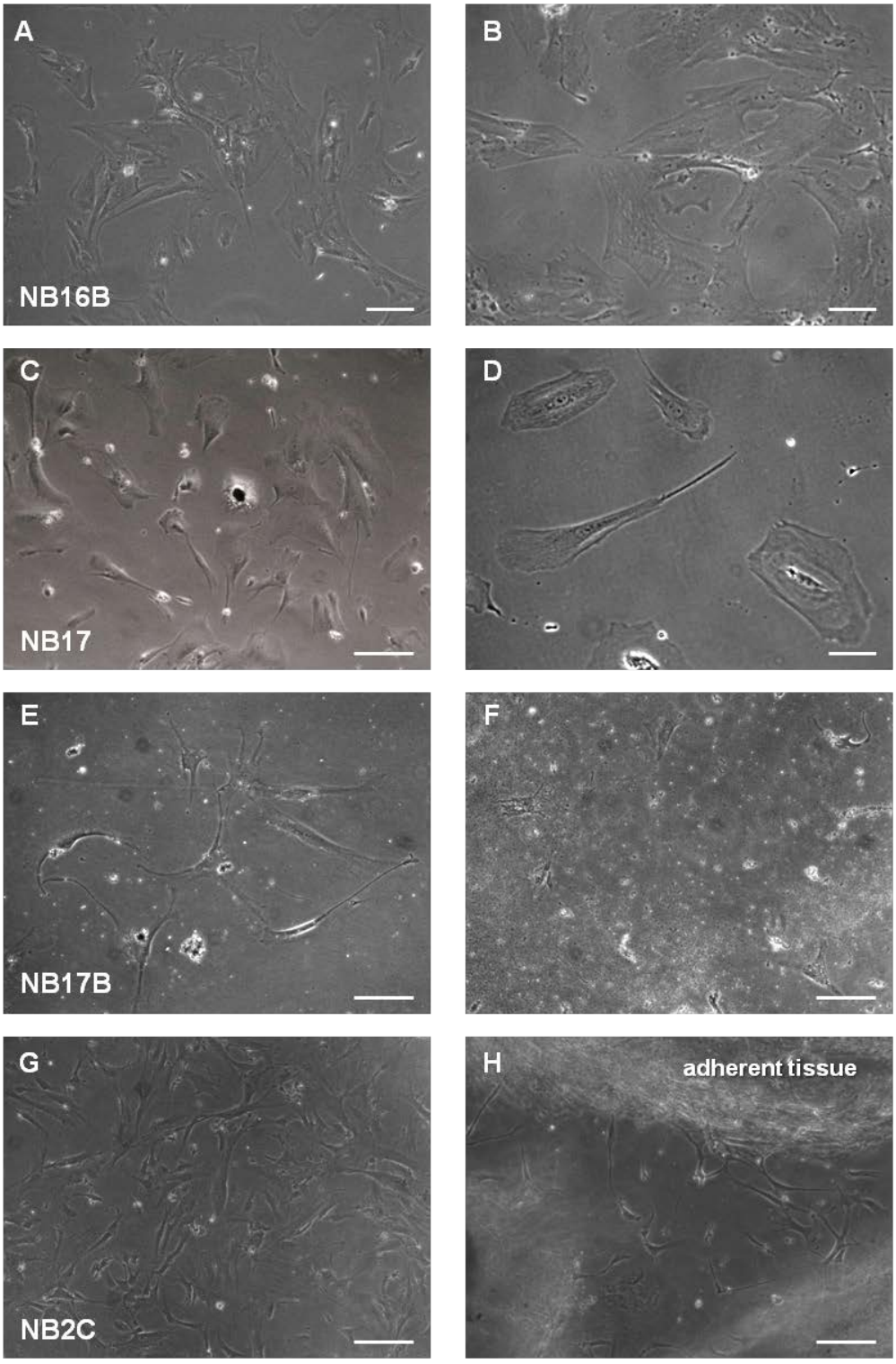

Figure 5.16. Primary neuroblastoma tumour tissues received from Alder Hey Children's Hospital. Tissues were mechanically dissociated and cultured in serum-containing medium. Single cells and tissue pieces adhered to the culture surface. Scale bars A-B, D, 20µm; C, E-H, 100µm.

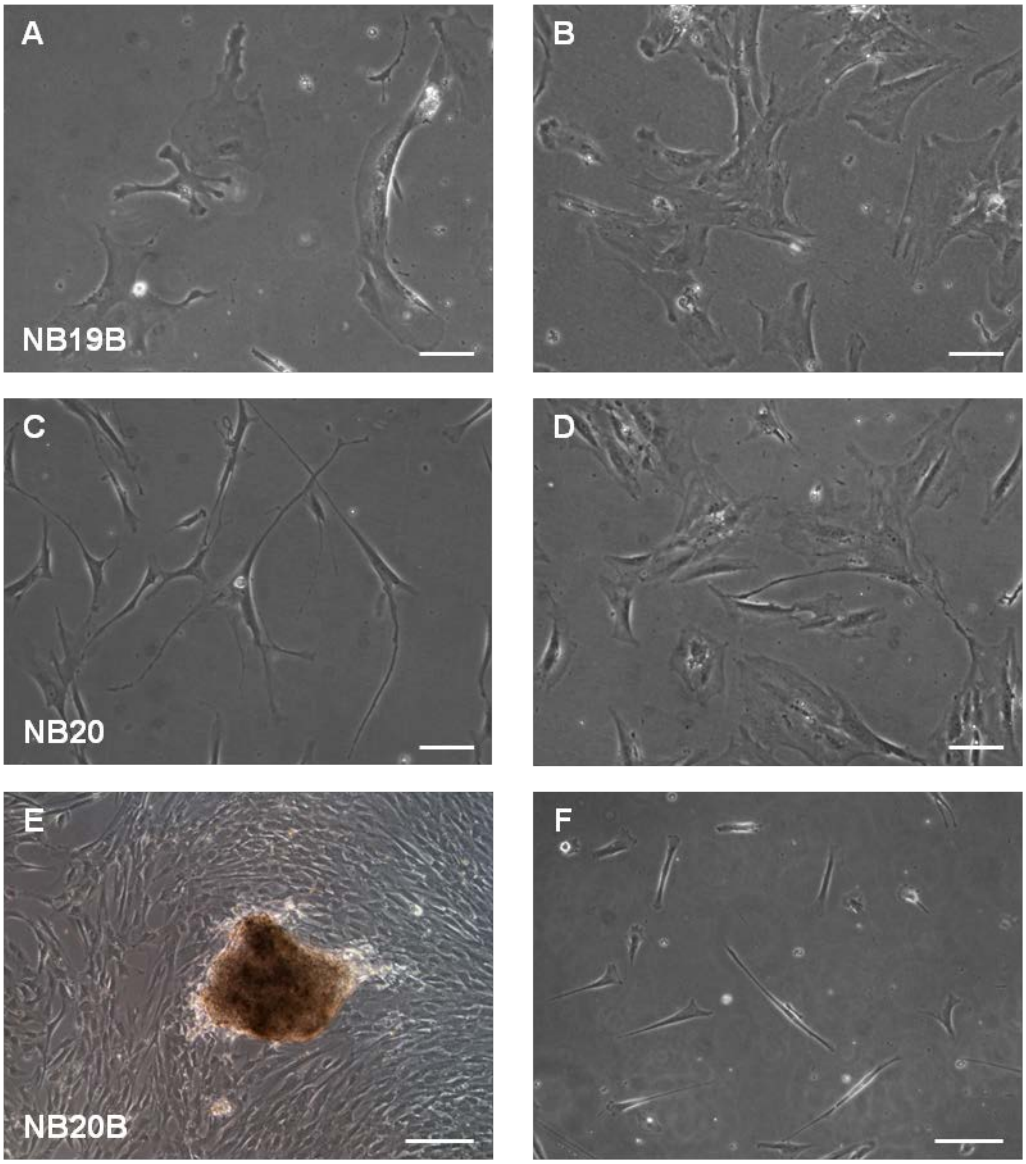

Figure 5.17. Additional primary neuroblastoma tumour tissues received from Alder Hey Children's Hospital, following tissue dissociation and adherent culture in serum-containing medium. Scale bars A-D, 20µm; E-F, 100µm.

The adherent cells of MYCN-amplified tumour NB19B were stained for the neuroblastoma protein markers MYCN and NB84 and the stem cell marker nestin (Figure 5.18). None of the cells expressed detectable MYCN or NB84, but the majority of cells did stain positively for nestin (Figure 5.18 G-L). Since this was a resected tumour and neuroblastoma patients often respond well to initial treatment, but succumb to a treatment-resistant relapse, it was possible that the cells being cultured were not malignant neuroblastoma cells.

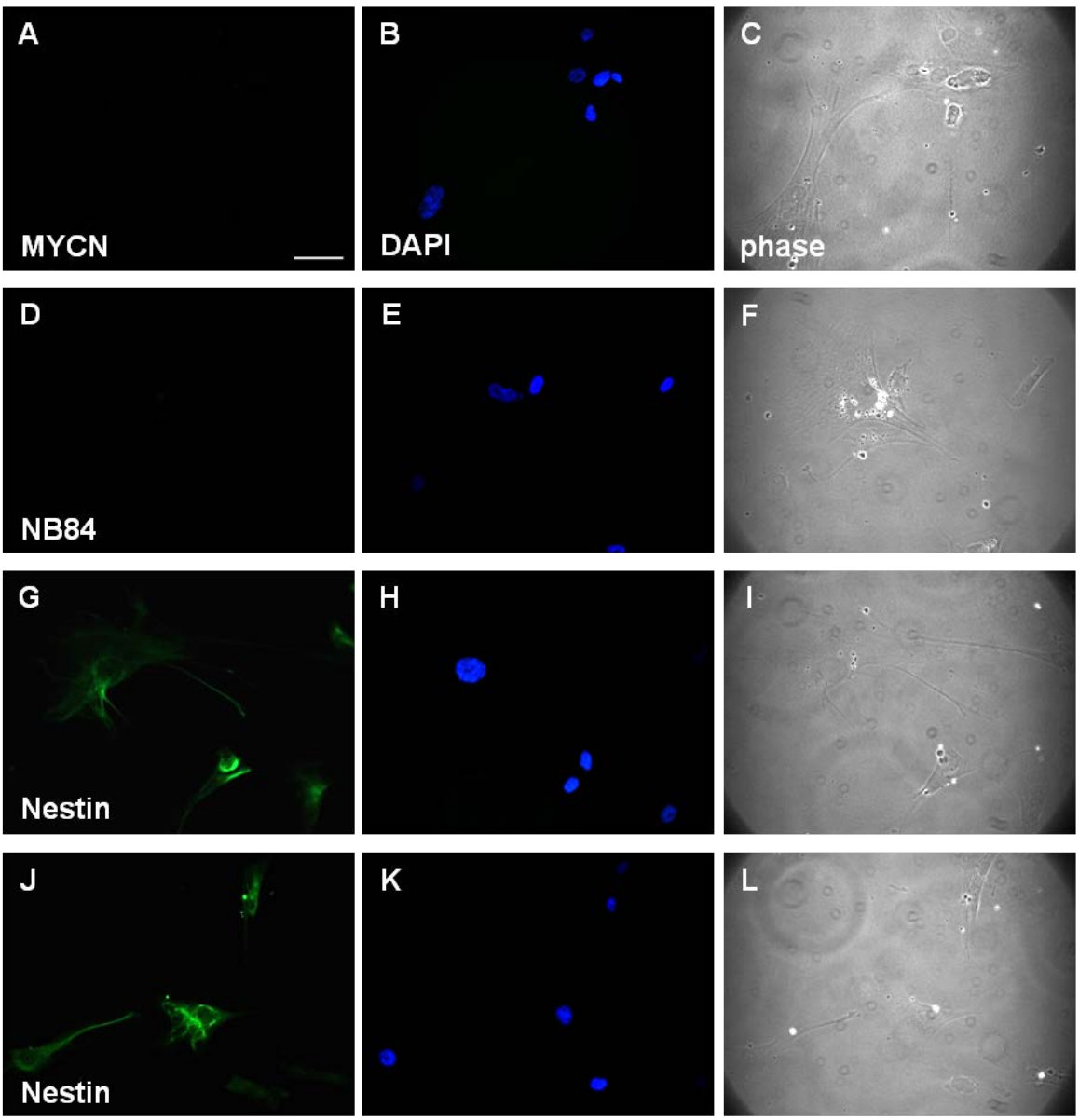

Figure 5.18. NB19B cells, following adherent culture in serum-containing medium, were trypsinised and cultured on 13mm glass coverslips. Cells were then stained using antibodies as labelled. Scale bar 50µm for all.

Methanol-fixed touchprints of MYCN-amplified tumour NB20 were received from the Alder Hey histopathologists, and these were stained for the stem cell markers CD133 and nestin to test the tumour's aggressiveness. Like the cultured NB19B cells, the entire tumour region on the touchprint of MYCN-amplified NB20 stained for nestin, and the majority of the cells seemed to stain for CD133 – expression of both proteins is associated with MYCN amplification (Sartelet et al. 2012; Thomas et al. 2004a).

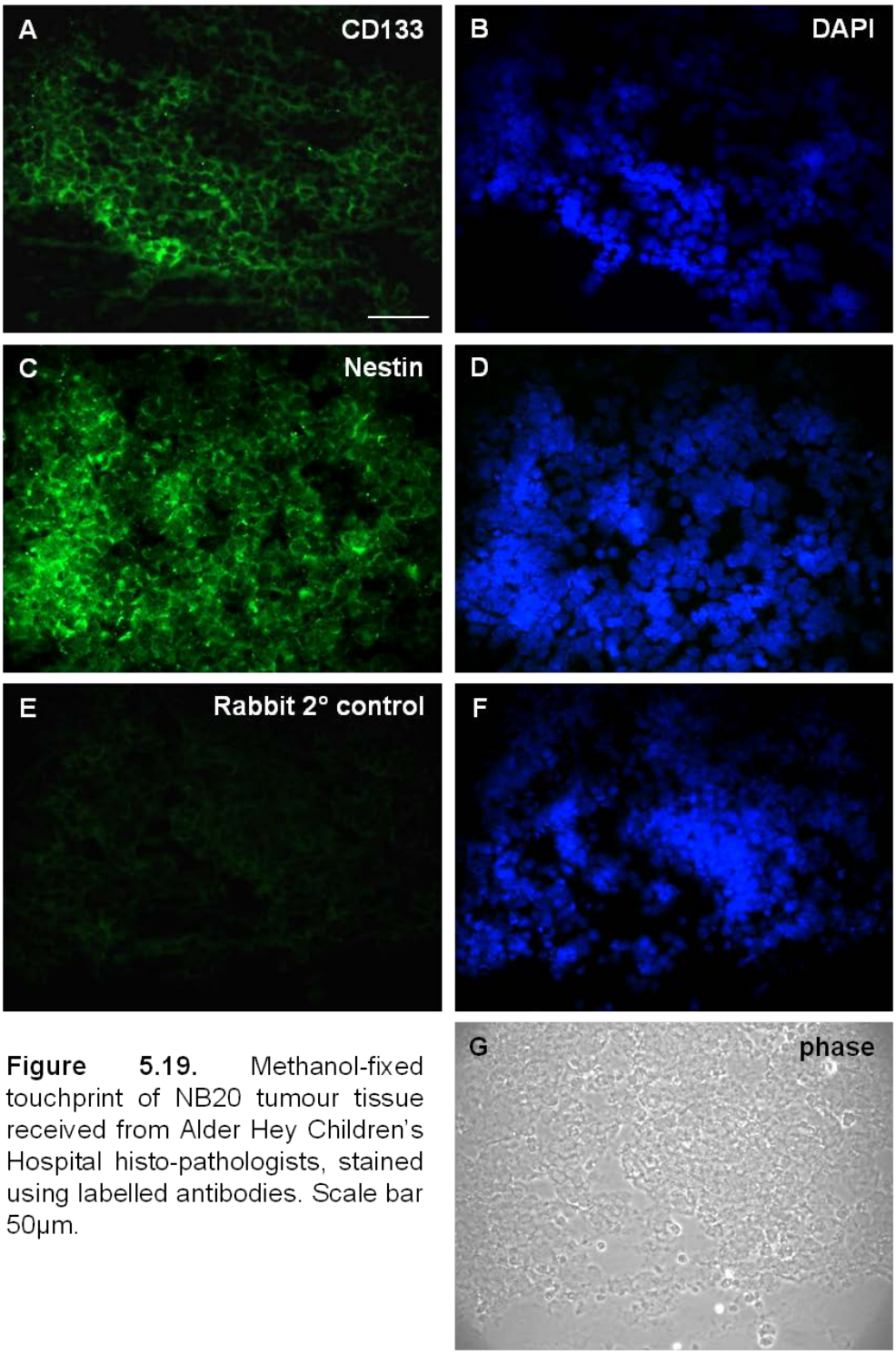

Figure 5.19. Methanol-fixed touchprint of NB20 tumour tissue received from Alder Hey Children's Hospital histo-pathologists, stained using labelled antibodies. Scale bar 50µm.

Following staining of adherent tumour cells by a number of group members, it was considered a distinct possibility that this culture method was not optimal for the culture of malignant neuroblastoma cells. Therefore future samples were cultured in serum-free “stem cell medium” as spheres (Figure 5.20). These spheres grew up to 500µm and following mechanical dissociation, further spheres were cultured for 1-3 passages before freezing.

For samples NB22, NB23 and NB24, bone marrow aspirates (taken at diagnosis) were also received. Bone marrow samples may be the most effective in producing primary neuroblastoma lines, as most neuroblastoma cell lines were originally derived from bone marrow samples. Bone marrow cells were cultured in serum-free medium as spheres (Hansford et al. 2007) (Figure 5.20), and frozen after 1-2 passages.

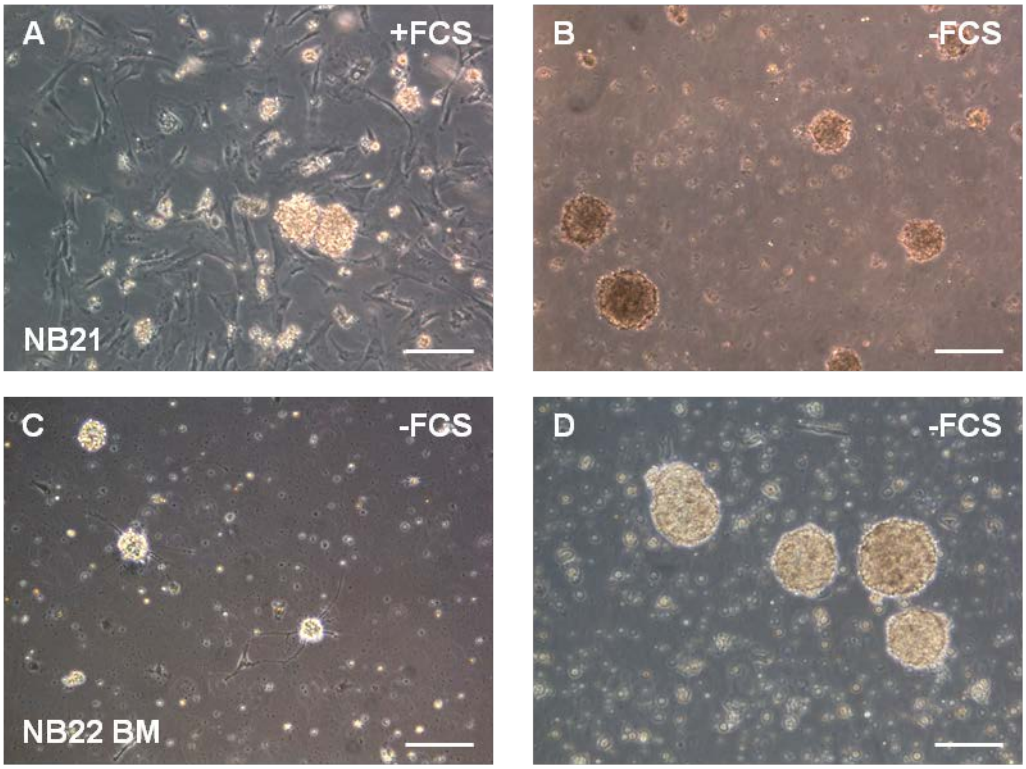

Figure 5.20. Neuroblastoma samples received from Alder Hey Children’s Hospital. A-B, primary tumour tissue following mechanical dissociation; C-D, bone marrow aspirates. A, cultured in serum-containing medium, B-D, non-adherent culture in serum-free medium. BM, bone marrow. Scale bars all 100µm.

5.3.3.2. Establishment of an *in vitro* system to assess the effect of the sympathetic ganglia on neuroblastoma cells

To test the influence and possible dependence of the Kelly cells on the sympathetic ganglia microenvironment for maintenance of a less aggressive phenotype, E10 sympathetic ganglia containing Kelly cells were dissected and placed into culture, either as dissociated cells or explants. E10 tissues were chosen because in their SG, the starting population of Kellys would all be MYCN deficient, therefore the effects of the ganglionic microenvironment could be efficiently tested. GFP-Kelly-containing tail tissue was cultured in parallel as a control. Following the discovery of MYCN re-expression at E14, the aim of these experiments was to investigate any differences between the behaviour of Kelly cells cultured with, but not necessarily in contact with SG cells, and Kelly cells integrated into explants, completely surrounded by and in contact with chick ganglion cells.

Preliminary experiments were performed to investigate whether the Kelly cells would survive being cultured on poly-L-lysine- and laminin-coated coverslips, in L15 sympathetic neuron medium in a CO_2-free incubator – the required SG culture conditions. Additionally, chick embryo tail cells were cultured on poly-L-lysine and laminin, in both L15 sympathetic neuron medium, cultured in a CO_2-free incubator, and RPMI medium in a 5% CO_2 incubator. EdU incorporation into both types of cells in all culture conditions indicated they were not only surviving, but proliferating in culture. Therefore sympathetic ganglia and pieces of tail tissue, both containing GFP Kellys that had survived in the embryonic tissues for 7 days, were either dissociated into single cells and placed into culture, or torn into small pieces and cultured as explants – all on coverslips coated with poly-L-lysine and laminin, in L15 medium and incubated at 37°C in 0% CO_2 for 3 days. EdU was added to the culture medium after 48 hours. These experiments were performed on two separate occasions, using tissues from at least 5 embryos each time.

As expected, in dissociated tail tissue, the majority of GFP-expressing Kelly cells had divided in the 24 hours prior to fixation (87%, n=572) (Figure 5.21 A-F and Figure 5.22 D), and almost all showed clear retention of MYCN expression (94%, n=363) (Figure 5.21 G-L, Figure 5.22 E). The results for Kelly cells within the explanted tail tissue (photographed in Figure 5.22 A-B) were almost identical, with 86% (n=780) having EdU incorporation (Figure 5.22 C+D) and 98% (n=373) displaying obviously high levels of the MYCN protein (Figure 5.22 E).

In the E10 sympathetic ganglia, it had been found that only 15% of the Kelly population were undergoing cell division (Figures 4.29, 4.30) and MYCN could not be detected by immunofluorescence in any of the Kelly cells (Figure 4.36 E-H, Figure 4.37 E-H, Figure 4.38). However, following dissociation of the tissue, meaning that the Kelly cells were not completely surrounded by SG cells, the proportion of proliferating cells had increased to 87% (n=377) (Figure 5.23 A-F, Figure 5.24 G), the same as those dissociated from the E10 tails. It was apparent from the E14 data that the loss of MYCN expression observed in the Kelly cells in the E10 SG was reversible, and this was also shown to be the case in the dissociated SG, where from an initial population of 0% MYCN-expressing Kellys, following 3 days in culture, 75% of the Kellys were found to express MYCN (n=148) (Figure 5.23 G-K, Figure 5.24 H). The cells' morphologies were similar to that observed for normal (undifferentiated) Kellys in culture. The sympathetic ganglion explants extended numerous axons, radiating out from the entire circumference (Figure 5.24 A-B), and some of the GFP Kellys within the explants also developed neurites which extended towards, and sometimes beyond, the edge of the SG tissue (Figure 5.24 C, arrows). Of the Kelly cells within the explants, 70% (n=248) had undergone cell division in the previous 24 hours (Figure 5.24 D+G), and although this was considerably more than the 15% proliferating in the SG *in vivo* at E10, and even the 22% at E14, it was in keeping with the chick SG cells. Perhaps most interesting was the fact that MYCN immunofluorescence could not be detected in any Kelly cells in the SG explants (Figure 5.24 E-F+H).

These results showed that the Kelly cells remained under the control of the sympathetic ganglia when put into culture, and implied that one or more factors within the sympathetic ganglionic environment were required for the maintenance of this downregulation.

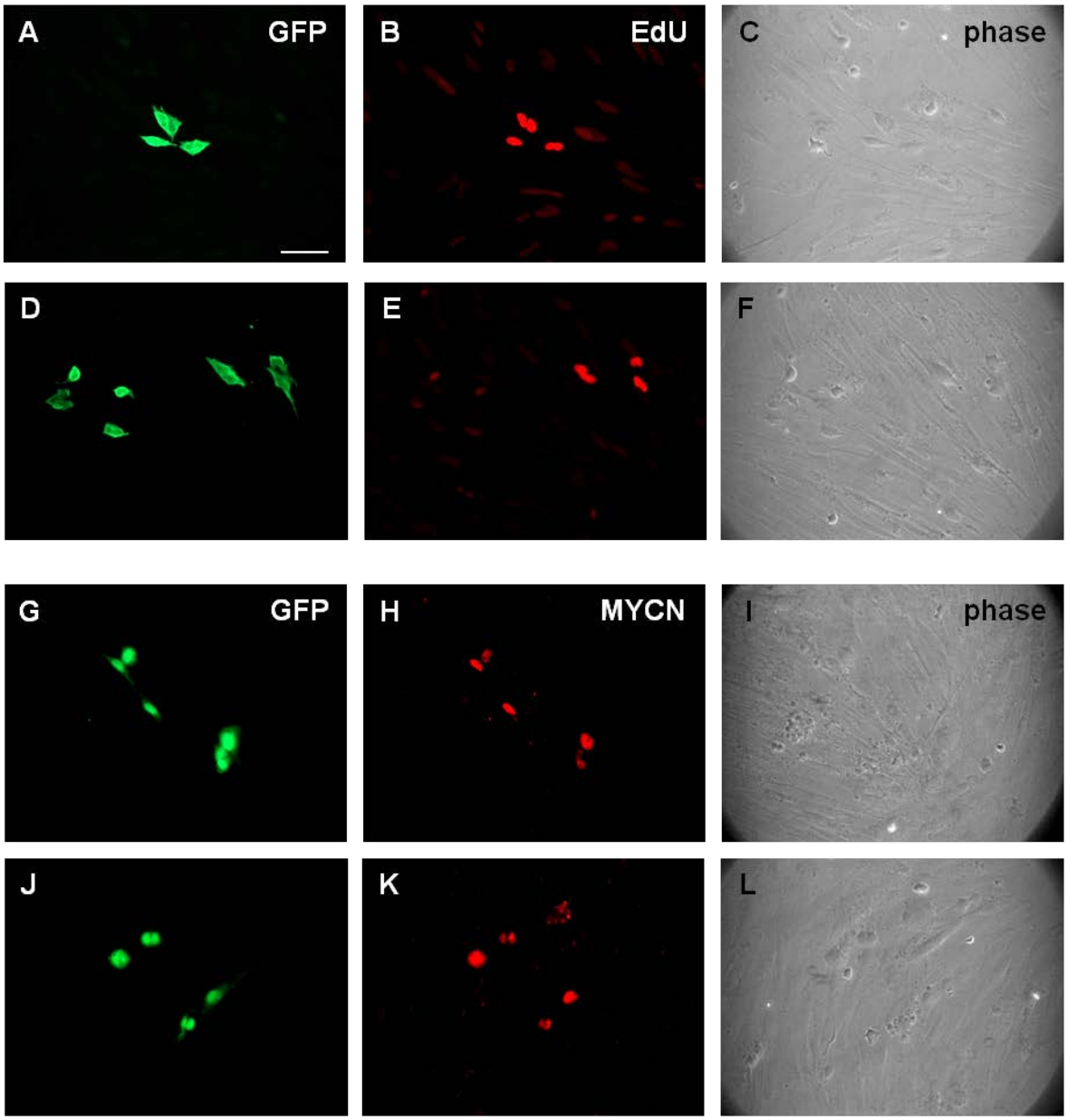

Figure 5.21. Following E3 intravenous injection of GFP-labelled Kelly cells, dissected E10 chick tail tissues containing GFP Kellys were dissociated into single cells and cultured on poly-L-lysine- and laminin-coated glass coverslips for 3 days. A-F, After 48 hours in culture, 5µM EdU was added to the culture medium, then after a further 24 hours, cells were fixed and EdU incorporation detected; G-I, MYCN immunofluorescence staining, following 3 days in culture. Scale bar 50µm for all.

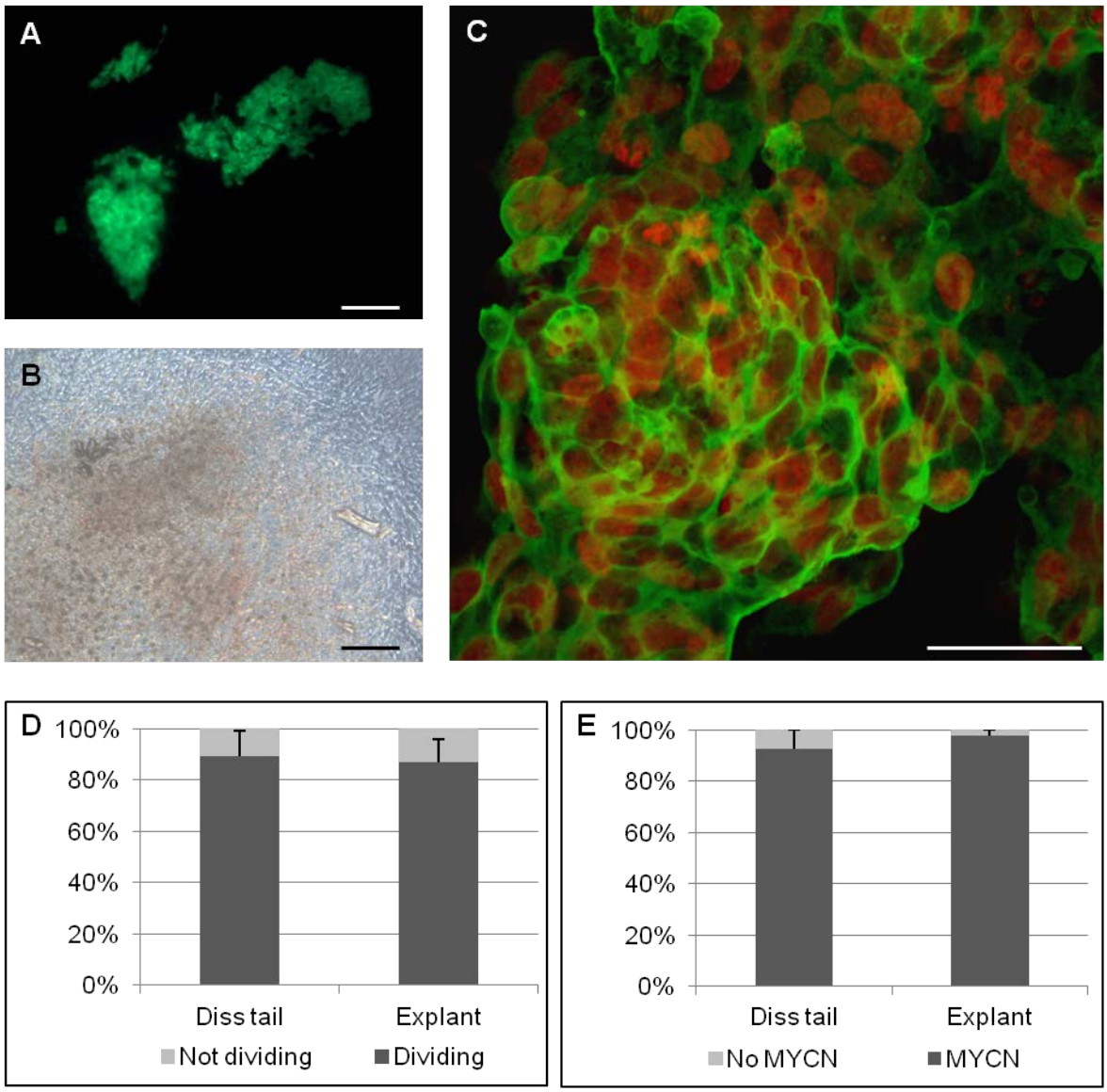

Figure 5.22. Tail tissue containing GFP-labelled Kellys (that had been injected intravenously at E3) was dissected from E10 embryos. This tissue was cultured *in vitro* as explants (A, fluorescence; B, brightfield) for 3 days. Tissues were then whole mount stained to detect EdU incorporation (C, compressed Z stack confocal image, green is anti-GFP antibody, red is EdU) and MYCN expression. Scale bars A-B, 200µm; C, 50µm. D-E, histograms to show the proportions of Kelly cells D, proliferating; E, expressing MYCN; in dissociated versus explanted tail tissue. Error bars display standard deviations from the mean value.

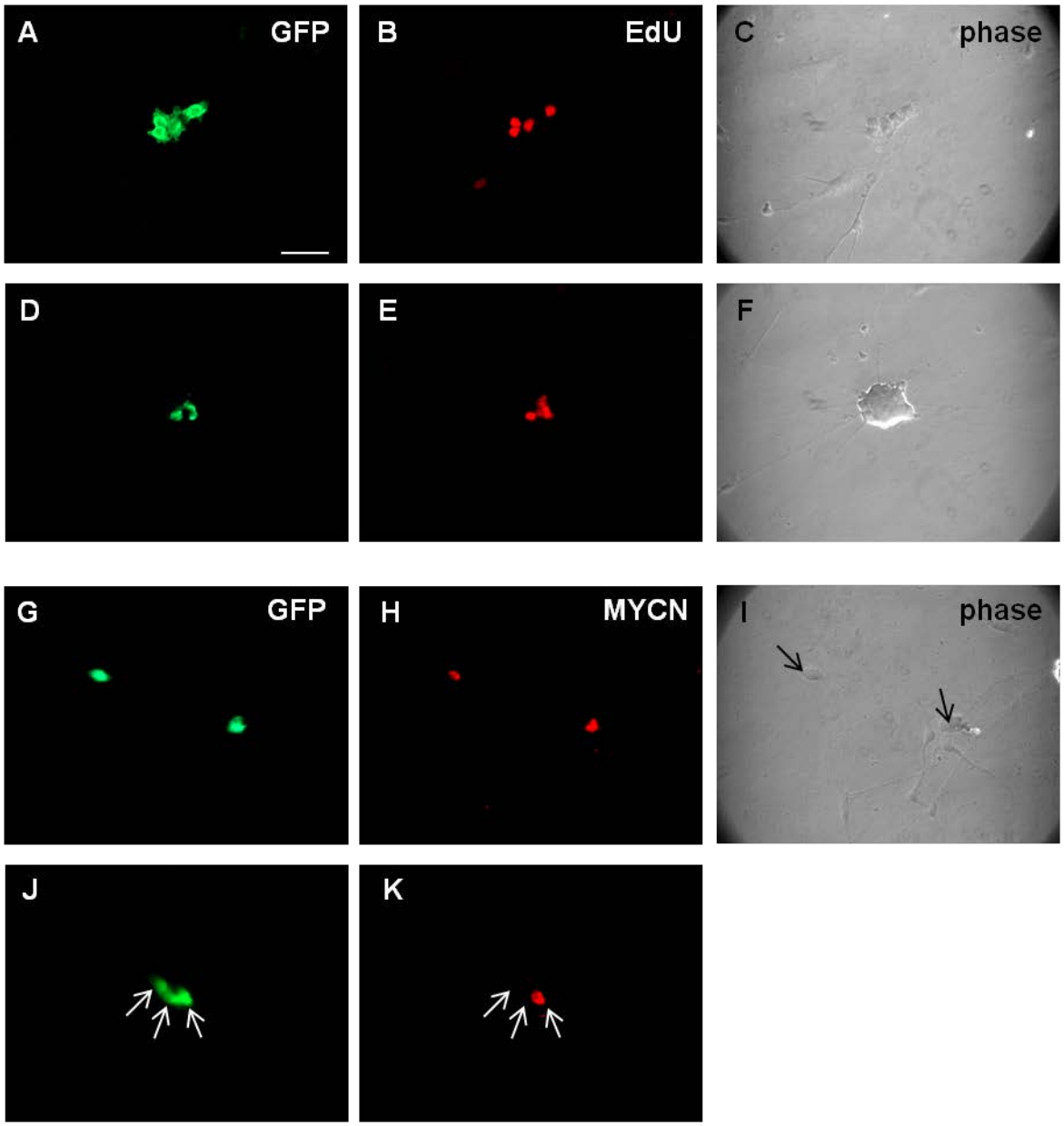

Figure 5.23. E10 chick sympathetic ganglia tissue, containing GFP-labelled Kellys that had been intravenously injected into the E3 embryos, were dissociated into single cells and cultured *in vitro* for 3 days. A-F, Following 48 hours in culture, 5µM EdU was added to the culture medium, then after a further 24 hours, cells were fixed and EdU incorporation detected; G-K, Following 3 days in culture, MYCN protein expression was detected by means of immunofluorescence. Arrows in I,J,K identify the individual Kelly cells. Scale bars 50µm.

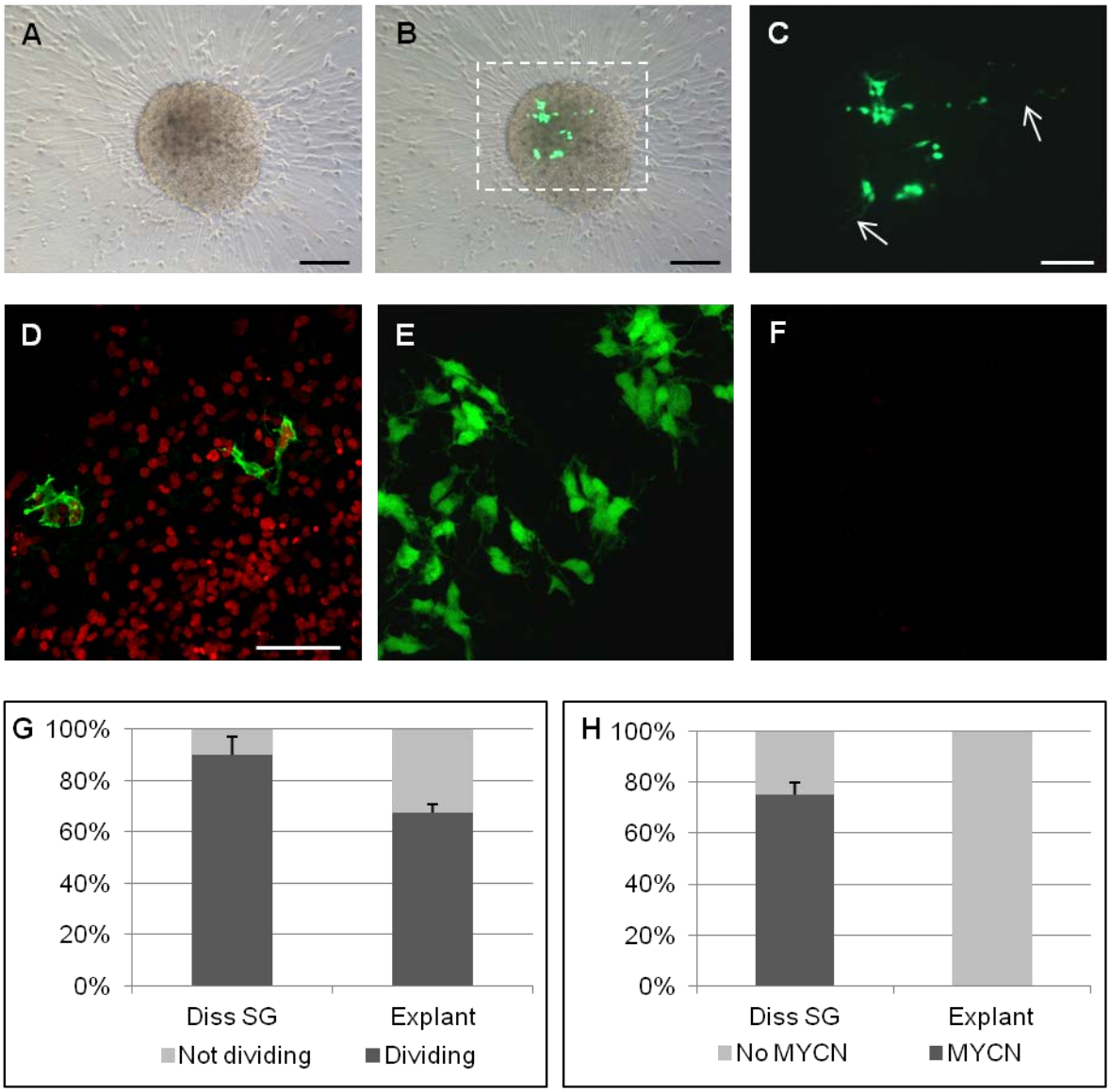

Figure 5.24. E10 chick sympathetic ganglia tissue containing GFP-Kellys (injected intravenously at E3) was explanted; and cultured *in vitro* for 3 days (A, brightfield; B, brightfield and GFP merged image; C, magnification of the GFP-labelled Kellys within the dashed box in B, arrows identify processes extending from Kelly cells). The sympathetic explants were then whole mount stained to detect EdU incorporation (D, green is anti-GFP antibody, red is EdU) and MYCN expression (E, green, GFP Kellys; F, red, lack of MYCN stain in Kellys shown in E). Scale bars A-B, 200µm; C, 100µm; D-F, 50µm. G-H, histograms to show the proportions of cells G, proliferating; H, expressing MYCN; in dissociated versus explanted SG tissue. Error bars show the standard deviations from the mean.

5.4. Discussion

5.4.1. Kelly cells within E14 chick tissues

Following the discovery that Kelly cells were showing reduced proliferation rates and MYCN downregulation in the sympathetic ganglia at E10, cells were allowed to survive in the chick embryos until E14. The distribution of cells was equivalent to that seen at E10, implying a lack of apoptosis of the cells between E10 and E14. The morphological data was consistent with an increased time spent within the various chick microenvironments. The GFP Kellys in the tail and meninges displayed a rounded morphology indistinguishable to that seen at E10, but the cell clumps were considerably larger, which was seemingly indicative of a proliferating population of cells. Indeed, the EdU incorporation revealed that half of the Kelly cells in the tail and meninges had divided in the 24 hours prior to sacrifice; an almost identical result to that attained at E10. MYCN immunofluorescence staining showed that the Kelly population continued to express this oncogenic protein. Thus once the Kellys had located to these two tissues, they appeared to form a somewhat stable population of cells that whether studied at E10 or E14, are consistent in appearance, proliferation rates and continue to express high levels of MYCN protein. These data are reflective of a tumourigenic population of cells.

In contrast, within the SG and ENS Kelly cells extended processes that were often much longer than those observed at E10, suggestive of cells proceeding further along the route of differentiation. Indeed, some of the cells expressed the neuronal protein GAP43. The proliferation data for Kellys in the sympathetic ganglia and gut showed cell division was markedly reduced compared to those cells in the tail and meninges, at 22% in the SG and 28% in the ENS. However surprisingly, proliferation in these two neural tissues was considerably higher than it had been between E9 and E10. The reduction in cell division observed at E10 may have been a temporary cessation due to cell migration, or permanent because of cell differentiation. If the former were true (particularly because Kellys at E10 did not stain for markers of differentiation) the relevant increase at E14 could have been down to Kellys that had finished migrating and re-entered the cell cycle. However, a lack of proliferation in a proportion of cells at E14 will have been permanent because of differentiation. The chick cells within both the sympathetic and gut were still clearly proliferating, therefore Kelly cell proliferation may well have been in keeping with the behaviour of the host environment. In addition, when coupled with the results for MYCN staining, an alternative explanation is possible. The single Kelly cells within the sympathetic ganglia that were completely surrounded by chick ganglion cells continued to display

downregulation of the MYCN protein, but those that were situated within small groups and somewhat shielded from the sympathetic ganglia microenvironment did show re-expression of MYCN. Therefore the increased fraction of proliferating cells may have been due to a proportion of cells upregulating their MYCN expression, resulting in a more aggressively dividing phenotype. However it is equally feasible, possibly more likely, that although none of the Kellys were expressing MYCN at E10, 15% were dividing, and since there were few clusters of cells observed at E10, the appearance of these by E14 suggests the proportion of proliferating cells resulted in the formation of small closely-associated groups of cells. It is therefore possible that following a reduction in contact with the SG environment, MYCN had been re-expressed in the shielded cells. Either way, it seems apparent that particularly at E14, there are two populations of cells within the SG.

5.4.2. SH-EP injections

The SH-EP experiments were completed in order to make a comparison between the MYCN-amplified, highly MYCN-expressing Kellys and the non-MYCN-amplified, non-MYCN-expressing wildtype SH-EPs, and also between the Kellys and the non-MYCN-amplified, yet MYCN-expressing SH-EP-MYCN cells – especially since the MYCN in the latter cells would not be able to be downregulated in response to the SG microenvironment. Since the wildtype SH-EPs were absent from the E10 embryos, even though large numbers of fluorescent cells were seen to be circulating following E3 injection, it was postulated that an initial lack of MYCN expression may have somehow prevented the cells' survival and/or ability to extravasate within the chick embryo. This was made more likely considering that although SK-N-AS cells were found within E10 tissues (work completed by Dr Anne Herrmann, University of Liverpool, UK), they were considerably few in number when compared to the MYCN-expressing Kellys and BE(2)Cs. The SH-EP-MYCN cells, the majority of which expressed relatively high levels of MYCN were therefore expected to behave in a similar way to the Kellys and BE(2)Cs, particularly in terms of location and survival, however it would be intriguing to discover how the constitutive MYCN expression would affect the cells within the SG, particularly in terms of proliferation and differentiation. However, the SH-EP-MYCN cells did not survive within the chick embryos: very few were observed at E7, and these had declined to a negligible number by E10.

The decrease in the proportion of cells expressing detectable levels of MYCN observed between subcloning of the SH-EP-MYCN cells and staining less than 10 passages later,

implies that although expression may be stable, it is definitely variable. The SH-EP-MYCN were not the constitutively highly MYCN-expressing line that had been hoped for.

It may be proposed that the apparent reprogramming of neuroblastoma cells by the chick embryo microevironment may be restricted to MYCN-amplified and/or highly MYCN-expressing cells. Particularly when it is considered that the Kelly and BE(2)C cell lines, both with high MYCN expression, exhibited good survival within the chick embryos, the SH-EP cells with little/no MYCN expression did not survive, and the SK-N-AS cells, with low-medium levels of MYCN, demonstrated limited (a median level of) survival. Alternatively, the lack of SH-EP survival may be a feature of this cell line, or due to an alternate, as yet undetermined, cause. To aid in the answering of this question, it would be useful to inject non-MYCN-amplified, yet highly MYCN-expressing neuroblastoma cell lines, as well as other lines lacking in MYCN expression (invariably non-amplified cells). Video analysis of SK-N-AS cells in the hours following intravenous injection has shown that cells grown in hypoxia (1% oxygen) extravasate much more quickly than those cultured in 21% oxygen (Dr Anne Herrmann, personal communication). It may be the case that lower proportions of cells extravasate from the blood system into body tissues in the less aggressive cells (for example non-MYCN-amplified lines), leading to considerably fewer in chick tissues when dissected at E10.

5.4.3. Primary neuroblastoma cell culture

An additional route of interest would be the injection of neuroblastoma cells derived from primary tumours. Sample size is small, as neuroblastoma is a rare disease, and only 3-4 samples are received on average each year from Alder Hey Children's Hospital. Various culture techniques were used, but considerably more efforts need to be made in characterising the cells before attempts at *in vivo* experimentation can begin. Bone marrow samples would seem to be the most promising in terms of establishing primary lines (Hansford et al. 2007), as the majority of neuroblastoma cell lines originate from bone marrow metastases. However, patient bone marrow samples will not always be positive for neuroblastoma cells, but this is not known at diagnosis. So for some samples – NB23 being one example in which the marrow was subsequently found to be negative for neuroblastoma cells – non-malignant cells, maybe haematopoietic stem/progenitor cells, will have been cultured and frozen. These may be useful as "normal" human control tissue.

Positive staining of neuroblastoma samples with smooth muscle actin antibodies (performed by Dr Dhanya Mullassery, University of Liverpool, UK), may suggest that cancer-associated myofibroblasts (CAMs) have predominantly been cultured. High proportions of CAMs within tumour tissue has been associated with a poor prognosis and increased metastasis in adult cancers such as breast and colon (Nakagawa et al. 2004; Yazhou et al. 2004). In neuroblastoma, the incidence of CAMs has been associated with Schwannian stroma-poor tumours, which generally correlate with a poor clinical outcome, and CAMs may also aid in the process of angiogenesis (Zeine et al. 2009). If, following characterisation of the adherent cultures, it is discovered that mostly CAMs that have been cultured, it may be useful to mix these with neuroblastoma cell lines or neuroblastoma tumour initiating cells (TICs) (received from Prof. David Kaplan, University of Toronto, Canada), both *in vitro* and *in vivo*, to study their (possibly aggressiveness-enhancing) effect.

5.4.4. Dissociation versus explant culture

Following the results from Kelly cells within the E14 sympathetic ganglia, where an increased proportion showed evidence of proliferation and some had re-expressed MYCN, it was necessary to further investigate the importance for the Kelly cells of intimate contact with SG microenvironment for maintenance of a less aggressive phenotype. Kelly-containing tail tissue was used as a control, and whether dissociated or explanted, almost all of the Kelly cells were proliferating and expressing MYCN, regardless of whether they were in close contact with the chick tail cells. For the E10 Kelly-containing sympathetic ganglia, in which MYCN expression had been downregulated, dissociation of the tissue, i.e. reduced/loss of contact between the Kelly cells and the chick SG cells, resulted in increased proliferation and a large proportion of the Kellys expressing detectable levels of MYCN following 3 days in culture. When the tissue was cultured as explants for 3 days, proliferation of the Kellys did increase, albeit to a lesser extent than in the dissociated cells, but this may still have been due to chick SG environmental influence, as the chick cells were dividing much more than had been recorded *in vivo*. No MYCN fluorescence was detected in any of the Kelly cells within the sympathetic explants. Kelly cell clusters the size of those seen at E14 were not observed in the SG explants, therefore all of the cells appeared to have some level of contact with the SG microenvironment. It remains unknown whether the sympathetic ganglia tissue is sufficient to initiate MYCN downregulation, but it appears that it is required for maintenance of this downregulation. A useful *in vitro* system has been established which will henceforth be useful to investigate likely candidate factors responsible for this downregulation.

Chapter Six:

Discussion

6.1. The chick embryo intravenous injection model

The chick embryo as a model organism has been invaluable in its contributions to furthering scientific knowledge in fields such as developmental biology: via gain- and more recently loss-of-function experiments using electroporation (Nakamura et al. 2004); neural crest cell fate maps, developed from imaging of labelled cells, allografts of NCCs from an alternate level, or grafting of exogenous cells, e.g. the creation of quail-chick chimeras (Burns & Le Douarin 2001; Erickson, Tosney & Weston 1980; Ezin, Fraser & Bronner-Fraser 2009); and has offered insights into the development of numerous body structures such as the limbs (Tickle, Summerbell & Wolpert 1975) and brain (Nico et al. 2001). In addition, the chick has had varied applications in the study of disease pathology, particularly tumour cell biology. In cancer research, the chick has aided numerous routes of investigation, including the study of medulloblastoma dissemination (Cage et al. 2012), glioma cell growth and invasion following injection into the brain ventricles (Cretu et al. 2005), and the use of the chorio-allantoic membrane (CAM) on which to grow cells from a variety of tumours such as colon carcinoma, squamous cell carcinoma and neuroblastoma, and analyse the extent of angiogenesis and metastasis (Cimpean, Ribatti & Raica 2008; Mangieri et al. 2009; Ossowski & Reich 1980; Stupack et al. 2006; Subauste et al. 2009). In terms of intravenous cell injection, the chick embryo has been published as a model for metastasis, following the injection of Lewis lung carcinoma cells into the chorio-allantoic vein at E12 (Bobek et al. 2004). However, intravenous injection at such an early time point and with the aim of reducing the tumourigenicity of neuroblastoma cells, such has been developed in this project, had never before been published.

Previous attempts to investigate the influence of an embryonic environment on tumour cells, as detailed in Chapter One, had been performed on malignant melanoma cells (Busch et al. 2008; Busch et al. 2007; Kulesa et al. 2006; Oppitz et al. 2007; Schriek et al. 2005). Although remarkable experiments which demonstrated that tumour cells can respond to an appropriate embryonic microenvironment and transform their behaviour and phenotype accordingly, the localised nature of the injections (into the neural tube or eye cup) meant that a relatively small number of cells could be administered (often less than 2000), and of these, only a small proportion responded to the environmental cues and migrated away from the neural crest. In comparison, the system of intravenous injection of single tumour cells at E3 developed in this project, allows the introduction of a greater number of cells (≥200,000), and although cells were not placed directly into the neural crest migratory pathway, they still targeted neural crest-derived tissues. Hence it was an efficient way of getting a much larger

number of cells into structures of interest (such as the sympathetic ganglia) for further investigation.

6.2. Brief overview of results

When injected intravenously at E3, while neural crest cell migration is still underway, MYCN-amplified neuroblastoma cells appeared to respond to guidance cues along the NC pathways and targeted specifically neural crest-derived tissues. Kelly cells integrated into neural tissues, i.e. the sympathetic ganglia and enteric nervous system within the gut, and showed reduced levels of proliferation compared to those situated within the non-neural tail and meninges – this was the case following analysis at both E10 and E14. In addition, expression of MYCN was downregulated in the SG – in all Kellys at E10 and in those in all-round contact with the ganglion cells at E14. This suggestion of a dependence on close contact with the SG microenvironment for the downregulation of the MYCN oncoprotein was supported by the explants versus dissociation culture experiments. Kelly cells within sympathetic ganglion tissue had undetectable levels of MYCN, whereas those that were dissociated from the tissue, therefore not in intimate contact with SG cells, often began to re-express MYCN. It was clear that the SG environment was critical for the maintenance of MYCN downregulation, however this was undoubtedly a reversible phenomenon, and it could not be determined from the experiments detailed in this project whether the sympathetic ganglia alone would be able to initiate this downregulation.

6.3. Routes of further investigation

The model established in this project provides opportunity to investigate the mechanism(s) by which MYCN is downregulated/controlled – both in normal development and in the Kelly cells – and also the consequences of this downregulation in the Kellys. Consequences would be expected to include alterations in neuroblastoma cell behaviour (potentially proliferation, apoptosis and/or differentiation), and the expression/repression of MYCN target genes.

The targeting of the cells is a fascinating observation, and one that may deserve further investigation – particularly if it is discovered that the sympathetic ganglion environment alone is not sufficient for Kelly cell reprogramming (see section 6.5) and the route of transformation

begins immediately upon experiencing the E3 chick embryo. However, if proven that the chick SG are sufficient for reprogramming, then regardless of how the Kellys reached their targets, what is of prime importance is how and why this reprogramming occurs. The elucidation of the potentially multiple signalling factors involved in the loss of MYCN, and indeed their signalling pathways may provide new therapeutic targets for neuroblastoma treatment. In addition, discovery of whether MYCN is controlled at the transcriptional level would lead to an alternative avenue of investigation: attempting to discover whether all MYCN-amplified neuroblastomas contain the appropriate regulatory sequences that would allow for MYCN transcriptional repression during normal sympathoadrenal development, and hence allow for downregulation following exposure to the appropriate factors in the embryo. Since the Kelly cells in the SG downregulate their MYCN, it is evident that they must retain the regulatory sequences, but it is not known whether this is the case for other cell lines. Even more important is to elucidate what these regulatory sequences are. In a clinical context, being able to control MYCN expression, particularly in MYCN-amplified tumours, is an exciting prospect in terms of novel therapies.

6.4. Consequences of MYCN downregulation

Studying the consequences of MYCN downregulation could provide insight into how the cells respond to this repression, i.e. whether downregulation of MYCN is the key to controlling tumour growth.

MYCN dowregulation has been studied by various groups on neuroblastoma cells *in vitro*. MicroRNAs (miRNAs) have been shown to be able to knock down endogenous MYCN protein levels, with the result of inhibition of proliferation and clonogenic growth in Kellys (Buechner et al. 2011). Short-hairpin RNA (shRNA) can also knock down MYCN expression in cultured MYCN-amplified cell lines following retroviral transmission. As a result of this, Kelly and SK-N-BE(2) cells differentiated into neurons, as judged by their morphology and staining for neurofilament and GAP43, and cell proliferation is also reduced by preventing transition of the cells from G1 to S phase of the cell cycle (Henriksen et al. 2011). The reduction of proliferation and induction of neuronal differentiation are both reflected in the results gained from the chick embryo injection model established in this project. In addition to the phenotypes mentioned above, an increase in apoptosis was observed in MYCN-amplified cells transfected with MYCN-siRNA (Iraci et al. 2011; Nara et al. 2007). Cells also began to express the neurotrophin receptors TrkA and p75, which are associated with a good prognosis in neuroblastoma (Nakagawara et al. 1993; Suzuki et al. 1993).

It has been demonstrated that MYCN directly represses the expression of TrkA and p75 when it forms a complex with Miz1 and SP1 and recruits the histone deacetylase HDAC1 to deacetylate the chromatin at the genes' promoter regions. Subsequent knockdown of MYCN using siRNA resulted in re-expression of the aforementioned neurotrophin receptors (Iraci et al. 2011). In addition, the differentiating agent retinoic acid, which itself has been shown to downregulate MYCN expression, also increases the number of TrkA receptors in LA-N-1 cells (Haskell et al. 1987). The prospect of TrkA and p75 being upregulated in response to the MYCN downregulation in the Kelly cells observed in our chick model is an exciting one, because of the possible consequences of expression of these proteins.

When neuroblastoma cells expressing high levels of TrkA (low stage and 4S) were grown *in vitro* in medium containing NGF, the result was enhanced survival as well as neuronal differentiation, but when these cells were cultured in the absence of NGF, many underwent apoptosis (Brodeur et al. 2009). These results were consistent with the behaviour of normal sympathetic neurons cultured with or without NGF (Oppenheim 1991). Advanced stage tumours with low TrkA expression did not undergo differentiation in response to NGF (Nakagawara & Brodeur 1997). However, in contrast, neuroblastoma cells initially lacking TrkA and p75 but then induced to re-express the receptors by MYCN knockdown, were exposed to NGF and this resulted in mass apoptosis (Iraci et al. 2011). This is supported by work in which MYCN-amplified neuroblastoma cells were induced to express TrkA, and this induced apoptosis by affecting levels of p53, caspase 3 and Bcl-2 (Lavoie et al. 2005). A possible explanation to these opposing behaviours is that the sudden induction of TrkA expression and shock of massively increased NGF detection led to the dramatic cellular response of apoptosis. An alternate explanation could involve the protein CCM2, as this has been shown to mediate TrkA-induced cell death (Harel et al. 2009), so the TrkA-expressing neuroblastoma cells that underwent differentiation in response to NGF may have been lacking CCM2. Whether the Kellys whose MYCN has been knocked down by the chick embryo sympathetic ganglia express CCM2 or not, the possibility of them being induced to express TrkA is exciting, as the prospect of them consequently undergoing either differentiation (as a small number did by E14) or apoptosis – possibly depending on the availability of NGF – are both appealing.

Following on from this project, it would be useful to first establish the response of Kelly cells to MYCN downregulation *in vitro*, which could be achieved by siRNA transfection. Expression of TrkA and p75 would be analysed, and in the event of a positive result, differentiation and apoptosis would be tested for, with and without the addition of NGF.

These data could then be used as a control, against which to compare the behaviour of Kelly cells *in vivo*. Kellys within the SG (whose MYCN has been downregulated) should be tested for TrkA and p75 expression at both E10 and E14, and perhaps in the explanted SG pieces after 3 days in culture. The next question would be, if the cells do express TrkA, do they respond by differentiation or apoptosis? A small proportion of Kellys at E14 have already been shown to express the neuronal protein GAP43, but since a wave of apoptosis of endogenous sympathetic neurons occurs around the time of hatching, likely in response to an abundance of neurotrophins, and for which the low affinity neurotrophin receptor p75 has been implicated (Bamji et al. 1998; Huang & Reichardt 2001), the same may occur in the Kelly cells expressing TrkA and p75.

As well as affecting the expression of neurotrophin receptors, loss of MYCN may result in a reduction of other MYCN targets which had previously contributed to an aggressive phenotype. Such genes may include hTERT (involved in cellular immortalisation), proteins involved in cell cycle progression such as cyclin D2, CDK4 and SKP2, the p53 inhibitor MDM2, Bmi-1 (involved in the self-renewal of cells and contributes to the prevention of apoptosis) and ODC1 (involved in polyamine synthesis) (Bell, Lunec & Tweddle 2007; Cetinkaya et al. 2007; Huang et al. 2011; Knoepfler, Cheng & Eisenman 2002; Lutz et al. 1996; Slack et al. 2005) . MYCN knockdown by siRNA in MYCN-amplified IMR-32 and BE(2)C cells has indeed been shown to modulate the expression of cell cycle related genes: SKP2 levels were reduced, whereas expression of DKK3 (a Wnt antagonist), p53 and TP53INP1 (a p53-inducible protein) increased (Bell, Lunec & Tweddle 2007). Another group have shown that loss of MYCN as a result of shRNA decreased Bmi-1 expression (Huang et al. 2011).

Downregulation of MYCN by antisense RNA constructs has been associated with a decrease in the levels of the Multidrug Resistance associated Protein (MRP) – a protein correlated with poor clinical outcome in neuroblastoma due to its inferred resistance to cytotoxic drugs (Haber et al. 1999; Norris et al. 1996). Therefore a therapeutic agent that effectively targeted MYCN would potentially be beneficial if used in conjunction with chemotherapeutic drugs.

Although the primary long term aim is to discover precisely what reduces MYCN levels in the chick embryo, it is important to assess the response of Kelly cells to a downregulation of MYCN, as this may be an indication of how MYCN-amplified primary neuroblastomas would respond to MYCN-reducing therapy.

6.5. Potential causes of MYCN downregulation

To be able to translate this research into the clinic, it is vital that the factors that prompt downregulation of MYCN in neural tissues are elucidated. In order to attempt this, one must examine genes upstream of MYCN that potentially control either transcription of the oncogene or stabilisation of its mRNA/protein product. Control of MYCN is however extremely complicated.

To begin to narrow down the potential regulators of MYCN expression in the chick embryos, it would first be helpful to answer the question of whether the SG alone can cause downregulation of MYCN. A relatively simple experiment could be performed entailing the dissociation of chick sympathetic ganglia into single cells and mixing with a small proportion (1-5%) GFP-Kelly cells, before culturing as “hanging drops” (Banerjee & Bhonde 2006) to allow close association of the cells. Staining of either frozen sections or whole mount staining of the entire resultant spheres with a MYCN antibody (alongside Kellys cultured in hanging drops with tail tissue as a positive control) may provide an indication of whether sympathetic ganglia alone are sufficient to knock down MYCN expression. If this culture system proves successful, the Kellys could be cultured with embryonic adrenal cells to discover the effect of these on the neuroblastoma cells’ behaviour. In addition, success with this technique would allow for easier analysis of both the consequences and causes of MYCN downregulation. In permitting greater numbers of Kelly cells to be “reprogrammed” (compared to the relatively few in each sympathetic chain in the chick embryos), qPCR could be performed as a more sensitive detection method than immunofluorescence. If, via the hanging drop method, MYCN downregulation was discovered to be a direct consequence of contact with the SG and/or alternative chick tissues, this would go some way to restricting the number of possible instigators of MYCN downregulation. In either case, future experiments should test the addition of activators and inhibitors of signalling pathways implicated in MYCN expression to identify the key pathways involved in our model system.

6.5.1. MYCN gene transcription

During normal embryonic development, MYCN is crucial, particularly for the developing nervous system (both CNS and PNS), lung, gut heart, liver and mesonephros. However, MYCN expression is completely repressed in almost all adult tissues (Stanton et al. 1992). This occurs epigenetically, at the transcriptional level, and this is likely to be the reason

behind the decrease in MYCN protein levels observed in Kelly cells within the chick SG. In MYCN-amplified neuroblastoma cell lines, induced differentiation results in a reduction of MYCN mRNA levels (Thiele, Reynolds & Israel 1985). The results obtained from Kelly cells in the E10 chick sympathetic ganglia reflect those obtained from cell lines *in vitro*, where inhibition of MYCN protein expression in MYCN-amplified LA-N-5 neuroblastoma cells resulted in reduced proliferation alongside a progression towards cellular differentiation (Negroni et al. 1991). In contrast, MYCN overexpression results in increased proliferation and cells being unable to differentiate in response to retinoic acid (Peverali et al. 1996), which could be considered to recapitulate the effects of the MYCN oncogene in highly MYCN-expressing tumours (Nara et al. 2007; Schweigerer et al. 1990).

Although some consideration should be given to proteins involved in activation of MYCN gene expression, such as E2F, SP1 and SP3 (Kramps et al. 2004; Strieder & Lutz 2003), in the context of this work, and considering that inhibition of a single protein with multiple cellular functions is unlikely to have a prolific effect on MYCN, it may be more appropriate to consider what may be actively downregulating the oncogene. Factors known to negatively modulate MYCN expression include BMPs, retinoic acid (RA), nitric oxide (NO) and vasoactive intestinal peptide (VIP), (Alvarez-Rodiguez et al. 2007; Chevrier et al. 2008; Ciani et al. 2004; Thiele, Reynolds & Israel 1985), all of which will have been encountered by the Kelly cells in the chick embryo. Retinoic acid is already used in neuroblastoma therapy as a differentiating agent, which also acts to reduce levels of MYCN in neuroblastoma cell lines (Messi et al. 2008; Thiele, Reynolds & Israel 1985). Using the *in vitro* explants culture system optimised in this project, or if successful, the hanging drop co-culture technique, it will be possible to investigate the effects on MYCN expression and cell behaviour of inhibiting these proteins

Sonic hedgehog (Shh) signalling has been shown to upregulate MYCN expression, with a resultant increase in proliferation in cerebellar granule precursors (Kenney, Cole & Rowitch 2003). BMP2 opposes Shh's activity by preventing MYCN expression via KLF10, with a consequent decrease in proliferation and promotion of differentiation (Alvarez-Rodiguez et al. 2007). The Kellys would have been exposed to BMPs released by the dorsal aorta upon aggregation in the primary sympathetic ganglia at E3.5 in the chick, but are unlikely to have been exposed later in development, therefore MYCN downregulation may have been initiated almost immediately upon sympathoadrenal targeting in the embryos. Nevertheless, a potential role for BMPs could be tested by the addition of a BMP antagonist such as noggin to the in vitro culture systems, to discover whether the subsequent loss of BMPs results in MYCN expression being upregulated.

Nitric oxide reduces proliferation in multiple cell types, including neuroblastoma, without affecting cell viability or apoptosis (Murillo-Carretero et al. 2002). It acts on several signalling pathways by activating transcription factors such as NF-κB and AP-1, which has the consequence of regulating a wide range of genes (Kroncke 2003). NO has been shown to inhibit MYCN expression, in turn reducing proliferation and promoting differentiation (Ciani et al. 2004). NO, as a result of its MYCN downregulation, reduces the levels of those ATP binding cassette (ABC) drug transporters under transcriptional control of MYCN – key proteins involved in chemotherapeutic drug resistance (Porro et al. 2010). It is not clear whether NO affects transcription of the MYCN gene, stability of its mRNA, or results in degradation of the protein. The neuronal form of nitric oxide synthase (nNOS) may be present in the chick SG (Bennett 1994; Domoto et al. 1995; Modin et al. 1994), therefore NO can be considered a candidate factor for MYCN downregulation in the Kellys. It would therefore be interesting to test nNOS inhibitors such as L-NAME in our *in vitro* culture systems (Kelly-containing sympathetic ganglia explants or hanging drops), to discover whether the loss of NO causes re-expression of MYCN. A positive result would go some way to confirming that NO is at least partly responsible for MYCN downregulation in the SG.

The sympathetic ganglia consist of both noradrenergic and cholinergic neurons. The former are characterised by their expression of tyrosine hydroxylase and dopamine-β-hydroxylase, and produce the neurotransmitter noradrenaline. Cholinergic neurons release the neuropeptide VIP, which acts as a vasodilator (Fahrenkrug 1989). Cholinergic neurons develop from noradrenergic sympathetic neurons which lose expression of TH and DBH. In the chick, they begin to express the cholinergic genes ChAT and VAChT from E7, with VIP-positive cells being detected at E10 (Duong, Geissen & Rohrer 2002). VIP induces differentiation of neuroblastoma cells (Pence & Shorter 1990), and also acts to reduce MYCN mRNA and therefore protein levels, particularly in MYCN-amplified cell lines (Chevrier et al. 2008). This effect is potentiated when added to cells in conjunction with RA, following which MYCN target genes SKP2 and TP531NP1 are downregulated (Chevrier et al. 2008). VIP inhibition would determine whether this peptide is contributing to maintenance of MYCN downregulation of Kellys in the sympathetic ganglia. However, its expression from E10 onwards makes it unlikely that VIP is one of the initiators of MYCN downregulation in the Kellys, which already have undetectable levels of MYCN when dissected at E10.

6.5.2. MYCN mRNA stability

It is also possible that the loss of MYCN observed in Kellys is due to mRNA instability. MYCN's mRNA stability is known to be affected by proteins such as MDM2, p53, p73 and HuD, as well as various microRNAs (miRNAs). Stabilisers of MYCN mRNA include MDM2, which increases stability in a p53-independent manner, resulting in an increase of protein translation and an abundance of MYCN in the cell (Gu et al. 2012). HuD, an RNA-binding protein specific to neurons, also stabilises MYCN mRNA, thereby inhibiting its decay (Manohar et al. 2002; Ross et al. 1997), and consequently contributing to neuroblastoma malignancy.

Overexpression of p53 has been shown to reduce MYCN protein levels, and this is proposed to be via destabilisation of the mRNA, which is then directed to the proteosome for degradation (Torres et al. 2010). The p53-related protein p73, despite inducing transcription of MYCN, also negatively regulates mRNA stability, leading to a reduction in protein levels (Horvilleur et al. 2008).

On the opposite strand to MYCN, an antisense gene has been discovered, N-cym, which is highly expressed only in MYCN-amplified cell lines, suggesting co-amplification with MYCN. The N-cym RNA has the potential to regulate the stability of MYCN mRNA (Scott et al. 2003).

MicroRNAs are endogenous short non-coding RNA molecules that bind (imperfectly) to complimentary nucleotide sequences within mRNA gene transcripts, with the consequence of preventing protein translation (Lewis et al. 2003). miR-34a is classed as a tumour suppressor, directly targeting, and preventing translation of MYCN. It has been mapped to chromosome 1p36, a region commonly deleted particularly in MYCN-amplified neuroblastomas, and the loss of miR-34a is likely to contribute to the malignant phenotype (Wei et al. 2008). Several other miRNAs have been identified as targeting MYCN, including miR-34c, -449, -29a, -29b, -29c, -101, -202 and -let-7e. These all reduce levels of MYCN protein when overexpressed in Kelly cells (Buechner et al. 2011). However, it is not known whether endogenous levels of any of the above miRNAs are sufficient to downregulate levels of MYCN protein, although this may be an interesting area for investigation.

6.5.3. MYCN protein stability

MYCN protein degradation as a result of phosphorylation is required for cell cycle exit and differentiation in cerebellar granule neuron precursors (Kenney, Widlund & Rowitch 2004). MYCN protein stability is directly influenced by glycogen synthase kinase 3 β (GSK3β), and indirectly via upstream PI3K/Akt signalling that converges on GSK3β (illustrated in Figure 1.10). Activation of this pro-survival pathway is associated with a poor prognosis in neuroblastoma (Opel et al. 2007).

PI3Ks are a family of lipid kinases that transmit signals from cell surface receptors such as Trks and ALK (Gustafson & Weiss 2010). Activating mutations in ALK, for example, may result in increased PI3K/Akt signal transduction, and therefore increased aggressiveness of neuroblastoma. PI3K phosphorylates PIP2 to PIP3, which allows translocation of both Akt and PDK1 to the plasma membrane, following which Akt is activated by phosphorylation at two distinct sites, by PDK1 and mTOR complex 2 (mTORC2) (Segerstrom et al. 2011). Active Akt then in turn activates mTOR which prevents MYCN S62 dephosphorylation (which may have otherwise been followed by ubiquitination and degradation), and Akt also blocks GSK3β-induced T58 phosphorylation of MYCN, which results in increased stability and transcription of growth-inducing target genes.

The tumour suppressor gene PTEN is able to dephosphorylate PIP3, thereby halting the PI3K/Akt/mTOR signalling cascade (Yin & Shen 2008). PTEN deletion may be expected to result in vastly increased pro-survival signal transmission, hence propagation of various cancers. However deletion of PTEN is rare in neuroblastoma, although inactivation of the gene by hypermethylation is much more common (Hoebeeck et al. 2009). Akt phosphorylation is associated with decreased survival in neuroblastoma, as well as often occurring alongside MYCN amplification (Opel et al. 2007). In addition, it has been shown that activated Akt and mTOR are found in neuroblastoma tumours, but not in normal adrenal medullas (Johnsen et al. 2008). It would be interesting to examine the activity of proteins along this pathway in Kelly cells in culture, compared to those within the E10 sympathetic ganglia with reduced levels of MYCN protein. For example, using an antibody that exclusively detects the phosphorylated Akt protein (pAkt), one may expect to find increased levels in MYCN-expressing Kellys *in vitro* or in the E10 chick tail, but reduced levels in the non-/low-MYCN-expressing cells within the SG.

Control of MYCN protein stability is clearly complex. However, a recent study using PI3K inhibitors reported degradation of MYCN protein resulting in “decreased angiogenesis and

improved survival" in mice with neuroblastoma (Chanthery et al. 2012). This demonstrates the potential of the PI3K/Akt/mTOR pathway as a therapeutic target in neuroblastoma, and suggests this may be an area worthy of further investigation.

Although testing the effects of inhibitors of various proteins along these pathways on the Kelly+SG *in vitro* systems, seems an obvious route of investigation, one would have to dissect the other pathways converging on these proteins, to ensure no adverse effects on fundamental cellular processes that may be assumed to be due to MYCN loss, but in fact because of disruption of vital signalling pathways.

6.6. Identification of MYCN regulatory DNA sequences

The amplified region of the MYCN gene in Kelly cells must contain the regulatory DNA sequences required to downregulate MYCN expression in response to SG environmental cues. Recently, MYCN amplicon sizes and positions were assessed in several MYCN-amplified neuroblastoma cell lines and a number of MYCN-amplified primary tumours (Blumrich et al. 2011). Amplicons ranged from 0.1 to 2.8Mb in size: for the Kellys it is roughly 1Mb (Figure 6.2). Although both the BE(2)C and IMR-32 lines' amplicons overlap with the Kellys', their overlap with each other's is only around 47kb. Therefore it would be useful to inject both of these cell lines at E3 to discover whether either (or both) responds to the sympathetic ganglia microenvironment by downregulation their MYCN expression. It has already been shown in this project that the BE(2)C cells target the same tissues and display the same morphologies as the Kelly cells at E10. However, cell proliferation and most importantly MYCN detection should be carried out on these cells, as well as the IMR-32. The results obtained could potentially narrow the specific region(s) of the MYCN amplicon required to allow cells to downregulate MYCN in response to factors within the SG environment. This region could be narrowed even further with the injection of additional cell lines. Injection of multiple cell lines would also be informative as to whether all/most MYCN amplicons contain the appropriate regulatory sequences to enable them to respond to signals within the embryo and downregulate MYCN.

Figure 6.1. Illustration of MYCN amplicons (blue) in MYCN-amplified neuroblastoma cell lines and primary tumours. Chromosomal gains are represented by red bars, chromosomal losses by green bars, and no change left blank. Attention is drawn to the Kelly cell line by a purple box. Adapted from Blumrich et al. 2011.

Potential repressor sequences may be able to be identified using the information gained from the experiments detailed immediately above, in conjunction with bioinformatics analysis and/or data gained from experiments to determine the cause of MYCN downregulation. A reporter gene, for example the dTomato plasmid, could then be inserted into the Kelly amplicon, placed under control of the proposed regulatory sequence, and tested by intravenous injection at E3 in the hope that in the sympathetic ganglia, tomato fluorescence would disappear along with the MYCN, but in the tail, the red fluorescence is still expressed. This reporter gene analysis could allow the identification of the appropriate enhancer and repressor sequences involved in the control of MYCN expression – in neuroblastoma cells and in embryonic development.

6.7. Concluding remarks

A new model system has been developed, in which MYCN-amplified neuroblastoma cells show neural crest targeting, and once incorporated into the sympathetic ganglia, are reprogrammed to a more benign phenotype. Repression of MYCN observed in the SG may be process involving multiple steps that also requires signals from the neural crest migratory stream, as well as those in the sympathetic ganglia. Factors from the migratory pathway only are likely to be inadequate, as MYCN expression is seen in the Kelly cells within the meninges and tail.

The ultimate aim is to decipher the mechanism(s) of MYCN downregulation, so that this could provide new therapeutic targets to control MYCN expression in MYCN-amplified neuroblastomas. The ideal scenario would be the ability to replicate the developmental

signals (still to be identified) in the chick model and persuade aggressively dividing tumour cells within patients to differentiate or apoptose without harming healthy tissues in the process. This would be a much less destructive treatment than is currently administered with cytotoxic drugs. However, any new druggable targets that can be translated into novel therapeutic agents would be a welcome discovery, for a disease in which despite intensive research, treatment is still failing high risk patients.

References

Adida, C., Berrebi, D., Peuchmaur, M., Reyes-Mugica, M. & Altieri, D.C. (1998a) 'Anti-apoptosis gene, survivin, and prognosis of neuroblastoma', *Lancet*, vol. 351, no. 9106.

Adida, C., Crotty, P.L., McGrath, J., Berrebi, D., Diebold, J. & Altieri, D.C. (1998b) 'Developmentally regulated expression of the novel cancer anti-apoptosis gene survivin in human and mouse differentiation', *American Journal of Pathology*, vol. 152, no. 1.

Aiken, C. (1997) 'Pseudotyping human immunodeficiency virus type 1 (HIV-1) by the glycoprotein of vesicular stomatitis virus targets HIV-1 entry to an endocytic pathway and suppresses both the requirement for Nef and the sensitivity to cyclosporin A', *J Virol*, vol. 71, no. 8, pp. 5871-5877.

Akitaya, T. & Bronnerfraser, M. (1992) 'EXPRESSION OF CELL-ADHESION MOLECULES DURING INITIATION AND CESSATION OF NEURAL CREST CELL-MIGRATION', *Developmental Dynamics*, vol. 194, no. 1, pp. 12-20.

Akudugu, J.M., Binder, A., Serafin, A., Slabbert, J., Giese, A. & Bohm, L. (2004) 'Changes in G1-phase populations in human glioblastoma and neuroblastoma cell lines influence p(66)/Be neutron-induced micronucleus yield', *Life Sciences*, vol. 75, no. 5, pp. 623-632.

Alajez, N.M., Shi, W., Hui, A.B.Y., Yue, S., Ng, R., Lo, K.W., Bastianutto, C., O'Sullivan, B., Gullane, P. & Liu, F.F. (2009) 'Targeted depletion of BMI1 sensitizes tumor cells to P53-mediated apoptosis in response to radiation therapy', *Cell Death and Differentiation*, vol. 16, no. 11, pp. 1469-1479.

Alam, G., Cui, H.J., Shi, H.L., Yang, L.Q., Ding, J., Mao, L., Maltese, W.A. & Ding, H.F. (2009) 'MYCN Promotes the Expansion of Phox2B-Positive Neuronal Progenitors to Drive Neuroblastoma Development', *American Journal of Pathology*, vol. 175, no. 2, pp. 856-866.

Alberts, B., Bray, D., Hopkin, K., Johnson, A., Lewis, J., Raff, M., Roberts, K. & Walter, P. (2010) *Essential Cell Biology*, Third edn, Garland Science, New York.

Alland, L., Muhle, R., Hou, H., Potes, J., Chin, L., SchreiberAgus, N. & DePinho, R.A. (1997) 'Role for N-CoR and histone deacetylase in Sin3-mediated transcriptional repression', *Nature*, vol. 387, no. 6628, pp. 49-55.

Allsopp, T.E. & Moss, D.J. (1989) 'A developmentally regulated chicken neuronal protein associated with the cortical cytoskeleton', *Journal of Neuroscience*, vol. 9, no. 1, pp. 13-24.

Alvarez-Rodiguez, R., Barzi, M., Berenguer, J. & Pons, S. (2007) 'Bone morphogenetic protein 2 opposes Shh-mediated proliferation in cerebellar granule cells through a TIEG-1-based regulation of Nmyc', *Journal of Biological Chemistry*, vol. 282, no. 51.

Andrae, J., Molander, C., Smits, A., Funa, K. & Nister, M. (2002) 'Platelet-derived growth factor-B and -C and active alpha-receptors in medulloblastoma cells', *Biochemical and Biophysical Research Communications*, vol. 296, no. 3.

Aoki, Y., Saint-Germain, N., Gyda, M., Magner-Fink, E., Lee, Y.H., Credidio, C. & Saint-Jeannet, J.P. (2003) 'Sox10 regulates the development of neural crest-derived melanocytes in Xenopus', *Developmental Biology*, vol. 259, no. 1, pp. 19-33.

Ayer, D.E. & Eisenman, R.N. (1993) 'A SWITCH FROM MYC-MAX TO MAD-MAX HETEROCOMPLEXES ACCOMPANIES MONOCYTE/MACROPHAGE DIFFERENTIATION', *Genes & Development*, vol. 7, no. 11.

Azarova, A.M., Gautam, G. & George, R.E. (2011) 'Emerging importance of ALK in neuroblastoma', *Seminars in Cancer Biology*, vol. 21, no. 4, pp. 267-275.

Baba, T., Convery, P.A., Matsumura, N., Whitaker, R.S., Kondoh, E., Perry, T., Huang, Z., Bentley, R.C., Mori, S., Fujii, S., Marks, J.R., Berchuck, A. & Murphy, S.K. (2009) 'Epigenetic regulation of CD133 and tumorigenicity of CD133+ovarian cancer cells', *Oncogene*, vol. 28, no. 2, pp. 209-218.

Baker, C.V.H., BronnerFraser, M., LeDouarin, N.M. & Teillet, M.A. (1997) 'Early-and late-migrating cranial neural crest cell populations have equivalent developmental potential in vivo', *Development*, vol. 124, no. 16.

Bamji, S.X., Majdan, M., Pozniak, C.D., Belliveau, D.J., Aloyz, R., Kohn, J., Causing, C.G. & Miller, F.D. (1998) 'The p75 neurotrophin receptor mediates neuronal apoptosis and is essential for naturally occurring sympathetic neuron death', *Journal of Cell Biology*, vol. 140, no. 4.

Banerjee, M. & Bhonde, R.R. (2006) 'Application of hanging drop technique for stem cell differentiation and cytotoxicity studies', *Cytotechnology*, vol. 51, no. 1.

Barbacid, M. (1994) 'THE TRK FAMILY OF NEUROTROPHIN RECEPTORS', *Journal of Neurobiology*, vol. 25, no. 11, pp. 1386-1403.

Bell, E., Chen, L.D., Liu, T., Marshall, G.M., Lunec, J. & Tweddle, D.A. (2010) 'MYCN oncoprotein targets and their therapeutic potential', *Cancer Letters*, vol. 293, no. 2, pp. 144-157.

Bell, E., Lunec, J. & Tweddle, D.A. (2007) 'Cell cycle regulation targets of MYCN identified by gene expression microarrays', *Cell Cycle*, vol. 6, no. 10, pp. 1249-1256.

Bell, E., Premkumar, R., Carr, J., Lu, X., Lovat, P.E., Kees, U.R., Lunec, J. & Tweddle, D.A. (2006) 'The role of MYCN in the failure of MYCN amplified neuroblastoma cell lines to G(1) arrest after DNA damage', *Cell Cycle*, vol. 5, no. 22.

Bellairs, R. & Osmond, M. (1998) *The Atlas of Chick Development*, Academic Press, London.

Bellmeyer, A., Krase, J., Lindgren, J. & LaBonne, C. (2003) 'The protooncogene c-Myc is an essential regulator of neural crest formation in Xenopus', *Developmental Cell*, vol. 4, no. 6, pp. 827-839.

Bennett, M.R. (1994) 'NITRIC-OXIDE RELEASE AND LONG-TERM POTENTIATION AT SYNAPSES IN AUTONOMIC GANGLIA', *General Pharmacology*, vol. 25, no. 8, pp. 1541-1551.

Berry, T., Luther, W., Bhatnagar, N., Jamin, Y., Poon, E., Sanda, T., Pei, D., Sharma, B., Vetharoy, W.R., Hallsworth, A., Ahmad, Z., Barker, K., Moreau, L., Webber, H., Wang, W., Liu, Q., Perez-Atayde, A., Rodig, S., Cheung, N.-K., Raynaud, F., Hallberg, B., Robinson, S.P., Gray, N.S., Pearson, A.D.J., Eccles, S.A., Chesler, L. & George, R.E. (2012) 'The ALK(F1174L) Mutation Potentiates the Oncogenic Activity of MYCN in Neuroblastoma', *Cancer cell*, vol. 22, no. 1, pp. 117-130.

Berthold, F. & Simon, T. (2005) 'Clinical Presentation', *Neuroblastoma*.

Bhatnagar, S.N. & Sarin, Y.K. (2012) 'Neuroblastoma: A Review of Management and Outcome', *Indian Journal of Pediatrics*, vol. 79, no. 6, pp. 787-792.

Blumrich, A., Zapatka, M., Brueckner, L.M., Zheglo, D., Schwab, M. & Savelyeva, L. (2011) 'The FRA2C common fragile site maps to the borders of MYCN amplicons in neuroblastoma and is associated with gross chromosomal rearrangements in different cancers', *Human Molecular Genetics*, vol. 20, no. 8.

Bobek, V., Plachy, J., Pinterova, D., Kolostova, K., Boubelik, M., Jiang, P., Yang, M. & Hoffman, R.M. (2004) 'Development of a green fluorescent protein metastatic-cancer chick-embryo drug-screen model', *Clinical & Experimental Metastasis*, vol. 21, no. 4.

Bouchard, C., Dittrich, O., Kiermaier, A., Dohmann, K., Menkel, A., Eilers, M. & Luscher, B. (2001) 'Regulation of cyclin D2 gene expression by the Myc/Max/Mad network: Myc-dependent TRRAP recruitment and histone acetylation at the cyclin D2 promoter', *Genes & Development*, vol. 15, no. 16.

Bourdeaut, F., Trochet, D., Janoueix-Lerosey, I., Ribeiro, A., Deville, A., Coz, C., Michiels, J.F., Lyonnet, S., Amiel, J. & Delattre, O. (2005) 'Germline mutations of the paired-like homeobox 2B (PHOX2B) gene in neuroblastoma', *Cancer Letters*, vol. 228, no. 1-2, pp. 51-58.

Breit, S., Ashman, K., Wilting, J., Rossler, J., Hatzi, E., Fotsis, T. & Schweigerer, L. (2000) 'The N-myc oncogene in human neuroblastoma cells: Down-regulation of an angiogenesis inhibitor identified as activin A', *Cancer Research*, vol. 60, no. 16.

Britsch, S., Li, L., Kirchhoff, S., Theuring, F., Brinkmann, V., Birchmeier, C. & Riethmacher, D. (1998) 'The ErbB2 and ErbB3 receptors and their ligand, neuregulin-1, are essential for development of the sympathetic nervous system', *Genes & Development*, vol. 12, no. 12, pp. 1825-1836.

Brodeur, G.M. (1995) 'MOLECULAR-BASIS FOR HETEROGENEITY IN HUMAN NEUROBLASTOMAS', *European Journal of Cancer*, vol. 31A, no. 4.

Brodeur, G.M. (2003) 'Neuroblastoma: Biological insights into a clinical enigma', *Nature Reviews Cancer*, vol. 3, no. 3, pp. 203-216.

Brodeur, G.M., Minturn, J.E., Ho, R., Simpson, A.M., Iyer, R., Varela, C.R., Light, J.E., Kolla, V. & Evans, A.E. (2009) 'Trk Receptor Expression and Inhibition in Neuroblastomas', *Clinical Cancer Research*, vol. 15, no. 10.

Brodeur, G.M. & Nakagawara, A. (1992) 'MOLECULAR-BASIS OF CLINICAL HETEROGENEITY IN NEUROBLASTOMA', *American Journal of Pediatric Hematology Oncology*, vol. 14, no. 2.

Brodeur, G.M., Pritchard, J., Berthold, F., Carlsen, N.L.T., Castel, V., Castleberry, R.P., Debernardi, B., Evans, A.E., Favrot, M., Hedborg, F., Kaneko, M., Kemshead, J., Lampert, F., Lee, R.E.J., Look, A.T., Pearson, A.D.J., Philip, T., Roald, B., Sawada, T., Seeger, R.C., Tsuchida, Y. & Voute, P.A. (1993) 'REVISIONS OF THE INTERNATIONAL CRITERIA FOR NEUROBLASTOMA DIAGNOSIS, STAGING, AND RESPONSE TO TREATMENT', *Journal of Clinical Oncology*, vol. 11, no. 8, pp. 1466-1477.

Brodeur, G.M., Seeger, R.C., Barrett, A., Berthold, F., Castleberry, R.P., Dangio, G., Debernardi, B., Evans, A.E., Favrot, M., Freeman, A.I., Haase, G., Hartmann, O., Hayes, F.A., Helson, L., Kemshead, J., Lampert, F., Ninane, J., Ohkawa, H., Philip, T., Pinkerton,

C.R., Pritchard, J., Sawada, T., Siegel, S., Smith, E.I., Tsuchida, Y. & Voute, P.A. (1988) 'INTERNATIONAL CRITERIA FOR DIAGNOSIS, STAGING, AND RESPONSE TO TREATMENT IN PATIENTS WITH NEURO-BLASTOMA', *Journal of Clinical Oncology*, vol. 6, no. 12, pp. 1874-1881.

Buechner, J., Tomte, E., Haug, B.H., Henriksen, J.R., Lokke, C., Flaegstad, T. & Einvik, C. (2011) 'Tumour-suppressor microRNAs let-7 and mir-101 target the proto-oncogene MYCN and inhibit cell proliferation in MYCN-amplified neuroblastoma', *British Journal of Cancer*, vol. 105, no. 2.

Burns, A.J. & Le Douarin, N.M. (1998) 'The sacral neural crest contributes neurons and glia to the post-umbilical gut: spatiotemporal analysis of the development of the enteric nervous system', *Development*, vol. 125, no. 21.

Burns, A.J. & Le Douarin, N.M. (2001) 'Enteric nervous system development: Analysis of the selective developmental potentialities of vagal and sacral neural crest cells using quail-chick chimeras', *Anatomical Record*, vol. 262, no. 1, pp. 16-28.

Burstyn-Cohen, T., Stanleigh, J., Sela-Donenfeld, D. & Kalcheim, C. (2004) 'Canonical Wnt activity regulates trunk neural crest delamination linking BMP/noggin signaling with G1/S transition', *Development*, vol. 131, no. 21.

Busch, C., Drews, U., Eisele, S.R., Garbe, C. & Oppitz, M. (2008) 'Noggin blocks invasive growth of murine B16-F1 melanoma cells in the optic cup of the chick embryo', *International Journal of Cancer*, vol. 122, no. 3, pp. 526-533.

Busch, C., Drews, U., Garbe, C., Eisele, S.R. & Oppitz, M. (2007) 'Neural crest cell migration of mouse B16-F1 melanoma cells transplanted into the chick embryo is inhibited by the BMP-antagonist noggin', *International Journal of Oncology*, vol. 31, no. 6, pp. 1367-1378.

Busch, C., Oppitz, M., Sailer, M.H., Just, L., Metzger, M. & Drews, U. (2006) 'BMP-2-dependent integration of adult mouse subventricular stem cells into the neural crest of chick and quail embryos', *Journal of Cell Science*, vol. 119, no. 21, pp. 4467-4474.

Butler, H. & Juurlink, B.H.J. (1987) *An atlas for staging mammalian and chick embryos*, CRC Press Inc., Florida.

Cage, T.A., Louie, J.D., Liu, S.R., Alvarez-Buylla, A., Gupta, N. & Hyer, J. (2012) 'Distinct patterns of human medulloblastoma dissemination in the developing chick embryo nervous system', *Clinical & Experimental Metastasis*, vol. 29, no. 4, pp. 371-380.

Calao, M., Sekyere, E.O., Cui, H.J., Cheung, B.B., Thomas, W.D., Keating, J., Chen, J.B., Raif, A., Jankowski, K., Davies, N.P., Bekkum, M.V., Chen, B., Tan, O., Ellis, T., Norris, M.D., Haber, M., Kim, E.S., Shohet, J.M., Trahair, T.N., Liu, T., Wainwright, B.J., Ding, H.F. & Marshall, G.M. (2012) Direct effects of Bmi1 on p53 protein stability inactivates oncoprotein stress responses in embryonal cancer precursor cells at tumor initiation, *Oncogene*, vol., [Online]. Available from: (Accessed.

Caren, H., Erichsen, J., Olsson, L., Enerback, C., Sjoberg, R.-M., Abrahamsson, J., Kogner, P. & Martinsson, T. (2008) 'High-resolution array copy number analyses for detection of deletion, gain, amplification and copy-neutral LOH in primary neuroblastoma tumors: Four cases of homozygous deletions of the CDKN2A gene', *Bmc Genomics*, vol. 9.

Caren, H., Kryh, H., Nethander, M., Sjoberg, R.-M., Trager, C., Nilsson, S., Abrahamsson, J., Kogner, P. & Martinsson, T. (2010) 'High-risk neuroblastoma tumors with 11q-deletion

display a poor prognostic, chromosome instability phenotype with later onset', *Proceedings of the National Academy of Sciences of the United States of America*, vol. 107, no. 9, pp. 4323-4328.

Carpenter, E.L. & Mosse, Y.P. (2012) 'Targeting ALK in neuroblastoma-preclinical and clinical advancements', *Nature reviews. Clinical oncology*, vol. 9, no. 7, pp. 391-399.

Castel, V., Segura, V. & Canete, A. (2010) 'Treatment of high-risk neuroblastoma with anti-GD2 antibodies', *Clinical & Translational Oncology*, vol. 12, no. 12, pp. 788-793.

Castleberry, R.P. (1997) 'Neuroblastoma', *European Journal of Cancer*, vol. 33, no. 9, pp. 1430-1437.

Cetinkaya, C., Hultquist, A., Su, Y., Wu, S., Bahram, F., Pahlman, S., Guzhova, I. & Larsson, L.-G. (2007) 'Combined IFN-gamma and retinoic acid treatment targets the N-Myc/Max/Mad1 network resulting in repression of N-Myc target genes in MYCN-amplified neuroblastoma cells', *Molecular Cancer Therapeutics*, vol. 6, no. 10.

Chanthery, Y.H., Gustafson, W.C., Itsara, M., Persson, A., Hackett, C.S., Grimmer, M., Charron, E., Yakovenko, S., Kim, G., Matthay, K.K. & Weiss, W.A. (2012) 'Paracrine Signaling Through MYCN Enhances Tumor-Vascular Interactions in Neuroblastoma', *Science Translational Medicine*, vol. 4, no. 115, p. 10.

Chatoo, W., Abdouh, M., David, J., Champagne, M.P., Ferreira, J., Rodier, F. & Bernier, G. (2009) 'The Polycomb Group Gene Bmi1 Regulates Antioxidant Defenses in Neurons by Repressing p53 Pro-Oxidant Activity', *Journal of Neuroscience*, vol. 29, no. 2, pp. 529-542.

Chen, L.D., Iraci, N., Gherardi, S., Gamble, L.D., Wood, K.M., Perini, G., Lunec, J. & Tweddle, D.A. (2010) 'p53 Is a Direct Transcriptional Target of MYCN in Neuroblastoma', *Cancer Research*, vol. 70, no. 4, pp. 1377-1388.

Chesler, L., Schlieve, C., Goldenberg, D.D., Kenney, A., Kim, G., McMillan, A., Matthay, K.K., Rowitch, D. & Weiss, W.A. (2006) 'Inhibition of phosphatidylinositol 3-kinase destabilizes Mycn protein and blocks malignant progression in neuroblastoma', *Cancer Research*, vol. 66, no. 16, pp. 8139-8146.

Cheung, M., Chaboissier, M.C., Mynett, A., Hirst, E., Schedl, A. & Briscoe, J. (2005) 'The transcriptional control of trunk neural crest induction, survival, and delamination', *Developmental Cell*, vol. 8, no. 2, pp. 179-192.

Chevrier, L., Meunier, A.C., Cochaud, S., Muller, J.M. & Chadeneau, C. (2008) 'Vasoactive intestinal peptide decreases MYCN expression and synergizes with retinoic acid in a human MYCN-amplified neuroblastoma cell line', *International Journal of Oncology*, vol. 33, no. 5, pp. 1081-1089.

Chin, L., Schreiberagus, N., Pellicer, I., Chen, K., Lee, H.W., Dudast, M., Cordoncardo, C. & Depinho, R.A. (1995) 'CONTRASTING ROLES FOR MYC AND MAD PROTEINS IN CELLULAR GROWTH AND DIFFERENTIATION', *Proceedings of the National Academy of Sciences of the United States of America*, vol. 92, no. 18.

Ciani, E., Severi, S., Contestabile, A. & Bartesaghi, R. (2004) 'Nitric oxide negatively regulates proliferation and promotes neuronal differentiation through N-Myc downregulation', *Journal of Cell Science*, vol. 117, no. 20.

Cimpean, A.M., Ribatti, D. & Raica, M. (2008) 'The chick embryo chorioallantoic membrane as a model to study tumor metastasis', *Angiogenesis*, vol. 11, no. 4, pp. 311-319.

Cohn, S.L., Pearson, A.D.J., London, W.B., Monclair, T., Ambros, P.F., Brodeur, G.M., Faldum, A., Hero, B., Iehara, T., Machin, D., Mosseri, V., Simon, T., Garaventa, A., Castel, V. & Matthay, K.K. (2009) 'The International Neuroblastoma Risk Group (INRG) Classification System: An INRG Task Force Report', *Journal of Clinical Oncology*, vol. 27, no. 2, pp. 289-297.

Cohn, S.L. & Tweddle, D.A. (2004) 'MYCN amplification remains prognostically strong 20 years after its "clinical debut"', *European Journal of Cancer*, vol. 40, no. 18, pp. 2639-2642.

Corbeil, D., Roper, K., Hellwig, A., Tavian, M., Miraglia, S., Watt, S.M., Simmons, P.J., Peault, B., Buck, D.W. & Huttner, W.B. (2000) 'The human AC133 hematopoietic stem cell antigen is also expressed in epithelial cells and targeted to plasma membrane protrusions', *Journal of Biological Chemistry*, vol. 275, no. 8.

Corvi, R., Amler, L.C., Savelyeva, L., Gehring, M. & Schwab, M. (1994) 'MYCN IS RETAINED IN SINGLE-COPY AT CHROMOSOME-2 BAND-P23-24 DURING AMPLIFICATION IN HUMAN NEUROBLASTOMA-CELLS', *Proceedings of the National Academy of Sciences of the United States of America*, vol. 91, no. 12, pp. 5523-5527.

Couly, G.F. & Ledouarin, N.M. (1987) 'MAPPING OF THE EARLY NEURAL PRIMORDIUM IN QUAIL CHICK CHIMERAS .2. THE PROSENCEPHALIC NEURAL PLATE AND NEURAL FOLDS - IMPLICATIONS FOR THE GENESIS OF CEPHALIC HUMAN CONGENITAL-ABNORMALITIES', *Developmental Biology*, vol. 120, no. 1.

Cretu, A., Fotos, J.S., Little, B.W. & Galileo, D.S. (2005) 'Human and rat glioma growth, invasion, and vascularization in a novel chick embryo brain tumor model', *Clinical & Experimental Metastasis*, vol. 22, no. 3, pp. 225-236.

Cui, H.J., Hu, B., Li, T., Ma, J., Alam, G., Gunning, W.T. & Ding, H.F. (2007) 'Bmi-1 is essential for the tumorigenicity of neuroblastoma cells', *American Journal of Pathology*, vol. 170, no. 4, pp. 1370-1378.

De, A., Lewis, X.Z. & Gambhir, S.S. (2003) 'Noninvasive imaging of lentiviral-mediated reporter gene expression in living mice', *Molecular Therapy*, vol. 7, no. 5, pp. 681-691.

De Bernardi, B., Nicolas, B., Boni, L., Indolfi, P., Carli, M., di Montezemolo, L.C., Donfrancesco, A., Pession, A., Provenzi, M., di Cataldo, A., Rizzo, A., Tonini, G.P., Dallorso, S., Conte, M., Gambini, C., Garaventa, A., Bonetti, F., Zanazzo, A., D'Angelo, P. & Bruzzi, P. (2003) 'Disseminated neuroblastoma in children older than one year at diagnosis: Comparable results with three consecutive high-dose protocols adopted by the Italian Co-Operative Group for Neuroblastoma', *Journal of Clinical Oncology*, vol. 21, no. 8, pp. 1592-1601.

Delannet, M. & Duband, J.L. (1992) 'TRANSFORMING GROWTH-FACTOR-BETA CONTROL OF CELL-SUBSTRATUM ADHESION DURING AVIAN NEURAL CREST CELL EMIGRATION INVITRO', *Development*, vol. 116, no. 1, pp. 275-287.

Demaison, C., Parsley, K., Brouns, G., Scherr, M., Battmer, K., Kinnon, C., Grez, M. & Thrasher, A.J. (2002) 'High-level transduction and gene expression in hematopoietic repopulating cells using a human immunodeficiency [correction of imunodeficiency] virus type 1-based lentiviral vector containing an internal spleen focus forming virus promoter', *Hum Gene Ther*, vol. 13, no. 7, pp. 803-813.

Diez-Torre, A., Andrade, R., Eguizabal, C., Lopez, E., Arluzea, J., Silio, M. & Arechaga, J. (2009) 'Reprogramming of melanoma cells by embryonic microenvironments', *International Journal of Developmental Biology*, vol. 53, no. 8-10, pp. 1563-1568.

Domoto, T., Teramoto, M., Tanigawa, K., Tamura, K. & Yasui, Y. (1995) 'ORIGINS OF NERVE-FIBERS CONTAINING NITRIC-OXIDE SYNTHASE IN THE RAT CELIAC-SUPERIOR MESENTERIC GANGLION', *Cell and Tissue Research*, vol. 281, no. 2, pp. 215-221.

Duband, J.-L. (2000) *Neural Crest Delamination and Migration: Integrating Regulations of Cell Interactions, Locomotion, Survival and Fate*, Duband, J.-L., Madame Curie Bioscience Database [Online], Available from: http://www.ncbi.nlm.nih.gov/books/NBK6397/ (Accessed).

Duong, C.V., Geissen, M. & Rohrer, H. (2002) 'The developmental expression of vasoactive intestinal peptide (VIP) in cholinergic sympathetic neurons depends on cytokines signaling through LIFR beta-containing receptors', *Development*, vol. 129, no. 6.

Eilers, M. & Eisenman, R.N. (2008) 'Myc's broad reach', *Genes & Development*, vol. 22, no. 20, pp. 2755-2766.

Engler, S., Thiel, C., Forster, K., David, K., Bredehorst, R. & Juhl, H. (2001) 'A novel metastatic animal model reflecting the clinical appearance of human neuroblastoma: Growth arrest of orthotopic tumors by natural, cytotoxic human immunoglobulin M antibodies', *Cancer Research*, vol. 61, no. 7, pp. 2968-2973.

Erickson, C.A., Duong, T.D. & Tosney, K.W. (1992) 'DESCRIPTIVE AND EXPERIMENTAL-ANALYSIS OF THE DISPERSION OF NEURAL CREST CELLS ALONG THE DORSOLATERAL PATH AND THEIR ENTRY INTO ECTODERM IN THE CHICK-EMBRYO', *Developmental Biology*, vol. 151, no. 1.

Erickson, C.A. & Goins, T.L. (1995) 'AVIAN NEURAL CREST CELLS CAN MIGRATE IN THE DORSOLATERAL PATH ONLY IF THEY ARE SPECIFIED AS MELANOCYTES', *Development*, vol. 121, no. 3, pp. 915-924.

Erickson, C.A. & Perris, R. (1993) 'THE ROLE OF CELL-CELL AND CELL-MATRIX INTERACTIONS IN THE MORPHOGENESIS OF THE NEURAL CREST', *Developmental Biology*, vol. 159, no. 1, pp. 60-74.

Erickson, C.A., Tosney, K.W. & Weston, J.A. (1980) 'ANALYSIS OF MIGRATORY BEHAVIOR OF NEURAL CREST AND FIBROBLASTIC CELLS IN EMBRYONIC-TISSUES', *Developmental Biology*, vol. 77, no. 1, pp. 142-156.

Evans, A.E., Dangio, G.J. & Randolph, J. (1971) 'PROPOSED STAGING FOR CHILDREN WITH NEUROBLASTOMA - CHILDRENS CANCER STUDY GROUP-A', *Cancer*, vol. 27, no. 2, pp. 374-&.

Ezin, A.M., Fraser, S.E. & Bronner-Fraser, M. (2009) 'Fate map and morphogenesis of presumptive neural crest and dorsal neural tube', *Developmental Biology*, vol. 330, no. 2, pp. 221-236.

Fagan, A.M., Zhang, H., Landis, S., Smeyne, R.J., SilosSantiago, I. & Barbacid, M. (1996) 'TrkA, but not TrkC, receptors are essential for survival of sympathetic neurons in vivo', *Journal of Neuroscience*, vol. 16, no. 19, pp. 6208-6218.

Fahrenkrug, J. (1989) 'VIP AND AUTONOMIC NEUROTRANSMISSION', *Pharmacology & Therapeutics*, vol. 41, no. 3, pp. 515-534.

Farrell, M., Waldo, K., Li, Y.X. & Kirby, M.L. (1999) 'A novel role for cardiac neural crest in heart development', *Trends in Cardiovascular Medicine*, vol. 9, no. 7, pp. 214-220.

Fichtner, I., Lemm, M., Becker, M. & Berthold, F. (1997) 'Effects of amifostine (WR-2721, ethyol) on tumor growth and pharmacology of cytotoxic drugs in human xenotransplanted neuroblastomas', *Anti-Cancer Drugs*, vol. 8, no. 2, pp. 174-181.

Fiddler, T.A., Smith, L., Tapscott, S.J. & Thayer, M.J. (1996) 'Amplification of MDM2 inhibits MyoD-mediated myogenesis', *Molecular and Cellular Biology*, vol. 16, no. 9, pp. 5048-5057.

Fukata, M. & Kaibuchi, K. (2001) 'Rho-family GTPases in cadherin-mediated cell-cell adhesion', *Nature Reviews Molecular Cell Biology*, vol. 2, no. 12.

Fukuzawa, M., Sugiura, H., Koshinaga, T., Ikeda, T., Hagiwara, N. & Sawada, T. (2002) 'Expression of vascular endothelial growth factor and its receptor Flk-1 in human neuroblastoma using in situ hybridization', *Journal of Pediatric Surgery*, vol. 37, no. 12, pp. 1747-1750.

Gammill, L.S., Gonzalez, C., Gu, C.H. & Bronner-Fraser, M. (2006) 'Guidance of trunk neural crest migration requires neuropilin 2/semaphorin 3F signaling', *Development*, vol. 133, no. 1, pp. 99-106.

Ganguli, G. & Wasylyk, B. (2003) 'p53-independent functions of MDM2', *Molecular Cancer Research*, vol. 1, no. 14, pp. 1027-1035.

Gaze, M.N., Hamilton, T.G. & Mairs, R.J. (1994) 'PHARMACOKINETICS AND EFFICACY OF I-131 METAIODOBENZYLGUANIDINE IN 2 NEUROBLASTOMA XENOGRAFTS', *British Journal of Radiology*, vol. 67, no. 798.

George, R.E., Sanda, T., Hanna, M., Frohling, S., Luther, W., II, Zhang, J., Ahn, Y., Zhou, W., London, W.B., McGrady, P., Xue, L., Zozulya, S., Gregor, V.E., Webb, T.R., Gray, N.S., Gilliland, D.G., Diller, L., Greulich, H., Morris, S.W., Meyerson, M. & Look, A.T. (2008) 'Activating mutations in ALK provide a therapeutic target in neuroblastoma', *Nature*, vol. 455, no. 7215, pp. 975-978.

Gestblom, C., Grynfeld, A., Ora, I., Ortoft, E., Larsson, C., Axelson, H., Sandstedt, B., Cserjesi, P., Olson, E.N. & Pahlman, S. (1999) 'The basic helix-loop-helix transcription factor dHAND, a marker gene for the developing human sympathetic nervous system, is expressed in both high- and low-stage neuroblastomas', *Laboratory Investigation*, vol. 79, no. 1, pp. 67-79.

Grandori, C., Cowley, S.M., James, L.P. & Eisenman, R.N. (2000) 'The Myc/Max/Mad network and the transcriptional control of cell behavior', *Annual Review of Cell and Developmental Biology*, vol. 16.

Gu, L., Zhang, H., He, J., Li, J., Huang, M. & Zhou, M. (2012) 'MDM2 regulates MYCN mRNA stabilization and translation in human neuroblastoma cells', *Oncogene*, vol. 31, no. 11, pp. 1342-1353.

Gustafson, W.C. & Weiss, W.A. (2010) 'Myc proteins as therapeutic targets', *Oncogene*, vol. 29, no. 9, pp. 1249-1259.

Haber, M., Bordow, S.B., Gilbert, J., Madafiglio, J., Kavallaris, M., Marshall, G.M., Mechetner, E.B., Fruehauf, J.P., Tee, L., Cohn, S.L., Salwen, H., Schmidt, M.L. & Norris, M.D. (1999) 'Altered expression of the MYCN oncogene modulates MRP gene expression and response to cytotoxic drugs in neuroblastoma cells', *Oncogene*, vol. 18, no. 17, pp. 2777-2782.

Haldi, M., Ton, C., Seng, W.L. & McGrath, P. (2006) 'Human melanoma cells transplanted into zebrafish proliferate, migrate, produce melanin, form masses and stimulate angiogenesis in zebrafish', *Angiogenesis*, vol. 9, no. 3, pp. 139-151.

Hall, B.K. & Ekanayake, S. (1991) 'Effects of growth factors on the differentiation of neural crest cells and neural crest cell-derivatives', *The International journal of developmental biology*, vol. 35, no. 4, pp. 367-387.

Hansford, L.M., McKee, A.E., Zhang, L.B., George, R.E., Gerstle, J.T., Thorner, P.S., Smith, K.M., Look, A.T., Yeger, H., Miller, F.D., Irwin, M.S., Thiele, C.J. & Kaplan, D.R. (2007) 'Neuroblastoma cells isolated from bone marrow metastases contain a naturally enriched tumor-initiating cell', *Cancer Research*, vol. 67, no. 23, pp. 11234-11243.

Harel, L., Costa, B., Tcherpakov, M., Zapatka, M., Oberthuer, A., Hansford, L.M., Vojvodic, M., Levy, Z., Chen, Z.Y., Lee, F.S., Avigad, S., Yaniv, I., Shi, L.M., Eils, R., Fischer, M., Brors, B., Kaplan, D.R. & Fainzilber, M. (2009) 'CCM2 Mediates Death Signaling by the TrkA Receptor Tyrosine Kinase', *Neuron*, vol. 63, no. 5, pp. 585-591.

Haskell, B.E., Stach, R.W., Werrbach-Perez, K. & Perez-Polo, J.R. (1987) 'Effect of retinoic acid on nerve growth factor receptors', *Cell and tissue research*, vol. 247, no. 1.

Hatzi, E., Breit, S., Zoephel, A., Ashman, K., Tontsch, U., Ahorn, H., Murphy, C., Schweigerer, L. & Fotsis, T. (2000) 'MYCN oncogene and angiogenesis: Down-regulation of endothelial growth inhibitors in human neuroblastoma cells - Purification, structural, and functional characterization', *Angiogenesis: from the Molecular to Integrative Pharmacology*, vol. 476.

Hatzi, E., Murphy, C., Zoephel, A., Ahorn, H., Tontsch, U., Bamberger, A.M., Yamauchi-Takihara, K., Schweigerer, L. & Fotsis, T. (2002) 'N-myc oncogene overexpression down-regulates leukemia inhibitory factor in neuroblastoma', *European Journal of Biochemistry*, vol. 269, no. 15.

Henion, P.D. & Weston, J.A. (1997) 'Timing and pattern of cell fate restrictions in the neural crest lineage', *Development*, vol. 124, no. 21, pp. 4351-4359.

Henriksen, J.R., Haug, B.H., Buechner, J., Tomte, E., Lokke, C., Flaegstad, T. & Einvik, C. (2011) 'Conditional expression of retrovirally delivered anti-MYCN shRNA as an in vitro model system to study neuronal differentiation in MYCN-amplified neuroblastoma', *Bmc Developmental Biology*, vol. 11.

Henriksson, M. & Luscher, B. (1996) 'Proteins of the Myc network: Essential regulators of cell growth and differentiation', *Advances in Cancer Research, Vol 68*, vol. 68.

Hirsch, M.R., Tiveron, M.C., Guillemot, F., Brunet, J.F. & Goridis, C. (1998) 'Control of noradrenergic differentiation and Phox2a expression by MASH1 in the central and peripheral nervous system', *Development*, vol. 125, no. 4, pp. 599-608.

Hiyama, E., Hiyama, K., Yokoyama, T., Matsuura, Y., Piatyszek, M.A. & Shay, J.W. (1995) 'CORRELATING TELOMERASE ACTIVITY LEVELS WITH HUMAN NEUROBLASTOMA OUTCOMES', *Nature Medicine*, vol. 1, no. 3, pp. 249-255.

Hoebeeck, J., Michels, E., Pattyn, F., Combaret, V., Vermeulen, J., Yigit, N., Hoyoux, C., Laureys, G., De Paepe, A., Spelernan, F. & Vandesompele, J. (2009) 'Aberrant methylation of candidate tumor suppressor genes in neuroblastoma', *Cancer Letters*, vol. 273, no. 2, pp. 336-346.

Hoehner, J.C., Gestblom, C., Hedborg, F., Sandstedt, B., Olsen, L. & Pahlman, S. (1996) 'A developmental model of neuroblastoma: Differentiating stroma-poor tumors' progress along an extra-adrenal chromaffin lineage', *Laboratory Investigation*, vol. 75, no. 5, pp. 659-675.

Hoffman, W.H., Biade, S., Zilfou, J.T., Chen, J.D. & Murphy, M. (2002) 'Transcriptional repression of the anti-apoptotic survivin gene by wild type p53', *Journal of Biological Chemistry*, vol. 277, no. 5, pp. 3247-3257.

Hogarty, M.D., Norris, M.D., Davis, K., Liu, X., Evageliou, N.F., Hayes, C.S., Pawel, B., Guo, R., Zhao, H., Sekyere, E., Keating, J., Thomas, W., Cheng, N.C., Murray, J., Smith, J., Sutton, R., Venn, N., London, W.B., Buxton, A., Gilmour, S.K., Marshall, G.M. & Haber, M. (2008) 'ODC1 Is a Critical Determinant of MYCN Oncogenesis and a Therapeutic Target in Neuroblastoma', *Cancer Research*, vol. 68, no. 23.

Horvilleur, E., Bauer, M., Goldschneider, D., Mergui, X., de la Motte, A., Benard, J., Douc-Rasy, S. & Cappellen, D. (2008) 'p73 alpha isoforms drive opposite transcriptional and post-transcriptional regulation of MYCN expression in neuroblastoma cells', *Nucleic Acids Research*, vol. 36, no. 13, pp. 4222-4232.

Hosoi, G., Hara, J., Okamura, T., Osugi, Y., Ishihara, S., Fukuzawa, M., Okada, A., Okada, S. & Tawa, A. (1994) 'LOW-FREQUENCY OF THE P53 GENE-MUTATIONS IN NEUROBLASTOMA', *Cancer*, vol. 73, no. 12.

Huang, E.J. & Reichardt, L.F. (2001) 'Neurotrophins: Roles in neuronal development and function', *Annual Review of Neuroscience*, vol. 24, pp. 677-736.

Huang, R., Cheung, N.-K.V., Vider, J., Cheung, I.Y., Gerald, W.L., Tickoo, S.K., Holland, E.C. & Blasberg, R.G. (2011) 'MYCN and MYC regulate tumor proliferation and tumorigenesis directly through BMI1 in human neuroblastomas', *Faseb Journal*, vol. 25, no. 12.

Huber, K. (2006) 'The sympathoadrenal cell lineage: Specification, diversification, and new perspectives', *Developmental Biology*, vol. 298, no. 2, pp. 335-343.

Huber, K., Kalcheim, C. & Unsicker, K. (2009) 'The development of the chromaffin cell lineage from the neural crest', *Autonomic Neuroscience Basic & Clinical*, vol. 151, no. 1, Sp. Iss. SI, pp. 10-16.

Hurlin, P.J., Queva, C. & Eisenman, R.N. (1997) 'Mnt, a novel Max-interacting protein is coexpressed with Myc in proliferating, rating cells and mediates repression at Myc binding sites', *Genes & Development*, vol. 11, no. 1.

Ikegaki, N., Bukovsky, J. & Kennett, R.H. (1986) 'IDENTIFICATION AND CHARACTERIZATION OF THE NMYC GENE-PRODUCT IN HUMAN NEUROBLASTOMA-CELLS BY MONOCLONAL-ANTIBODIES WITH DEFINED SPECIFICITIES', *Proceedings of*

the National Academy of Sciences of the United States of America, vol. 83, no. 16, pp. 5929-5933.

Iraci, N., Diolaiti, D., Papa, A., Porro, A., Valli, E., Gherardi, S., Herold, S., Eilers, M., Bernardoni, R., Della Valle, G. & Perini, G. (2011) 'A SP1/MIZ1/MYCN Repression Complex Recruits HDAC1 at the TRKA and p75NTR Promoters and Affects Neuroblastoma Malignancy by Inhibiting the Cell Response to NGF', *Cancer Research*, vol. 71, no. 2, pp. 404-412.

Iwahara, T., Fujimoto, J., Wen, D.Z., Cupples, R., Bucay, N., Arakawa, T., Mori, S., Ratzkin, B. & Yamamoto, T. (1997) 'Molecular characterization of ALK, a receptor tyrosine kinase expressed specifically in the nervous system', *Oncogene*, vol. 14, no. 4, pp. 439-449.

Jellinger, K. (1978) 'GLIOBLASTOMA MULTIFORME - MORPHOLOGY AND BIOLOGY', *Acta Neurochirurgica*, vol. 42, no. 1-2.

Jessen, K.R. & Mirsky, R. (2005) 'The origin and development of glial cells in peripheral nerves', *Nature Reviews Neuroscience*, vol. 6, no. 9, pp. 671-682.

Jiang, X.B., Rowitch, D.H., Soriano, P., McMahon, A.P. & Sucov, H.M. (2000) 'Fate of the mammalian cardiac neural crest', *Development*, vol. 127, no. 8, pp. 1607-1616.

Johnsen, J.I., Segerstrom, L., Orrego, A., Elfman, L., Henriksson, M., Kagedal, B., Eksborg, S., Sveinbjornsson, B. & Kogner, P. (2008) 'Inhibitors of mammalian target of rapamycin downregulate MYCN protein expression and inhibit neuroblastoma growth in vitro and in vivo', *Oncogene*, vol. 27, no. 20, pp. 2910-2922.

Johnston, M.C., Noden, D.M., Hazelton, R.D., Coulombre, J.L. & Coulombre, A.J. (1979) 'ORIGINS OF AVIAN OCULAR AND PERIOCULAR TISSUES', *Experimental Eye Research*, vol. 29, no. 1, pp. 27-43.

Kalluri, R. & Zeisberg, M. (2006) 'Fibroblasts in cancer', *Nature Reviews Cancer*, vol. 6, no. 5.

Kang, J., Rychahou, P.G., Ishola, T.A., Mourot, J.M., Evers, B.M. & Chung, D.H. (2008) 'N-myc is a novel regulator of PI3K-mediated VEGF expression in neuroblastoma', *Oncogene*, vol. 27, no. 28, pp. 3999-4007.

Kapur, R.P. (2000) 'Colonization of the murine hindgut by sacral crest-derived neural precursors: Experimental support for an evolutionarily conserved model', *Developmental Biology*, vol. 227, no. 1, pp. 146-155.

Kasemeier-Kulesa, J.C., Bradley, R., Pasquale, E.B., Lefcort, F. & Kulesa, P.M. (2006) 'Eph/ephrins and N-cadherin coordinate to control the pattern of sympathetic ganglia', *Development*, vol. 133, no. 24, pp. 4839-4847.

Kee, Y. & Bronner-Fraser, M. (2005) 'To proliferate or to die: role of Id3 in cell cycle progression and survival of neural crest progenitors', *Genes & Development*, vol. 19, no. 6.

Kenney, A.M., Cole, M.D. & Rowitch, D.H. (2003) 'Nmyc upregulation by sonic hedgehog signaling promotes proliferation in developing cerebellar granule neuron precursors', *Development*, vol. 130, no. 1, pp. 15-28.

Kenney, A.M., Widlund, H.R. & Rowitch, D.H. (2004) 'Hedgehog and PI-3 kinase signaling converge on Nmyc1 to promote cell cycle progression in cerebellar neuronal precursors', *Development*, vol. 131, no. 1.

Kerr, J.F.R., Wyllie, A.H. & Currie, A.R. (1972) 'APOPTOSIS - BASIC BIOLOGICAL PHENOMENON WITH WIDE-RANGING IMPLICATIONS IN TISSUE KINETICS', *British Journal of Cancer*, vol. 26, no. 4, pp. 239-&.

Kitamura, K., Takiguchihayashi, K., Sezaki, M., Yamamoto, H. & Takeuchi, T. (1992) 'AVIAN NEURAL CREST CELLS EXPRESS A MELANOGENIC TRAIT DURING EARLY MIGRATION FROM THE NEURAL-TUBE - OBSERVATIONS WITH THE NEW MONOCLONAL-ANTIBODY, MEBL-1', *Development*, vol. 114, no. 2, pp. 367-378.

Knoepfler, P.S., Cheng, P.F. & Eisenman, R.N. (2002) 'N-myc is essential during neurogenesis for the rapid expansion of progenitor cell populations and the inhibition of neuronal differentiation', *Genes & Development*, vol. 16, no. 20.

Kogner, P., Barbany, G., Dominici, C., Castello, M.A., Raschella, G. & Persson, H. (1993) 'COEXPRESSION OF MESSENGER-RNA FOR TRK PROTOONCOGENE AND LOW-AFFINITY NERVE GROWTH-FACTOR RECEPTOR IN NEUROBLASTOMA WITH FAVORABLE PROGNOSIS', *Cancer Research*, vol. 53, no. 9, pp. 2044-2050.

Koizumi, H., Hamano, S., Doi, M., Tatsunami, S., Nakada, K., Shinagawa, T. & Tadokoro, M. (2006) 'Increased occurrence of caspase-dependent apoptosis in unfavorable neuroblastomas', *American Journal of Surgical Pathology*, vol. 30, no. 2.

Korshunov, A., Remke, M., Kool, M., Hielscher, T., Northcott, P.A., Williamson, D., Pfaff, E., Witt, H., Jones, D.T.W., Ryzhova, M., Cho, Y.J., Wittmann, A., Benner, A., Weiss, W.A., von Deimling, A., Scheurlen, W., Kulozik, A.E., Clifford, S.C., Collins, V.P., Westermann, F., Taylor, M.D., Lichter, P. & Pfister, S.M. (2012) 'Biological and clinical heterogeneity of MYCN-amplified medulloblastoma', *Acta Neuropathologica*, vol. 123, no. 4, pp. 515-527.

Kramps, C., Strieder, V., Sapetschnig, A., Suske, G. & Lutz, W. (2004) 'E2F and Sp1/Sp3 synergize but are not sufficient to activate the MYCN gene in neuroblastomas', *Journal of Biological Chemistry*, vol. 279, no. 7, pp. 5110-5117.

Krams, M., Hero, B., Berthold, F., Parwaresch, R., Harms, D. & Rudolph, P. (2003) 'Full-length telomerase reverse transcriptase messenger RNA is an independent prognostic factor in neuroblastoma', *American Journal of Pathology*, vol. 162, no. 3.

Kroncke, K.D. (2003) 'Nitrosative stress and transcription', *Biological Chemistry*, vol. 384, no. 10-11, pp. 1365-1377.

Krull, C.E., Lansford, R., Gale, N.W., Collazo, A., Marcelle, C., Yancopoulos, G.D., Fraser, S.E. & BronnerFraser, M. (1997) 'Interactions of Eph-related receptors and ligands confer rostrocaudal pattern to trunk neural crest migration', *Current Biology*, vol. 7, no. 8, pp. 571-580.

Kulesa, P.M. & Gammill, L.S. (2010) 'Neural crest migration: Patterns, phases and signals', *Developmental Biology*, vol. 344, no. 2, pp. 566-568.

Kulesa, P.M., Kasemeier-Kulesa, J.C., Teddy, J.M., Margaryan, N.V., Seftor, E.A., Seftor, R.E.B. & Hendrix, M.J.C. (2006) 'Reprogramming metastatic melanoma cells to assume a neural crest cell-like phenotype in an embryonic microenvironment', *Proceedings of the*

National Academy of Sciences of the United States of America, vol. 103, no. 10, pp. 3752-3757.

LaBonne, C. & Bronner-Fraser, M. (1998a) 'Induction and patterning of the neural crest, a stem cell-like precursor population', *Journal of Neurobiology*, vol. 36, no. 2, pp. 175-189.

LaBonne, C. & Bronner-Fraser, M. (1998b) 'Neural crest induction in Xenopus: evidence for a two-signal model', *Development*, vol. 125, no. 13, pp. 2403-2414.

Lallier, T.E. & Bronnerfraser, M. (1988) 'A SPATIAL AND TEMPORAL ANALYSIS OF DORSAL-ROOT AND SYMPATHETIC-GANGLION FORMATION IN THE AVIAN EMBRYO', *Developmental Biology*, vol. 127, no. 1, pp. 99-112.

Langley, K. & Grant, N.J. (1999) 'Molecular markers of sympathoadrenal cells', *Cell and Tissue Research*, vol. 298, no. 2.

Larsson, L.-G. & Henriksson, M.A. (2010) 'The Yin and Yang functions of the Myc oncoprotein in cancer development and as targets for therapy', *Experimental Cell Research*, vol. 316, no. 8, pp. 1429-1437.

Larsson, L.G., Pettersson, M., Oberg, F., Nilsson, K. & Luscher, B. (1994) 'EXPRESSION OF MAD, MXI1, MAX AND C-MYC DURING INDUCED-DIFFERENTIATION OF HEMATOPOIETIC-CELLS - OPPOSITE REGULATION OF MAD AND C-MYC', *Oncogene*, vol. 9, no. 4.

Lasorella, A., Boldrini, R., Dominici, C., Donfrancesco, A., Yokota, Y., Inserra, A. & Iavarone, A. (2002) 'Id2 is critical for cellular proliferation and is the oncogenic effector of N-Myc in human neuroblastoma', *Cancer Research*, vol. 62, no. 1.

Lavoie, J.F., LeSauteur, L., Kohn, J., Wong, J., Furtoss, O., Thiele, C.J., Miller, F.D. & Kaplan, D.R. (2005) 'TrkA induces apoptosis of neuroblastoma cells and does so via a p53-dependent mechanism', *Journal of Biological Chemistry*, vol. 280, no. 32, pp. 29199-29207.

Le Douarin, N.M. (1982) *The Neural Crest*, Cambridge University Press, Cambridge.

Lee, L.M.J., Seftor, E.A., Bonde, G., Cornell, R.A. & Hendrix, M.J.C. (2005) 'The fate of human malignant melanoma cells transplanted into zebrafish embryos: Assessment of migration and cell division in the absence of tumor formation', *Developmental Dynamics*, vol. 233, no. 4, pp. 1560-1570.

Lewis, B.P., Shih, I.H., Jones-Rhoades, M.W., Bartel, D.P. & Burge, C.B. (2003) 'Prediction of mammalian microRNA targets', *Cell*, vol. 115, no. 7, pp. 787-798.

Li, J. & Kretzner, L. (2003) 'The growth-inhibitory Ndrg1 gene is a Myc negative target in human neuroblastomas and other cell types with overexpressed N- or c-myc', *Molecular and Cellular Biochemistry*, vol. 250, no. 1-2, pp. 91-105.

Lim, K.C., Lakshmanan, G., Crawford, S.E., Gu, Y., Grosveld, F. & Engel, J.D. (2000) 'Gata3 loss leads to embryonic lethality due to noradrenaline deficiency of the sympathetic nervous system', *Nature Genetics*, vol. 25, no. 2, pp. 209-212.

Longo, L., Borghini, S., Schena, F., Parodi, S., Albino, D., Bachetti, T., Da Prato, L., Truini, M., Gambini, C., Tonini, G.P., Ceccherini, I. & Perri, P. (2008) 'PHOX2A and PHOX2B genes are highly co-expressed in human neuroblastoma', *International Journal of Oncology*, vol. 33, no. 5, pp. 985-991.

Lutz, W., Stohr, M., Schurmann, J., Wenzel, A., Lohr, A. & Schwab, M. (1996) 'Conditional expression of N-myc in human neuroblastoma cells increases expression of alpha-prothymosin and ornithine decarboxylase and accelerates progression into S-phase early after mitogenic stimulation of quiescent cells', *Oncogene*, vol. 13, no. 4, pp. 803-812.

Mains, R.E. & Patterso.Ph (1973) 'PRIMARY CULTURES OF DISSOCIATED SYMPATHETIC NEURONS .1. ESTABLISHMENT OF LONG-TERM GROWTH IN CULTURE AND STUDIES OF DIFFERENTIATED PROPERTIES', *Journal of Cell Biology*, vol. 59, no. 2, pp. 329-345.

Mangieri, D., Nico, B., Coluccia, A.M.L., Vacca, A., Ponzoni, M. & Ribatti, D. (2009) 'An alternative in vivo system for testing angiogenic potential of human neuroblastoma cells', *Cancer Letters*, vol. 277, no. 2, pp. 199-204.

Manohar, C.F., Short, M.L., Nguyen, A., Nguyen, N.N., Chagnovich, D., Yang, Q.W. & Cohn, S.L. (2002) 'HuD, a neuronal-specific RNA-binding protein, increases the in vivo stability of MYCN RNA', *Journal of Biological Chemistry*, vol. 277, no. 3, pp. 1967-1973.

Maris, J.M., Hogarty, M.D., Bagatell, R. & Cohn, S.L. (2007) 'Neuroblastoma', *Lancet*, vol. 369, no. 9579.

Maris, J.M., Kyemba, S.M., Rebbeck, T.R., White, P.S., Sulman, E.P., Jensen, S.J., Allen, C., Biegel, J.A. & Brodeur, G.M. (1997) 'Molecular genetic analysis of familial neuroblastoma', *European Journal of Cancer*, vol. 33, no. 12, pp. 1923-1928.

Maris, J.M., Weiss, M.J., Guo, C., Gerbing, R.B., Stram, D.O., White, P.S., Hogarty, M.D., Sulman, E.P., Thompson, P.M., Lukens, J.N., Matthay, K.K., Seeger, R.C. & Brodeur, G.M. (2000) 'Loss of heterozygosity at 1p36 independently predicts for disease progression but not decreased overall survival probability in neuroblastoma patients: A Children's Cancer Group study', *Journal of Clinical Oncology*, vol. 18, no. 9.

Massari, M.E. & Murre, C. (2000) 'Helix-loop-helix proteins: Regulators of transcription in eucaryotic organisms', *Molecular and Cellular Biology*, vol. 20, no. 2.

Matthay, K.K. (1997) 'Neuroblastoma: biology and therapy', *Oncology (Williston Park, N.Y.)*, vol. 11, no. 12, pp. 1857-1866; discussion 1869-1872, 1875.

McLennan, R. & Krull, C.E. (2002) 'Ephrin-As cooperate with EphA4 to promote trunk neural crest migration', *Gene Expression*, vol. 10, no. 5-6.

McMahon, S.B., Wood, M.A. & Cole, M.D. (2000) 'The essential cofactor TRRAP recruits the histone acetyltransferase hGCN5 to c-Myc', *Molecular and Cellular Biology*, vol. 20, no. 2.

Mertens, F., Johansson, B., Hoglund, M. & Mitelman, F. (1997) 'Chromosomal imbalance maps of malignant solid tumors: A cytogenetic survey of 3185 neoplasms', *Cancer Research*, vol. 57, no. 13.

Messi, E., Florian, M.C., Caccia, C., Zanisi, M. & Maggi, R. (2008) 'Retinoic acid reduces human neuroblastoma cell migration and invasiveness: effects on DCX, LISI, neurofilaments-68 and vimentin expression', *Bmc Cancer*, vol. 8, p. 12.

Meulemans, D. & Bronner-Fraser, M. (2004) 'Gene-regulatory interactions in neural crest evolution and development', *Developmental Cell*, vol. 7, no. 3, pp. 291-299.

Mintz, B. & Illmensee, K. (1975) 'NORMAL GENETICALLY MOSAIC MICE PRODUCED FROM MALIGNANT TERATOCARCINOMA CELLS', *Proceedings of the National Academy of Sciences of the United States of America*, vol. 72, no. 9, pp. 3585-3589.

Mizuseki, K., Kishi, M., Matsui, M., Nakanishi, S. & Sasai, Y. (1998) 'Xenopus Zic-related-1 and Sox-2, two factors induced by chordin, have distinct activities in the initiation of neural induction', *Development*, vol. 125, no. 4, pp. 579-587.

Modin, A., Weitzberg, E., Hokfelt, T. & Lundberg, J.M. (1994) 'NITRIC-OXIDE SYNTHASE IN THE PIG AUTONOMIC NERVOUS-SYSTEM IN RELATION TO THE INFLUENCE OF N-G-NITRO-L-ARGININE ON SYMPATHETIC AND PARASYMPATHETIC VASCULAR CONTROL IN-VIVO', *Neuroscience*, vol. 62, no. 1, pp. 189-203.

Molenaar, J.J., Ebus, M.E., Koster, J., Santo, E., Geerts, D., Versteeg, R. & Caron, H.N. (2010) 'Cyclin D1 is a direct transcriptional target of GATA3 in neuroblastoma tumor cells', *Oncogene*, vol. 29, no. 18, pp. 2739-2745.

Molofsky, A.V., Pardal, R., Iwashita, T., Park, I.K., Clarke, M.F. & Morrison, S.J. (2003) 'Bmi-1 dependence distinguishes neural stem cell self-renewal from progenitor proliferation', *Nature*, vol. 425, no. 6961.

Moore, K.L. & Persaud, T.V.N. (2003) *Before We Are Born: Essentials of Embryology and Birth Defects*, Sixth edn, Saunders, Pennsylvania.

Morales, A.V., Barbas, J.A. & Nieto, M.A. (2005) 'How to become neural crest: From segregation to delamination', *Seminars in Cell & Developmental Biology*, vol. 16, no. 6, pp. 655-662.

Moriguchi, T., Takako, N., Hamada, M., Maeda, A., Fujioka, Y., Kuroha, T., Huber, R.E., Hasegawa, S.L., Rao, A., Yamamoto, M., Takahashi, S., Lim, K.C. & Engel, J.D. (2006) 'Gata3 participates in a complex transcriptional feedback network to regulate sympathoadrenal differentiation', *Development*, vol. 133, no. 19, pp. 3871-3881.

Morin, X., Cremer, H., Hirsch, M.R., Kapur, R.P., Goridis, C. & Brunet, J.F. (1997) 'Defects in sensory and autonomic ganglia and absence of locus coeruleus in mice deficient for the homeobox gene Phox2a', *Neuron*, vol. 18, no. 3.

Mosse, Y.P., Laudenslager, M., Longo, L., Cole, K.A., Wood, A., Attiyeh, E.F., Laquaglia, M.J., Sennett, R., Lynch, J.E., Perri, P., Laureys, G., Speleman, F., Kim, C., Hou, C., Hakonarson, H., Torkamani, A., Schork, N.J., Brodeur, G.M., Tonini, G.P., Rappaport, E., Devoto, M. & Maris, J.M. (2008) 'Identification of ALK as a major familial neuroblastoma predisposition gene', *Nature*, vol. 455, no. 7215, pp. 930-U922.

Mourali, J., Benard, A., Lourenco, F.C., Monnet, C., Greenland, C., Moog-Lutz, C., Racaud-Sultan, C., Gonzalez-Dunia, D., Vigny, M., Mehlen, P., Delsol, G. & Allouche, M. (2006) 'Anaplastic lymphoma kinase is a dependence receptor whose proapoptotic functions are activated by caspase cleavage', *Molecular and Cellular Biology*, vol. 26, no. 16, pp. 6209-6222.

Mullassery, D. (2011) *Neuroblastoma: Understanding current treatments and investigating novel strategies*, University of Liverpool, UK.

Murillo-Carretero, M., Ruano, M.J., Matarredona, E.R., Villalobo, A. & Estrada, C. (2002) 'Antiproliferative effect of nitric oxide on epidermal growth factor-responsive human neuroblastoma cells', *Journal of Neurochemistry*, vol. 83, no. 1, pp. 119-131.

Murphy, D.M., Buckley, P.G., Bryan, K., Das, S., Alcock, L., Foley, N.H., Prenter, S., Bray, I., Watters, K.M., Higgins, D. & Stallings, R.L. (2009) 'Global MYCN Transcription Factor Binding Analysis in Neuroblastoma Reveals Association with Distinct E-Box Motifs and Regions of DNA Hypermethylation', *Plos One*, vol. 4, no. 12.

Muth, D., Ghazaryan, S., Eckerle, I., Beckett, E., Poehler, C., Batzler, J., Beisel, C., Gogolin, S., Fischer, M., Henrich, K.-O., Ehemann, V., Gillespie, P., Schwab, M. & Westermann, F. (2010) 'Transcriptional Repression of SKP2 Is Impaired in MYCN-Amplified Neuroblastoma', *Cancer Research*, vol. 70, no. 9, pp. 3791-3802.

Nakagawa, H., Liyanarachchi, S., Davuluri, R.V., Auer, H., Martin, E.W., de la Chapelle, A. & Frankel, W.L. (2004) 'Role of cancer-associated stromal fibroblasts in metastatic colon cancer to the liver and their expression profiles', *Oncogene*, vol. 23, no. 44, pp. 7366-7377.

Nakagawa, S. & Takeichi, M. (1995) 'NEURAL CREST CELL-CELL ADHESION CONTROLLED BY SEQUENTIAL AND SUBPOPULATION-SPECIFIC EXPRESSION OF NOVEL CADHERINS', *Development*, vol. 121, no. 5.

Nakagawara, A. (1998) 'Molecular basis of spontaneous regression of neuroblastoma: role of neurotrophic signals and genetic abnormalities', *Human cell*, vol. 11, no. 3, pp. 115-124.

Nakagawara, A. (2005) 'Molecular and Developmental Biology of Neuroblastoma', *Neuroblastoma*.

Nakagawara, A., Arimanakagawara, M., Scavarda, N.J., Azar, C.G., Cantor, A.B. & Brodeur, G.M. (1993) 'ASSOCIATION BETWEEN HIGH-LEVELS OF EXPRESSION OF THE TRK GENE AND FAVORABLE OUTCOME IN HUMAN NEUROBLASTOMA', *New England Journal of Medicine*, vol. 328, no. 12, pp. 847-854.

Nakagawara, A. & Brodeur, G.M. (1997) 'Role of neurotrophins and their receptors in human neuroblastomas: a primary culture study', *European Journal of Cancer*, vol. 33, no. 12, pp. 2050-2053.

Nakamura, H., Katahira, T., Sato, T., Watanabe, Y. & Funahashi, J. (2004) 'Gain- and loss-of-function in chick embryos by electroporation', *Mechanisms of Development*, vol. 121, no. 9, pp. 1137-1143.

Nara, K., Kusafuka, T., Yoneda, A., Oue, T., Sangkhathat, S. & Fukuzawa, M. (2007) 'Silencing of MYCN by RNA interference induces growth inhibition, apoptotic activity and cell differentiation in a neuroblastoma cell line with MYCN amplification', *International Journal of Oncology*, vol. 30, no. 5.

Negroni, A., Scarpa, S., Romeo, A., Ferrari, S., Modesti, A. & Raschella, G. (1991) 'DECREASE OF PROLIFERATION RATE AND INDUCTION OF DIFFERENTIATION BY A MYCN ANTISENSE DNA OLIGOMER IN A HUMAN NEUROBLASTOMA CELL-LINE', *Cell Growth & Differentiation*, vol. 2, no. 10.

Nickerson, H.J., Matthay, K.K., Seeger, R.C., Brodeur, G.M., Shimada, H., Perez, C., Atkinson, J.B., Selch, M., Gerbing, R.B., Stram, D.O. & Lukens, J. (2000) 'Favorable biology and outcome of stage IV-S neuroblastoma with supportive care or minimal therapy: A Children's Cancer Group study', *Journal of Clinical Oncology*, vol. 18, no. 3, pp. 477-486.

Nico, B., Frigeri, A., Nicchia, G.P., Quondamatteo, F., Herken, R., Errede, M., Ribatti, D., Svelto, M. & Roncali, L. (2001) 'Role of aquaporin-4 water channel in the development and integrity of the blood-brain barrier', *Journal of Cell Science*, vol. 114, no. 7.

Nikiforov, M.A., Popov, N., Kotenko, I., Henriksson, M. & Cole, M.D. (2003) 'The Mad and Myc basic domains are functionally equivalent', *Journal of Biological Chemistry*, vol. 278, no. 13, pp. 11094-11099.

Norris, M.D., Bordow, S.B., Marshall, G.M., Haber, P.S., Cohn, S.L. & Haber, M. (1996) 'Expression of the gene for multidrug-resistance-associated protein and outcome in patients with neuroblastoma', *New England Journal of Medicine*, vol. 334, no. 4, pp. 231-238.

Opel, D., Poremba, C., Simon, T., Debatin, K.M. & Fulda, S. (2007) 'Activation of Akt predicts poor outcome in neuroblastoma', *Cancer Research*, vol. 67, no. 2, pp. 735-745.

Oppenheim, R.W. (1991) 'CELL-DEATH DURING DEVELOPMENT OF THE NERVOUS-SYSTEM', *Annual Review of Neuroscience*, vol. 14, pp. 453-501.

Oppitz, M., Busch, C., Schriek, G., Metzger, M., Just, L. & Drews, U. (2007) 'Non-malignant migration of B16 mouse melanoma cells in the neural crest and invasive growth in the eye cup of the chick embryo', *Melanoma Research*, vol. 17, no. 1, pp. 17-30.

Ossowski, L. & Reich, E. (1980) 'EXPERIMENTAL-MODEL FOR QUANTITATIVE STUDY OF METASTASIS', *Cancer Research*, vol. 40, no. 7, pp. 2300-2309.

Otto, T., Horn, S., Brockmann, M., Eilers, U., Schuttrumpf, L., Popov, N., Kenney, A.M., Schulte, J.H., Beijersbergen, R., Christiansen, H., Berwanger, B. & Eilers, M. (2009) 'Stabilization of N-Myc Is a Critical Function of Aurora A in Human Neuroblastoma', *Cancer Cell*, vol. 15, no. 1, pp. 67-78.

Pahlman, S. & Hoehner, J.C. (1996) 'Neurotrophin receptors, tumor progression and tumor maturation', *Molecular Medicine Today*, vol. 2, no. 10, pp. 432-438.

Pahlman, S., Stockhausen, M.T., Fredlund, E. & Axelson, H. (2004) 'Notch signaling in neuroblastoma', *Seminars in Cancer Biology*, vol. 14, no. 5, pp. 365-373.

Park, J.R., Eggert, A. & Caron, H. (2008) 'Neuroblastoma: Biology, prognosis, and treatment', *Pediatric Clinics of North America*, vol. 55, no. 1, pp. 97-+.

Pattyn, A., Morin, X., Cremer, H., Goridis, C. & Brunet, J.F. (1999) 'The homeobox gene Phox2b is essential for the development of autonomic neural crest derivatives', *Nature*, vol. 399, no. 6734, pp. 366-370.

Pence, J.C. & Shorter, N.A. (1990) 'INVITRO DIFFERENTIATION OF HUMAN NEUROBLASTOMA-CELLS CAUSED BY VASOACTIVE-INTESTINAL-PEPTIDE', *Cancer Research*, vol. 50, no. 16.

Perri, P., Bachetti, T., Longo, L., Matera, I., Seri, M., Tonini, G.P. & Ceccherini, I. (2005) 'PHOX2B mutations and genetic predisposition to neuroblastoma', *Oncogene*, vol. 24, no. 18, pp. 3050-3053.

Peverali, F.A., Orioli, D., Tonon, L., Ciana, P., Bunone, G., Negri, M. & DellaValle, G. (1996) 'Retinoic acid-induced growth arrest and differentiation of neuroblastoma cells are counteracted by N-myc and enhanced by max overexpressions', *Oncogene*, vol. 12, no. 2, pp. 457-462.

Pierce, G.B., Pantazis, C.G., Caldwell, J.E. & Wells, R.S. (1982) 'SPECIFICITY OF THE CONTROL OF TUMOR-FORMATION BY THE BLASTOCYST', *Cancer Research*, vol. 42, no. 3, pp. 1082-1087.

Pina-Oviedo, S., Urbanska, K., Radhakrishnan, S., Sweet, T., Reiss, K., Khalili, K. & Del Valle, L. (2007) 'Effects of JC virus infection on anti-apoptotic protein survivin in progressive multifocal leukoencephalopathy', *American Journal of Pathology*, vol. 170, no. 4.

Porro, A., Chrochemore, C., Cambuli, F., Iraci, N., Contestabile, A. & Perini, G. (2010) 'Nitric Oxide Control of MYCN Expression and Multi Drug Resistance Genes in Tumours of Neural Origin', *Current Pharmaceutical Design*, vol. 16, no. 4, pp. 431-439.

Postovit, L.-M., Seftor, E.A., Seftor, R.E.B. & Hendrix, M.J.C. (2006) 'A three-dimensional model to study the epigenetic effects induced by the microenvironment of human embryonic stem cells', *Stem Cells*, vol. 24, no. 3, pp. 501-505.

Pozniak, C.D., Radinovic, S., Yang, A., McKeon, F., Kaplan, D.R. & Miller, F.D. (2000) 'An anti-apoptotic role for the p53 family member, p73, during developmental neuron death', *Science*, vol. 289, no. 5477.

Raabe, E.H., Laudenslager, M., Winter, C., Wasserman, N., Cole, K., LaQuaglia, M., Maris, D.J., Mosse, Y.P. & Maris, J.M. (2008) 'Prevalence and functional consequence of PHOX2B mutations in neuroblastoma', *Oncogene*, vol. 27, no. 4, pp. 469-476.

Reiff, T., Tsarovina, K., Majdazari, A., Schmidt, M., del Pino, I. & Rohrer, H. (2010) 'Neuroblastoma Phox2b Variants Stimulate Proliferation and Dedifferentiation of Immature Sympathetic Neurons', *Journal of Neuroscience*, vol. 30, no. 3, pp. 905-915.

Reissmann, E., Ernsberger, U., FrancisWest, P.H., Rueger, D., Brickell, P.M. & Rohrer, H. (1996) 'Involvement of bone morphogenetic protein-4 and bone morphogenetic protein-7 in the differentiation of the adrenergic phenotype in developing sympathetic neurons', *Development*, vol. 122, no. 7, pp. 2079-2088.

Roffers-Agarwal, J. & Gammill, L.S. (2009) 'Neuropilin receptors guide distinct phases of sensory and motor neuronal segmentation', *Development*, vol. 136, no. 11, pp. 1879-1888.

Ross, R.A., Lazarova, D.L., Manley, G.T., Smitt, P.S., Spengler, B.A., Posner, J.B. & Biedler, J.L. (1997) 'HuD, a neuronal-specific RNA-binding protein, is a potential regulator of MYCN expression in human neuroblastoma cells', *European Journal of Cancer*, vol. 33, no. 12, pp. 2071-2074.

Santiago, A. & Erickson, C.A. (2002) 'Ephrin-B ligands play a dual role in the control of neural crest cell migration', *Development*, vol. 129, no. 15, pp. 3621-3632.

Sartelet, H., Imbriglio, T., Nyalendo, C., Haddad, E., Annabi, B., Duval, M., Fetni, R., Victor, K., Alexendrov, L., Sinnett, D., Fabre, M. & Vassal, G. (2012) 'CD133 expression is associated with poor outcome in neuroblastoma via chemoresistance mediated by the AKT pathway', *Histopathology*, vol. 60, no. 7, pp. 1144-1155.

Sasselli, V., Pachnis, V. & Burns, A.J. (2012) 'The enteric nervous system', *Developmental Biology*, vol. 366, no. 1, pp. 64-73.

Sawai, S., Shimono, A., Wakamatsu, Y., Palmes, C., Hanaoka, K. & Kondoh, H. (1993) 'DEFECTS OF EMBRYONIC ORGANOGENESIS RESULTING FROM TARGETED DISRUPTION OF THE N-MYC GENE IN THE MOUSE', *Development*, vol. 117, no. 4, pp. 1445-1455.

Schmidt, M., Lin, S.Y., Pape, M., Ernsberger, U., Stanke, M., Kobayashi, K., Howard, M.J. & Rohrer, H. (2009) 'The bHLH transcription factor Hand2 is essential for the maintenance of

noradrenergic properties in differentiated sympathetic neurons', *Developmental Biology*, vol. 329, no. 2, pp. 191-200.

Schober, A., Krieglstein, K. & Unsicker, K. (2000) 'Molecular cues for the development of adrenal chromaffin cells and their preganglionic innervation', *European Journal of Clinical Investigation*, vol. 30, pp. 87-90.

Schriek, G., Oppitz, M., Busch, C., Just, L. & Drews, U. (2005) 'Human SK-Mel 28 melanoma cells resume neural crest cell migration after transplantation into the chick embryo', *Melanoma Research*, vol. 15, no. 4, pp. 225-234.

Schwab, M. (2005) 'Molecular Cytogenetics', *Neuroblastoma*.

Schwab, M., Alitalo, K., Klempnauer, K.H., Varmus, H.E., Bishop, J.M., Gilbert, F., Brodeur, G., Goldstein, M. & Trent, J. (1983) 'AMPLIFIED DNA WITH LIMITED HOMOLOGY TO MYC CELLULAR ONCOGENE IS SHARED BY HUMAN NEURO-BLASTOMA CELL-LINES AND A NEURO-BLASTOMA TUMOR', *Nature*, vol. 305, no. 5931, pp. 245-248.

Schwab, M. & Bishop, J.M. (1988) 'SUSTAINED EXPRESSION OF THE HUMAN PROTOONCOGENE MYCN RESCUES RAT EMBRYO CELLS FROM SENESCENCE', *Proceedings of the National Academy of Sciences of the United States of America*, vol. 85, no. 24.

Schwab, M., Westermann, F., Hero, B. & Berthold, F. (2003) 'Neuroblastoma: biology and molecular and chromosomal pathology', *Lancet Oncology*, vol. 4, no. 8.

Schweigerer, L., Breit, S., Wenzel, A., Tsunamoto, K., Ludwig, R. & Schwab, M. (1990) 'AUGMENTED MYCN EXPRESSION ADVANCES THE MALIGNANT PHENOTYPE OF HUMAN NEUROBLASTOMA-CELLS - EVIDENCE FOR INDUCTION OF AUTOCRINE GROWTH-FACTOR ACTIVITY', *Cancer Research*, vol. 50, no. 14.

Scott, D., Elsden, J., Pearson, A. & Lunec, J. (2003) 'Genes co-amplified with MYCN in neuroblastoma: silent passengers or co-determinants of phenotype?', *Cancer Letters*, vol. 197, no. 1-2, pp. 81-86.

Segerstrom, L., Baryawno, N., Sveinbjornsson, B., Wickstrom, M., Elfman, L., Kogner, P. & Johnsen, J.I. (2011) 'Effects of small molecule inhibitors of PI3K/Akt/mTOR signaling on neuroblastoma growth in vitro and in vivo', *International Journal of Cancer*, vol. 129, no. 12, pp. 2958-2965.

Sela-Donenfeld, D. & Kalcheim, C. (1999) 'Regulation of the onset of neural crest migration by coordinated activity of BMP4 and Noggin in the dorsal neural tube', *Development*, vol. 126, no. 21.

Shojaei-Brosseau, T., Chompret, A., Abel, A., de Vathaire, F., Raquin, M.A., Brugieres, L., Feunteun, J., Hartmann, O. & Bonaiti-Pellie, C. (2004) 'Genetic epidemiology of neuroblastoma: A study of 426 cases at the Institut Gustave-Roussy in France', *Pediatric Blood & Cancer*, vol. 42, no. 1, pp. 99-105.

Singh, S.K., Hawkins, C., Clarke, I.D., Squire, J.A., Bayani, J., Hide, T., Henkelman, R.M., Cusimano, M.D. & Dirks, P.B. (2004) 'Identification of human brain tumour initiating cells', *Nature*, vol. 432, no. 7015, pp. 396-401.

Sjostrom, S.K., Finn, G., Hahn, W.C., Rowitch, D.H. & Kenney, A.M. (2005) 'The Cdk1 complex plays a prime role in regulating N-myc phosphorylation and turnover in neural precursors', *Developmental Cell*, vol. 9, no. 3, pp. 327-338.

Slack, A., Chen, Z.W., Tonelli, R., Pule, M., Hunt, L., Pession, A. & Shohet, J.M. (2005) 'The p53 regulatory gene MDM2 is a direct transcriptional target of MYCN in neuroblastoma', *Proceedings of the National Academy of Sciences of the United States of America*, vol. 102, no. 3, pp. 731-736.

Smith, A.G., Popov, N., Imreh, M., Axelson, H. & Henriksson, M. (2004) 'Expression and DNA-binding activity of MYCN/max and Mnt/max during induced differentiation of human neuroblastoma cells', *Journal of Cellular Biochemistry*, vol. 92, no. 6, pp. 1282-1295.

Soderholm, H., Ortoft, E., Johansson, I., Ljungberg, J., Larsson, C., Axelson, H. & Pahlman, S. (1999) 'Human achaete-scute homologue 1 (HASH-1) is downregulated in differentiating neuroblastoma cells', *Biochemical and Biophysical Research Communications*, vol. 256, no. 3, pp. 557-563.

Sommer, L., Shah, N., Rao, M. & Anderson, D.J. (1995) 'The cellular function of MASH1 in autonomic neurogenesis', *Neuron*, vol. 15, no. 6.

Spitz, R., Hero, B., Ernestus, K. & Berthold, F. (2003) 'Deletions in chromosome arms 3p and 11q are new prognostic markers in localized and 4s neuroblastoma', *Clinical Cancer Research*, vol. 9, no. 1, pp. 52-58.

Stanton, B.R., Perkins, A.S., Tessarollo, L., Sassoon, D.A. & Parada, L.F. (1992) 'LOSS OF N-MYC FUNCTION RESULTS IN EMBRYONIC LETHALITY AND FAILURE OF THE EPITHELIAL COMPONENT OF THE EMBRYO TO DEVELOP', *Genes & Development*, vol. 6, no. 12A, pp. 2235-2247.

Straub, J.A., Sholler, G.L.S. & Nishi, R. (2007) 'Embryonic sympathoblasts transiently express TrkB in vivo and proliferate in response to brain-derived neurotrophic factor in vitro', *Bmc Developmental Biology*, vol. 7.

Strieder, V. & Lutz, W. (2003) 'E2F proteins regulate MYCN expression in neuroblastomas', *Journal of Biological Chemistry*, vol. 278, no. 5.

Stupack, D.G., Teitz, T., Potter, M.D., Mikolon, D., Houghton, P.J., Kidd, V.J., Lahti, J.M. & Cheresh, D.A. (2006) 'Potentiation of neuroblastoma metastasis by loss of caspase-8', *Nature*, vol. 439, no. 7072, pp. 95-99.

Subauste, M.C., Kupriyanova, T.A., Conn, E.M., Ardi, V.C., Quigley, J.P. & Deryugina, E.I. (2009) 'Evaluation of metastatic and angiogenic potentials of human colon carcinoma cells in chick embryo model systems', *Clinical & Experimental Metastasis*, vol. 26, no. 8.

Suzuki, T., Bogenmann, E., Shimada, H., Stram, D. & Seeger, R.C. (1993) 'LACK OF HIGH-AFFINITY NERVE GROWTH-FACTOR RECEPTORS IN AGGRESSIVE NEUROBLASTOMAS', *Journal of the National Cancer Institute*, vol. 85, no. 5, pp. 377-384.

Takahashi, K. & Yamanaka, S. (2006) 'Induction of pluripotent stem cells from mouse embryonic and adult fibroblast cultures by defined factors', *Cell*, vol. 126, no. 4, pp. 663-676.

Takenobu, H., Shimozato, O., Nakamura, T., Ochiai, H., Yamaguchi, Y., Ohira, M., Nakagawara, A. & Kamijo, T. (2011) 'CD133 suppresses neuroblastoma cell differentiation via signal pathway modification', *Oncogene*, vol. 30, no. 1.

Tamm, I., Wang, Y., Sausville, E., Scudiero, D.A., Vigna, N., Oltersdorf, T. & Reed, J.C. (1998) 'IAP-family protein Survivin inhibits caspase activity and apoptosis induced by Fas (CD95), Bax, caspases, and anticancer drugs', *Cancer Research*, vol. 58, no. 23.

Thiele, C.J., Reynolds, C.P. & Israel, M.A. (1985) 'DECREASED EXPRESSION OF N-MYC PRECEDES RETINOIC ACID-INDUCED MORPHOLOGICAL-DIFFERENTIATION OF HUMAN NEURO-BLASTOMA', *Nature*, vol. 313, no. 6001, pp. 404-406.

Thiery, J.P., Duband, J.L. & Delouvee, A. (1982) 'PATHWAYS AND MECHANISMS OF AVIAN TRUNK NEURAL CREST CELL-MIGRATION AND LOCALIZATION', *Developmental Biology*, vol. 93, no. 2, pp. 324-343.

Thomas, S.K., Messam, C.A., Spengler, B.A., Biedler, J.L. & Ross, R.A. (2004a) 'Nestin is a potential mediator of malignancy in human neuroblastoma cells', *Journal of Biological Chemistry*, vol. 279, no. 27.

Thomas, W.D., Raif, A., Hansford, L. & Marshall, G. (2004b) 'N-myc transcription molecule and oncoprotein', *International Journal of Biochemistry & Cell Biology*, vol. 36, no. 5, pp. 771-775.

Tickle, C., Summerbell, D. & Wolpert, L. (1975) 'POSITIONAL SIGNALING AND SPECIFICATION OF DIGITS IN CHICK LIMB MORPHOGENESIS', *Nature*, vol. 254, no. 5497, pp. 199-202.

Torres, J., Regan, P.L., Edo, R., Leonhardt, P., Jeng, E.I., Rappaport, E.F., Ikegaki, N. & Tang, X.X. (2010) 'Biological effects of induced MYCN hyper-expression in MYCN-amplified neuroblastomas', *International Journal of Oncology*, vol. 37, no. 4, pp. 983-991.

Trochet, D., Bourdeaut, F., Janoueix-Lerosey, I., Deville, A., de Pontual, L., Schleiermacher, G., Coze, C., Philip, N., Frebourg, T., Munnich, A., Lyonnet, S., Delattre, O. & Amiel, J. (2004) 'Germline mutations of the paired-like homeobox 2B (PHOX2B) gene in neuroblastoma', *American Journal of Human Genetics*, vol. 74, no. 4, pp. 761-764.

Tsarovina, K., Pattyn, A., Stubbusch, J., Muller, F., van der Wees, J., Schneider, C., Brunet, J.F. & Rohrer, H. (2004) 'Essential role of Gata transcription factors in sympathetic neuron development', *Development*, vol. 131, no. 19, pp. 4775-4786.

Tweddle, D.A., Pearson, A.D.J., Haber, M., Norris, M.D., Xue, C.Y., Flemming, C. & Lunec, J. (2003) 'The p53 pathway and its inactivation in neuroblastoma', *Cancer Letters*, vol. 197, no. 1-2, pp. 93-98.

Valentiner, U., Valentiner, F.U. & Schumacher, U. (2008) 'Expression of CD44 is associated with a metastatic pattern of human neuroblastoma cells in a SCID mouse xenograft model', *Tumor Biology*, vol. 29, no. 3, pp. 152-160.

van Limpt, V., Chan, A., Schramm, A., Eggert, A. & Versteeg, R. (2005) 'Phox2B mutations and the Delta-Notch pathway in neuroblastoma', *Cancer Letters*, vol. 228, no. 1-2, pp. 59-63.

van Limpt, V., Schramm, A., Lakeman, A., van Sluis, P., Chan, A., van Noesel, M., Baas, F., Caron, H., Eggert, A. & Versteeg, R. (2004) 'The Phox2B homeobox gene is mutated in sporadic neuroblastomas', *Oncogene*, vol. 23, no. 57, pp. 9280-9288.

Van Roy, N., De Preter, K., Hoebeeck, J., Van Maerken, T., Pattyn, F., Mestdagh, P., Vermeulen, J., Vandesompele, J. & Speleman, F. (2009) 'The emerging molecular

pathogenesis of neuroblastoma: implications for improved risk assessment and targeted therapy', *Genome medicine*, vol. 1, no. 7, pp. 74-74.

Vanderlugt, N.M.T., Domen, J., Linders, K., Vanroon, M., Robanusmaandag, E., Teriele, H., Vandervalk, M., Deschamps, J., Sofroniew, M., Vanlohuizen, M. & Berns, A. (1994) 'POSTERIOR TRANSFORMATION, NEUROLOGICAL ABNORMALITIES, AND SEVERE HEMATOPOIETIC DEFECTS IN MICE WITH A TARGETED DELETION OF THE BMI-1 PROTOONCOGENE', *Genes & Development*, vol. 8, no. 7.

Vita, M. & Henriksson, M. (2006) 'The Myc oncoprotein as a therapeutic target for human cancer', *Seminars in Cancer Biology*, vol. 16, no. 4, pp. 318-330.

Wakamatsu, Y., Watanabe, Y., Nakamura, H. & Kondoh, H. (1997) 'Regulation of the neural crest cell fate by N-myc: Promotion of ventral migration and neuronal differentiation', *Development*, vol. 124, no. 10, pp. 1953-1962.

Wei, J.S., Song, Y.K., Durinck, S., Chen, Q.R., Cheuk, A.T.C., Tsang, P., Zhang, Q., Thiele, C.J., Slack, A., Shohet, J. & Khan, J. (2008) 'The MYCN oncogene is a direct target of miR-34a', *Oncogene*, vol. 27, no. 39, pp. 5204-5213.

Weiss, W.A., Aldape, K., Mohapatra, G., Feuerstein, B.G. & Bishop, J.M. (1997) 'Targeted expression of MYCN causes neuroblastoma in transgenic mice', *Embo Journal*, vol. 16, no. 11, pp. 2985-2995.

Westermann, F., Muth, D., Benner, A., Bauer, T., Henrich, K.O., Oberthur, A., Brors, B., Beissbarth, T., Vandesompele, J., Pattyn, F., Hero, B., Konig, R., Fischer, M. & Schwab, M. (2008) 'Distinct transcriptional MYCN/c-MYC activities are associated with spontaneous regression or malignant progression in neuroblastomas', *Genome Biology*, vol. 9, no. 10, p. 39.

Weston, J.A. & Butler, S.L. (1966) 'TEMPORAL FACTORS AFFECTING LOCALIZATION OF NEURAL CREST CELLS IN CHICKEN EMBRYO', *Developmental Biology*, vol. 14, no. 2, pp. 246-&.

Wilson, P.A. & Hemmatibrivanlou, A. (1995) 'INDUCTION OF EPIDERMIS AND INHIBITION OF NEURAL FATE BY BMP-4', *Nature*, vol. 376, no. 6538, pp. 331-333.

Wolffe, A.P. (1997) 'Transcriptional control - Sinful repression', *Nature*, vol. 387, no. 6628, pp. 16-17.

Woods, W.G., Tuchman, M., Robison, L.L., Bernstein, M., Leclerc, J.M., Brisson, L.C., Brossard, J., Hill, G., Shuster, J., Luepker, R., Byrne, T., Weitzman, S., Bunin, G. & Lemieux, B. (1996) 'A population-based study of the usefulness of screening for neuroblastoma', *Lancet*, vol. 348, no. 9043, pp. 1682-1687.

Yazhou, C., Wenlv, S., Weidong, Z. & Licun, W. (2004) 'Clinicopathological significance of stromal myofibroblasts in invasive ductal carcinoma of the breast', *Tumor Biology*, vol. 25, no. 5-6, pp. 290-295.

Yin, A.H., Miraglia, S., Zanjani, E.D., AlmeidaPorada, G., Ogawa, M., Leary, A.G., Olweus, J., Kearney, J. & Buck, D.W. (1997) 'AC133, a novel marker for human hematopoietic stem and progenitor cells', *Blood*, vol. 90, no. 12, pp. 5002-5012.

Yin, Y. & Shen, W.H. (2008) 'PTEN: a new guardian of the genome', *Oncogene*, vol. 27, no. 41, pp. 5443-5453.

Zeine, R., Salwen, H.R., Peddinti, R., Tian, Y., Guerrero, L., Yang, Q., Chlenski, A. & Cohn, S.L. (2009) 'Presence of cancer-associated fibroblasts inversely correlates with Schwannian stroma in neuroblastoma tumors', *Modern Pathology*, vol. 22, no. 7.

Zhu, S.Z., Lee, J.S., Guo, F., Shin, J., Perez-Atayde, A.R., Kutok, J.L., Rodig, S.J., Neuberg, D.S., Helman, D., Feng, H., Stewart, R.A., Wang, W.C., George, R.E., Kanki, J.P. & Look, A.T. (2012) 'Activated ALK Collaborates with MYCN in Neuroblastoma Pathogenesis', *Cancer Cell*, vol. 21, no. 3, pp. 362-373.

Zimmerman, K.A., Yancopoulos, G.D., Collum, R.G., Smith, R.K., Kohl, N.E., Denis, K.A., Nau, M.M., Witte, O.N., Toranallerand, D., Gee, C.E., Minna, J.D. & Alt, F.W. (1986) 'DIFFERENTIAL EXPRESSION OF MYC FAMILY GENES DURING MURINE DEVELOPMENT', *Nature*, vol. 319, no. 6056, pp. 780-783.